Regulation of the PP2AC, PP4C, PP6C and alpha4 signalling axis in the myocardium: roles in calcium homeostasis and hypertrophy

A thesis submitted in partial fulfilment for the degree of Doctor of Philosophy by

Olga Eleftheriadou

Faculty of Science, Engineering and Computing
Kingston University London

January 2017

Declaration

I declare that while registered for a research degree at Kingston University, I have not been a registered candidate or enrolled student for another award at any other academic or professional institution. All material contained in the thesis is my own original work, and any references to or use of other sources and collaborative contributions have been clearly acknowledged within the text. None of the work presented here has been used in any other submission for an academic award.

Abstract

Cardiac physiology and hypertrophy are regulated by the phosphorylation status of most proteins, which is controlled by the opposing reactions of protein kinases and phosphatases (PP). The type 2A protein phosphatase family is comprised of PP2A, PP4 and PP6, due to the high amino acid homology of their catalytic subunits (PP2ACα/β, PP4C and PP6C). The activity and expression of this family are partly regulated by alpha4, a common regulatory protein that is essential in type 2A phosphatase holoenzyme biogenesis. In the heart, more than 98% of protein dephosphorylation is mediated by serine/ threonine protein phosphatases, of which type 2A protein phosphatases along with protein phosphatase 1, contribute approximately 90%. Currently, the role(s) of type 2A protein phosphatases and their regulation by alpha4 in the heart is poorly defined and requires detailed investigation.

In this study, quantitative PCR analysis demonstrated that PP2ACβ mRNA was most abundant in H9c2 cardiomyocytes and neonatal rat ventricular myocytes (NRVM) whilst, in adult rat ventricular myocytes (ARVM), PP2ACα mRNA was the most abundantly transcribed. Surprisingly, immunoblotting analysis, using catalytic subunit-specific antibodies, identified the expression of all type 2A protein phosphatase catalytic subunits in H9c2 cardiomyocytes and NRVM, however, ARVM only expressed PP2AC and PP6C protein. PP4C protein expression was only detectable in ARVM following proteasomal inhibition with compound MG132. Using siRNA to selectively knockdown type 2A protein phosphatase catalytic subunits, it was revealed that PP2ACα alone dephosphorylates $Ca_V1.2$-Ser1928. The

data also suggested that PP2ACα, PP2ACβ and PP4C dephosphorylate phospholemman at both Ser63 and Ser68 in cardiomyocytes. siRNA-mediated knockdown of alpha4 protein expression rapidly reduced the expression of all type 2A catalytic subunits. Interestingly, expression of both PP2AC and alpha4 protein expression was elevated in pressure overload-induced left ventricular (LV) hypertrophy. Even though PP6C expression was unchanged, expression of PP6C regulatory subunits (i) SIT4-associated protein 1 (SAP1) and (ii) ankyrin repeat domain (ANKRD) 28 and 44 proteins were upregulated, whereas SAP2 expression was downregulated in hypertrophied LV tissue. Co-immunoprecipitation experiments revealed that the cellular association between alpha4 protein and PP2AC or PP6C subunits was either unchanged or reduced in hypertrophied LV tissue, respectively. Exposure of cardiomyocytes to hydrogen peroxide increased levels of H2AX phosphorylation (γH2AX), indicating hydrogen peroxide-induced DNA damage, which was unaffected by the knockdown of PP6C, however, levels of both total H2AX and γH2AX were diminished by the knockdown of alpha4 protein.

The novel findings in this study collectively, demonstrate the differences in the expression, stability, substrate specificity and altered alpha4-mediated regulation of the type 2A protein phosphatases in normal and hypertrophied myocardium and provide new insights into the molecular mechanisms involved in cardiac calcium homeostasis and DNA repair and thereby help to identify potential targets for the development of new and improved therapies against cardiac pathological hypertrophy.

Acknowledgments

First of all, I want to thank my principal supervisor Dr Andrew K. Snabaitis for his support, continuous patience and encouragement as well as his contribution of time and ideas throughout my PhD studies. Without his invaluable guidance, this dissertation would not have been possible.

Also, I am very grateful to the rest of my supervisor team: Prof Michael J. Shattock and Dr Ali Ryan, for all their support and insightful comments on my work. The guidance they offered, motivated me to widen my research from various perspectives.

I would also like to thank my examiners, Prof Jian-Mei Li and Prof Tony Walker for the enjoyable discussion during my viva and for their suggestions on the thesis revision.

I would like to thank King's College of London for allowing me to work occasionally at the Rayne Institute. I would also like to acknowledge Dr Andrii Boguslavskyi, Dr Shiney Reji, Dr Asvi Francois and Dr Richard Heads, for their contribution in key experiments described in this thesis. Their expertise and thorough demonstration of the experimental processes were greatly appreciated.

A special thank you goes to Dr Brian E. Wadzinski, who kindly donated the catalytic subunit-specific antibodies used in this study. Further, I want to thank Dr Ioannou Niko and Prof Helmout Modjtahedi for providing me specific cell lysates. Also, I thank the British Heart Foundation for funding this PhD. My grateful thanks are also

extended to Prof Edith Sim, for the opportunity she provided me to join their team as an intern and her friendly advice during my studies.

I am particularly grateful to Dr Michael R. Longman, Dr Cowan Jonathan, Dr Polycarpou Elena, Dr Vargo Elizabeth, Dr Griffin Ruth, Nico Lambri, Dr Crescente Vincenzo, Holland Sinead, Goncalves Da Silva Ronni and Dr Mulcahy-Ryan Lauren for their support and friendship.

Finally, I would like to thank my parents, my sister and my husband for all their constant love and encouragement. Their precious support was indispensable for the realisation of this research.

List of Publications

Eleftheriadou, O., Boguslavskyi, A., Longman, M.R., Cowan, J., Francois, A., Heads, R.J., Wadzinski, B.E., Ryan, A., Shattock, M.J. and Snabaitis, A.K., 2017. Expression and regulation of type 2A protein phosphatases and alpha4 signalling axis in cardiac health and hypertrophy. Basic Research in Cardiology 112, doi:10.1007/s00395-017-0625-2. (Copy attached).

List of Presentations

Expression and regulation of the type 2A protein phosphatase-alpha4 signalling axis in cardiac health and hypertrophy.
Poster presentation; The British Pharmacological Society (BPS) annual meeting, London, UK, December 2016.

"Matters of the Heart": Role of the type 2A protein phosphatase family.
Oral presentation; The three-minutes thesis competition, Kingston University London, Kingston upon Thames, UK, February 2016.

Expression of the type 2A protein phosphatases in cardiac health and disease.
Poster presentation; 34th International Society for Heart Research European Section (ISHR-ES) meeting, July 2015, Bordeaux, France.

Expression of the type 2A protein phosphatases in cardiac health and disease.
Poster presentation; The British Society for Cardiovascular Research (BSCR) Autumn meeting, Reading, UK, September 2014.

Expression of the type 2A protein phosphatases in cardiac health and disease.
Oral and poster presentation; Interdisciplinary Hub Conference for the Study of Health and Age-related conditions (IhSHA), Kingston University London, Kingston upon Thames, UK, June 2014.

Contents

List of Tables

List of Figures

Abbreviations

Abs	Absorbance
ACTB	β-actin
Ang-II	Angiotensin II
ANKRD	Ankyrin repeat domain
AraC	Cytosine arabinoside
ARVMs	Adult rat ventricular myocytes
ATM	Ataxia-telangiectasia mutated
atm	atmosphere
ATP	Adenosine-5'-triphosphate
ATR	ATM- and Rad3-Related
BCA	Bicinchoninic acid
BSA	Bovine serum albumin
BW	Body weight
C	Catalytic subunit
Ca^{2+}	Calcium ions
CAL	Calibrator gene
CaMKII	Ca^{2+}/calmodulin–dependent kinase II
cAMP	Cyclic adenosine monophosphate
$Ca_V1.2$	LTCC $\alpha 1_C$ subunit
cDNA	Complementary DNA
cm	Centimetre
CRE	cAMP response element
CREB	CRE binding protein
CV	Coefficient of variation
DMEM	Dulbecco's Modified Eagle Medium
DMSO	Dimethyl sulfoxide
DNA	Deoxyribonucleic acid
DNA-PK	DNA-dependent protein kinase
dsDNA	double-stranded DNA
E1	Ubiquitin-activating enzyme
E2	Ubiquitin-conjugating enzyme
E3	Ubiquitin ligase enzyme
ECL	Enhanced chemiluminescence
EDTA	Ethylenediaminetetraacetic acid disodium salt dihydrate
EGTA	Ethylene-bis(oxyethylenenitrilo)tetraacetic acid
E_{NA}	Na^+ equilibrium potential
ERK	Extracellular signal-regulated kinase
ERK1/2	Extracellular signal-regulated kinases 1/2
ET-1	Endothelin-1
FBS	Foetal bovine serum
FC	Fold-change

FXYD1	FXYD-domain containing ion transport regulator 1
g	Grams
g	Relative centrifugal force
GAPDH	Glyceraldehyde-3-phosphate dehydrogenase
GOI	Gene of interest
GPCRs	G protein-coupled receptors
GTS	Targeted gene of treated samples
h	Hour
H^+	Hydrogen ion
H2AX	Histone 2A variant X
HCl	Hydrochloride acid
HEPES	4-(2-Hydroxyethyl)piperazine-1-ethanesulfonic acid
HW	Heart weight
I_{Ca}	calcium current
I_{CaL}	L-type Ca^{2+} current
IGBP1	Immunoglobulin binding protein 1
I_K	Potassium current
I_{K1}	Inward rectifying potassium current
I_{Kr}	Rapid component of the delayed rectifier potassium current
I_{Ks}	Slow component of the delayed rectifier potassium current
I_{Kur}	Ultrarapid delayed rectifier potassium current
I_{Na}	Sodium current
$I_{Na/Ca}$	Na^+/Ca^{2+}-exchanger current
IP	Immunoprecipitation
IP3	Inositol 1,4,5-triphosphate
I_{to}	Transient outward K^+ current
K^+	Potassium ions
kg	Kilograms
L	Litter
Leu	Leucine residue
LV	Left ventricular
LVW	Left ventricular weight
Lys	Lysine residue
M	Molar
MAPK	Mitogen-activated protein kinase
mg	Milligram
min	Minutes
ml	millilitre
mM	Millimolar
mRNA	Messenger RNA
MTT	3-(4, 5-dimethylthiazol-2-yl)-2, 5-diphenyltetrazolium bromide
Na^+	Sodium ion
NADPH	Nicotinamide adenine dinucleotide phosphate
NCX	Na^+/Ca^{2+}-exchanger
NF	Normalisation factor
NKA	Na^+/K^+ ATPase
no-RT	No reverse transcriptase

NRQ	Normalised relative quantities
NRVMs	Neonatal rat ventricular myocytes
NT	Non-treated
PBS	Phosphate buffered saline
PCR	Polymerase chain reaction
PKA	Protein kinase A
PKC	Protein kinase C
PKG	Protein kinase G
PLM	Phospholemman
PP	Protein phosphatase
PP1	Protein phosphatase 1
PP2A	Protein phosphatase 2A
PP2B	protein phosphatase 2B or calcineurin
PP4	Protein phosphatase 4
PP6	Protein phosphatase 6
PR65	Regulatory subunit of PP2A
qPCR	Quantitative polymerase chain reaction
r	Pearson coefficient of correlation
redox	reduction–oxidation
RIN	RNA integrity number
RNA	Ribonucleic acid
RNAi	RNA interference
ROS	Reactive oxygen species
rpm	Revolutions per minute
RQ	Relative quantity
RT	Reverse transcription
RT-PCR	Reverse transcriptase polymerase chain reaction
RyR2	Ryanodine receptor type 2
SAP	Sit4-associated protein
SD	Standard deviation
SDS	Sodium dodecyl sulfate
SEM	Standard error of the mean
Ser	Serine residue
SERCA	SR Ca^{2+}-ATPase
si	Small interfering
siAlph4	ON-TARGET plus™ Rat Igbd1 siRNA SMARTpool
siC	ON-TARGET plus™ Non-Targeting siRNA
siPP2Cα	ON-TARGET plus™ Rat Ppp2ca siRNA SMARTpool
siPP2Cβ	ON-TARGET plus™ Rat Ppp2cb siRNA SMARTpool
siPP4C	ON-TARGET plus™ Rat PPP4C siRNA SMARTpool
siPP6C	ON-TARGET plus™ Rat PPP6C siRNA SMARTpool
siRNA	Small interfering Ribonucleic acid
siTox	TOX™ Transfection Control
TAC	Transaortic constriction
Tap42	PP2A-associated protein 42
TBE	Tris-borate-EDTA
TBST buffer	1xTris-based buffer containing Tween-20 0.1 % (v/v)

Thr	Threonine residue
TL	Tibia length
TOX-siRNA	TOX™ Transfection Control siRNA
Tris	tris(hydroxymethyl)aminomethane
Ub	Ubiquitin
unk	Unknown sample
V_m	Membrane potential
α-AR	α-adrenergic receptor
β-AR	β-adrenergic receptor
γH2AX	Phosphorylated H2AX
µg	Microgram
µl	Microlitre
µM	Micromolar

Chapter 1

General Introduction

1.1 Prevalence of cardiovascular disease in the UK

Cardiovascular disease still remains one of the leading causes of death worldwide (Naghavi M et al., 2015; Roth et al., 2015; Townsend et al., 2016) and is the second leading cause of death in the UK[1]. Cardiac hypertrophy (section 1.2), is a major predictor of cardiovascular morbidity and mortality (Levy et al., 1990; Brown et al.; Havranek et al., 2008; Okwuosa et al., 2015). It is associated with nearly all forms of heart failure and other cardiovascular diseases, such as essential hypertension, coronary heart disease and is also considered an independent risk for myocardial infarction, arrhythmia and sudden death (Kannel et al., 1987; Koren et al., 1991; Brown et al.; East et al., 2003; Frenneaux, 2004; Smits and Smits, 2004; Meijs et al., 2007).

Heart failure, is a cardiovascular condition where the heart cannot pump blood sufficiently to the rest of the body and is associated with increasing mortality rates and hospitalisation (Nicol et al., 2008; McMurray et al., 2012; Guha and McDonagh, 2013; Ponikowski et al., 2014; Bhatnagar et al., 2015; Gerber et al., 2015). In the UK, more than 500,000 people have been diagnosed with heart failure according to

[1]British Heart Foundation cardiovascular disease statistics compendium 2017; https://www.bhf.org.uk/research/heart-statistics/heart-statistics-publications/cardiovascular-disease-statistics-2017

British Heart Foundation statistics 2017[2]. Most common causes of heart failure are hypertensive and coronary heart disease (Velagaleti and Vasan, 2007; Dunlay et al., 2009). The primary abnormality is impaired function of the left ventricle and fall in cardiac output (McMurray et al., 2012). Several compensatory mechanisms exist in mammals to augment cardiac output sufficiently which mainly include the Frank-Starling mechanism (Katz, 2002), development of ventricular hypertrophy (section 1.2.5) and increased sympathetic drive to the heart (section 1.3.3). However, over time, all these adaptive mechanisms, become maladaptive and may trigger progression to a decompensated phenotype and heart failure (Hein et al., 2003; Gradman and Alfayoumi, 2006; El-Armouche and Eschenhagen, 2008).

Current therapies for heart failure provide only symptomatic relief or provisionally impede disease progression (McMurray et al., 2012; Ponikowski et al., 2014). Thus, a better understanding of the molecular mechanisms underlying cardiac pathophysiology may provide new possibilities for the development of new and improved therapies to prevent or treat pathological cardiac hypertrophy, heart failure and other types of cardiovascular disease.

1.2 Cardiac hypertrophy

1.2.1 Cardiac growth

In mammals, the heart is one of the first organs to form and function during fetal development (Cleaver and Krieg, 2010). Under normal conditions, cardiomyocytes comprise approximately 70-80% of the adult heart's mass, even though they represent nearly one-third of the total cell population (Nag, 1980; Popescu et al., 2006). Though, prenatal cardiac growth depends on hyperplasia of cardiomyocytes,

[2]Cardiovascular statistics – British Heart Foundation UK facts sheet; https://www.bhf.org.uk/research/heart-statistics

shortly after birth, most cardiomyocytes exit the cell cycle and lose their ability to divide (Li et al., 1996; Porrello et al., 2008; Maillet et al., 2013; Alkass et al., 2015). Subsequent growth of the heart, during postnatal development, is primarily reliant on hypertrophy (enlargement) of individual cardiomyocytes (Li et al., 1996; Porrello et al., 2008; Mollova et al., 2013; Senyo et al., 2013; Alkass et al., 2015; Bergmann et al., 2015). Nevertheless, recent studies have provided evidence of cardiomyocyte turnover (most studies report < 1% per year) during a human lifespan that gradually declines with age, which is thought to contribute to the development of the heart along with hypertrophy (Bergmann et al., 2009; Mollova et al., 2013; Bergmann et al., 2015).

Cardiac hypertrophy can be defined as an increase in cardiac mass due to an enlargement in cardiomyocyte size, which is achieved by an increase in protein synthesis and the number of sarcomeres in the component myofibrils. In response to an increase in workload, imposed by physiological or pathological stimulation, the heart undergoes hypertrophic growth to normalise ventricular wall stress. Depending on the stimulus, cardiac hypertrophy can be divided into physiological and pathological hypertrophy, which are characterised by distinct remodelling and molecular mechanisms, discussed in the following sections (sections 1.2.2-1.2.5) (review by Maillet et al., 2013).

1.2.2 Physiological and pathological cardiac hypertrophy

Cardiac hypertrophy, that occurs in normal growth (postnatal hypertrophy), pregnancy or chronic exercise training, is usually referred to as physiological hypertrophy. This type of cardiac hypertrophy is characterised by normal or enhanced contractile function, normal morphology and organisation of heart structure (Pluim et al., 2000; Schannwell et al., 2002; Iemitsu et al., 2003; Konhilas

et al., 2004; Eghbali et al., 2005) (Figure 1.1). In contrast, cardiac hypertrophy, induced in settings of a disease such as hypertension, aortic stenosis or following heart injury (myocardial infarction), is referred to as pathological hypertrophy. Pathological hypertrophy is mostly considered irreversible and is commonly associated with contractile dysfunction, interstitial fibrosis, upregulation of fetal cardiac genes (such as atrial and brain natriuretic peptides) and increased mortality (Levy et al., 1990; Hein et al., 2003; McMullen et al., 2003; Drazner et al., 2004; de Simone et al., 2008).

1.2.3 Concentric and eccentric hypertrophy

Cardiac hypertrophy is typically caused by pressure or volume overload, leading to different forms of left ventricular (LV) hypertrophy with distinct morphology, molecular mechanisms and gene expression profiles, at least at an early stage (Figure 1.1). Therefore, physiological and pathological hypertrophy have been subdivided into concentric and eccentric hypertrophy (review by Maillet et al., 2013).

Physiological stimulus can result in concentric or eccentric hypertrophy, however, this category of remodelling is considered reversible. Isometric or static exercise, such as weightlifting, results in a pressure load on the heart and leads to concentric hypertrophy with a small or no change in chamber volume whilst, isotonic exercise such as running or pregnancy, increases venous return to the heart, which results in volume overload and eccentric hypertrophy characterised by chamber enlargement and a proportional change in wall thickness (McMullen et al., 2003; Mihl et al., 2008; Xiao et al., 2014). Pathological stimulus, such as hypertension or aortic stenosis, produces an increase in systolic wall stress and results in concentric hypertrophy, which is characterised by an increase in relative wall thickness and

cardiac mass, with a reduction in left ventricular volume, where the addition of new sarcomeres in parallel increases cardiomyocyte size. Alternatively, a pathological stimulus such as chronic myocardial infarction or valvular insufficiency, causes an increase in diastolic wall stress and can lead to wall dilation with the preferential lengthening of cardiomyocytes by the addition of new sarcomeres in series (Grossman et al., 1975; McMullen et al., 2003).

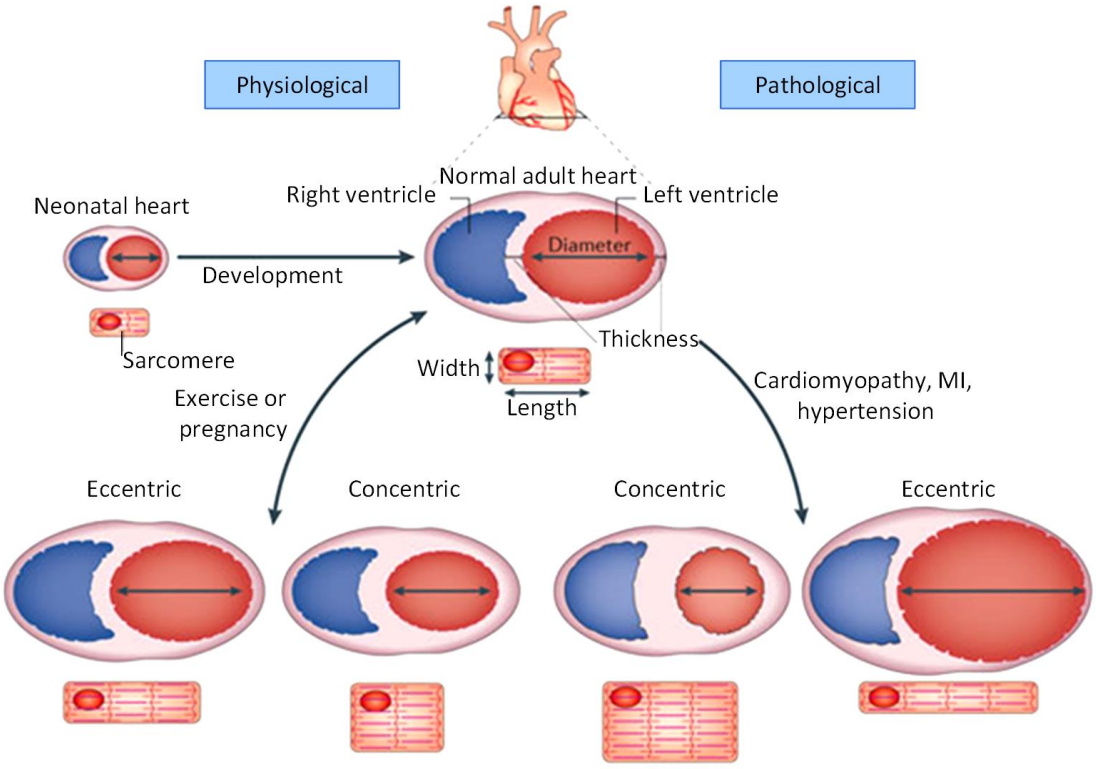

Figure 1.1 Different forms of cardiac hypertrophy (taken from Maillet et al., 2013). Postnatal hypertrophy is associated with the normal development of the postnatal heart until adulthood. Physiological hypertrophy during pregnancy or in response to chronic exercise training, is reversible and characterised by normal cardiac morphology and function. In contrast, hypertrophy that occurs in settings of disease is detrimental to cardiac structure and function and can lead to heart failure. Pressure overload stimulus causes thickening of the left ventricle wall due to the addition of sarcomeres in parallel and results in concentric hypertrophy. Volume overload stimulus induces an increase in muscle mass via the addition of sarcomeres in series and results in eccentric hypertrophy. MI: Myocardial infarction.

1.2.4 Molecular mechanisms of physiological LV hypertrophy

Cardiac hypertrophy is typically stimulated by intracellular signal transduction

pathways in response to either neuroendocrine factors or mechanical stretch–sensing apparatus (review by Maillet et al., 2013). The molecular mechanism for the pregnancy-induced LV hypertrophy (eccentric phenotype) is poorly understood yet, however, postnatal and exercise-induced hypertrophy is stimulated by high serum levels of growth factors such as insulin-like growth factor 1 (IGF1). IGF1 is involved in the activation of phosphoinositide 3-kinase and protein kinase B, which regulate the progress of physiological hypertrophy (Figure 1.2) (McMullen et al., 2003; Luo et al., 2005). In a previous study, transgenic mice, with reduced phosphoinositide 3-kinase activity, showed suppressed developmental growth and attenuated physiological hypertrophy in response to exercise training (Luo et al., 2005).

1.2.5 Molecular mechanisms of pathological LV hypertrophy

1.2.5.1 Concentric hypertrophy

In response to pathological pressure overload, autocrine or paracrine neurohormonal factors, such as angiotensin II (Ang-II), endothelin-1 (ET-1) or noradrenaline, are released and induce cardiomyocyte growth (Schunkert et al., 1990; Arai et al., 1995; Rapacciuolo et al., 2001; Yayama et al., 2004) (Figure 1.2). Ang-II, ET-1 or noradrenaline bind to their cognate G protein-coupled receptors (e.g. Ang-II receptors, ET-1 receptors or α_1-adrenergic receptors, respectively) that are coupled to heterotrimeric G_q proteins of the G protein family and cause the dissociation of the Gα ($G\alpha_{q/11}$) and Gβγ subunits (Lambright et al., 1994; Sondek et al., 1996; review by Rockman et al., 2002). The activated $G\alpha_{q/11}$ then activates phospholipase C, which catalyses the cleavage of the phospholipid phosphatidylinositol 4,5-bisphosphate into inositol 1,4,5-triphosphate (IP_3) and diacylglycerol (Rozengurt, 1986; Trepel et al., 1988; Simon et al., 1991). IP_3 production induces intracellular

calcium (Ca^{2+}) release from the sarcoplasmic reticulum via stimulation of the IP_3 receptors to activate the Ca^{2+}/calmodulin–dependent kinase II (CaMKII) and calcineurin (Molkentin et al., 1998). However, due to the low density of IP_3 receptors on the sarcoplasmic reticulum of ventricular cardiomyocytes, calcineurin/CAMKII activation is primarily driven by Ca^{2+} released during β-adrenergic receptor stimulation or introduced into the cell via the transient receptor potential canonical channels 3 and 6 subtypes, which can be activated by their association with phospholipase C or diacylglycerol (Mackenzie et al., 2004; Nakayama et al., 2010; Wu et al., 2010). Overall, calcineurin (also known as protein phosphatase 2B (PP2B)) is a Ca^{2+}-dependent protein phosphatase that activates the nuclear factor of activated T cells family of transcription factors, which in turn enhance the transcription of hypertrophic genes that, in their majority, are typically maladaptive (Molkentin et al., 1998; Wilkins et al., 2004). Diacylglycerol activates serine/ threonine-protein kinase C (PKC), which in turn enables the MEK1/2 (mitogen-activated protein kinase (MAPK)/ extracellular signal-regulated kinase (ERK) kinases 1/2)-ERK1/2 signalling pathway resulting in increased protein synthesis and cell growth (Raman and Cobb, 2003; Harris et al., 2004). The MEK1/2-ERK1/2 pathway is suggested to drive the adaptive cardiac hypertrophy response, however, association of the MEK1/2-ERK1/2 complex with the Gβγ subunits enhances autophosphorylation of ERK2 at Thr188 residue and its localisation in the nucleus, resulting in the activation of transcription factors and increased transcription of hypertrophic genes (Bueno and Molkentin, 2002; Harris et al., 2004; Lorenz et al., 2009). The latter event has been suggested to induce maladaptive cardiac hypertrophy (Lorenz et al., 2009; Ruppert et al., 2013; Mutlak and Kehat, 2015).

In addition to neurohormonal-dependent stimulation of cardiac hypertrophy,

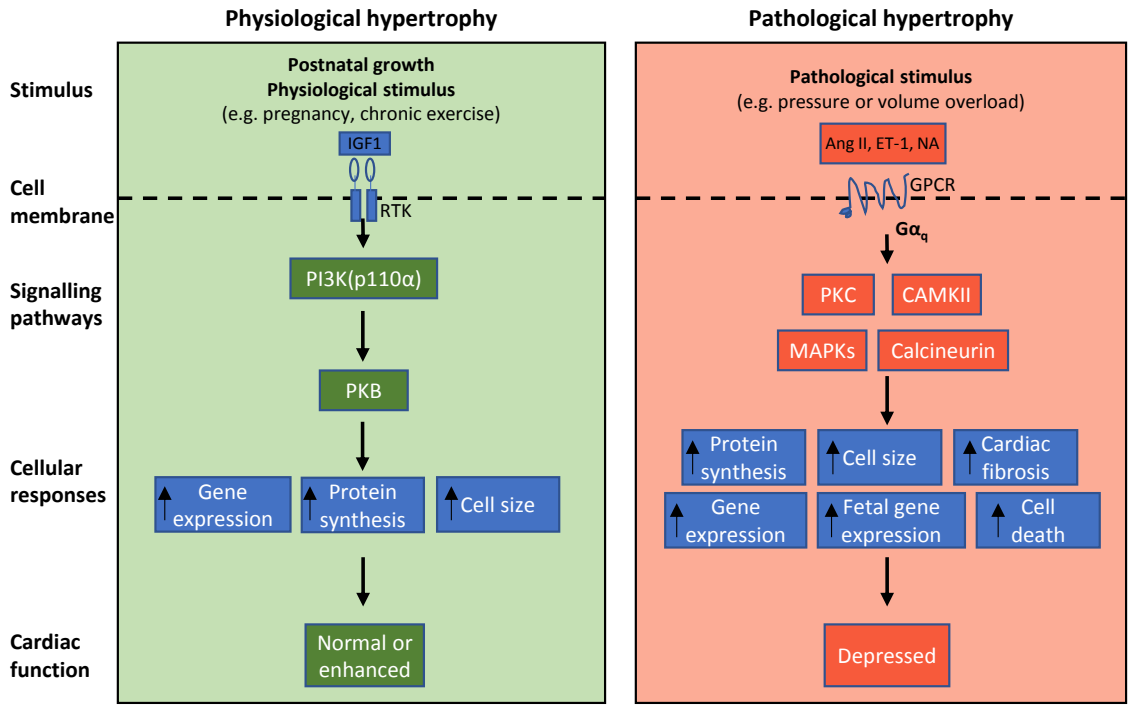

Figure 1.2 A schematic illustration of signalling pathways involved in the induction of physiological or pathological cardiac hypertrophy (adapted from Bernardo et al., 2010). Ang II: angiotensin II; ET-1: endothelin-1; GPCR: G protein-coupled receptor; IGF-1: insulin-like growth factor 1; MAPK: mitogen-activated protein kinase; NA: noradrenaline; PI3K (p110α): phosphoinositide 3-kinase p110α; RTK: receptor tyrosine kinase.

cardiomyocytes can detect directly hemodynamic stress (e.g. pressure overload) by an internal sensory apparatus, resulting in activation of stress-activated protein kinases (SAPKS) p38 kinases and c-Jun N-terminal kinases branches of the mitogen-activated protein kinase (MAPK) cascade, which in turn activate transcription factors, followed by the induced transcription of hypertrophic genes (Gupta et al., 1996; Weinberg et al., 1999; Braz et al., 2003; Raman and Cobb, 2003; Sopontammarak et al., 2005). Nevertheless, in many studies, their role in the development of pathological cardiac hypertrophy appears to be contradictory. Activation of JNK has been suggested to either induce a maladaptive cardiac phenotype or protect the heart in a setting of pathological pressure overload (Choukroun et al., 1999; Minamino et al., 2002; Sadoshima et al., 2002; Liang and Molkentin, 2003; Liu et al., 2009). Moreover, evidence has shown an anti-apoptotic

or anti-hypertrophic role of p38 kinases (p38α subfamily), whilst other studies demonstrated an association between the activated p38 and induction of maladaptive cardiac phenotype and/ or cardiomyocyte apoptosis (Wang et al., 1998; Zhang et al., 2000; Behr et al., 2001; Braz et al., 2003; Kaiser et al., 2004; Nishida et al., 2004).

1.2.5.2 Eccentric hypertrophy

Pathological cardiac hypertrophy, induced by volume overload due to valvular insufficiency or chronic myocardial infarction, results in eccentric pathological hypertrophy. Such a stress mainly activates ERK5 and has been associated with progression to dilated cardiomyopathy and sudden death (Nicol et al., 2001).

1.3 Excitation-contraction of ventricular cardiomyocytes

1.3.1 Action potential of ventricular cardiomyocytes

The action potential (i.e. the electrical impulse that initiates contraction) of a typical ventricular cardiomyocyte (Figure 1.3A-C) is divided into 5 phases (0-4), beginning and ending with phase 4 (Figure 1.4) (Bers, 2001; Nattel and Carlsson, 2006; Giudicessi and Ackerman, 2012). At phase 4 (resting phase), the membrane baseline potential is at a steady voltage, (between -80 mV to -90 mV), mainly due to a constant K^+ ion efflux (inward rectifying K^+ current, I_{K1}) through the rectifier K^+ channels and the activity of the Na^+/K^+-ATPase (influx of K^+) (Inagaki et al., 1996; Bers, 2001; Nattel and Carlsson, 2006). At this stage, voltage-gated Na^+ and Ca^{2+} channels are closed. Phase 0 of the action potential begins with the depolarisation of the cell to its threshold due to the passive entrance of Na^+ from a neighbouring cardiomyocyte or pacemaker cell, through the gap junctions (formed primarily of connexin 43) causing an inward Na^+ current (I_{Na}) that exceeds the I_K (Spragg and Kass, 2005; Boyett et al., 2006). Voltage-gated Na^+ "fast" channels (mainly $Na_V1.5$) are then triggered to open (Maier et al., 2002; Blechschmidt et al., 2008), allowing Na^+ influx

into the cell. This increase in the Na^+ inward current (I_{Na}) causes a rapid further depolarisation of the cell membrane towards the Na^+ equilibrium potential (E_{Na} = +70 mV). Meanwhile, at V_m=-40 mV, the voltage-gated L-type Ca^{2+} channels (primarily $Ca_V1.2$ in

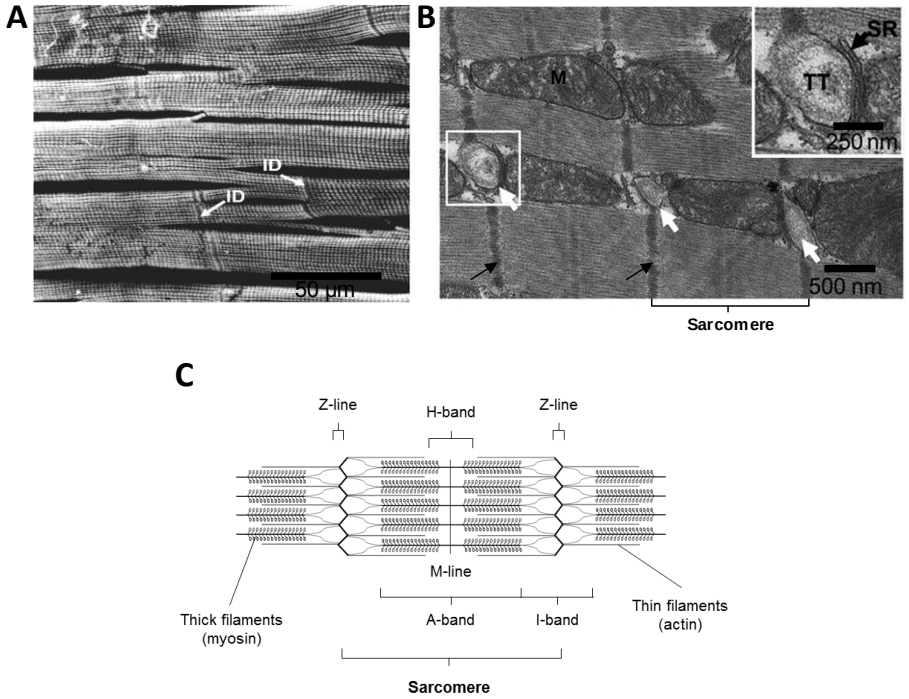

Figure 1.3 Cardiomyocyte structure and sarcomere organisation. The major cellular constituents of the adult myocardium are the cardiomyocytes (>90% in human myocardium) (Banerjee et al., 2007; Mollova et al., 2013; Alkass et al., 2015). (**A**) A backscattered electron microscopy image of cardiomyocytes in normal human left ventricular myocardium, reproduced by Kanzaki et al. (2010), shows that cardiomyocytes are striated, branched, cells that cross-link with those around them in three dimensions. Cell-cell connections by intercalated discs (ID, white arrows) and sarcomere striation are observed; scale bar = 50 µm. ID: intercalated disc. (**B**) Transmission electron microscopy image showing the transverse tubules (white arrows) and Z line (black arrows) formed between adjacent sarcomeres in healthy human myocardium, reproduced by Zhang et al. (2013); scale bar 500 nM. Box insert shows higher resolution of the transverse tubule (TT)-sarcoplasmic reticulum (SR) dyadic junction marked by the white square; scale bar: 250 nM. TT: transverse tubule; SR: sarcoplasmic reticulum; M: mitochondria. (**C**) A simplified schematic diagram of the thin (actin) and thick (myosin) filaments arrangement in the sarcomere, the basic cardiomyocyte contractile apparatus. Thin filaments are attached to the Z-lines and expand towards the centre of the sarcomere whilst, thick filaments, are positioned at the centre of the sarcomere. The central A-band is determined by the length of the thick filaments which are flanked by the thin filaments. The centre of the thick filaments is known as M-line. The I-band consists only thin filaments, and the area of the thick filaments which is not flanked by thin filaments is known as H-band. Z-lines contain mainly α-actinin that crosslinks thin filaments from adjacent sarcomeres.

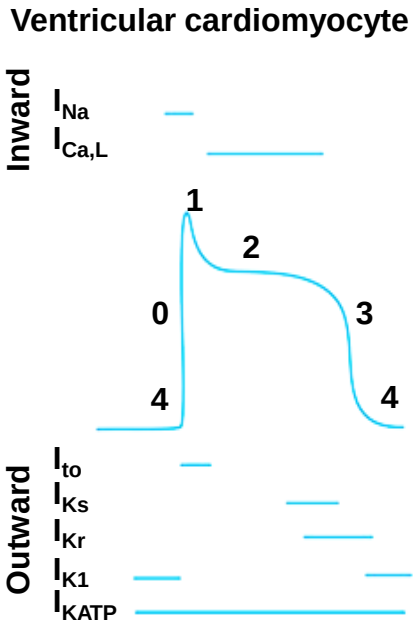

Figure 1.4 Action potential of ventricular cardiomyocytes (taken from Giudicessi and Ackerman, 2012). A diagram of the phases (0-4) of a typical ventricular cardiomyocyte action potential is shown. Timing and portion of the inward and outward currents of the action potential are indicated with blue (ventricular cardiomyocyte) or orange (nodal cardiomyocyte) bars. SA: Sinoatrial; AV: atrioventricular; $I_{Ca,L}$: Ca^{2+} current (through L-type Ca^{2+} channels); I_{K1}: inward rectifier K^+ current; I_{KATP}: ATP-sensitive K^+ current; I_{Kr}: rapid component of the delayed rectifier K^+ current; I_{Ks}: slow component of the delayed-rectifier K^+ current; I_{Na}: Na^+ current; I_{to}: transient outward K^+ current.

ventricles) open and cause a "slow" inward Ca^{2+} current (I_{Ca}) $K_v1.4$) and produce a transient outward (Mangoni et al., 2003; Takemura et al., 2005; Zhang et al., 2005). During that stage, the ventricular cardiomyocytes membrane potential (V_m) may reach a peak at +30-50 mV due to the continuous leak of K^+ (Bers, 2001). Depolarisation rapidly shuts off the outward $I_{K1,}$ but voltage-gated K^+ channels are activated ($K_v4.2$, $K_v4.3$ and K^+ current, called I_{to} (Bers, 2001; Giudicessi and Ackerman, 2012). At peak potential, where the inward current (I_{Na}+I_{Ca}) is equal to the outward current (mainly due to K^+), the voltage-gated Na^+ channels close, inactivating I_{Na}. The next phase is phase 1 (rapid repolarisation phase), where an initial rapid repolarisation is induced mainly due to the inactivation of I_{Na} and activation of transient outward I_{to}. Phase 2 (plateau phase), is the longest phase of the action potential. I_{to} is inactivated, however, the voltage-gated L-type Ca^{2+} channels are still open, and the main inward is I_{Ca} is balanced by the delayed rectifier K^+ currents I_{Ks}, I_{Kur}, and I_{Kr} ($K_v7.1$, $K_v1.5$ and $K_v11.1$ channels, respectively), leading to the plateau (Bers, 2001; Giudicessi and Ackerman, 2012). This stage becomes significant in the excitation-contraction coupling process (see

section 1.3.2). During phase 3 (late repolarisation), the voltage-gated L-type calcium channels are closing. The cells are repolarised with the V_m returning to its resting potential, due to the persistent outward K^+ currents (mainly by I_{K1} increase) (Bers, 2001; Giudicessi and Ackerman, 2012). Furthermore, the extra cytosolic concentrations of Na^+ and Ca^{2+} ($[Na^+]_i$ and $[Ca^{2+}]_i$, respectively) are mainly extruded from the cell by the sarcolemmal Na^+/ K^+-ATPase (NKA), which in turn restores the loss of intracellular K^+ during the repolarisation phase and the forward mode of Na^+/Ca^{2+}-exchanger, increasing inward $I_{Na/Ca}$ (Ca efflux) (Bers, 2001; Nattel and Carlsson, 2006).

1.3.2 Cardiac excitation-contraction coupling

Electrical excitation (section 1.3.1) of the cardiomyocyte leads to contraction. This process is called excitation-contraction coupling and is well characterised in ventricular cardiomyocytes (Bers, 2002). Calcium (Ca^{2+}) is the critical mediator of cardiac excitation-contraction coupling, that can act as an intracellular secondary messenger and drive contraction. Depolarisation of the sarcolemma by the inward I_{Na} current during the action potential activates the L-type Ca^{2+}-channels, which allows free Ca^{2+} to enter the cell (also termed inward Ca^{2+} current (I_{Ca})) (Scriven et al., 2000; Bers, 2001; Takemura et al., 2005). In addition, during depolarisation, the inward I_{Na}, may trigger Ca^{2+} influx via the reverse mode of the Na^+/Ca^{2+}-exchanger (NCX), contributing to an early increase in $[Ca^{2+}]_i$ (Bers, 2001; Lines et al., 2006). The L-type Ca^{2+} channels are primarily located at sarcolemma invaginations into the cell interior, called t-tubules (transverse tubules), in close proximity to type 2 ryanodine receptors (RyR2), which are the Ca^{2+} release channels of the sarcoplasmic reticulum in cardiomyocytes, the primary intracellular calcium store (Nakai et al., 1990; Scriven et al., 2000; Brette et al., 2004; Zhang et al., 2013). An increase in local cytosolic free Ca^{2+} concentration ($[Ca^{2+}]_i$) near the RyR2, primarily due to the

L-type Ca^{2+} channels activity, binds to and activates them to releases free Ca^{2+} (also termed Ca^{2+} sparks) from the sarcoplasmic reticulum, in a process known as "Ca^{2+} induced Ca^{2+} release" (CICR) (Bers, 2001; Bers, 2002). CICR may increase $[Ca^{2+}]_i$ approximately 10-fold in ventricular cardiomyocytes, as several thousand sparks are activated synchronically (high density of RyR2), which causes inactivation of the I_{Ca} (Bers, 2001). The cytosolic free Ca^{2+} then binds to the thin filament troponin complex, specifically at troponin C, which results in subsequent formation of actin-myosin cross-bridges to produce contraction of the cardiomyocytes along the muscle's major axis (Bers, 2001). Muscle contraction occurs when the central bipolar myosin thick filaments use ATPase-generated force to pull the thin filaments, sliding the two types of filaments across each other to reduce sarcomere length.

Following contraction, the Ca^{2+} dissociates from troponin C, disrupting the actin-myosin interaction on myofilaments (Hazard et al., 1998; Bers, 2001) and is removed from the cytosol by four mechanisms, involving sarcoplasmic reticulum Ca^{2+}-ATPase (SERCA2a), sarcolemmal NCX, sarcolemmal Ca^{2+}-ATPase or mitochondrial Ca^{2+} uniport, to allow relaxation of the cardiomyocytes (diastole) (Bers, 2002). The activator Ca^{2+} is predominantly reuptaken into the sarcoplasmic reticulum through the SERCA2a. Under normal conditions, the sarcoplasmic reticulum usually reuptakes an equal fraction of activator Ca^{2+} that was released. This fraction usually corresponds to approximately 70% or more of the activator Ca^{2+} present in the cytosol, depending on the species (Bers, 1997; Pieske et al., 1999; Puglisi et al., 1999; Shannon et al., 2000; Bers, 2001; MacLennan and Kranias, 2003). The activity of SERCA2a is regulated by phospholamban (Bers, 2001; MacLennan and Kranias, 2003; Vangheluwe et al., 2005). At low levels of cytosolic $[Ca^{2+}]_i$, dephosphorylated phospholamban inhibits SERCA2a activity.

However, at high levels of $[Ca^{2+}]_i$, the Ca^{2+}-calmodulin–dependent protein kinase (CaMKII), a serine/threonine-specific protein kinase, is activated (Saucerman and Bers, 2008). CAMKII phosphorylates phospholamban at the threonine 17 residue and relieves its inhibitory function (Bers, 2001; MacLennan and Kranias, 2003; Vangheluwe et al., 2005). Phospholamban can also be phosphorylated at serine16 by the serine/threonine-protein kinase A (PKA) and increase SERCA2a activity, in response to β-adrenergic receptor stimulation, (see section 1.3.3) (Bers, 2002; MacLennan and Kranias, 2003). An important fraction (up to 28%) of the activator Ca^{2+} is extruded by the forward mode of the sarcolemmal NCX due to the increased $[Ca^{2+}]_I$, which favours the Ca^{2+} efflux (Bers, 1997; Pieske et al., 1999; Puglisi et al., 1999; Shannon et al., 2000; Bers, 2001; MacLennan and Kranias, 2003; Liao et al., 2012). Only a small fraction of the activator Ca^{2+} is removed from the cytosol by the sarcolemmal Ca^{2+}-ATPase or mitochondrial Ca^{2+} uniport (Bers, 2001). The latter appears to have a major role in activation of oxidative metabolism (Territo et al., 2000; reviewed by Griffiths et al., 2010).

The excitation-contraction coupling is regulated by the activation of the G protein-coupled receptors (GPCRs) which are driven by the stimulation of the sympathetic or parasympathetic nervous system, causing changes in the phosphorylation status of many cardiac proteins and affecting the cardiac rate and output eventually (Bers, 2001). The mechanism is further described in section 1.3.3.

1.3.3 Autonomic control of cardiomyocyte contraction

The autonomic nervous system controls the heart rate (chronotropy), conduction velocity through the atrioventricular node (dromotropy), the force of contraction (inotropy) and rate of relaxation (lusitropy). Therefore, the autonomic nervous system can regulate cardiac output, in response to circulatory requirements of the

body. It is divided into two interacting systems: the sympathetic and parasympathetic system (Sherwood, 2011; Shen et al., 2012). Overall, activation of the sympathetic neurons, under physiological (i.e. exercise; section 1.2.4) or pathological conditions (i.e. pressure overload; section 1.2.5), causes the release of noradrenaline, a catecholamine, which activates Gs protein-coupled receptors, such as the β-adrenergic receptors on cardiac myocytes (Bers, 2002).

β_1-adrenergic receptor is the abundant subtype and is functional at both t-tubules and surface sarcolemma of ventricular cardiomyocytes (Brodde, 1991; Moniotte et al., 2001; Cros and Brette, 2013). When the sympathetic transmitter noradrenaline binds to β_1-adrenergic receptors, $G\alpha_s$ subunit is activated and dissociates from the $G\beta\gamma$ dimer (Figure 1.5). $G\alpha_s$ then activates the adenylate cyclase to increase cAMP, which in turn binds to and activates cAMP-dependent protein kinase A (PKA) (Defer et al., 2000; Pierce et al., 2002). PKA then directly phosphorylates several local substrates on serine/ threonine residues, involved in excitation-contraction coupling, such as L-type voltage-gated Ca^{2+} channels, RyR2, phospholamban, troponin I and phospholemman, through its interaction with various A-kinase anchoring proteins (AKAPS) (reviewed by Diviani et al., 2011). Phosphorylation of the L-type voltage-gated Ca^{2+} channels, $Ca_V1.2$, by PKA, has been commonly reported to upregulate its activity, thereby, increasing inward I_{Ca} and $[Ca^{2+}]_i$ (Osterrieder et al., 1982; Gao et al., 1997; Hulme et al., 2006a; Shi et al., 2012). RyR2 has been shown to increase calcium release from the sarcoplasmic reticulum and $[Ca^{2+}]_i$, when phosphorylated by PKA (Marx et al., 2000b; Xiao et al., 2005; Xiao et al., 2006; Huke and Bers, 2008b). Phosphorylation of phospholamban by PKA, relieves its inhibition of SERCA2a, thereby, accelerating activator Ca^{2+} reuptake by the sarcoplasmic reticulum (Bers, 2002; MacLennan and Kranias, 2003). The sarcomeric protein troponin I, which is part of the troponin complex on thin actin filaments, has been shown to reduce myofilament sensitivity to Ca^{2+} when phosphorylated by PKA whilst, PKA-phosphorylated myosin-binding protein C has

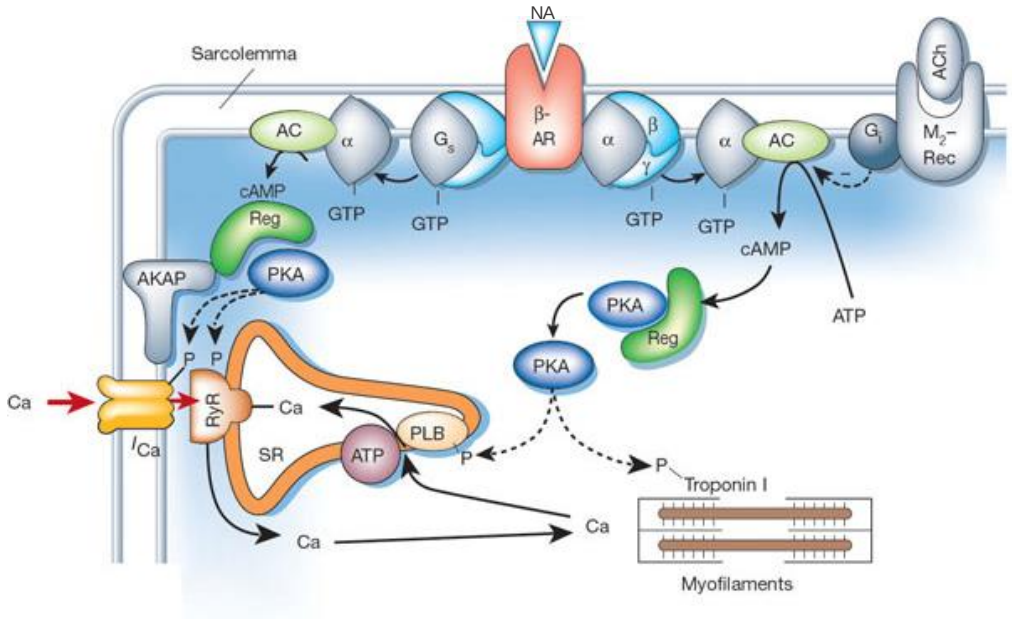

Figure 1.5 β-αdrenergic receptor stimulation by sympathetic and parasympathetic system activation and phosphorylation of targets relevant to excitation-contraction coupling (taken from Bers, 2002). NA: noradrenaline; AC: adenylyl cyclase; ACh: acetylcholine; AKAP: A kinase anchoring protein; β-AR: β-adrenergic receptor; M_2-Rec: M_2-muscarinic receptor; PLB: phospholamban; Reg: PKA regulatory subunit; SR: sarcoplasmic reticulum. Ca: calcium cations (Ca^{2+}); ATP: Ca^{2+}-ATPase; RyR: ryanodine receptor.

been identified as a factor that accelerates cardiomyocyte relaxation (Stelzer et al., 2007; Kooij et al., 2013). Recent studies have emphasised the importance of PKA-phosphorylation of phospholemman, an accessory protein of NKA, which increases the NKA affinity for $[Na^+]_i$, which in turn activates inward $I_{Na/Ca}$ (Ca^{2+} efflux) (Pavlović et al., 2007; Despa et al., 2008).

PKA may also indirectly amplify the phosphorylation of several cardiac proteins related to excitation-contraction coupling (such as phospholamban, phospholemman, RyR2) by phosphorylation of protein phosphatase inhibitor-1 at Thr35 and subsequent inhibition of serine/ threonine protein phosphatase 1 (PP1) (Bers, 2001; El-Armouche et al., 2003). In addition, the excessive $[Ca^{2+}]_i$, increases the serine/ threonine CAMKII activation, which in turn can also phosphorylate substrates involved in Ca^{2+} handling, such as $Ca_V1.2$, RyR2, phospholamban, in a similar

manner to PKA (Bers, 2001; MacLennan and Kranias, 2003; Rodriguez et al., 2003; Xiao et al., 2005; Huke and Bers, 2008b; Blaich et al., 2010). Furthermore, inhibition of PP1, prevents dephosphorylation (de-activation) of CAMKII, thereby, increasing its activity (Blitzer et al., 1998).

Cardiac β_2-adrenergic receptors are coupled to both G_s and G_i proteins (Xiao et al., 1995; Kilts et al., 2000). Even though activation of β_2-adrenergic receptors by noradrenaline enhances cAMP production and PKA phosphorylation of $Ca_V1.2$ (Xiao et al., 1994; Chen-Izu et al., 2000), many studies have demonstrated dissociation with PKA-dependent phosphorylation of phospholamban, troponin I and positive inotropic effect, probably due to the inhibitory function of $G\alpha_i$ towards the adenylate cyclase (Xiao et al., 1994; Xiao et al., 1995; Kuschel et al., 1999; Chen-Izu et al., 2000). Nevertheless, β_2-adrenergic receptors have been shown to co-localise with a subpopulation of $Ca_V1.2$ channels at the sarcolemma surface (Balijepalli et al., 2006), where it appears to be more functionally present (100 more *vs* t-tubules) (Cros and Brette, 2013). Collectively these observations suggest a very localised β_2-adrenergic receptor-mediated PKA activation specifically near $Ca_V1.2$, thereby regulating local I_{CaL}, in contrast to β_1-adrenergic receptor stimulation which appears to activate PKA more globally.

In the normal heart, sympathetic stimulation shortens the action potential and increases cardiac output. The combined phosphorylation of $Ca_V1.2$ and RyR2, rapidly increases I_{Ca} and $[Ca^{2+}]_i$ thereby, accelerating contractility, which is characterised as a positive inotropic effect. The positive lusitropic effect of β-adrenergic receptor stimulus is mediated by the increased sarcoplasmic reticulum Ca^{2+} reuptake due to phosphorylation of phospholamban primarily and the increased Ca^{2+} insensitivity of filaments due to troponin I phosphorylation, resulting in accelerated cardiac relaxation (Bers, 2002; Sigg and Hezi-Yamit, 2009). Continuous

catecholamine stimulation of β-adrenergic receptor induces severe myocardial damages, including cardiac hypertrophy and apoptosis and has been implicated in heart failure and sudden death (Bogoyevitch et al., 1996; Communal et al., 1998; Antos et al., 2001; Marks, 2001).

1.4 Serine/ threonine phosphatases

Reversible protein phosphorylation, principally on serine or threonine residues, is a ubiquitous post-translational protein modification that is central to the regulation of most cellular functions and signal transduction pathways, by altering protein activity and/ or subcellular localisation (Virshup and Shenolikar, 2009). This mechanism (Figure 1.6) is strictly controlled by the opposing activities of protein kinases and protein phosphatases (Berg et al., 2015).

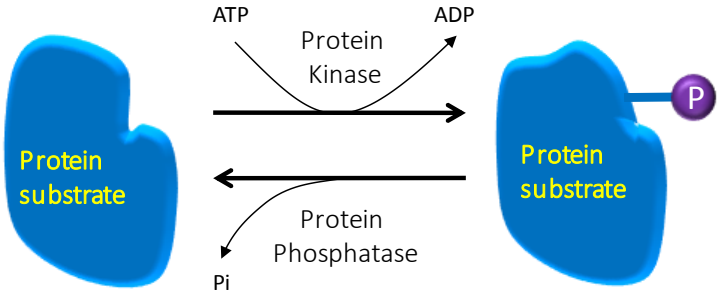

Figure 1.6 A simplistic model of reversible protein phosphorylation. Phosphorylation is a post-translation protein modification in which a phosphate from adenosine triphosphate (ATP) is covalently attached to the hydroxyl residues in the side chain of the amino acids tyrosine, serine, or threonine by a kinase protein, thereby, altering the conformation, activity and/ or subcellular localisation of the protein. Reversible phosphorylation (also known as dephosphorylation) is accomplished by protein phosphatases, which catalyse the hydrolytic removal of the phosphate group attached to the protein and release inorganic phosphate (Pi) into the cytosolic environment. ATP: adenosine triphosphate; ADP: adenosine diphosphate; P: phosphate group, Pi: inorganic phosphate.

In humans, approximately 98% of protein phosphorylation events occur at serine/ threonine residues (Olsen et al., 2006). Currently, more than 400 protein serine/ threonine-specific kinases (PSKs), are thought to be encoded in the human genome

(Anderson et al., 2006; Shi, 2009). Nevertheless, there are only approximately 30 protein serine/ threonine-specific phosphatases (PSPs) (Cohen, 2004; Shi, 2009). PSPs are classified into three major families, based on signature sequence motifs on their catalytic subunit and biochemical properties: i) phosphoprotein phosphatases (PPPs), such as PP1, PP2A, PP4, PP6, PP2B, PP5, and PP7, ii) metal-dependent protein phosphatases (PPMs), such as PP2C and iii) the aspartate-based phosphatases represented by FCP/ SCP (TFIIF- associating component of RNA polymerase II CTD phosphatase/ small CTD phosphatase) (Shi, 2009). Even though much fewer PSPs (30) are encoded, compared to the number of PSKs (428), the assembly of several PPP family members to holoenzymes, using a shared catalytic subunit and a large number of regulatory subunits, results in a great diversity (Janssens and Goris, 2001; Cohen, 2002; Shi, 2009; Virshup and Shenolikar, 2009). Serine/ threonine protein phosphatases (predominantly PP1, PP2A) have been shown to regulate a broad array of cardiac proteins involved in Ca^{2+} handling and hypertrophy (review by: Heijman et al., 2013; Weber et al., 2015).

1.5 Type 2A protein phosphatase family in the heart

Interestingly, PP1 and PP2A contribute to approximately 90% of protein phosphatase activity in the heart (MacDougall et al., 1991; Lüss et al., 2000; Virshup and Shenolikar, 2009). PP2A is an abundant and highly conserved evolutionary PPP (Shi, 2009; Virshup and Shenolikar, 2009; Lillo et al., 2014). Its catalytic subunit (PP2AC) is estimated to represent 0.1-1% of total cellular protein in some tissues (Shi, 2009; Virshup and Shenolikar, 2009). This thesis is focused on the serine/ threonine type 2A protein phosphatase family of the PPPs, which includes PP2A, PP4 and PP6 (Cohen et al., 1990; Shi, 2009; Virshup and Shenolikar, 2009; Lillo et al., 2014) and their role and regulation in cardiac pathophysiology.

PP2A, PP4 and PP6 catalytic subunits (PP2AC, PP4C and PP6C, respectively) share approximately 60-65% amino acid identity in humans (Kloeker et al., 2003) and are highly conserved among eukaryotic species (approximately 80%) (Cohen et al., 1990; Brautigan, 2013; Lillo et al., 2014). Crystallographic data suggest that their catalytic subunit is highly conserved and bind to two metal ions Mn^{2+} and Fe^{3+}, which are thought to play a catalytic role through the activation of a water molecule for the dephosphorylation reaction (Cho and Xu, 2007; Shi, 2009). PP2AC, PP4C and PP6C C-terminals share a region of three 100% conserved residues (YFL) (Favre et al., 1994; Hwang et al., 2016) and a group of conserved residues at their N-terminal fragment, shown to regulate binding of PP2AC with alpha4 (Jiang et al., 2013b), the common regulator of type 2A PP family catalytic subunits (Nanahoshi et al., 1999; Kong et al., 2009; LeNoue-Newton et al., 2016). Furthermore, PP2AC, PP4C and PP6C have also been characterised by a sensitivity to enzymatic inhibition by okadaic acid and other natural toxins (Brewis et al., 1993; Hastie and Cohen, 1998; Prickett and Brautigan, 2006).

1.5.1 PP2A holoenzyme assembly and activity

1.5.1.1 PP2A holoenzyme assembly

The functional PP2A holoenzyme exists as a heterotrimeric complex, containing a core dimer (a ~36 kDa catalytic (C) subunit and a ~65 kDa scaffold (A) subunit) bound to a regulatory (B) subunit (review by Janssens and Goris, 2001). However, the C subunit can also exist in a complex with the A subunit, forming the core dimer AC, or in association with alpha4 protein (Kremmer et al., 1997; Murata et al., 1997; review by Janssens and Goris, 2001; Jiang et al., 2013). As it can be seen in figure 1.7, the core dimer formation precedes the recruitment of a regulatory B-subunit (Xu et al., 2006). The A and C subunits exist in two forms, PP2AAα or PP2Aaβ and

PP2ACα or PP2ACβ (see section 3.1.1 for gene transcription), respectively, which are expressed in varying degrees (Green et al., 1987; Arino et al., 1988; Hemmings et al., 1990; DeGrande et al., 2013). The B subunit exists in variable isoforms which are subdivided into 4 distinct gene families, B, B', B'' and B''', encoding 13 different regulatory proteins, from which only 12 were found to be transcribed in the heart (except PP2R2C) (review by Janssens and Goris, 2001; DeGrande et al., 2013). The recruitment of these B subunits is regulated, at least in part, by post-translational modifications of the catalytic subunit (see section 1.5.4) (review by Sents et al., 2013). Thus, numerous PP2A heterotrimeric holoenzymes can be formed with distinct substrate specificity, activity and subcellular localisation (review by Janssens and Goris, 2001; Zwaenepoel et al., 2008; DeGrande et al., 2013).

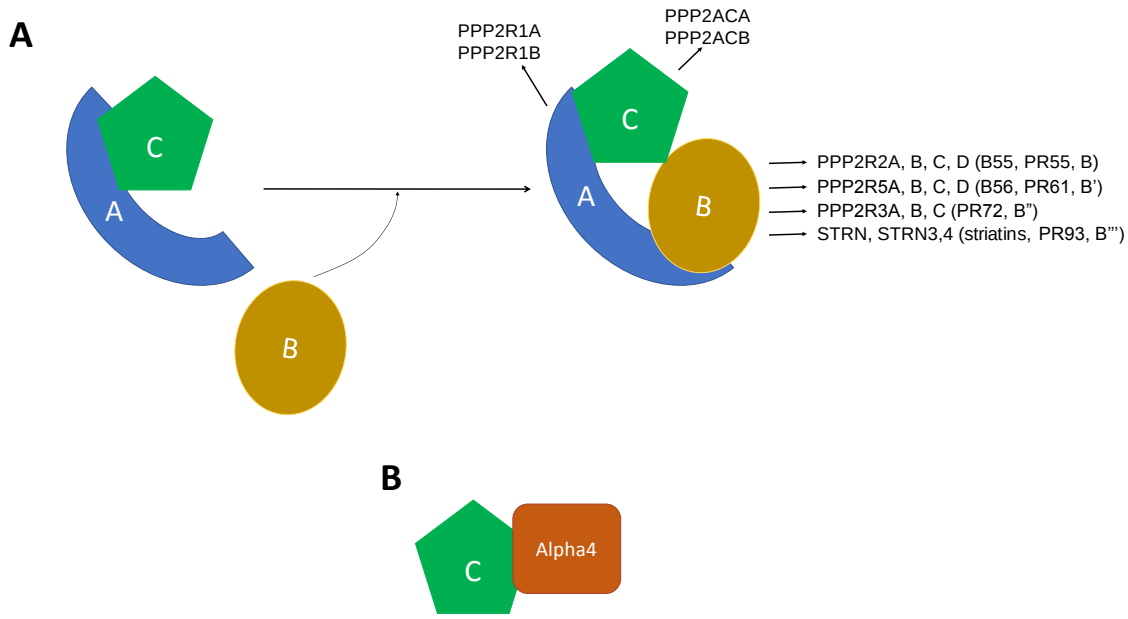

Figure 1.7 Schematic illustration of the PP2A holoenzyme and non-canonical PP2AC-alpha4 complex (adapted from Sents et al., 2013). (**A**) The core enzyme is comprised of the scaffold (A) and catalytic (C) forming a dimer (AC). A third regulatory B (B, B', B'' or B''') subunit can be associated with the AC dimmer. (**B**) Non-canonical PP2AC-alpha4 complex, where alpha4 can bind other potential substrates (i.e. Mid1).

1.5.1.2 PP2AC activity in cardiomyocytes

The diversity of PP2A holoenzyme formation and distinct substrate targeting, have

defined PP2A as a master regulator of major cellular processes, including cell growth, DNA damage repair and apoptosis (McConnell et al., 2007; Kong et al., 2009; review by Wlodarchak and Xing, 2016). In cardiomyocytes, PP2A activity is associated with multiple proteins involved in membrane excitability, excitation-contraction coupling and hypertrophic signalling. PP2AC has been shown to downregulate the activity of Na^+ channel $Na_V1.5$ (Baba et al., 2004), $Ca_V1.2$ via the recruitment of B56 or PR59 subunits (Gao et al., 1997; Hulme et al., 2006a; Xu et al., 2010; Shi et al., 2012), and the ryanodine receptor (RyR2) via the recruitment of B56α or B56δ isoform (Terentyev et al., 2009; Belevych et al., 2011). It has also been suggested to dephosphorylate troponin I (Jideama et al., 2006), connexin 43 (Ai et al., 2011), phospholamban and protein phosphatase inhibitor-1 protein (El-Armouche et al., 2006a). A limitation of many of these studies is the use of common phosphatase inhibitors, which as described in Chapter 4 (section 4.5.1) may also affect other members of the PPP family.

1.5.2 PP4 holoenzyme assembly and activity

PP4 is the eukaryotic homologue of yeast Pph3p (Brewis and Cohen, 1992; Brautigan, 2013). The active PP4 holoenzyme (Figure 1.8) exists as a heterodimer (low activity) consisting of the catalytic subunit (PP4C) and a regulatory subunit (R1, R2 or R4) or as a heterotrimer formed by PP4C and any two regulatory subunits (R1, R2, R3 (isoforms PP4R3α or PP4R3β)), except for R4, which does not bridge with the rest regulatory subunits (Kloeker and Wadzinski, 1999; Hastie et al., 2000; Chen et al., 2008a). Furthermore, PP4C has been shown to interact directly with alpha4 protein (Gingras et al., 2005; Kong et al., 2009; LeNoue-Newton et al., 2016). There is no information in the existing literature about the function of PP4 towards cardiac proteins. A known function of PP4 is the activation of the two transcription factors c-Rel and NF-κB (Hu et al., 1998). In addition, the PP4C/R2/R3

heterotrimeric is suggested to promote cisplatin resistance in mammalian cells (Gingras et al., 2005; Hastie et al., 2006). PP4 has been found to localise to the centrosome in mammalian cells (Brewis et al., 1993) is thought to regulate centrosome maturation and meiosis, as shown in *C. elegans* (Helps et al., 1998; Sumiyoshi et al., 2002). PP4 has also been shown to coordinate DNA damage repair in the non-homologous end-joining repair process of DNA double-strand breaks and cell cycle checkpoints (Gingras et al., 2005; Liu et al., 2012; Shaltiel et al., 2014). Recent studies have provided evidence for post-translational modification of PP4C, which may affect the recruitment of the regulatory subunits (section 1.5.4.4) (Lee and Lee, 2014; Hwang et al., 2016).

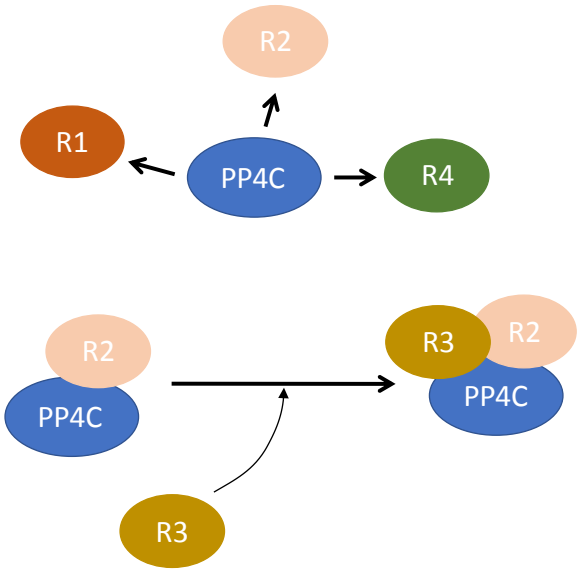

Figure 1.8 Schematic illustration of PP4 holoenzyme assembly. PP4 functional holoenzyme is thought to be formed by the interaction of PP4C with either R1, R2 orR4 subunit creating a dimer, or a trimer with the association of PP4C and any tow of the regulatory subunits.

1.5.3 PP6C holoenzyme assembly and activity

The PP6C subunit is a homologue of the budding yeast sit4p (Arndt et al., 1989). Functional mammalian protein PP6 is thought to form an active heterotrimeric holoenzyme (Figure 1.9) with the catalytic subunit (PP6C), a Sit4-associated protein (SAP) domain subunit (SAP1-3) and an ankyrin repeat domain subunit (ANKRD28,

44 or 52) (Luke et al., 1996; Stefansson and Brautigan, 2006; Stefansson et al., 2008; Guergnon et al., 2009). Similar to PP4C, there is no information in the existing literature about the role of PP6 in cardiomyocytes. Overall, studies suggest that SAP1 facilitates PP6C-mediated dephosphorylation and activation of DNA-PK (Mi et al., 2009; Douglas et al., 2010; Hosing et al., 2012), which in turn phosphorylates H2AX at Ser139 (Andegeko et al., 2001; Falck et al., 2005). Phosphorylated H2AX (γH2AX) is required for the process of DNA double-strand break by non-homologous end-joining (Bassing et al., 2002; Meador et al., 2008; Shrivastav et al., 2008b; Shrivastav et al., 2008a). Recent evidence suggests that SAP1-3 proteins play a role in cell cycle related to mTORC1 inhibition in mammalian cells, a mechanism that appears to be homologues in the yeast (SAP2, SAP3) (Morales-Johansson et al., 2009; Wengrod et al., 2015). SAP2 and SAP3 have been implicated in homology-directed repair of DNA in cancer tissue (Zhong et al., 2011). The reported functionality of the ANKRD proteins is limited to ANKRD28 protein. PP6C:SAP1:ANKRD28 holoenzyme is thought to be involved in regulating the inhibitory subunit of nuclear factor kappa B epsilon degradation in response to tumour necrosis factor α (Stefansson and Brautigan, 2006). More recently ANKRD28 was found to interact with the tumour suppressor breast cancer protein 1 (Vincent et al., 2016).

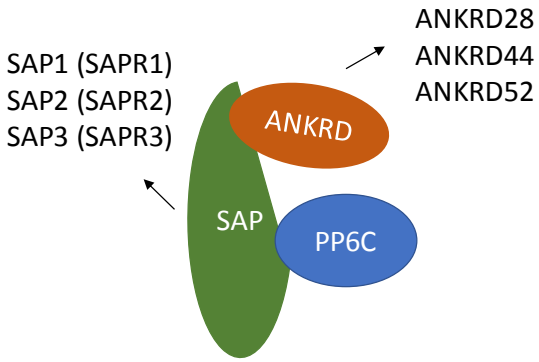

Figure 1.9 Schematic illustration of PP6 holoenzyme. The functional trimeric holoenzyme is formed by the PP6C, SAP and ANKRD subunits.

1.5.4 Type 2A protein phosphatase catalytic subunit post-translational modification

The majority of post-translational modifications have been characterised on PP2AC. The C-terminal conserved tail (^{304}TPDYFL^{309}) of PP2AC undergoes two forms of post-translational modifications, which affect PP2A activity and/ or holoenzyme assembly: i) threonine 304 (Thr304) or tyrosine 307 (Tyr307) phosphorylation (Chen et al., 1992; Longin et al., 2007), and ii) leucine 309 (Leu309) carboxymethylation (Favre et al., 1994; Lee et al., 1996). In addition, PP2AC has been shown to be subjected to ubiquitination and proteasome-mediated degradation (Trockenbacher et al., 2001; McConnell et al., 2010; Watkins et al., 2012; Udeshi et al., 2013; Xu et al., 2014).

1.5.4.1 PP2AC phosphorylation at Thr304 and Tyr307

PP2AC is subjected to phosphorylation at Thr304 and/ or Tyr307 which has been reported to reduce PP2AC activity (Chen et al., 1992; Longin et al., 2007; Schmitz et al., 2010). Thr304 phosphorylation is thought to selectively inhibit holoenzyme assembly with the PR55/B subfamily, whereas Tyr307 phosphorylation is thought to affect interaction with the PR61 (B′) subunits. In addition, PP2AC has shown the ability of autodephosphorylation (review by Janssens and Goris, 2001).

1.5.4.2 PP2AC carboxylmethylation at Leu309

PP2AC carboxylmethylation at Leu309 by leucine carboxylmethyltransferase-1 increases its activity and holoenzyme assembly by facilitating the association of PP2AC with the subfamily regulatory subunits (Favre et al., 1994; Lee et al., 1996; review by Janssens and Goris, 2001; Xu et al., 2006; Longin et al., 2007; DeGrande et al., 2013). For example, PP2AC-Leu309 carboxylmethylation is required for the recruitment of PR55/B (review by Janssens and Goris, 2001; DeGrande et al., 2013).

This modification is reversed by the protein phosphatase methylesterase-1 (Ogris et al., 1999; Longin et al., 2007; review by Sents et al., 2013). Leucine carboxylmethyltransferase-1 appears to interact only with active PP2A holoenzymes and convert them into substrate-specific holoenzymes (Stanevich et al., 2011). Furthermore, in a recent study, PP2AC carboxylmethylation was proposed to alter the subcellular distribution of PP2AC in cardiomyocytes in response to G_iPCR stimulation (Longman et al., 2014).

1.5.4.3 PP2AC ubiquitination

The process of ubiquitination requires the synergy of three enzymes, called E1 (Ub-activating enzymes), E2 (Ub-conjugating enzymes) and E3 (Ub ligases), that work sequentially in a cascade resulting in the attachment of an ubiquitin (Ub) molecule, which is a highly conserved small protein, to a lysine residue of a target protein (monoubiquitination) (Figure 1.10) (Hershko et al., 1983). Moreover, Ub can be attached to more than one lysine residue of the same protein substrate (multiubiquitination) and/ or can be targeted for ubiquitination itself via repeated ubiquitination cycles, since it contains lysine residues (Lys6, Lys11, Lys27, Lys29, Lys33, Lys48, and Lys63), leading to the formation of an Ub chain (polyubiquitination) (Chau et al., 1989; Nguyen et al., 2014). The process of ubiquitination can be reversed by a group of enzymes called deubiquitinases (Nguyen et al., 2014). Depending on the type of ubiquitination, proteins can be targeted for degradation by the proteasome 26S (Hershko et al., 1983; Chau et al., 1989; Nguyen et al., 2014), an ATP-dependent protease complex (Hough et al., 1986; Eytan et al., 1989b; da Fonseca et al., 2012). It was thought that mono- and multi-ubiquitinated proteins, which are usually involved in many cellular processes such as DNA repair and gene expression, are less preferred by the 26S proteasome-

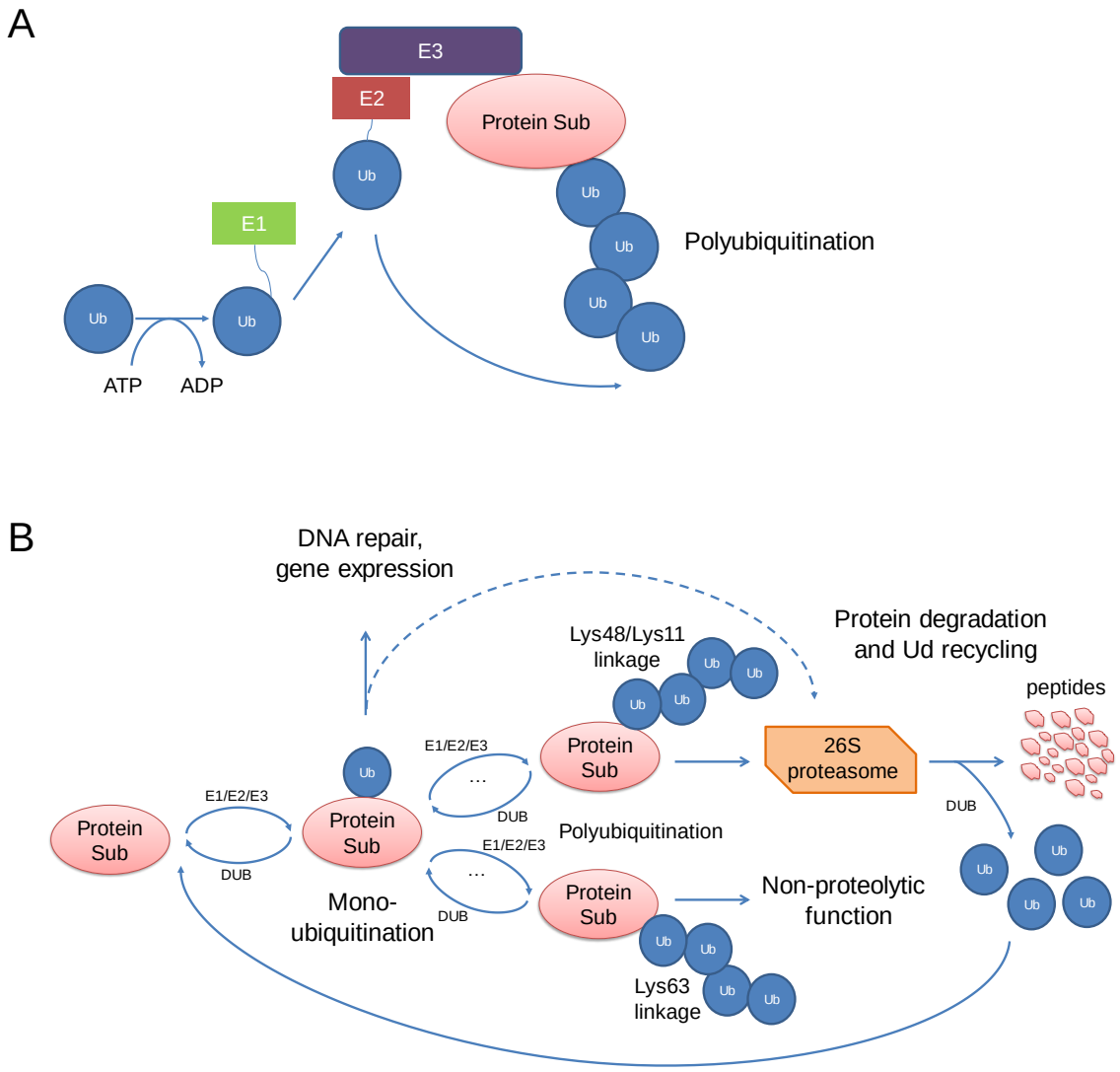

Figure 1.10 Simplified schematic representation of the ubiquitin-proteasome-mediated system (UPS) (inspired by Nguyen et al., 2014). (**A**) Enzymatic cascade during mono- and poly-ubiquitination. First, the Ub molecule is attached by a thioester bond to a cysteine of the E1 enzyme in an adenosine-5'-triphosphate (ATP)-dependent manner and the Ub molecule is then delivered to the active site cysteine of the E2 enzyme. The E3 enzyme then binds both the E2 enzyme carrying the Ub molecule and the target protein substrate to transfer the Ub molecule onto the amino group of a lysine amino acid to generate an isopeptide bond, resulting in protein substrate ubiquitination. This process may result in monoubiquitination (one Ub attached to the protein), multiubiquitination (Ub molecules are attached to multiple lysine residues on protein), or polyubiquitination (Ub is attached on the lysine of another Ub, therefore, creating Ub-linked chain on the lysine residue of the targeted protein. (**B**) Determination of the fate of the protein substrate depends on the type of ubiquitination and type of the substrate-conjugated polyubiquitin chain. E1: ubiquitin-activating enzyme, E2: ubiquitin-conjugating enzyme, E3: ubiquitin ligase, DUB: deubiquitinating enzymes, Ub: ubiquitin, Sub: substrate, Lys: Lysine, ATP: adenosine-5'-triphosphate.

mediated degradation mechanism than polyubiquitinated proteins (Thrower et al., 2000; Hoege et al., 2002; Minsky et al., 2008). Nevertheless, a recent study showed that mammalian protein substrates following mono- or poly-ubiquitination were degraded by proteasome 26S with a similar frequency in human cells (Braten et al., 2016). Proteins which are conjugated with polyUb chains, formed by linked Ub molecules through the Ub Lys48 or Lys11 residues (at least four ubiquitin molecules), are known to be recognised by the 26S proteasome (Figure 3.1B) (Chau et al., 1989; Deng et al., 2000; Thrower et al., 2000; Jin et al., 2008; Nathan et al., 2013). On the other hand, protein polyubiquitination, where the attached polyUb chain is formed by linked Ub molecules through the Ub Lys63 residue is involved in non-proteolytic processes such as kinase activation and DNA repair (Deng et al., 2000; Thrower et al., 2000; Hoege et al., 2002; Jin et al., 2008; Nathan et al., 2013). The role of other lysine polyUb topologies is not yet well understood. Once the protein substrate is bound to the 26S proteasome, the Ub molecules are released from the protein substrate by the activity of a deubiquitinating enzyme, allowing Ub recycling (Komander et al., 2009).

Many studies have demonstrated that PP2AC is subjected to ubiquitination and proteasome-mediated degradation (Trockenbacher et al., 2001; McConnell et al., 2010; Watkins et al., 2012; Udeshi et al., 2013; Xu et al., 2014). In addition, in a recent proteomic study, it was shown that both PP2A catalytic subunits (PP2ACα and PP2ACβ) contain lysine residues, that can be targeted for ubiquitination (Udeshi et al., 2013). Thus, ubiquitination can affect the biogenesis of PP2A holoenzymes. Ubiquitination of PP2AC has been shown to be achieved mainly by two ligase E3 enzymes: i) E3 ligase Mid1 interacting with alpha4 and PP2AC and ii) Cullin3 (Trockenbacher et al., 2001; McConnell et al., 2010; Watkins et al., 2012; Udeshi et al., 2013; Xu et al., 2014). Interestingly, even though alpha4 recruits Mid1 E3

ligase, its interaction with PP2AC has been shown to either i) promote (Trockenbacher et al., 2001; Watkins et al., 2012) or ii) prevent the ubiquitin-mediated degradation of PP2AC, via either the binding of PP2AC with the alpha4 ubiquitin-interacting motif or by the monoubiquitination of alpha4 itself within its C-terminal domain, which may weaken the association of Mid1 with the E2 ubiquitin conjugating enzyme (Kong et al., 2009; McConnell et al., 2010; LeNoue-Newton et al., 2011; Jiang et al., 2013a; review by Sents et al., 2013).

1.5.4.4 PP4C and PP6C carboxymethylation

Recent studies support a similar mechanism for PP4C and PP6C. Leucine carboxylmethyltransferase-1-mediated carboxylmethylation of PP4C-Leu307 was suggested to facilitate either PP4C:R1, PP4C:R2 or PP4C:R3 complex formation (Lee and Lee, 2014; Hwang et al., 2016). While evidence has shown that PP6C is methylated on its C-terminal, the position is not confirmed yet (Kloeker et al., 1997; Lee and Lee, 2014; Hwang et al., 2016).

1.5.5 Association of type 2A protein phosphatases and the alpha4 regulatory protein

Alpha4 is the homolog of yeast Tap42 protein (Di Como and Arndt, 1996; Onda et al., 1997). It was first identified as an immunoglobulin binding protein (IGBP1) in B cells (Inui et al., 1995). In yeast, Tap42 is involved in the target of rapamycin (TOR) pathway that links nutrient and energy availability to cell growth (Di Como and Arndt, 1996; Jiang and Broach, 1999).

Alpha4 protein can interact directly with the catalytic subunit of PP2A, PP4 and PP6, making it a common regulator of the type 2A family phosphatases (Nanahoshi et al., 1999; Kloeker et al., 2003; Hwang et al., 2016; LeNoue-Newton et al., 2016). Deletion of alpha4 protein has been shown to lead to progressive loss of all PP2A,

PP4, and PP6 catalytic subunits and phosphatase complexes and apoptosis (Kong et al., 2009; LeNoue-Newton et al., 2016). Hence, alpha4 plays an important role in the stability of the type 2A protein phosphatase catalytic subunits and biogenesis of their holoenzymes (review by Sents et al., 2013).

Overall, it has been proposed, that alpha4 binding with the PP2AC, i) serves a critical role in protection of PP2AC from proteasome-mediated degradation (Kong et al., 2009; McConnell et al., 2010; LeNoue-Newton et al., 2011; Jiang et al., 2013a), however, evidence shows that this interaction may also ii) enhance proteasome-mediated degradation of the catalytic subunits (Trockenbacher et al., 2001; Watkins et al., 2012; McDonald et al., 2014), or iii) either inhibit their activity or altering their specificity towards target substrates (Nanahoshi et al., 1999; Jacinto et al., 2001; Prickett and Brautigan, 2006; Kong et al., 2009).

1.5.6 Type 2A protein phosphatase family in heart disease

From the type 2A protein phosphatase family, only PP2A has been characterised and studied in the heart, except for some initial reports related to the expression of PP4C or PP6C in heart and other tissues (Brewis et al., 1993; Bastians and Ponstingl, 1996; Kloeker et al., 2003). In patients with atrial fibrillation, fibrosis and heart failure, both overexpression and downregulation of PP2AC has been reported, which was associated with altered Ca^{2+}- and Na^{+}- handling in cardiomyocytes (Jelicks and Siri, 1995; Marx et al., 2000b; Pieske et al., 2002; Baartscheer et al., 2003; Despa et al., 2008; El-Armouche et al., 2011; DeGrande et al., 2013). Studies in animal models, investigating the consequences of either the overexpression or deletion of PP2ACα in the heart, demonstrated impaired cardiac function and development of hypertrophy or heart failure (Gergs et al., 2004; Li et al., 2016). These studies collectively, many of which are discussed in depth in sections 5.5 and 6.5, highlight the importance of phosphatase activity regulation in heart disease.

1.6 Dissertation focus

Given the importance of PP2A in cardiac pathophysiology and the lack of knowledge about the type 2A protein phosphatase role and regulation in the heart, this thesis aims to investigate: i) the expression of the PP2AC (PP2ACα and PP2ACβ), PP4C, PP6C in cardiomyocytes, ii) their expression and aspects of their regulation in pathological LV hypertrophy and iii) the possible roles of individual members of the type 2A protein phosphatase family and alpha4 signalling axis in the regulation of either calcium handling or DNA repair in cardiomyocytes.

Chapter 2

General Methods

This chapter covers methods which are relevant to more than one chapter in this thesis. Methods which are specific to a chapter are described in the relevant "Specific methods" section of that chapter.

2.1 Animal tissue

Animal tissue used in this study was obtained in accordance with the UK Home Office Guidance on the Operation of the Animals (Scientific Procedures) Act 1986 (UK), the Directive of the European Parliament (2010/63/EU), and received approval by the local ethics review board at King's College London. All protocols were performed by home office licensed individuals.

2.2 Cell culture

All solutions, glassware and plasticware for *in vitro* cell culture were pre-sterilised or sterilised by autoclaving for 15 min at 121^{o}C and 1.2 atm. Heat-sensitive solutions were sterilised by filtration through 0.2-μm sterile syringe filters (Corning Inc., USA). Mammalian cell culture work was performed in a laminar air-flow hood (Thermo Fisher Scientific, USA), decontaminated with 70% (v/v) industrial methylated spirit (IMS) prior to and after use. The surface of all materials was wiped by 70% (v/v) industrial methylated spirit before entering the laminar air-flow hood.

Cell cultures were maintained at 37°C in a humidified incubator (Thermo Fisher Scientific) in an atmosphere of 5% CO_2 and 95% air.

2.2.1 Culturing of H9c2 cardiomyocytes

The embryonic rat cardiomyocyte-derived H9c2 cell line was obtained from the American Type Culture Collection (#CRL-1446; ATCC, UK). H9c2 cardiomyocytes were cultured in Gibco™ Dulbecco's modified Eagle's medium (DMEM) supplemented with 10% (v/v) Gibco™ heat-inactivated Fetal Bovine Serum (FBS) from Thermo Fisher Scientific, 100 IU/ml penicillin and 100 µg/ml streptomycin (Sigma-Aldrich, USA). This is referred to as complete culture medium. Complete culture medium was further filtered through 0.2-µm filter units (Thermo Fisher Scientific) and stored at 4^{o}C until required. Cells were grown in cell culture treated 75 cm^2 flasks, 6-well or 96-well plates at 37°C in a humidified atmosphere of 5% CO_2 and 95% air. The culture medium was renewed every 2 to 3 days according to the manufacturer's instructions.

H9c2 cardiomyocytes were passaged upon reaching 80% confluency (Figure 2.1C). The medium was removed, and the cells were trypsinised in 5 ml of 0.25% (w/v) Trypsin - 0.53 mM EDTA (Fisher Scientific) for 1-3 minutes at 37^{o}C. The disrupted cell layer was observed through a Motic® AE31 Elite inverted microscope (Ted Pella Inc., USA) every minute. The cell suspension was gently aspirated by pipetting and mixed with 10 ml of complete culture medium in a 50-ml falcon tube to inactivate trypsin. Cells were centrifuged at 150 *g* for 3 minutes at room temperature. The supernatant was removed, and the pellet was gently resuspended into 10 ml of complete culture medium. Cell clumps were dispersed by gently passing the cell suspension once through a 10-ml syringe with an attached 25-gauge needle (0.5 mm diameter). Cells were subcultured into new 75 cm^2 flasks or culture

plates, in a subcultivation ratio of 1:10, unless otherwise was stated. Cells were allowed to settle at least 24 hours prior to any treatment at 37°C in 5% CO_2 and 95% air. Cultured H9c2 cardiomyocytes between passage numbers 4 to 12 were used for experiments, starting from the purchased batch. A new culture was established from frozen stocks every two to three months.

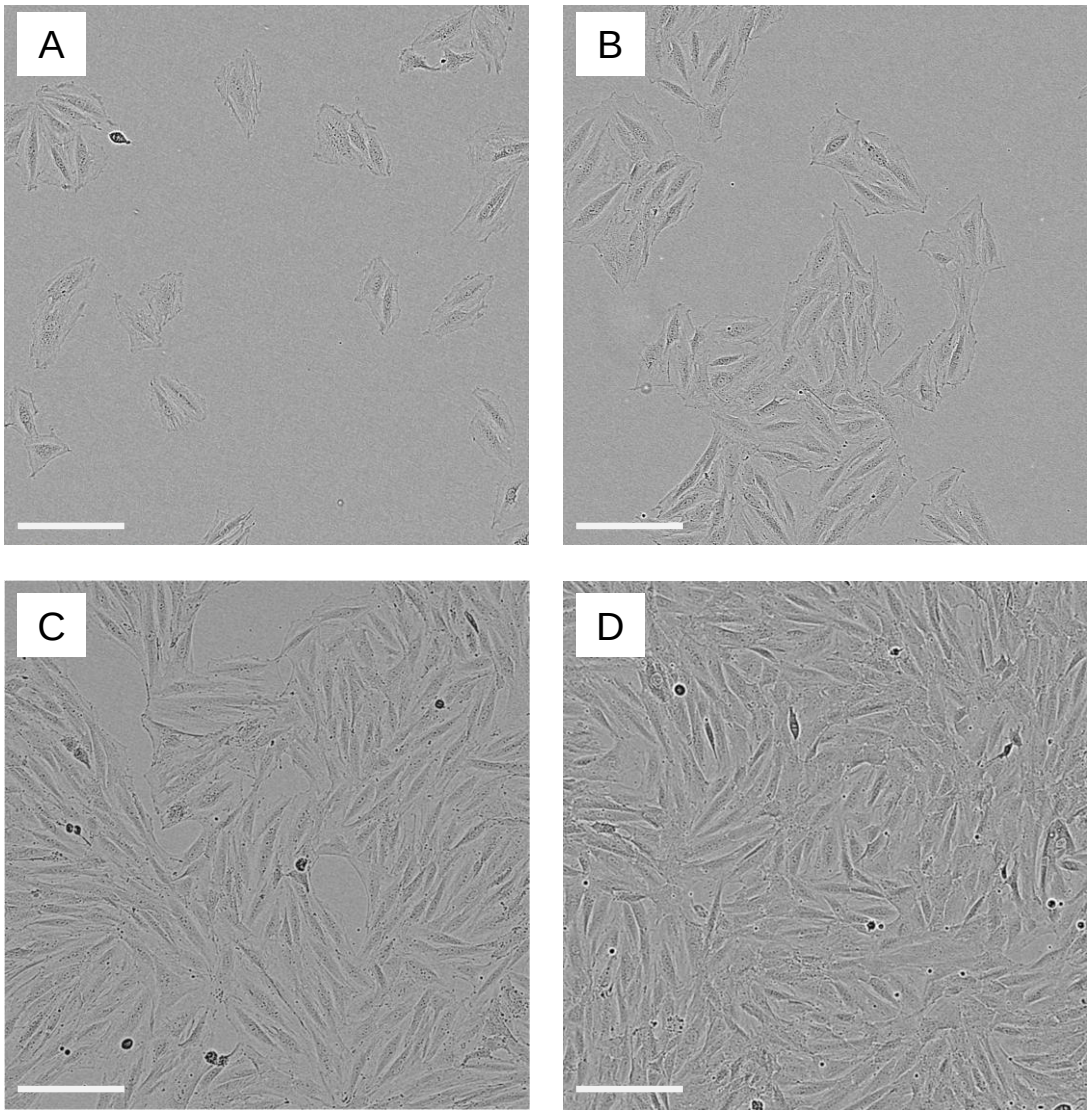

Figure 2.1 Images of H9c2 cardiomyocytes by IncuCyte® ZOOM System (Essen BioScience, USA) with 15%, 30%, 80% and 100% confluency after 1, 3, 6 or 7 days in culture. Scale bars, 200 µm.

2.2.1.2 Cryopreservation and recovery of H9c2 cardiomyocytes

H9c2 cardiomyocytes were grown in 75 cm^2 flasks until 80% confluency was achieved. Cells were trypsinised as described above and resuspended in complete culture medium. The cell number was counted by trypan blue exclusion assay (section 2.2.3), and the cell suspension was centrifuged at 150 *g* for 3 minutes at room temperature. The supernatant was removed, and the cell pellet was resuspended in an appropriate volume of cryopreservation medium (complete culture medium supplemented with sterile-filtered 5% (v/v) DMSO (Sigma-Aldrich)) at a cell density of $1x10^6$ cells/ ml. The cell suspension in cryopreservation medium was transferred to 1.5-2.0-ml cryovials and then placed into a cryo-freezing container (NALGENE, USA) filled with 100% isopropanol. The cryo-freezing container, containing the cryovials, was cooled in a -80°C freezer, allowing the control of cooling rate at 1°C per minute. After a minimum of 4 hours to ensure that a stable temperature has been reached, the cryovials containing the frozen cells were stored in the vapour phase of a liquid nitrogen container.

To recover stocks of H9c2 cardiomyocytes cryopreserved in liquid nitrogen, the cryovials containing the frozen cells were quickly taken out and thawed rapidly by gentle agitation in a 37°C water bath (1-2 minutes). Once the cell suspension was thawed completely, it was transferred to a 75 cm^2 flask containing 10 ml of pre-warmed complete culture medium. The cells were allowed to settle overnight at 37°C, in 5% CO_2, 95% air and the medium was renewed to remove any traces of DMSO.

2.2.2 Isolation of adult rat ventricular myocytes (ARVMs)

Adult rat ventricular myocytes (ARVM) were isolated from the hearts of 200-250 g

Wistar adult male rats (B & K Universal Ltd, UK) by Dr Shiney Reji[3], using a collagenase-based enzymatic digestion technique (Snabaitis et al., 2005).

Rats were anaesthetised by an intraperitoneal injection of 50 mg/kg sodium pentobarbitone (Sagatal, Rhone Merieux, Ireland), followed by an intraperitoneal injection of 150 IU heparin (Leo Laboratories Ltd, Ireland) to prevent blood clot formation in the excised heart. Unconsciousness was confirmed by the loss of pedal reflex, and the chest cavity was opened by cutting around the rib cage and through the diaphragm. The heart was rapidly excised with an adequate length of aorta and pulmonary trunk intact and soaked in ice-cold modified Krebs solution (Solution A; 130 mM NaCl, 0.4 mM NaH_2PO_4, 1.4 mM MgCl, 0.75 mM $CaCl_2$, 4.2 mM HEPES, 220 mM taurine, 4.5 mM KCl, 10 mM creatine and 10 mM glucose, pH 7.3). Excess tissue was removed, and a blunt stainless-steel cannula was placed into the aorta as quickly as possible and tied with a 4/0 surgical silk suture (Johnson and Johnson, USA). The heart was then immediately mounted on the Langendorff Perfusion system and was perfused for 5 min with modified Krebs solution Solution A at 37ºC to remove any residual vascular blood, followed by perfusion with calcium-free solution A containing 100 µM EGTA for 4 min. The heart was then perfused for 8 min with solution A containing 100 µM $CaCl_2$ and 1 mg/ml collagenase (Type II; Worthington Biochemical Corporation, USA). The ventricles were then cut into small pieces to increase the surface area for collagenase digestion and incubated in 10 ml of collagenase solution (gassed with 100 % O_2, 37 ºC) for a further 10 minutes. The tissue was gently triturated for less than 2 minutes, using a 2-ml plastic dropping pipette to facilitate cell dispersion, until a uniform suspension was obtained. This mixture was then filtered through a nylon mesh (mesh size 200 µm) to separate isolated ARVMs from the undigested ventricular tissue. The suspension

[3]Cardiovascular Division, King's College London, The Rayne Institute, St. Thomas' Hospital, London, United Kingdom.

was left to settle for 8-10 minutes allowing the cardiac myocytes to sediment into a loose pellet. The supernatant was removed, and the pellet was resuspended in solution A containing 500 µM $CaCl_2$ and 1% (w/v) bovine serum albumin (BSA). ARVMs were then left to sediment and form a loose pellet for a further 8-10 minutes. The supernatant was removed, and the pellet was resuspended in solution A containing 1 mM $CaCl_2$. ARVMs were left to settle at room temperature for 2 hours prior to use in experiments.

2.2.2.1 Culturing of ARVM

Culture plates (6-well) were coated with laminin by placing 1.5 ml of 15 µg/ml laminin (Sigma-Aldrich) solution in each well for 2 hours at 37^{o}C under sterile conditions and then rinsed once with modified M199 medium supplemented with 10% (v/v) heat-inactivated FBS, 100 I.U./ml penicillin, 100 µg/ml streptomycin, 2 mM creatine, 2 mM carnitine and 5 mM taurine (obtained from Sigma-Aldrich), prior to use (Snabaitis et al., 2005). This is referred to as M199 supplemented medium.

Freshly isolated ARVM (section 2.2.2) were allowed to settle for 2 hours at room temperature and form a loose pellet by sedimentation due to gravity. The ARVM were briefly centrifuged at 50 *g*, and the storage solution was removed. ARVMs were resuspended in M199 supplemented medium, and following cell counting (section 2.2.3), ARVMs were seeded at 200,000 cells per well into 6-well laminin coated cell culture plates (see above). ARVMs were allowed to adhere for 2 hours at 37^{o}C, in 5% CO_2, 95% air (Figure 2.2). The culture medium was then replaced with fresh M199 supplemented medium, prior to any treatment. The cultures were maintained for 24 to 48 hours at 37^{o}C, in 5% CO_2, 95% air.

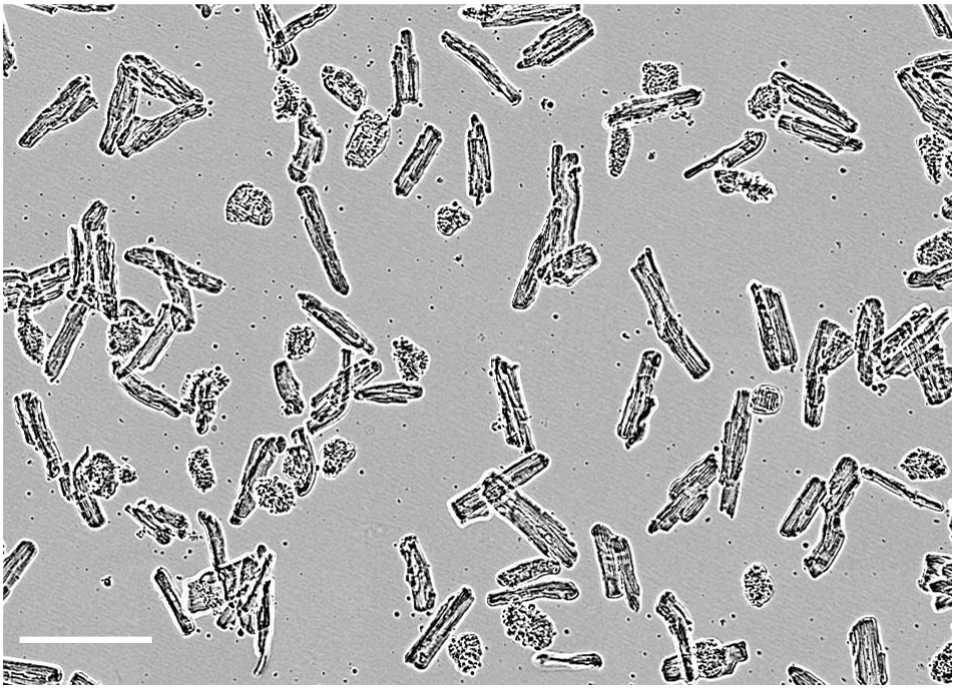

Figure 2.2 Image of adult rat ventricular myocytes (ARVMs) under the microscope, showing both healthy (rod-shaped) and dead (round) myocytes. Scale bar, 150 µm.

2.2.3 Determination of H9c2 cardiomyocyte number

The cell quantification assay was carried out using a modification of the protocol suggested in the Sigma-Aldrich manual from "Cook Book" Volume 12, 2010 and the method described by Strober, (2015). 50 µl of a single-cell suspension was gently mixed with 50 µl of sterile-filtered 0.4% (w/v) trypan blue solution (Sigma-Aldrich) (dilution factor of 2). The mixture was allowed to sit at room temperature for one minute, and then 10 µl of it was added to two counting chambers of a haemocytometer-like FastRead-102 disposable counting slide from Immune Systems Ltd (Paignton, UK). Viable cells were counted within 3-5 minutes from at least two 4 x 4 grids of each chamber, as viewed under the microscope with the help of a hand-held mechanical counter. The count was repeated twice. Viable cells excluded trypan blue, while dead cells stained blue due to trypan blue uptake.

The final cell density was given by the following formula:

$$\text{cells/ml} = \frac{\text{total counts x } 10^4 \text{ x sample dilution factor}}{\text{number of complete 4 x 4 grids counted}}$$

2.3 Knockdown of protein expression by small interfering RNA

2.3.1 siRNA transfection of H9c2 cardiomyocytes

H9c2 cardiomyocytes were cultured as described previously (section 2.2.1) in 6-well or 96-well plates with a subcultivation ratio of 1:10 and were maintained in DMEM, medium supplemented with 10% FBS, 100 IU/ml penicillin and 100 μg/ml streptomycin, in 5% CO_2 at 37°C, until they reached 30% confluency. All transfections were performed using DharmaFECT#1 Transfection Reagent (GE Healthcare, Dharmacon Inc., USA). ON-TARGET plus™ Non-Targeting Control Pool (GE Healthcare, Dharmacon Inc.), composed of four different non-targeting siRNAs and designed to not target any known genes in the rat cell was used as a negative control (Baum et al., 2010). TOX™ Transfection Control (GE Healthcare, Dharmacon Inc.) was used as a positive control to evaluate transfection efficiency. Cells, successfully transfected, underwent apoptosis and cell death in 24 to 48 hours. Other siRNAs used in this study were the ON-TARGET plus™ Rat alpha4 (also known as IGBP1) siRNA SMARTpool against the rat alpha4 mRNA, the ON-TARGET plus™ Rat Ppp2ca siRNA SMARTpool and ON-TARGET plus™ Rat Ppp2cb siRNA SMARTpool against the rat PP2A alpha (PP2ACα) and beta (PP2ACβ) catalytic subunit mRNAs respectively, the ON-TARGET plus™ Rat PPP4C siRNA SMARTpool specific for the rat PP4 catalytic subunit mRNA and the ON-TARGET plus™ Rat PPP6C siRNA SMARTpool against rat PP6 catalytic subunit mRNA (GE Healthcare, Dharmacon Inc.) presented in Table 2.1. The transfection mix was prepared using a ratio of 1 μl of DharmaFECT#1 transfection

Table 2.1 List of siRNAs

siRNA	Target	siRNA sequence	Abbreviation	Cat. No
ON-TARGET plus™ Rat Igbd siRNA SMARTpool of four ON-TARGET plus siRNAs	Alpha4 (Rat)	5’ CCAGCAAGCGUCUAGAUCA 3’ 5’ UUGAGAAGGCUGCCGGAAU 3’ 5’ AAGCAGAUGAUGAGCGUGU 3’ 5’ CUUGAUUUGUUCAGCCGAA 3’	siAlpha4	L-100452-02-0005
ON-TARGET plus™ Rat Ppp2ca siRNA SMARTpool of four ON-TARGET plus siRNAs	PP2Cα (Rat)	5’ UCAUGGAACUCUUUAGAAU 3’ 5’ CGAUGAGUGUUUAAGGAAA 3’ 5’ CCACAUGUCACUCGUCGUA 3’ 5’ GGGAGCUGGUUAUACCUUU 3’	siPP2Cα	L-097852-02-0005
ON-TARGET plus™ Rat Ppp2cb siRNA SMARTpool of four ON-TARGET plus siRNAs	PP2Cβ (Rat)	5’ CGGCAGAUCACACAAGUAU 3’ 5’ UUUAGUAGAUGGACAGAUA 3’ 5’ CAGAGCGUAUCACAAUAUU 3’ 5’ UGACUCUUCUUGUAGCAUU 3’	siPP2Cβ	L-097830-02-0005

siRNA	Target	siRNA sequence	Abbreviation	Cat. No
ON-TARGET plus™ Rat PPP4C siRNA SMARTpool of four ON-TARGET plus siRNAs	PP4C (Rat)	5’ GGUUCGAUAUCCUGACCGA 3’ 5’ GCAGUGAUGUGGUCGCCCA 3’ 5’ GUCAAGGCCCUGUGCGCUA 3’ 5’ CUGUGUGGUCAGCGCCUAA 3’	siPP4C	L-083916-02-0005
ON-TARGET plus™ Rat PPP6C siRNA SMARTpool of four ON-TARGET plus siRNAs	PP6C (Rat)	5’ CUAAGUGGCCUGACCGUAU 3’ 5’ CGAACUAUUGAGCGAAAUC 3’ 5’ UAACGCAGGUGUACGGAUU 3’ 5’ GUUUAUGUUUGACGAGAAG 3’	siPP6C	L-093177-02-0005
ON-TARGET plus™ Non-Targeting Control Pool of four ON-TARGET plus Non-Targeting siRNAs		Commercially sensitive information	siC	D-001810-10-20
TOX™ Transfection Control		Commercially sensitive information	siTOX	D-001500-01-05

reagent (Dharmacon) per 50 pmoles of siRNA in a DNase/ RNase-free microcentrifuge tube and was allowed to incubate on ice for 20 minutes to form siRNA:DharmaFECT#1 complexes. The transfection mix was then added to an appropriate volume of antibiotic-free DMEM with 10% FBS for a final siRNA concentration of 50 nM. The culture medium was then replaced by the transfection medium. Cells were incubated at 37°C in 5% CO_2 for 1 to 4 days. For longer incubation (e.g. 8 days), the transfection medium was replaced every 4 days. The cells were then trypsinised and collected for total RNA purification (section 2.4.1) or lysed for immunoblotting analysis (section 2.5.1).

2.3.2 Recognition of siRNA off-target effects towards non-target mRNAs

Even a single base mismatch between the sequences of the siRNA antisense strand and the mRNA target at the open reading frame can abolish gene expression silencing (Elbashir et al., 2001a; Elbashir et al., 2001c; Holen et al., 2002; Amarzguioui et al., 2003). Nevertheless, partial sequence complementation of 8 nucleotides, between the siRNA seed region sequence (position 1-8 nt) and 3'-untranslated regions (3'-UTRs) of non-target mRNAs can introduce siRNA off-target effects (Jackson et al., 2003; Birmingham et al., 2006; Jackson et al., 2006; review by Jackson and Linsley, 2010; Ui-Tei, 2013). Therefore, to identify siRNA-mediated off-target effects towards a specific non-target substrate, the sequence complementation was investigated between the siRNA and the non-target mRNA (open reading frame and 3'-UTR region). Rejection of a candidate siRNA due to unwanted off-target effects was based on mismatches of ≤4 nucleotides cut-off between the siRNA and a non-target mRNA corresponding open reading frame sequence and/or complementation of 8 nucleotides between the siRNA seed region and a non-target mRNA 3'-UTR (Elbashir et al., 2001c; Holen et al., 2002; Amarzguioui et al., 2003; Jackson et al., 2003; Birmingham et al., 2006; Jackson et

al., 2006; review by Jackson and Linsley, 2010; Ui-Tei, 2013). cDNA sequences were obtained from GenBank®[4] (Benson et al., 2000), genetic sequence database, and was converted to mRNA, using BioEdit v7.1.3 software (Hall, 1999). The open reading frame region was selected by BioEdit v7.1.3 software. Multiple mRNA sequence alignment was performed by EMBOSS Needle[5] alignment tool (Rice et al., 2000).

2.4 Determination of gene expression by quantitative real-time polymerase chain reaction

Quantitative real-time PCR, also known as quantitative PCR (qPCR) is a powerful technique for the investigation of gene expression (Wong and Medrano, 2005). The RNA preparation, evaluation and reverse transcription into cDNA, followed by the detection and quantification of amplification products in real time by qPCR, are described below in sections 2.4.1-2.4.5.

2.4.1 Purification of total RNA from mammalian cells

Total RNA was isolated from H9c2 cells, neonatal rat ventricular myocytes (NRVMs) or ARVMs and purified using the RNeasy Plus Mini kit (Qiagen, UK) according to the manufacturer's instructions. To promote an RNase-free environment, all equipment and working surfaces were decontaminated with RNaseZap (Qiagen) before use. Only RNase-free water and plasticware were used for this protocol.

In brief, following cell counting (section 2.2.3), H9c2 cardiomyocytes (~$1.2 \bullet 10^6$

[4]Free accessed via the National Centre for Biotechnology Information (NCBI) website; http://www.ncbi.nlm.nih.gov/GenBank®/.
[5]Free accessed via the European Bioinformatics (EMBL-EBI) website; http://www.ebi.ac.uk/Tools/psa/emboss_needle/nucleotide.html.

cells, unless otherwise was stated), NRVMs (~$2 \bullet 10^6$ cells) or ARVMs (~$1 \bullet 10^7$ cells), were centrifuged at 50 *g* for 3 minutes at room temperature. The supernatant was removed, and the cell pellet was immediately resuspended in 300 µl of RNAprotect cell reagent (Qiagen) by vortexing, providing immediate stabilisation of the RNA in the cells. The suspension was transferred to a 1.5 ml centrifuge tube and either stored at -20^{o}C (long-term) or processed immediately for total RNA purification in the following way. The suspension was centrifuged at 5,000 *g* for 5 minutes at room temperature. The supernatant was removed, and the cell pellet was dissolved in an appropriate volume of RLT Plus buffer (Qiagen) containing 1% (v/v) β-mercaptoethanol (National Diagnostics, USA). The lysate was passed through a QIAshredder spin column (Qiagen) for complete homogenisation. The homogenised lysate was transferred to a genomic DNA eliminator spin column and centrifuged at 8,000 *g* for 1 minute at room temperature. An equal volume of ethanol 70% (v/v) was added to the flow-through and mixed by pipetting. Up to 700 µl of the sample was transferred to an RNeasy spin column (Qiagen) placed in a 2-ml collection tube and centrifuged at 8,000 *g* for 15 seconds at room temperature. The flow-through was discarded, and 700 µl of the RW1 buffer (Qiagen) were added to the RNeasy spin column. The column was centrifuged at 8,000 *g* for 15 seconds at room temperature, and the flow-through was discarded, 500 µl of the RPE buffer (Qiagen) was added to the RNeasy spin column and centrifuged at 8,000 *g* for 15 seconds at room temperature. The flow-through was discarded, and the last step was repeated except that the column was centrifuged for 2 minutes. The flow-through was then discarded, and the RNeasy spin column was placed in a new 2-ml collection tube and centrifuged at 8,000 *g* for 1 minute at room temperature. The RNeasy spin column was then placed in a new 1.5-ml collection tube, and 30-50 µl of RNase-free water was added directly to the spin column membrane. The column was centrifuged at 8,000 *g* for 1 minute at room temperature to elute the RNA. RNA concentration,

purity and quality were estimated as it is described in section 2.4.2. Aliquots of RNA were flash-frozen in liquid nitrogen and stored at -80ºC until required later. All RNA aliquots were subjected to only one freeze-thaw cycle.

2.4.2 Quality assessment of total RNA

2.4.2.1 Total RNA quantification and quality control by NanoVue Plus

The concentration and purity of RNA solutions were determined using the ultraviolet/visible spectrophotometer NanoVue Plus (GE Healtcare, USA). The operation was performed according to the manufacturer's instructions. RNase-free water was used for background correction, and total RNA concentration was quantified at 260 nm. The purity of the RNA sample was determined by the 260/280 nm and 260/230 absorbance (abs) ratios, revealing any possible contamination of the RNA solution with peptides or residual buffers, respectively. Pure RNA preparations are expected to have both ratios ≥2.0. RNA samples with an absorbance ratio at OD260/280 ≥2.0 and OD260/230 >1.8 were used for further analysis.

2.4.2.2 Quantification of RNA integrity using 2100 Bioanalyzer

The integrity of RNA was evaluated using a 2100 Bioanalyzer (Agilent Technologies, UK) and an Agilent RNA 6000 Nano Kit. The software and algorithm classify total RNA by calculating an RNA integrity number (RIN) from 1 to 10, with 1 corresponding to the most degraded RNA profile and 10 to the most intact (Schroeder et al., 2006). The preparation of all samples was completed according to the Agilent RNA 6000 Nano Kit Guide (Manual Part Number G2938-90034, Edition 08/2006) in the following way. Each RNA chip contains an interconnected set of microchannels, used for separation of nucleic acid fragments based on their size as they are driven through it electrophoretically. All reagents were equilibrated at room

temperature for 30 minutes before use. The electrodes of the 2100 Bioanalyzer were decontaminated by washing with RNase ZAP (Qiagen) for 1 minute followed by a wash with RNase-free water for 10 seconds. A volume of 550 µl of the Agilent Nano gel matrix was passed through the spin filter by centrifugation at 1,500 *g* for 10 minutes at room temperature. Aliquots of 65 µl of the filtered gel matrix were transferred into microcentrifuge tubes and were stored at 4°C for up to 4 weeks. Prior to use, 1 µl of the provided dye solution was added to the filtered 65 µl gel aliquot and mixed by vortexing followed by a centrifugation step at 13,000 *g* for 10 minutes at room temperature and the gel-dye mix was used within one day. An RNA chip was placed on the chip priming station, and 9 µl of the gel-dye mix was pipetted into the well, marked "". The plunger was positioned at the 1-ml and the chip priming station was closed. The syringe plunger was pressed down until it was held by the clip, was then released after 30 seconds and 5 seconds later the plunger was pulled back to the 1 ml position. The priming station was opened, and 9 µl of the gel-dye mix was pipetted in each of the wells, marked "". A volume of 5µl of the Nano marker was added into the 12 sample wells and to the ladder well, marked "". The RNA samples and the ladder were heat-denatured at 70°C for 2 minutes to minimise secondary structures. From each RNA sample, 1µl containing 25-500 ng RNA was added in each of the 12 sample wells and 1µl of the ladder into the ladder well. The chip was placed in an appropriate vortexer (IKA - Model MS3; Staufen, Germany) and was vortexed for 1 minute at 2,400 rpm. The chip was inserted in the Agilent 2100 Bioanalyzer within 5 minutes and analysed. The analysis was performed via Agilent's 2100 expert software selecting the "Eukaryotic Total RNA Nano" assay. The RNA integrity number (RIN) was estimated for each sample. Only RNA samples with RIN index close to 9 or above 7 were selected for qPCR analysis, when extracted from H9c2 cardiomyocytes or neonatal (NRVMs) and adult (ARVMs) rat ventricular myocytes respectively, unless otherwise was stated (Fleige

and Pfaffl, 2006; Schroeder et al., 2006).

2.4.2.3 RNA quality evaluation by agarose gel electrophoresis

Inspection of the 28S and 18S ribosomal RNA bands (Rio et al., 2010) was performed by agarose gel electrophoresis to evaluate the integrity and overall quality of a total RNA preparation before using it for other applications. Electrophoresis was performed in a horizontal electrophoresis apparatus (Bio-Rad Laboratories, USA). Since ribonucleotides contain a phosphate group, overall, the RNA molecules are negatively charged and can migrate in an electric field towards the positively charged anode.

The protocol used here is a modification from the publication by Rio et al., 2010 and only RNase-free water was used (Millipore water purification system Elix®; Merck Millipore, USA). Agarose gels were prepared and contained 1% (w/v) agarose (Fisher Scientific) dissolved in 100 ml 1X Tris-borate-EDTA (TBE) buffer (89 mM Tris-base, 89 mM boric acid, 2 mM EDTA, pH 8). The solution was heated in a microwave oven until the agarose melted and the solution was clear. The agarose gel was then complemented with 1 µl of 10,000X SYBR® Safe DNA Gel Stain solution (Invitrogen, USA) mixed carefully and poured into the gel tray. Appropriate size well combs were inserted, and the agarose gel was left to polymerise for 30 minutes. Appropriate volume of each sample containing 100 ng RNA was transferred to an RNase-free 0.5-ml microtube. RNase- free water was added up to a 10 µl final volume and the RNA sample was mixed with 2 µl of 6X loading buffer (0.25% (w/v) bromophenol blue, 40% (w/v) sucrose). Each prepared sample and a 1kb Plus DNA ladder (Thermo Fisher Scientific, Life Technologies Corporation) was loaded into each well and electrophoresis was run at 80 V for 1 hour. After electrophoresis, the gels were visualised by the Molecular Imager GelDoc XR+ Imaging System using

ultraviolet exposure combined with the XcitaBlue™ Conversion Screen and the Image Lab 4.0.1 software (Bio-Rad Laboratories).

2.4.3 Two-step reverse transcriptase polymerase chain reaction (RT-PCR)

All equipment and working surfaces were decontaminated with DNaseZAP and RNaseZAP (Ambion Inc., USA) prior to use. Only RNase/DNase-free water and plasticware were used for this protocol. RNA was reverse transcribed into cDNA using oligo-dT primers via a two-step reverse transcription (RT) process using the NanoScript 2 Reverse Transcription kit, (Primerdesign Ltd, UK), according to the manufacturer's instructions. Oligo-dT primers bind to the polyA tail of messenger RNA (mRNA), targeting the RT reaction preferentially to the 3'end of the mRNA fraction and reducing non-specific priming on the ribosomal fraction of total RNA. The first step is the 'annealing' step in which the RT primers are annealed to the denatured RNA template. This step reduces secondary structures in the RNA template that may impede long cDNA synthesis. Appropriate volume of each RNA template containing 0.5 to 1 µg RNA, 1 µl of Oligo-dT primers mix and appropriate volume of RNase/DNase-free water up to final volume 10 µl were added into an RNase-free 0.5 ml microtube. Each sample was heated to 65°C for 5 minutes and then immediately transferred to an ice water bath and allowed to cool for 5 minutes. In the second 'extension' step, the mRNA is reverse transcripted into first strand cDNA by the nanoScript 2 enzyme, starting at the primer binding sites whilst the original RNA template in the RNA/cDNA hybrid is degraded. For this step, 10 µl of a mix containing 2 µl of nanoScript 2 10X buffer, 1 µl dNTP mix, 2 µl DTT 100 mM, 4 µl RNase/ DNase-free water and 1 µl of nanoScript 2 enzyme were added to each of the samples from the previous step on ice. The samples were mixed briefly by vortex followed by a brief pulse centrifugation and incubated at 55^{o}C for 20 minutes. Each reaction was then heat-inactivated at 75^{o}C for 15 minutes. A no-

reverse transcriptase (no-RT) control was included for every RNA template. The synthesised cDNA and no-RT samples were diluted to 5ng/µl with RNase/DNase-free water (Fisher Scientific) and were further analysed by qPCR or stored at -20^{o}C until use.

2.4.4 SYBR Green quantitative polymerase chain reaction

qPCR was performed using the Precision™ 2X Master Mix with SYBRgreen fluorescent dye (Primerdesign Ltd, UK) and the Stratagene Mx3005P qPCR system (Agilent Technologies), according to the manufacturer's instructions. In qPCR, a thermostable DNA polymerase amplifies a fragment of the cDNA template in cycles (Wong and Medrano, 2005). After every cycle, the number of the copies is doubled, leading to an exponential amplification of targets. SYBR Green is a commonly used double-strand DNA dye, which fluoresces when binding to the amplified DNA. The amount of the fluorescence emitted during amplification is directly proportional to the amount of amplified DNA and is monitored during the whole PCR process (usually 30-50 cycles).

All equipment and working surfaces were decontaminated with DNaseZAP and RNaseZAP (Ambion Inc.) prior to use. Only RNase/DNase-free water and plasticware were used. Verified quantitative PCR primers pairs specific to rat genes *PP2ACα*, *PP2ACβ*, *PP4C*, *PP6C*, *GAPDH* (Glyceraldehyde-3-phosphate dehydrogenase) and *ACTB* (β-actin) were obtained from Primerdesign Ltd (Table 2.2). Each qPCR reaction contained 5 µl diluted cDNA (25 ng in total), 10 µl Precision™ 2X qPCR Master Mix (Primerdesign Ltd), 1 µl of 6 µM primer mix and 4 µl RNase/DNase-free water (20 µl reaction). A no-RT control and a no-template control were included as negative controls for each gene to test for DNA contamination (such as genomic DNA or PCR product from a previous run).

qPCR reactions for all the genes of interest were performed in biological triplicates, and technical duplicates in the same bright white real-time PCR 96-well plates (Primerdesign Ltd) sealed with optical adhesive seals. The qPCR run conditions were as follows: one cycle of 10 minutes at 95°C for enzyme activation, followed by 40 cycles of 15 seconds at 95°C for denaturation and 1 minute at 60°C for data collection.

Table 2.2 Primers for qPCR

Gene (species)	Primers	T*m* (°C)	Accession No
PP2ACα **(Rat)**	**Forward** **5'-TTACCGAGAGCGTATCACCATA-3'**	**57**	**NM_017039**
	Reverse **5'-TTTCCGTATTTCCTTAAACACTCATC-3'**	**57.3**	
PP2ACβ (Rat)	**Forward** **5'-TCGTGACTGGTTAAGGGAAAGG-3'**	**58.5**	**NM_017040**
	Reverse **5'-AAACTCCAACTCTATAATCCATGCC-3'**	**58**	
PP4C **(Rat)**	**Forward** **5'-TGACATCCACGGACAATTCTATG-3'**	**57.3**	**NM_134359**
	Reverse **5'-CAGCAGGAGGAGGAAGGTTT-3'**	**57.3**	
PP6C **(Rat)**	**Forward** **5'-GGCT TGTTCTTCCTAAAATGGC-3'**	**56.7**	**NM_133589**
	Reverse **5'-TTCCAAGAGCAGATCACAAA CATA-3'**	**57.4**	
GAPDH (Rat)	**Commercially sensitive information**		**NM_017008**
ACTB (Rat)	**Commercially sensitive information**		**NM_ 031144**

2.4.5 Relative quantification in qPCR

The cycle in which fluorescence can be detected whilst exceeding the baseline fluorescence is termed quantitation cycle (Cq) according to the MIQE guidelines (Bustin et al., 2009). The mean Cq standard deviation (SD) was less than 0.2 Cq (usually SD less than 0.35 Cq is accepted) between technical replicates (D'Haene et al., 2010). Unknown samples with at least 5 Cq values below (32-fold difference) the respective no-RT and no-template controls were further analysed (Zornhagen et al., 2015). Multiple reference genes were used in this study to limit normalisation variations (Vandesompele et al., 2002; Bustin et al., 2009). Relative quantification was performed using two approaches, the comparative Cq method and the qbase$^+$ software approach, described in sections 2.4.5.2 and 2.4.5.3, respectively.

2.4.5.1 Validation of reference genes

Two reference genes were chosen from literature search, glyceraldehyde-3-phosphate dehydrogenase and β-actin, for normalisation of genes of interest in rat cardiomyocytes (Villeneuve et al., 2009; Tan et al., 2012; Ellison et al., 2013; Zheng et al., 2013; Pooja et al., 2015). Validation of the reference genes was performed by measuring the standard deviation (SD) of the average Cq values, coefficient of variation (CV) and Pearson coefficient of correlation (*r*) using the BestKeeper© v1.0 software, an excel based tool that scores the reference genes based on a repeated pairwise correlation analysis (Pfaffl et al., 2004). More stable genes should have an *r* value that equals to or is close to 1 and SD less than 1.

2.4.5.2 Relative quantification by Cq comparative method

The comparative Cq method, also known as ΔΔCq method, was used to compare gene expression normalised to a single validated gene (Livak and Schmittgen, 2001;

Schmittgen and Livak, 2008). Firstly, the mean Cq value of the technical replicates for each gene was calculated for each sample. Then, the difference between the averaged Cq values for each gene of interest (GOI) and the reference genes (either GAPDH or ACTB) was calculated for each sample by the following equation:

$$\Delta\text{Cq (GOI)} = \text{mean Cq (GOI)} - \text{mean Cq (references)}$$

One of the genes of interest or the targeted gene from the control sample was chosen as the calibrator gene (CAL) and the difference in the ΔCq values between the other genes of interest (GOI) or targeted gene of treated samples (GTS), and the calibrator was calculated using the formula:

$$\Delta\Delta\text{Cq (GOI or GTS)} = \Delta\text{Cq(GOI or GTS)} - \Delta\text{Cq(CAL)}$$

The fold-change between the genes of interest or targeted gene of treated samples *vs* the calibrator gene was calculated by applying ΔΔCq to the following equation:

$$\text{Fold change} = 2^{-\Delta\Delta\text{Cq}}$$

Fold change of the calibrator gene or sample was equal to 1. The other normalised relative quantity values (fold changes) were then averaged between all biological replicates and presented in a graph with the standard error (SEM) of the mean. Fold change equal to 1.0 indicated no difference in the mRNA expression of a gene of interest relative to the mRNA expression of the calibrator gene. Fold change less than 1.0 could be converted to fold decrease in the mRNA expression by the following formula (Schmittgen and Livak, 2008):

$$\text{Fold decrease} = -1/\text{Fold change}$$

which could then be interpreted using the absolute value.

2.4.5.3 Relative quantification by modified qbase$^+$ software approach

When investigating potential differences in the transcription level of a gene due to treatment compared to the control or between different cell types, it is generally recommended to use more than one validated references for more reliable normalisation (Vandesompele et al., 2002). In order to use two reference genes for normalisation in qPCR relative quantification, a qbase$^+$ workflow approach (Hellemans et al., 2007) was preferred.

As mentioned previously, the mean Cq value of the technical replicates for each gene was calculated for each sample. Then, the relative quantity (RQ) of each gene of interest (GOI) in the unknown sample (unk) in relation to the control sample was calculated based on the following formula (Pfaffl, 2001):

$$\mathrm{RQ(GOI)}_{unk} = \mathrm{E(GOI)}_{unk}^{\mathrm{Cq(GOI)}_{control} - \mathrm{Cq(GOI)}_{unknown}}$$

where E corresponds to the qPCR efficiency. In this study, the amplification of all genes has been normalised to 100% by PrimerDesign (UK) therefore, E equals 2.

Next, the normalisation factor (NF) based on the geometric mean of *n* number reference genes RQ is calculated for each unknown and control sample:

$$\mathrm{NF}_{unk} = \sqrt[n]{\mathrm{RQ}_{unk}\left(\mathrm{REF}_{1,unk}\right) \cdot \mathrm{RQ}\left(\mathrm{REF}_{2,unk}\right) \cdot \ldots \cdot \mathrm{RQ}(\mathrm{REF}_{n,unk})}$$

where $\mathrm{REF}_{1,unk}$ corresponds to reference gene 1, $\mathrm{REF}_{2,unk}$ corresponds to reference gene 2 and $\mathrm{REF}_{n,unk}$ corresponds to reference gene *n* in the unknown sample.

Then, the normalised relative quantities (NRQ) of each gene of interest (GOI) in the unknown or control sample is calculated, based on the ratio of the RQ value of an

unknown sample versus a control expressed in comparison to the corresponding NF by the following formula (Hellemans et al., 2007):

$$\mathrm{NRQ(GOI)}_{unk} = \mathrm{RG}_{unk}/\mathrm{NF}_{unk}$$

The NRQ (GOI) represents the fold change of the GOI in the unknown in relation to the control sample. The method mentioned above can be applied when using a single reference for normalisation by the following equitation (Pfaffl, 2001):

$$\mathrm{NRQ\ (GOI)}_{unk} = \frac{\mathrm{E(GOI)}_{unk}^{\mathrm{Cq(GOI)}_{control} - \mathrm{Cq(GOI)}_{unknown}}}{\mathrm{E(REF)}_{unk}^{\mathrm{Cq(REF)}_{control} - \mathrm{Cq(REF)}_{unknown}}}$$

The NRQ (GOI) of the control sample was equal to 1. The other NRQ (GOI) values for each unknown sample were then averaged between all biological replicates and presented in a graph with the standard error (SEM) of the mean. Fold changes less than 1.0 could be converted to fold decrease in the mRNA expression as described in section 2.4.5.2.

2.5 Protein expression analysis by western blotting (immunoblotting)

2.5.1 Protein sample preparation

Cells in culture plates or flasks were washed with ice-cold PBS and then lysed with an appropriate volume of modified 1X Laemmli sample buffer (Laemmli, 1970) containing 10% (v/v) glycerol, 43.75 mM Tris-base, pH 6.8, 2% (w/v) SDS, 0.03% (w/v) bromophenol blue and 3 % (v/v) β-mercaptoethanol. Cells were further lysed with a scraper and samples were collected into centrifuge tubes. Cells in suspension were lysed by the addition of an appropriate volume (2:1) of modified 3X Laemmli sample buffer (Laemmli, 1970) containing 30% (v/v) Glycerol, 131.25 mM Tris-

HCl, pH 6.8, 6% (w/v) SDS, 0.09% (w/v) bromophenol blue and 9 % (v/v) β-mercaptoethanol. Samples were boiled for 5 minutes at 95^{o}C and then stored at -20°C until required later.

2.5.2 SDS-polyacrylamide gel electrophoresis (PAGE)

Prior to use, the samples were briefly vortexed after thawing, followed by a quick spin down. An equal volume of protein samples was separated by SDS-PAGE using polyacrylamide gels. To be able to determine the size of the proteins, 3 µl of Precision Plus Protein™ dual colour standards (Bio-Rad, USA) were run alongside to the samples. Depending on the molecular weight of the protein of interest, 6% to 15% percent resolving gels (375 mM Tris-HCl, pH 8.7, 0.1% (w/v) SDS, 6%-12% (w/v) acrylamide, 0.1% (v/v) TEMED, 0.1% (w/v) APS) and 4% stacking gels (500 mM Tris-HCl, pH 6.8, 4% (w/v) acrylamide, 0.1% (w/v) SDS, 0.1% (v/v) TEMED, 0.1% (w/v) APS) were used. Protein gels were resolved in running buffer (25 mM Tris, 190 mM glycine, 0.1% (w/v) SDS) at 180V until the blue dye front ran off the bottom of the resolving gel.

2.5.3 Determination of protein expression by western blotting

Following the SDS-PAGE of proteins, each gel was transferred to either 0.20 or 0.45 µm pore size Hybond-P PVDF (GE Healthcare, UK), 0.45 µm pore size Hybond ECL nitrocellulose (GE Healthcare, UK) or 0.45 µm pore size EMD Millipore Immobilon-FL PVDF (Merck Millipore) membrane, using the ECL Semi-dry Blotter TE 77 (GE Healthcare). A stack was assembled in the following order: three sheets of Whatman paper (6.0 × 8.5 cm) were placed on the anode, one PVDF or nitrocellulose membrane (6.0 × 8.5 cm), a protein gel (6.0 × 8.5 cm) and three more sheets of Whatman paper (6.0 × 8.5 cm). Each layer of the transfer stack was soaked in transfer buffer (48 mM Tris-HCl, pH 8.3, 0.037% (w/v) SDS, 39 mM Glycine,

20% (v/v) Methanol), while the PVDF membrane was firstly prewetted with methanol for 10 seconds and then soaked in transfer buffer. Proteins were transferred to PVDF or nitrocellulose membranes at 0.8 mA per cm^2 of the gel surface for 2 hours. After the end of the transfer, the membranes were incubated with either 5% (w/v) Marvel skimmed milk powder or 3% (w/v) BSA in TBS-T buffer (TBS buffer (20 mM Tris-HCl, 130 mM NaCl, pH 7.6) containing 0.1% (v/v) Tween-20) for 2 hours with constant agitation on an orbital shaker at room temperature. Each membrane was then incubated with 10 ml primary antibody (diluted in 1 % (w/v) dried milk in TBS-T) overnight at 4°C with constant agitation. The membranes were then washed five times every 20 minutes with TBS-T buffer. Blots were then incubated for 1 hour with an appropriate horseradish peroxidase (HRP)-linked secondary antibody (1:1000 diluted in milk 1% (w/v) in TBS-T, 10ml) or with IRDye® 680RD-conjugated secondary antibodies (1:15,000 diluted in milk 1 % (w/v) in TBS-T, 10ml) when being prepared for enhanced chemiluminescence (ECL) analysis or LI-COR Odyssey® CLx Imaging System (LI-COR Biosciences, USA) respectively. Membranes were then washed four times every 15 minutes with TBS-T. A list of the antibodies and working dilutions used in this study is presented in table 2.3.

2.5.3.1 Quantitative western blotting using the enhanced chemiluminescence (ECL) detection system

Proteins were visualised using the ECL western blotting detection reagents and analysis system (GE Healthcare) according to the manufacturer's instructions. Blots were incubated with the chemiluminescence reagent (GE Healthcare) for 1 min, placed in a cassette and then, exposed to a piece of Amersham Hyperfilm ECL (18 × 24 cm) (GE Healthcare) in a dark room. The development of the films was performed by a FUJI Medical film processor RG II (Fujifilm, Japan). The blots were

Table 2.3 List of antibodies and working dilutions.

Antibody	Dilution factor	Supplier, Cat No#
Sheep polyclonal anti-PP2AC	1:1,000	Custom made[6] (Kloeker et al., 2003)
Sheep polyclonal anti-PP4C	1:1,000	Custom made[6] (Kloeker et al., 2003)
Sheep polyclonal anti-PP6C	1:1,000	Custom made[6] (Kloeker et al., 2003)
Mouse monoclonal anti-alpha4	1:1,000	Cell Signaling Technology, #5699
Rabbit polyclonal anti-alpha4	1:1,000	Bethyl Laboratories, #A300-417A-1
Goat polyclonal anti-Actin (I-19)	1:2,000	Santa Cruz Biotechnology Inc, #sc-1616
Mouse monoclonal anti-Ubiquitin (P4D1)	1:500	Santa Cruz Biotechnology, Inc., #sc- 8017
Rabbit polyclonal anti-phospho-CaV1.2 (Ser1928)	1:1,000	LifeSpan BioSciencies, #LS-C145147C
Rabbit polyclonal anti-phospho-PLM (Ser63)	1:5,000	Custom made[7] (Fuller et al., 2009)
Rabbit polyclonal anti-phospho-PLM (Ser68)	1:15,000	Custom made[7] (Fuller et al., 2009)
Rabbit polyclonal anti-ANKRD28	1:1,500	Bethyl laboratories, #A300-974A
Rabbit polyclonal anti-ANKRD44	1:1,000	LSBio, #LS-C178736
Rabbit polyclonal anti-ANKRD52	1:1,000	LSBio, #LS-C15372
Goat polyclonal anti-SAP1 (V-14)	1:1,000	Santa Cruz Biotechnology, #sc-109864
Mouse monoclonal anti-SAP2 (H-3)	1:500	Santa Cruz Biotechnology, #sc-376678
Rabbit polyclonal anti-SAP3	1:1,000	ProteintechTM, #16944-1-AP

[6]Kindly donated dy Dr B. E. Wadzinski, School of Medicine, University of Vanderbilt (USA).
[7]Kindly donated by Prof M. J. Shattock, Cardiovascular Division, King's College London, The Rayne Institute, St. Thomas' Hospital, London, United Kingdom.

Antibody	Dilution factor	Supplier, Cat No#
Rabbit polyclonal anti-H2AX	1:1,000	Cell Signaling Technology, #2595
Rabbit polyclonal anti-phospho-Histone H2AX (Ser139)	1:1,000	Cell Signaling Technology, #2577
HRP-conjugated sheep anti-mouse secondary	1:1,000	GE Healthcare, #NA931
HRP-conjugated horse anti-mouse secondary	1: 1,000	Cell Signaling Technology, #7076
HRP-conjugated donkey anti-goat secondary	1:2,000	Santa Cruz Biotechnology Inc, #sc-2020
HRP-conjugated donkey anti-rabbit secondary	1:1,000	GE Healthcare, #NA934V
HRP-conjugated goat anti-rabbit secondary	1:1,000	Cell Signaling Technology, #7074S
HRP-conjugated donkey anti-sheep secondary	1:1,000	Santa Cruz Biotechnology, Inc., #sc-2916
Alexa Fluor® 647 conjugated donkey anti-sheep secondary	1:1,000	Millipore, #AP184SA6
IRDye® 680RD donkey anti-Goat secondary	1:15,000	LI-COR Biosciences, #926-68074
IRDye® 680RD donkey anti-rabbit secondary	1:15,000	LI-COR Biosciences, #926-68073

scanned by Model GS-800 Calibrated Imaging Densitometer (Bio-Rad Technologies), and bands on the film were quantified using Quantity One 1-D v4.6.2 analysis software (Bio-Rad Technologies).

2.5.3.2 Quantitative fluorescent western blotting

Membranes were incubated with IRDye® 680RD-conjugated secondary antibodies (1:15,000 diluted in 1 % (w/v) milk in TBS-T, 10ml). Signal intensities of the fluorophore channel 700 nm were determined using a LI-COR Odyssey® CLx

Imaging System (resolution: 169 µm, scan quality: medium-lowest) and analysed with the Image Studio™ v5.x software (LI-COR Biosciences, USA).

2.5.4 Total protein staining with Coomassie Blue R-250

After western blotting analysis, PVDF and nitrocellulose membranes were immersed in coomassie blue (2.4 mM Coomassie Blue R-250, 10% (v/v) acetic acid, 50% (v/v) methanol) for 30 min with agitation to stain the membrane for total protein and confirm the efficiency of protein transfer from the gel to the membrane. The coomassie blue stained membranes were destained with 50% (v/v) methanol, 10% (v/v) acetic acid solution, which was changed regularly until the proteins bands were visible.

2.6 Measuring cell viability with MTT assay

The MTT assay, first developed by Mosmann in 1983 (Mosmann, 1983), was used to determine the number of viable and metabolically active cells. It is based on the enzymatic reduction of a water-soluble yellow tetrazolium salt, 3-(4, 5-dimethylthiazol-2-yl)-2, 5-diphenyltetrazolium bromide (MTT), which forms a water-insoluble purple formazan crystal in the mitochondria of metabolically active cells and must then be dissolved for calorimetric measurement. The absorbance value is directly proportional to cell number. The protocol was modified and is described below.

Cells were cultured in 96-well flat-bottomed culture plates (100 µl per well) to the required confluency and were allowed to adhere at least 24 hours prior to any treatment. The cells were treated as per experimental design and incubation times. At the end of the experiment, the medium was removed and replaced with 100 µl of MTT reagent (Merck Millipore) 0.5 mg/ml solution made in pre-warmed DMEM

without phenol red. The plate was then kept in the dark and incubated at 37°C, 5% CO_2, 95% air for 4 hours. After incubation, the MTT solution was carefully removed, and 100 µl of DMSO was added to each well (samples and blanks) to lyse the cells, using a multichannel pipette. The plate was covered in foil and was shaken gently for 15 minutes on an orbital plate shaker at room temperature. The absorbance of each well was measured at 540 nm by the Infinite M200 PRO plate reader from TECAN (UK) and analysed using the Magellan™ v7 data analysis software (Magellan, Taiwan). The raw 540 nm absorbance readings were corrected by subtracting the mean absorbance of the blank wells (wells without cells). The relative cell viability was calculated as $[Abs]_{sample}/[Abs]_{control}\times100\%$.

2.7 Statistical analysis

Each experiment was repeated at least three times ($n\geq3$), and statistical analysis was performed using GraphPad Prism v6.07 software (GraphPad Software, Inc., USA). Data were presented as mean values ± standard error of the mean (SEM). For comparison of data between 2 groups, an appropriately tailed unpaired Student's t-test was used. To compare more than two groups, one-way ANOVA followed by either a Dunnett's or Tukey's post-hoc multiple comparisons tests was used. Differences were considered statistically significant at the 95% confidence level, where $p<0.05$.

Chapter 3

Expression of the Type 2A Protein Phosphatases in Cardiomyocytes

3.1 Introduction

3.1.1 Transcriptional regulation of PP2ACα, PP2ACβ, PP4C and PP6C subunits

3.1.1.1 Regulation of PP2ACα and PP2ACβ transcription

The PP2A catalytic subunit exists in two forms, PP2ACα and PP2ACβ, which are encoded by two different genes. The *PPP2ACα* gene is localised to human chromosome 5q23-q31 (Jones et al., 1993), whilst the *PPP2ACβ* gene is mapped to human chromosome 8p21-p12 (Imbert et al., 1996). Approximately 100-150 bp upstream the major transcription start sites of PP2ACα (position at 205 nucleotides upstream the translation codon, ATG, in human) and PP2ACβ (positions at 409 and 423 nucleotides upstream the translation codon, ATG, in human) have been reported to be sufficient for full transcriptional promoter activity (Khew-Goodall et al., 1991). PP2ACα is commonly predominant in nature at the mRNA level (Khew-Goodall and Hemmings, 1988; Khew-Goodall et al., 1991; Sunahori et al., 2009). This was at least partly explained by the distinct content of transcriptional factor binding sites in PP2ACα and PP2ACβ promoter region, which may affect the level of transcription (Khew-Goodall and Hemmings, 1988; Khew-Goodall et al., 1991; Sunahori et al., 2009). Both PP2ACα and PP2ACβ promoters are lacking the TATA

box sequence and contain several transcription factor Sp1 (specificity protein 1) binding sites which differ in number and location (Khew-Goodall et al., 1991; Sunahori et al., 2009). Nevertheless, the PP2ACα promoter region contains a cAMP response element (CRE) motif (26 bp upstream of the transcription start site) that is absent in the PP2ACβ promoter (Khew-Goodall et al., 1991; Sunahori et al., 2009). Binding of the CRE binding protein (CREB) or Sp1 protein to the CRE or Sp1 sites, respectively, enhances the promoter activity (Khew-Goodall et al., 1991; Sunahori et al., 2009). Moreover, PP2ACα transcription appears to be regulated epigenetically, through the methylation of a CpG site within the CRE motif in its promoter region, which can suppress the promoter activity by affecting CREB binding (Sunahori et al., 2011).

3.1.1.2 Regulation of PP4C transcription

Similar to PP2AC, the PP4 catalytic subunit amino acid sequence is highly conserved across eukaryotic species (Brewis and Cohen, 1992; Brautigan, 2013). The *PPP4C* gene has been mapped to human chromosome 16p11-p12 (Bastians et al., 1997a). Two major transcription start sites have been identified (positions at 53 and 84 nucleotides upstream the translation codon, ATG, in human) (Huang et al., 1997). The 5'-flanking sequence, 500 bp upstream the translation start site, is lacking the TATA box, but contain other transcription factor binding sites including several AP1, AP2 (activator proteins 1 and 2), and gamma-IRE (IFN-gamma response element) sites upstream of the second transcription site and a Sp1 binding site between the two major transcription start sites (Huang et al., 1997). Nevertheless, the regulation of PP4C transcription in eukaryotic cells is yet to be investigated.

3.1.1.3 Regulation of PP6C transcription

The PP6 catalytic subunit (PP6C) is also found to be conserved across eukaryotic species (Brautigan, 2013). The human *PPP6C* gene has been localised to chromosome Xq22.3 (Bastians et al., 1997b). The regulation of PP6C transcription remains unclear, however, it has been shown previously that PP6C transcription was enhanced in high-density epithelial cells, accompanied by the expression of elevated protein levels of PP6C (Ohama et al., 2013). Thus, a correlation between PP6C expression and cell density-dependent feedback signalling was proposed (Ohama et al., 2013).

3.1.2 Post-translational regulation of type 2A protein phosphatase catalytic subunits by the ubiquitin-proteasome-mediated system

The ubiquitin-proteasome system, described in figure 1.10, is (i) a primary pathway for degradation of damaged and miss-folded proteins in mammalian cells and (ii) a critical cellular protein post-translational regulatory mechanism, therefore, it plays a critical role in many cellular processes such as the cell cycle, cell division, apoptosis and cell signalling (Fuchs et al., 1998; El-Khodor et al., 2001; Terret et al., 2003; Siu et al., 2011). In the cardiovascular system, dysregulation of ubiquitin-proteasome system activity has been related to several diseases including myocardial ischemia, certain cardiomyopathies and heart failure (Bulteau et al., 2001; Herrmann et al., 2003; Powell et al., 2005; Depre et al., 2006; Predmore et al., 2010). All type 2A protein phosphatase catalytic subunits are ubiquitously expressed, and their expression can be subjected to post-translational regulation by the ubiquitin-proteasome system (Trockenbacher et al., 2001; McConnell et al., 2010; Udeshi et al., 2013; Xu et al., 2014).

3.2 Specific objectives

Very little is known regarding the expression and regulation of PP4 and PP6 in healthy mammalian myocardium. Therefore, the experiments performed in this study aim to:

1. detect the mRNA and protein expression of PP2ACα, PP2ACβ, PP4C and PP6C in H9c2 cardiomyocytes, neonatal rat ventricular myocytes (NRVMs) and adult rat ventricular myocytes (ARVMs).

2. investigate whether the expression levels of type 2A protein phosphatase catalytic subunits are dependent on 26S proteasome activity in ARVMs.

3.3 Methods

3.3.1 Neonatal rat ventricular myocyte isolation and cell culture

3.3.1.1 Isolation of neonatal rat ventricular myocytes (NRVMs)

NRVMs were isolated from three litters of between eight to twelve 1-2 day old Sprague Dawley neonatal rat pups by Dr Asvi Francois[8] at the BSU within Waterloo campus of King's College London, using a collagenase/ pancreatin-based enzymatic digestion technique (Punn et al., 2000) and pooled together. All dissection equipment, glassware and plasticware were either pre-sterilised or sterilised by autoclaving (15 min, 121^{o}C, 1.2 atm). Solutions were either pre-sterilised or sterilised by autoclaving (15 min, 121^{o}C, 1.2 atm) or filtration through 0.2-µm sterile syringe filters (Corning Inc., USA). During the procedure, surgical equipment not being used was kept in 70% ethanol.

Neonates were separated from the mother in a different laboratory room and were euthanised by cervical dislocation. Following euthanasia, the neonates were rinsed briefly in 70% (v/v) ethanol to sterilise the tissue. The chest of the animals was opened carefully using small blunt ended scissors. The heart was removed using blunt ended scissors, and the attached lungs were separated from the heart with sharp-ended scissors. The hearts were then transferred into a 90-mm sterile petri dish containing ice-cold ADS buffer (0.68% NaCl (w/v), 0.476% HEPES (w/v), 0.012% NaH_2PO_4 (w/v), 0.1% glucose (w/v), 0.04% KCl (w/v), 0.01% $MgSO_4$ (w/v), pH 7.35) and were dissected into 1 mm pieces using small surgical scissors. This procedure was repeated for all the hearts.

In a laminar air-flow hood, the petri dish containing the hearts in ADS buffer was

[8]Cardiovascular Division, King's College London, The Rayne Institute, St. Thomas' Hospital, London, United Kingdom.

placed on ice. Curved sharp ended scissors were used to slice the hearts into very fine pieces. The heart-ADS buffer solution was then transferred into a 50-ml falcon centrifuge tube and allowed to settle at room temperature and form a loose pellet by sedimentation due to gravity. The supernatant was carefully aspirated off and 7 ml of enzyme solution (ADS buffer supplied with 0.5 mg/ml collagenase (Worthington Biochemical Corporation, USA) and 0.6 mg/ml Gibco™ pancreatin (Thermo Fisher Scientific, Life Technologies Corporation) was added to the heart pieces. The mixture was placed in a water bath at 37^{o}C for 7 min, swirling the tube from time to time. The heart pieces were then allowed to settle and form a loose pellet by sedimentation due to gravity. The supernatant was then discarded, and 7 ml of the enzyme solution was added. The mixture was placed in the water bath for 7-min incubation at 37^{o}C step, and the heart pieces were then left to sediment by gravity. The supernatant was aspirated off, and the cardiomyocytes were then isolated from the heart fragments by eight cycles of enzymatic digestion as described below.

The settled heart pieces were mixed with 7 ml of the enzyme solution by pipetting. The tube was incubated at 37^{o}C for 15 min and was swirled from time to time. After the heart pieces settled by sedimentation due to gravity, the supernatant containing the isolated cardiomyocytes was transferred to a 15-ml falcon centrifuge tube and mixed with 2 ml sterile-filtered FBS by pipetting to stop the collagenase-pancreatin digestion. The mixture was then centrifuged at 150 *g* for 6 min at room temperature. The supernatant was discarded, and the pelleted cells were resuspended in 6 ml of pre-plating medium (referred to as medium I) containing 2:1 (v/v) plating medium:Gibco™ Foetal Calf Serum (Thermo Fisher Scientific, Life Technologies Corporation). The plating medium (referred to as medium II) contained 4:1 (v/v) Gibco™ DMEM: Gibco™ M199 medium, supplemented with 0.5% (v/v) Gibco™ Horse Serum, 5% (v/v) Gibco™ Foetal Calf Serum (Thermo Fisher Scientific, Life

Technologies Corporation), 100 IU/ml penicillin and 100 μg/ml streptomycin (Sigma-Aldrich). The cell suspension was then transferred to a 50-ml falcon centrifuge tube which was placed in a standard incubator (37ºC, 5% CO_2), leaving the lid half open to allow CO_2 calibration. This digestion process was followed by another seven digestion cycles of the settled heart pieces. All digests were pooled into the same 50-ml falcon centrifuge tube which was centrifuged at 150 *g* for 6 min at room temperature, and the supernatant was gently aspirated off. The cell pellet was then resuspended in 50 ml of equal volumes of medium I and medium II. 12.5 ml of the cell suspension were transferred into four uncoated 90-mm petri dishes, which were placed in an incubator at 37ºC, 5% CO_2 for 60-90 min, to allow non-myocyte cells to adhere. Following the 60-90 min incubation, the medium, containing mostly cardiomyocytes (>95%), was transferred into a new 50-ml falcon centrifuge tube and cell number was counted using the trypan blue exclusion test as described in Chapter 2 (section 2.2.3).

3.3.1.2 Cell culture of NRVMs and inhibition of fibroblast growth

Culture 6-well plates (Thermo Fisher Scientific, Nalge Nunc International) were pre-coated with gelatin by placing 2 ml of 1% (w/v) gelatin (Sigma-Aldrich) solution into each well for 2 hours at 37^{o}C under sterile conditions and then washed with pre-warmed sterile PBS, prior to use. NRVMs were plated at a density of 2×10^{6} cells per well on gelatin-coated 6-well culture plates and maintained in plating medium for 24 hours. The medium was then replaced with serum-free maintenance medium containing 4:1 (v/v) DMEM:M199, supplemented with 100 IU/ml penicillin and 100 μg/ ml streptomycin for 48 hours prior to experimentation. Fibroblast growth was inhibited by the addition of 20 μM cytosine arabinoside (AraC), a DNA replication inhibitor, in the maintenance medium for 48 hours (Mesquita et al., 2014). Plates were incubated at 37°C in a humidified incubator (5% CO_2 and 95% air).

3.3.2 Inhibition of 26S proteasome activity in ARVMs

Freshly isolated ARVMs were cultured as described in Chapter 2 (section 2.2.2). Compound MG132 (TOCRIS, USA), a potent cell-permeable inhibitor (IC_{50} = 100 nM) of the 26S proteasome (Lee and Goldberg, 1996; Tsubuki et al., 1996), was used in ARVMs to reduce the 26S proteasome-mediated degradation of the ubiquitin-conjugated cellular protein. Cultured ARVMs were treated with 1 µM of MG132 (dissolved in sterile-filtered DMSO; final concentration of 0.1% (v/v) DMSO in the cell culture) for 0, 2, 4, 8 and 24 hours at 37^{o}C, 5% CO_2. Samples were prepared for immunoblotting analysis as described in Chapter 2 (section 2.5.1).

3.3.3 Quantification of transcript levels of PP2ACα, PP2ACβ, PP4C and PP6C by qPCR analysis

Total RNA was isolated from H9c2 cardiomyocytes (~1.2×10^6 cells), NRVMs (~2×10^6 cells) and ARVMs (~1×10^7 cells), using an RNeasy Plus Mini kit (Qiagen) (section 2.4.1). The quality and quantity of total RNA samples and cDNA preparation were performed as described in Chapter 2 (section 2.4). Relative mRNA levels of all genes were measured by qPCR analysis using the comparative Cq method (Livak and Schmittgen, 2001; Schmittgen and Livak, 2008). Two candidate reference genes, β-actin (ACTB) and glyceraldehyde-3-phosphate dehydrogenase (GAPDH), were validated by the BestKeeper© v1.0 software (Pfaffl et al., 2004) and used for normalisation. Data were presented in a graph as fold change ($2^{-\Delta\Delta Cq}$) of the mRNA expression of type 2A protein phosphatase catalytic subunits relative to PP2ACα (calibrator gene) mRNA expression.

3.3.4 Comparison of PP2ACα, PP2ACβ, PP4C and PP6C mRNA expression by qPCR analysis in NRVM with and without cytosine arabinoside (AraC)

Total RNA isolation, validation and cDNA preparation were performed as described in Chapter 2 (section 2.4). Fold change in the mRNA expression of either PP2ACα, PP2ACβ, PP4C or PP6C in NRVMs treated with 20 μM AraC, relative to the mRNA expression in the untreated NRVMs, was calculated based on the qbase^{+} software approach (Hellemans et al., 2007) and presented in a graph. Two candidate reference genes, ACTB and GAPDH, were validated by the BestKeeper© v1.0 software (Pfaffl et al., 2004) and used in combination for more accurate normalisation (Vandesompele et al., 2002; Bustin et al., 2009). Selection of differentially expressed genes, relevant to biological response, was based on fold difference in the relative mRNA expression (≥2-fold down- or upregulation) with a *P*-value ($p<0.05$) cut-off (Guo et al., 2006; Huang et al., 2015; Qin et al., 2015; Song et al., 2015; Sun et al., 2016).

3.3.5 Western blotting analysis

Protein sample preparation, SDS-PAGE and immunoblotting analysis were performed as described in Chapter 2 (section 2.5) to detect the expression of total PP2AC (both PP2ACα, PP2ACβ), PP4C, PP6C and ubiquitin in H9c2 cardiomyocytes, NRVMs and ARVMs. Details about the antibodies and working dilutions used in this chapter are presented in table 2.3.

3.4 Results

3.4.1 Transcript expression profile of type 2A protein phosphatases in H9c2 cardiomyocytes, NRVMs and ARVMs

The transcript expression profile of the type 2A protein phosphatase catalytic subunits was examined in rat embryonic heart-derived H9c2 cell line, neonatal and adult cardiomyocytes. The first step in this process was to validate the quality of RNA isolated from H9c2 cardiomyocytes, NRVMs and ARVMs, followed by an evaluation of the candidate reference genes and finally mRNA quantification using qPCR analysis as described below.

3.4.1.1 Validation of RNA quality for qPCR analysis

Total RNA samples, showing an absorbance ratio of A260/A280 ≥2.0 and A260/A230 >1.8, were considered to be of high purity and were further tested for RNA integrity. The RNA integrity of total RNA samples isolated from H9c2 cardiomyocytes or ARVM was initially evaluated by electrophoresis in agarose gels. As shown in figure 3.1, all ribosomal RNA bands had discernible lower edges, indicating good RNA quality. The RNA integrity was then determined using a 2100 Bioanalyzer (Agilent Technologies). The RNA integrity number (RIN) values scored 9.5-10.0, 7.3-8.8 or 7.4-8.7, when total RNA was isolated from H9c2 cardiomyocytes, NRVMs or ARVMs, respectively. As expected, RNA integrity was better preserved (RIN >9.0) in total RNA samples isolates from a cell line compared to isolations from primary cells (Fleige and Pfaffl, 2006; Schroeder et al., 2006). As it can be seen in figure 3.2, clear 18S and 28S ribosomal peaks were present in all the samples, even though additional peaks were present at samples with RIN scores between 7 to 9. These data suggested isolation of good-quality RNA which could be used in qPCR analysis (Fleige and Pfaffl, 2006; Schroeder et al., 2006).

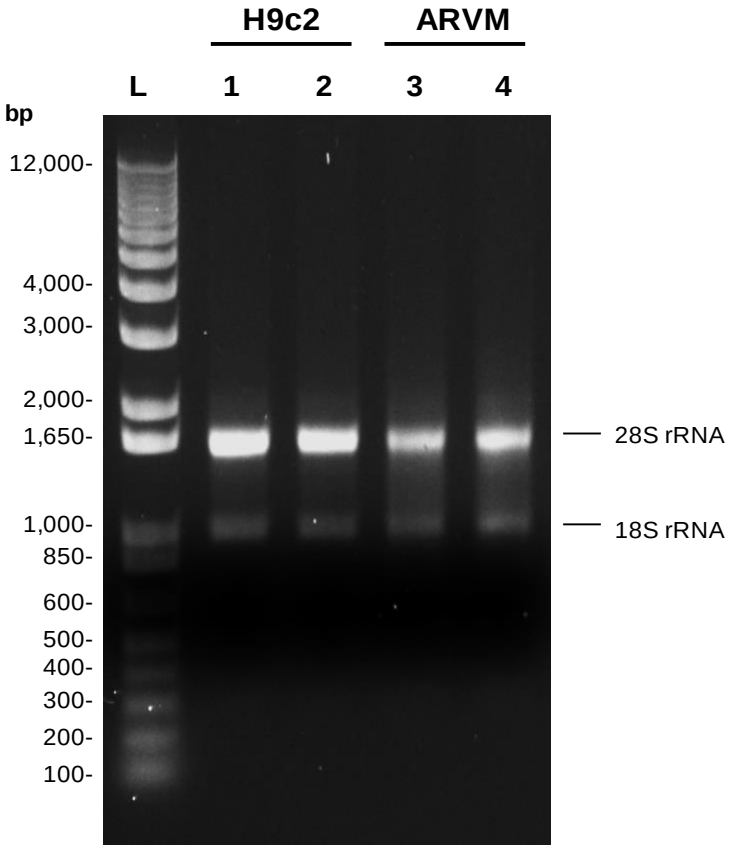

Figure 3.1 Electrophoresis of total RNA isolated from H9c2 cardiomyocytes (lanes 1-2) or ARVMs (lanes 3-4). 100-200 ng of total RNA was run on 1% (w/v) agarose gel. A 1kb Plus DNA ladder was run alongside the samples (lane L). Data are representative of three individual RNA isolations.

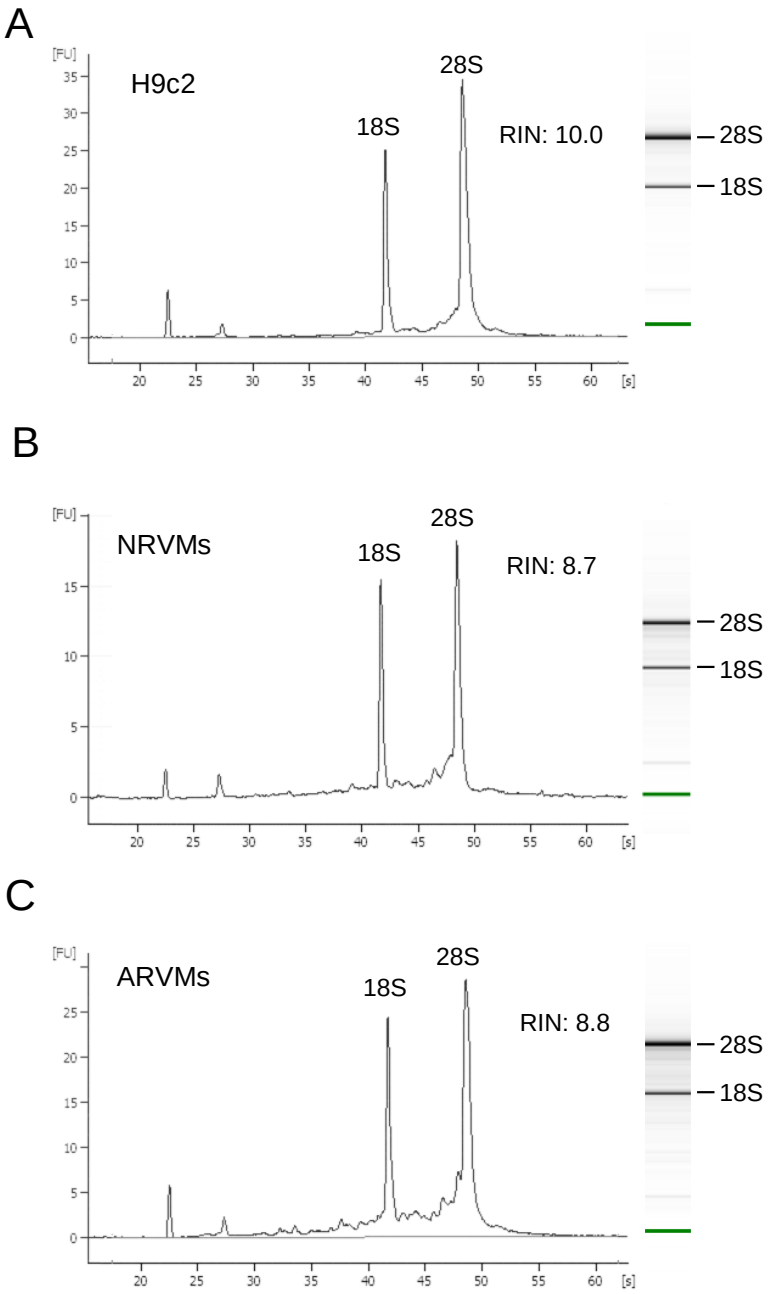

Figure 3.2 Electropherograms and calculated RIN values of total RNA obtained by the RNeasy protect cell mini kit (Qiagen) from (**A**) H9c2 cardiomyocytes, (**B**) NRVMs or (**C**) ARVMs. Total RNA was analysed using an Agilent RNA 6000 Nano Assay and 2100 Bioanalyzer (Agilent Technologies). The two peaks represent the 28S and 18S ribosomal RNAs. Data are representative of three individual RNA isolations.

3.4.1.2 Validation of ACTB and GAPDH reference genes

Two candidate reference genes, GAPDH and ACTB, were validated for data normalisation. The SD of the average Cq values, the coefficient variation (CV) and the Pearson coefficient of correlation (r) were estimated by the BestKeeper© v1.0

software (Pfaffl et al., 2004) for each reference gene across the three biological replicates in each cell type (H9c2 cardiomyocytes, NRVMs and ARVMs), which are shown in table 3.1. The reference genes, ACTB and GAPDH, had an SD less than 1, showed very strong correlation ($0.96 \leq r \leq 1$) and had a low coefficient variation (CV≤3.2%). According to these data, both reference genes met the criteria determined by Pfaffl et al. (2004), showing high stability across the biological replicates and were considered suitable for use in the subsequent qPCR analysis.

Table 3.1 Expression stability of the reference genes (ACTB and GAPDH) in H9c2 cardiomyocytes, NRVMs and ARVMs, was determined by calculating the coefficient variation (CV), standard deviation (SD) and Pearson coefficient of correlation (*r*), of each candidate reference gene Cq values (n=3), using the BestKeeper© v1.0 software (Pfaffl et al., 2004).

Cell type	Reference gene	CV (%)	SD	*r*
H9c2 cardiomyocytes	ACTB	0.99	0.17	1.00
	GAPDH	2.31	0.42	1.00
NRVMs	ACTB	3.02	0.59	1.00
	GAPDH	2.09	0.40	1.00
ARVMs	ACTB	3.32	0.69	0.98
	GAPDH	2.29	0.41	0.96

3.4.1.3 mRNA expression levels of PP2ACα, PP2ACβ, PP4C and PP6C in H9c2 cardiomyocytes, NRVMs and ARVMs

Prior to qPCR data analysis, the Cq values of PP2ACα, PP2ACβ, PP4C, PP6C, GAPDH or ACTB genes in the unknown samples were compared with the ones in the no-RT or no-template control reactions, to estimate the percentage of genomic DNA contamination. In all unknown samples, difference in the Cq values of each gene between the no-RT or no-template control reactions and the unknown samples

was equal to or higher than 5 Cq, showing that 3% or less of the amplification in the unknown samples was attributable to unwanted signals (e.g. genomic DNA template), therefore, it was considered not significant.

The mRNA expression of PP2ACβ, PP4C and PP6C relative to the expression of PP2ACα mRNA was determined in H9c2 cardiomyocytes, NRVMs and ARVMs (Figure 3.3). In H9c2 cardiomyocytes, PP2ACβ mRNA expression was significantly ($p<0.05$) higher (1.22-fold), while PP4C and PP6C mRNA expression was significantly ($p<0.05$) less (2.05-fold and 2.94-fold, respectively) compared to the PP2ACα mRNA expression levels (Figure 3.3A), when data was normalised to either ACTB or GAPDH reference genes. In NRVMs, the mRNA expression of PP2ACβ was significantly ($p<0.05$) higher (3.26-fold change) compared to the PP2ACα mRNA expression levels (Figure 3.3B). On the other hand, PP4C and PP6C mRNA expression levels were less expressed (2.91-fold and 5.40-fold, respectively), relative to the mRNA expression levels of PP2ACα, however, these results were not statistically significant (Figure 3.3B). The same results were confirmed when data were normalised to either ACTB or GAPDH reference genes. In ARVMs, mRNA levels of PP2ACβ, PP4C and PP6C were significantly less expressed (2.72-fold, 15.32-fold and 5.57-fold, respectively), compared to the PP2ACα mRNA expression levels (Figure 3.3C) upon data normalisation with either ACTB or GAPDH reference genes. These data showed that all genes, encoding the type 2A protein phosphatase catalytic subunits, were transcribed in H9c2 cardiomyocytes, NRVMs and ARVMs. In addition, relative mRNA expression levels of PP2ACα, PP2ACβ, PP4C and PP6C, normalised with either ACTB or GAPDH, were identical, therefore, for simplicity, only data normalised with ACTB were shown and discussed. Interestingly, as it can be seen in figures 3.3A and 3.3C, the relative mRNA expression profile of PP2ACα,

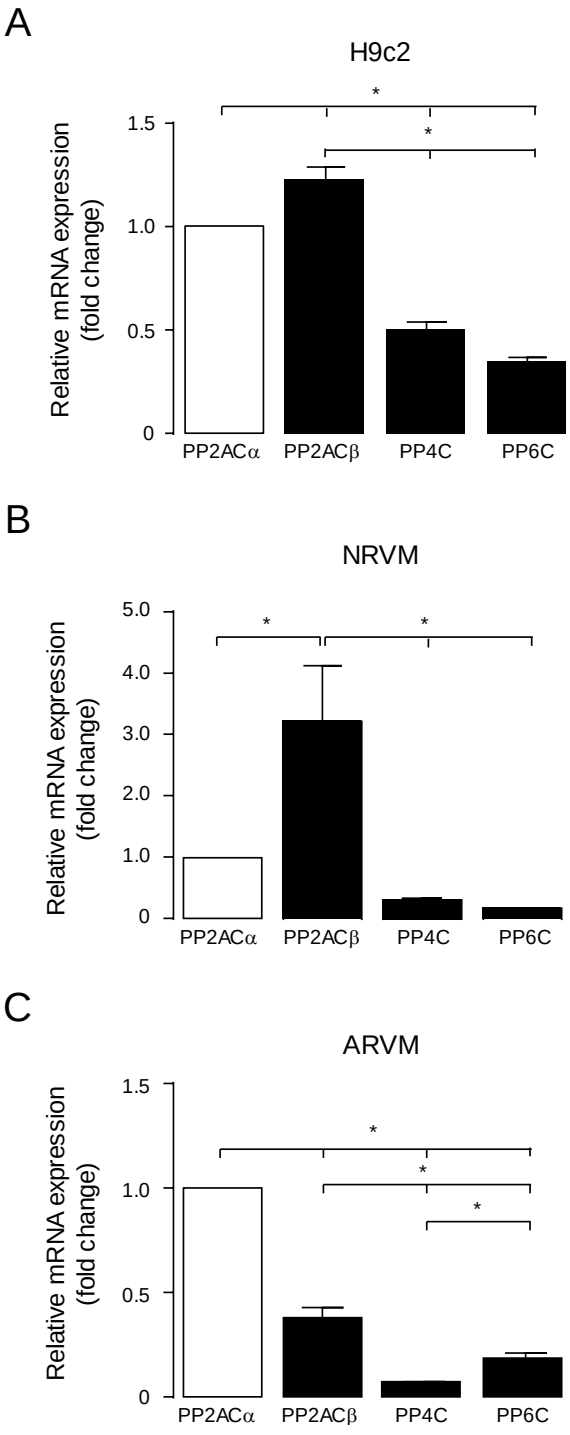

Figure 3.3 Fold change of the mRNA expression levels of the catalytic subunits of type 2A protein phosphatases, relative to PP2ACα mRNA expression and normalised with ACTB (or GAPDH) (PrimerDesign) in (**A**) H9c2 cardiomyocytes, (**B**) NRVMs and (**C**) ARVMs was validated by qPCR analysis and calculated by the comparative Cq method. Values are plotted as mean ± SEM of three biological replicates (RNA isolations), run in duplicate reactions. Statistical comparison was made by one-way ANOVA followed by Tukey's post-hoc multiple comparisons tests; *p<0.05.

PP2ACβ, PP4C and PP6C appears to differ between H9c2 cardiomyocytes (PP2ACβ>PP2ACα>PP4C>PP6C) and ARVMs (PP2ACα>PP2ACβ>PP6C>PP4C). On the other hand, the relative mRNA expression profile of type 2A protein phosphatase catalytic subunits in NRVMs (PP2ACβ>PP2ACα≃PP4C≃PP6C) was similar to the H9c2 cardiomyocytes (Figures 3.3A and 3.3B).

3.4.2 Effects of cytosine arabinoside (AraC) treatment in the mRNA expression levels of PP2ACα, PP2ACβ, PP4C and PP6C in NRVMs

To determine whether the transcript expression of type 2A protein phosphatase catalytic subunits in NRVMs may be affected by fibroblast contamination in the culture, the mRNA levels of PP2ACα, PP2ACβ, PP4C and PP6C were determined and compared by qPCR in untreated NRVMs and NRVMs treated with 20 μM cytosine arabinoside (AraC) to inhibit fibroblast growth (Novoyatleva et al., 2010; Mesquita et al., 2014; Sun et al., 2014).

3.4.2.1 Validation of RNA quality for qPCR analysis

Total RNA samples with an absorbance ratio A260/A280 ≥2.0 and A260/A230 >1.8, were considered to be of high purity and were tested for RNA integrity by a 2100 Bioanalyzer (Agilent Technologies). The RNA integrity number (RIN) values scored between 7.4 to 8.7. As it can be seen in figure 3.4, all the samples showed clear 18S and 28S ribosomal peaks, even though additional peaks were present. These data suggested isolation of RNA with good quality that could be used for qPCR analysis.

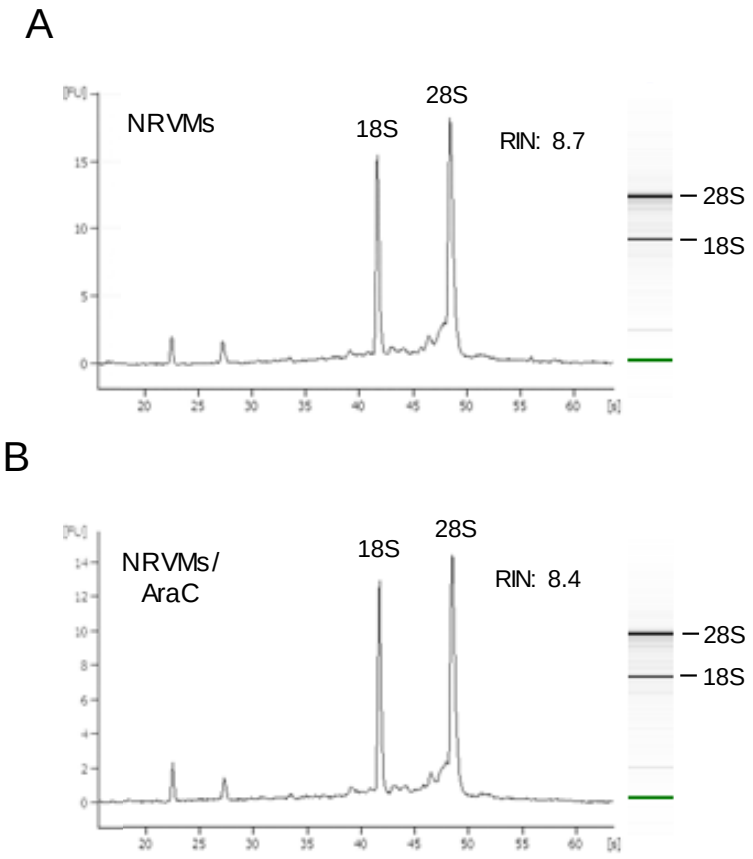

Figure 3.4 Electropherograms and calculated RIN values of total RNA obtained by the RNeasy protect cell mini kit (Qiagen) from (**A**) untreated NRVMs and (**B**) treated with 20 µM cytosine arabinoside (AraC) for 48 hours. Total RNA was analysed using an Agilent RNA 6000 Nano Assay and 2100 Bioanalyzer (Agilent Technologies). The two peaks represent the 28S and 18S ribosomal RNAs. Data are representative of three individual RNA isolations.

3.4.2.2 Validation of ACTB and GAPDH reference genes

Two reference genes, ACTB and GAPDH, were validated across all the biological replicates and experimental conditions by the BestKeeper© v1.0 software (Pfaffl et al., 2004) to decide whether they were appropriate for further use. Table 3.2 shows that both ACTB and GAPDH had SD of less than 1 and showed low coefficient variation (CV≤3.45%) and significantly ($p<0.001$) strong correlation ($r\cong1$). Therefore, both reference genes were considered stable and suitable for use in qPCR analysis (Pfaffl et al., 2004). In addition, an unpaired Student's t-test among the Cq values of each reference gene in NRVMs with and without AraC treatment showed no significant differences.

Table 3.2 Expression stability of the reference genes (ACTB and GAPDH) in untreated NRVMs and NRVMs treated with cytosine arabinoside (AraC) was determined by calculating the coefficient of variation (CV), standard deviation (SD) and coefficient of correlation (*r*), of each candidate reference gene Cq values (n=6), using BestKeeper© v1.0 software.

Cell type	Reference gene	CV (%)	SD	*r*
NRVMs	ACTB	3.02	0.59	1.00
	GAPDH	2.09	0.40	1.00
NRVMs (AraC)	ACTB	2.72	0.53	1.00
	GAPDH	3.45	0.66	1.00

3.4.2.3 Comparison of mRNA expression levels of PP2ACα, PP2ACβ, PP4C and PP6C in NRVMs with and without cytosine arabinoside (AraC)

First, the Cq values of PP2ACα, PP2ACβ, PP4C, PP6C, GAPDH or ACTB genes in the unknown samples were compared with the ones in the no-RT or no-template control reactions, to evaluate the percentage of genomic DNA contamination. In both untreated NRVM and NRVM treated with 20 µM AraC, the Cq values of each gene in the unknown samples differed from the no-RT or no-template control reactions at least 5 Cq values, suggesting that 3% or less of the amplification in the unknown samples was attributable to the genomic DNA template and was considered not significant.

The mRNA expression levels of type 2A protein phosphatase catalytic subunits were determined in NRVMs treated with AraC relative to the ones in the untreated NRVMs. Figure 3.5 shows that the mRNA expression levels of PP2ACα (1.19-fold change), PP2ACβ (1.23-fold change), PP4C (1.30-fold change) and PP6C (1.01-fold change) in NRVMs treated with AraC were not significantly altered compared to the mRNA expression levels in the untreated NRVMs. These data suggest that: i) the

AraC treatment does not significantly affect the mRNA expression of the type 2A protein phosphatase catalytic subunits in NRVMs and ii) fibroblast contamination can be considered minimal in the untreated NRVMs.

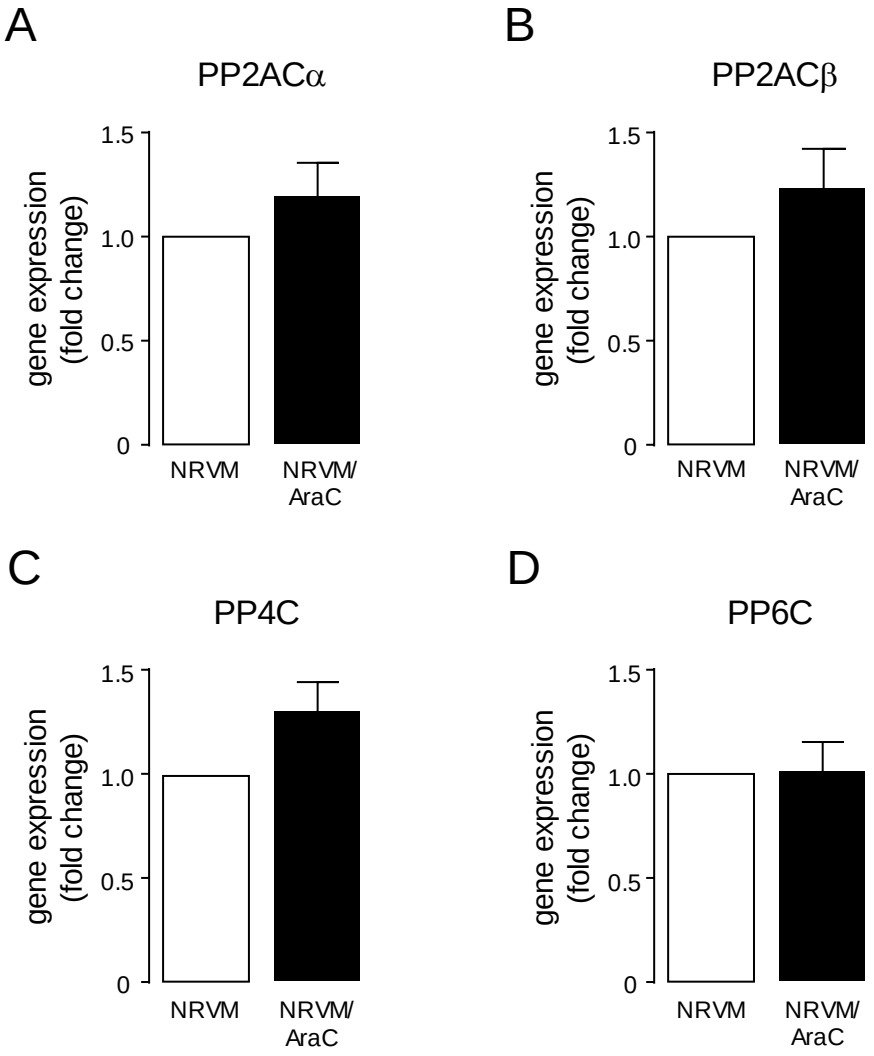

Figure 3.5 Fold change of the mRNA expression levels of (**A**) PP2ACα, (**B**) PP2ACβ, (**C**) PP4C and (**D**) PP6C in NRVMs treated with 20 µM cytosine arabinoside (AraC) for 48 hours, relative to the expression levels in the untreated NRVMs and normalised with multiple reference genes (ACTB and GAPDH), was calculated using the the qbase^{+} software approach. Data represent mean values ± SEM of three individual biological replicates. Statistical comparison was made by a two-tailed unpaired Student's t-test. No significant changes were observed between the untreated NRVM and treated with AraC.

3.4.3 Detection of protein expression of PP2AC, PP4C and PP6C in cardiomyocytes

The protein expression of type 2A protein phosphatase catalytic subunits was

investigated in rat embryonic heart-derived H9c2 cardiomyocytes and ARVMs. Figure 3.6A shows that total PP2AC was not significantly different between H9c2 cardiomyocytes and ARVMs. Surprisingly, PP4C protein expression was not detected in ARVM lysates, whilst it was expressed in H9c2 cardiomyocytes (Figure 3.6B). Furthermore, PP6C expression was significantly ($p<0.05$) higher (3.4-fold) in ARVM compared to the H9c2 cardiomyocytes.

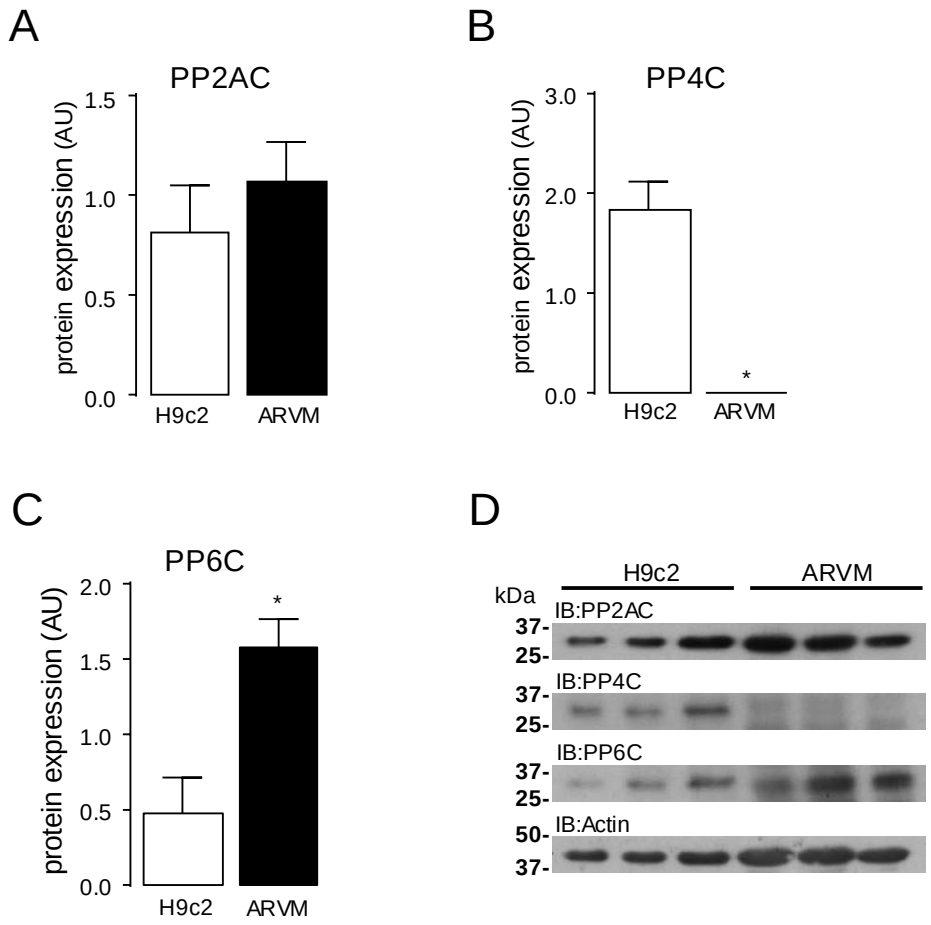

Figure 3.6 Protein expression of the type 2A protein phosphatase catalytic subunits, in H9c2 cardiomyocytes and ARVMs, was analysed by SDS-PAGE (using 12% polyacrylamide gels) and immunoblotting using catalytic subunit-specific antibodies to PP2AC, PP4C and PP6C. Protein levels of (**A**) total PP2AC, (**B**) PP24C and (**C**) PP6C were quantified by densitometry and normalised to actin. All data represent mean values ± SEM of three individual experiments (cell lysates). Statistical comparison was made by a two-tailed unpaired Student's t-test; *$p<0.05$. (**D**) Representative immunoblots (IB) of total PP2AC, PP4C and PP6C protein expression.

In addition, the expression of type 2A protein phosphatases was determined in NRVMs with and without AraC. Figure 3.7 (A-C) shows that total PP2AC, PP4C

and PP6C protein expression was not significantly altered in NRVMs treated with AraC when compared to the untreated NRVMs.

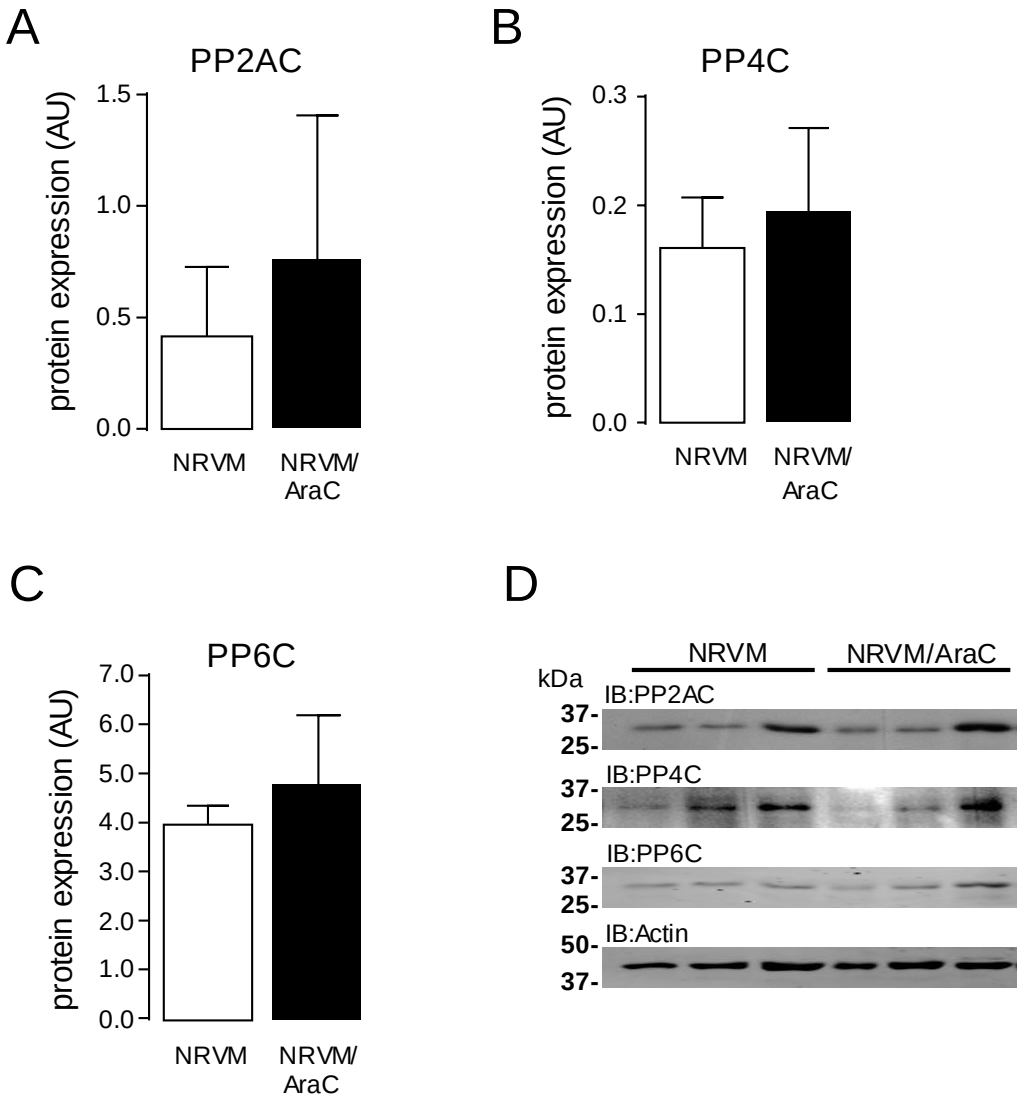

Figure 3.7 Protein expression of the type 2A protein phosphatase catalytic subunits, in untreated NRVMs and NRVMs treated with 20 µM cytosine arabinoside (AraC) for 48 hours, was determined by immunoblotting analysis, using subunit-specific antibodies to PP2AC, PP4C and PP6C. Prior to immunoblotting, proteins from each sample were resolved by SDS-PAGE (on 12% polyacrylamide gels). Levels of (**A**) total PP2AC, (**B**) PP4C and (**C**) PP6C protein expression were quantified by densitometry or LI-COR Odyssey® CLx Imaging System and normalised to actin. All data represent mean values ± SEM of three individual experiments (cell lysates). Statistical comparison was made by a two-tailed unpaired Student's t-test. No significant changes were observed between the untreated NRVM and treated with AraC. (**D**) Representative immunoblots (IB) of total PP2AC, PP4C and PP6C protein expression.

Taken together, these data showed that total PP2AC and PP6C were expressed at the

protein level in H9c2 cardiomyocytes, NRVMs and ARVMs whilst, PP4C expression was detected only in H9c2 cardiomyocytes and NRVMs, indicating a differential protein expression of PP4C during cardiomyocyte development. Furthermore, the protein expression levels of type 2A protein phosphatase catalytic subunits were not significantly altered in NRVMs with and without AraC treatment.

3.4.4 Effect of proteasome-mediated degradation in type 2A protein phosphatase catalytic subunits expression in ARVMs

As shown in figure 3.6B, PP4C protein expression was not detected in ARVMs, whereas transcription of PP4C mRNA was detected (Figure 3.3C). A possible explanation for these results could be that the 26S proteasome mediates degradation of PP4 in ARVM. Therefore, the compound MG132 was used to inhibit proteasome activity in ARVMs. Figure 3.8A clearly shows that levels of protein ubiquitination were elevated after 4-24 hours exposure of ARVMs to 1 μM MG132. As it can be seen in figures 3.8C and 3.8E, the protein expression of total PP2AC and PP6C was not significantly ($p=0.47$ and $p=0.64$, respectively) altered, following MG132-mediated proteasome inhibition for 2-24 hours, compared to the untreated cells. Interestingly, in figure 3.8B, western blotting revealed an apparent increase in PP4C protein levels in samples where proteasome activity was inhibited for two or more hours, compared to the untreated ARVMs. Even though the data in figure 3.8D were not statistically significant ($p=0.22$) due to experimental variability/ difficulty in quantification, these results indicate that the protein expression levels of PP4C may be regulated by the 26S proteasome-mediated degradation mechanism, which could explain the absence of PP4C in the adult cardiomyocytes.

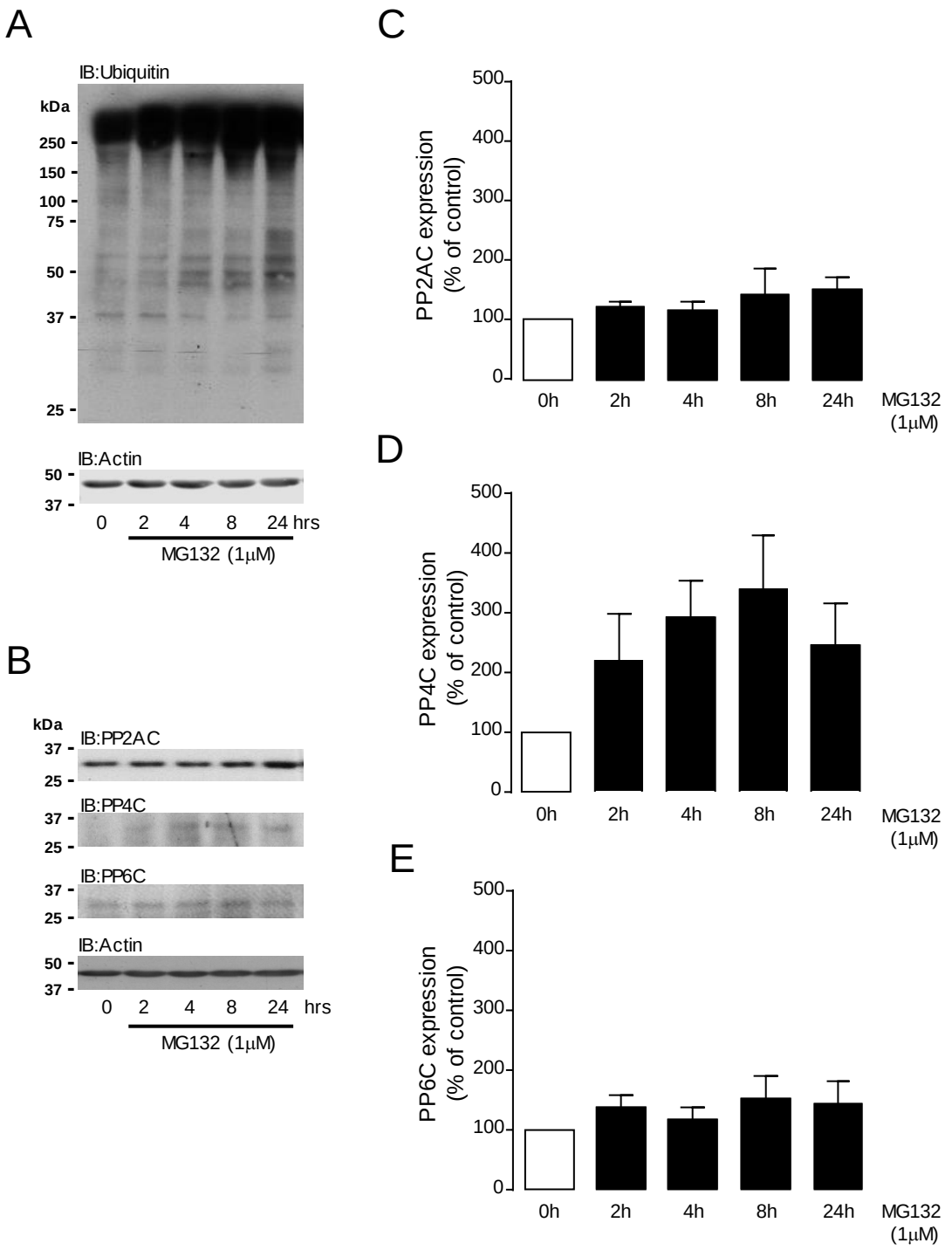

Figure 3.8 The expression of ubiquitin-conjugated cellular proteins and total PP2AC, PP4C and PP6C in cultured ARVMs, exposed to MG132 (1 μM) for 0, 2, 4, 8 and 24 hours, was analysed by SDS-PAGE (on 12% polyacrylamide gels) and immunoblotting, using an anti-ubiquitin antibody and subunit-specific antibodies to ubiquitin PP2AC, PP4C and PP6C. (**A-B**) Representative immunoblots (IB) of (**A**) ubiquitin-conjugated cellular proteins and (**B**) total PP2AC, PP4C and PP6C. Protein expression levels of (**C**) total PP2AC, (**D**) PP4C and (**E**) PP6C were quantified by densitometry or LI-COR Odyssey® CLx Imaging System and normalised to actin. All data represent mean values ± SEM of three individual experiments. Statistical analysis was performed with one-way Anova. No significant differences were observed (*vs* 0h).

3.5 Discussion

3.5.1 Expression of the type 2A protein phosphatase catalytic subunits in cardiomyocytes

Out of the three members of the type 2A protein phosphatase family (PP2A, PP4 and PP6), the protein expression and regulation of PP2A catalytic subunits (PP2ACα and PP2ACβ) in cardiomyocytes has been studied the most (Khew-Goodall and Hemmings, 1988; DeGrande et al., 2013; Longman et al., 2014) and has been shown to be associated with cardiac dysfunction and heart failure (Gergs et al., 2004; DeGrande et al., 2013; Hoehn et al., 2015; Li et al., 2016). Nonetheless, very little is known regarding the expression of PP4 and PP6 catalytic subunits (PP4C and PP6C respectively) in cardiac tissue.

H9c2 cardiomyocytes, NRVMs and ARVMs are widely used in cardiovascular research to explore signalling pathways associated with cardiac hypertrophy, calcium homeostasis and heart failure and to investigate potential cardioprotection targets (Simpson et al., 1982; Wang and Proud, 2002; Patten and Hall-Porter, 2009; Oyama et al., 2011; Wijnker et al., 2011; Shi et al., 2012; Pavlovic et al., 2013). An original finding of this study is that all type 2A protein phosphatase catalytic subunit transcripts were present in rat embryonic heart-derived H9c2 cardiomyocytes, as well as in neonatal and adult rat ventricular myocytes. Comparison of the mRNA relative expression profile of PP2ACα, PP2ACβ, PP4C and PP6C between the three cell types revealed great similarity between H9c2 cardiomyocytes (PP2ACβ>PP2ACα>PP4C>PP6C) and NRVMs (PP2ACβ>PP2ACα≃PP4C≃PP6C), while the relative transcript profile in ARVMs (PP2ACα>PP2ACβ>PP6C>PP4C) differed from the other two cell types (section 3.4.1.3). Furthermore, it was shown that total PP2AC and PP6C protein expression was detected in H9c2

cardiomyocytes, neonatal and adult rat ventricular myocytes (section 3.4.3). The latter results are in line with those observed in previous studies, reporting the expression of either PP2AC or PP6C subunits in the adult heart tissue (Khew-Goodall et al., 1991; Bastians and Ponstingl, 1996; Kloeker et al., 2003; Stefansson and Brautigan, 2006). In an earlier study, Brewis et al., (1993), reported the mRNA expression of PP4C in the rodent heart but did not investigate the protein expression levels (Brewis et al., 1993). Even though the PP4C transcript was present in H9c2 cardiomyocytes, NRVMs and ARVMs, at the protein level it was only detected in H9c2 cardiomyocytes and NRVMs. Interestingly, PP4C protein expression was not detected in ARVMs. The latter result is in agreement with Kloeker and co-workers' (2003) findings, showing that PP4C was either absent or of a very low abundance in rat adult cardiac tissue. Taken together, these results suggest that there may be an association between the type 2A protein phosphatase catalytic subunit expression and the heart developmental stage.

Myocardial overexpression of PP2ACα in transgenic mice has been shown to lead to severely impaired cardiac function, eccentric cardiac hypertrophy and dilated cardiomyopathy (Gergs et al., 2004; Hoehn et al., 2015). On the other hand, Dong et al. (2015) showed that conditional loss of PP2ACα in the postnatal mouse heart, at postnatal day 6.5, resulted in postnatal eccentric hypertrophy at postnatal day 11 but no cardiomyocyte disarray was observed. In the same study, Dong and co-workers (2015) claimed that conditional loss of PP2ACα in the adult mouse heart did not cause any visible phenotype (Dong et al., 2015). Another recent study by Li and co-workers, (2016), demonstrated that deletion of PP2ACα expression in the heart of adult mice led to cardiomyocyte hypertrophy after (10 days) or heart failure after (60 days), using a tamoxifen-inducible, myocardial cell-specific PP2ACα knockout mouse model (Li et al., 2016). Collectively, these studies outline a critical role for

PP2ACα in cardiac function and health, which is not yet fully understood, however, it appears to be strictly balanced. In addition, the last two studies indicate that PP2ACβ cannot compensate for the long-term absence of PP2ACα, suggesting that these catalytic subunits may have distinguished roles in cardiac function, despite having 97% amino acid sequence identity (Arino et al., 1988). Nonetheless, the role of PP2ACβ in cardiac function has remained unclear. In this chapter, the data suggested no significant differences in the total PP2AC protein expression between H9c2 cardiomyocytes and ARVMs, however, a significant difference in the relative mRNA expression between PP2ACα and PP2ACβ in each cell type was observed. In H9c2 cardiomyocytes, PP2ACβ mRNA expression was significantly ($p<0.05$) 1.22-fold higher and in ARVM significantly ($p<0.05$) 2.72-fold less compared to the PP2ACα mRNA expression levels. Furthermore, in NRVM, PP2ACβ mRNA was expressed significantly ($p<0.05$) 3.26-fold higher when compared to PP2ACα mRNA expression levels. Considering that total PP2AC protein has been shown to be under a strict autoregulatory mechanism at the level of translation (Baharians and Schonthal, 1998), it is tempting to suggest that although the total PP2AC protein expression was at a similar level in both H9c2 cardiomyocytes and ARVMs, the contribution of each catalytic subunit in the cell function of each of the above cell types and consequently NRVMs, may differ according to the differential stage of the cardiomyocytes (terminally differentiated or not). Nevertheless, without a specific antibody distinguishing between the two subunits, it is very hard to provide further evidence at the protein level.

As described in Chapter 1 (section 1.5.4.3), PP2AC subunits have been shown to be targeted for polyubiquitination and proteasome degradation (Trockenbacher et al., 2001; McConnell et al., 2010; Watkins et al., 2012; Udeshi et al., 2013; Xu et al., 2014). In addition, Xu et al. (2014), reported that both Lys48 and Lys63 ubiquitin

chains were formed in total PP2AC, suggesting that PP2AC polyubiquitination is not only linked with 26S proteasome-mediated degradation but may be involved in facilitating protein-protein interaction (Xu et al., 2014). Therefore, in this study, H9c2 cardiomyocytes were treated with MG132 to enhance the expression of polyubiquitinated PP2AC subunits. As figure 3.8C showed, the protein expression levels of the unmodified total PP2AC were not significantly altered. This result is not surprising as part of the total PP2AC content in the lysate would be expected to be subjected to polyubiquitination, however, no polyubiquitinated PP2AC was detected on the immunoblot. A possible explanation for this result could be that the signal may be below the limits of detection since polyubiquitinated proteins would be spread across the immunoblot due to different degrees of ubiquitination.

Even though the expression of PP6C in normal cardiac tissue was first identified by Bastians and Postingl, in 1996 (Bastians and Ponstingl, 1996), its regulation and involvement in cardiac function still remain unknown. A recent proteomic study revealed that PP6C has ubiquitination sites (Lys8, Lys132, Lys188, Lys219, and Lys231) (Udeshi et al., 2013), but there is no other report available, demonstrating the type of ubiquitination PP6C may undergo in native conditions. A study was conducted, presented in this chapter, to determine if PP6C undergoes proteasome-mediated degradation in ARVMs. Like PP2AC protein expression, the protein expression levels of the unmodified PP6C were not significantly changed even though the 26S proteasome was inhibited and no additional bands were identified on the immunoblot as ubiquitinated forms of PP6C.

The data in this chapter showed that PP4C protein levels were detected in H9c2 cardiomyocytes and NRVMs but not in ARVMs, even though the transcript was expressed, suggesting that PP4C expression may be developmentally regulated in cardiomyocytes. Furthermore, since a proteomic study of Udeshi et al. (2013),

showed that PP4C has ubiquitination sites (Lys26, Lys63, and Lys183) (Udeshi et al., 2013), the results in this chapter raised the possibility of PP4C to be post-translationally regulated in the ARVMs by a 26S proteasome-mediated degradation mechanism. To date, no other study has investigated the type of ubiquitin modifications in PP4C, except the one of Udeshi et al. (2013), in which PP4C endogenous ubiquitination sites were identified. Interestingly, in the present study, PP4C protein expression levels were detected when proteasome activity was inhibited by MG132 (2-24 hours). However, it was not possible to discern additional higher molecular weight protein bands on the immunoblot as ubiquitinated PP4C forms at this stage.

In early postnatal life, the growth of cardiomyocytes switches from hyperplastic to hypertrophic, however, this process is not yet well understood (Porrello et al., 2008; Bergmann et al., 2015). The data in this chapter suggested that PP4C expression may be developmentally adapted and regulated by a proteasome-mediated degradation system in the heart. Such a mechanism could explain why PP4C protein was expressed in the rat embryonic heart-derived H9c2 cell line and neonatal rat ventricular myocytes but was absent or at very low abundance in the adult rat ventricular myocytes, without proteasome inhibition treatment, whereas the PP4C transcript was present. The regulation of PP4C at the mRNA level has been proposed by Hu et al., (2001) to be developmentally dependent in the mouse. In their study, quantity and tissue-expression-preference for global PP4C mRNA were altered during embryonic development or between different adult tissues (Hu et al., 2001).

3.5.2 Effects of cytosine arabinoside (AraC) treatment on the expression of type 2A protein phosphatase catalytic subunits in NRVMs

Even if fibroblast contamination in NRVM culturing is expected to be less than 5%

(Punn et al., 2000), in many studies cytosine arabinoside (AraC) has been used to inhibit fibroblast growth in the culture (Tanaka et al., 1994; Novoyatleva et al., 2010; Mesquita et al., 2014; Sun et al., 2014). Therefore, the expression of type 2A protein phosphatases was examined in NRVMs treated with AraC, to exclude potential expression of these genes attributed to fibroblast contamination. The data in figures 3.5 and 3.7 show that type 2A protein phosphatase catalytic subunits were not significantly different at the mRNA and protein expression level in NRVMs with or without AraC, therefore, their expression in NRVMs was not affected by any fibroblast content or AraC treatment in the culture.

3.6 Summary

In summary, in this chapter, the relative mRNA expression profile of all type 2A family protein phosphatase catalytic subunits was shown to be similar in rat embryonic heart-derived H9c2 cell line and NRVMs and differed in ARVMs. The protein expression of all type 2A protein phosphatase catalytic subunits was detected in all cell types (H9c2 cardiomyocytes, NRVMs and ARVMs) except for PP4C in ARVMs, which was either absent or the signal was below the limits of detection. However, PP4C was detected in ARVM only when the proteasome was inhibited. PP2ACβ mRNA was abundant in H9c2 cardiomyocytes and NRVM whilst, PP2ACα mRNA was most abundant in ARVM. Furthermore, total PP2AC protein expression was similar in H9c2 cardiomyocytes and ARVM, however, PP6C protein content was greater in ARVM. In addition, it was shown that the expression of PP2ACα, PP2ACβ, PP4C and PP6C was not significantly altered in NRVM with and without fibroblast growth inhibition. Finally, since all type 2A protein phosphatase catalytic subunits were expressed in H9c2 cardiomyocytes, it was demonstrated that these cells could be further used as an appropriate model to investigate and distinguish the specificity of PP2ACα, PP2ACβ, PP4C and PP6C towards cardiac protein substrates associated with cardiac calcium homeostasis, DNA repair and hypertrophy.

Chapter 4

Characterisation of siRNA-Mediated Silencing of Type 2A Protein Phosphatase Catalytic Subunits and Alpha4 Regulatory Protein

4.1 Introduction

RNA interference (RNAi) defines the phenomenon of using small double-stranded (ds) RNA oligomers to inhibit gene expression. It was firstly described in 1998 by Fire and co-workers (Fire et al., 1998) in the nematode worm *C. elegans* and was later found in a wide range of organisms including plants (Waterhouse et al., 1998; Hamilton and Baulcombe, 1999) and mammals (Wianny and Zernicka-Goetz, 2000). Since then, RNAi has frequently been used as a tool for post-transcriptional gene silencing in basic science, allowing extensive characterisation of gene function in various organisms (Elbashir et al., 2001b; Zender et al., 2003; Bart et al., 2006; Zhou et al., 2006; Khatri and Rajam, 2007; Qin and Cheng, 2010; Troegeler et al., 2014).

4.1.1 siRNA-mediated RNAi mechanism

The presence of dsRNA in cells triggers the RNA interference (RNAi) machinery, a process that has been described extensively in the literature (Fire et al., 1998; Hamilton and Baulcombe, 1999; Hammond et al., 2000; Zamore et al., 2000; Bernstein et al., 2001; Rana, 2007). Figure 4.1 shows a simplified schematic

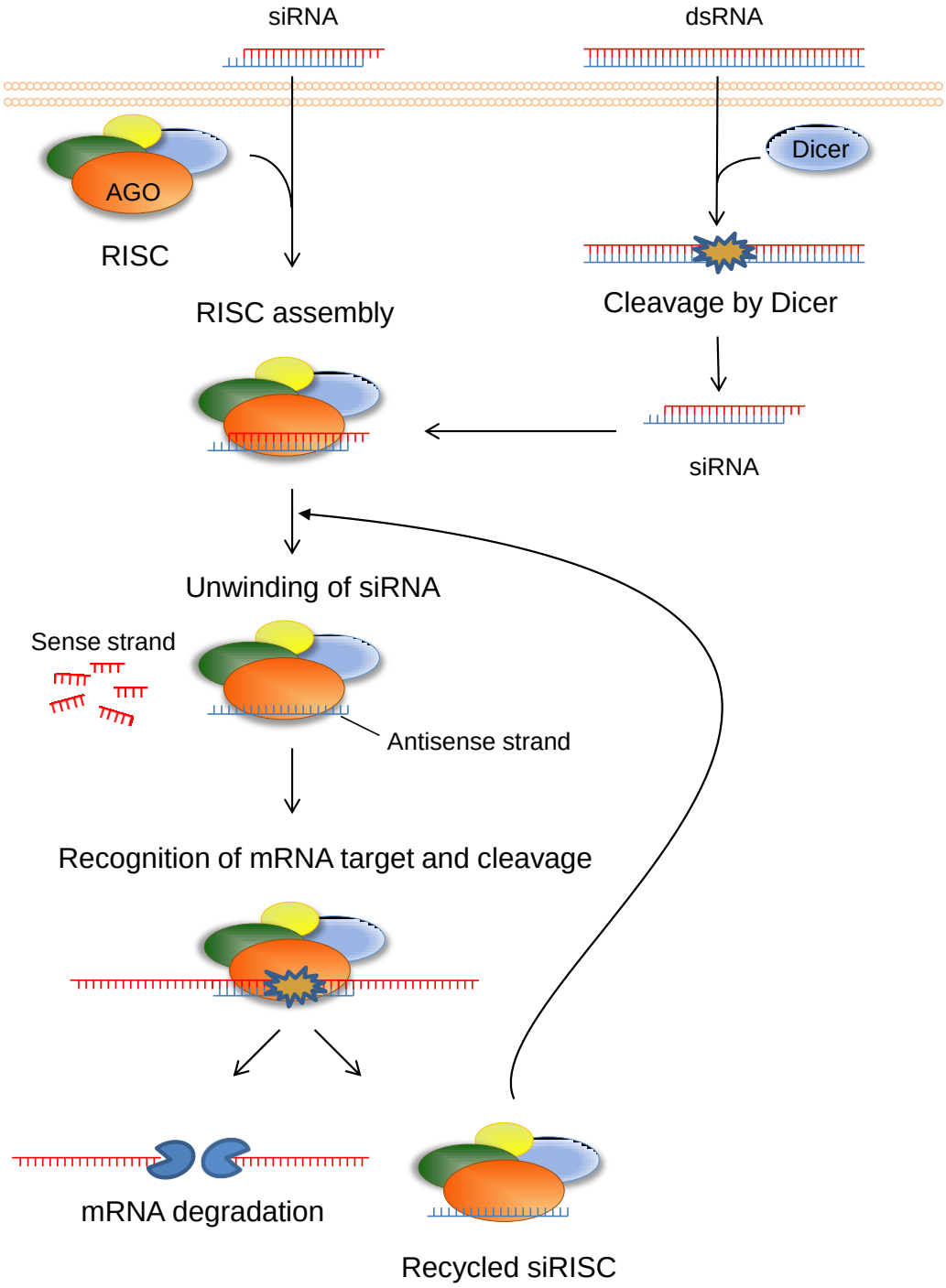

Figure 4.1 Simplified schematic representation of the RNAi mechanism (inspired by Rana, 2007). Long double-stranded RNA (dsRNA) is introduced into the cell and is cleaved into a small interfering RNA (siRNA) by Dicer. Alternatively, chemically synthesised siRNA can be introduced directly into the cell. The double stranded siRNA is then incorporated into the RNA-induced silencing complex (RISC) and is unwound, resulting in the cleavage of the sense strand of RNA by an argonaute protein (AGO) and released from RISC. The sense strand is further degraded by cellular nucleases, while the antisense strand guides the siRNA:RISC (siRISC) complex towards a target complementary mRNA, inducing mRNA degradation and resulting in suppression of protein expression. The mRNA is further degraded by cellular nucleases whereas, the siRISC complex can carry out multiple cleavage events.

overview, representing the RNAi process. Artificial siRNAs are commonly used in mammalian systems for gene expression silencing since long dsRNA (>30 bp) can activate the immune response during RNAi experiments (Nanduri et al., 1998; Elbashir et al., 2001b).

4.1.2 Overcoming the challenges of in vitro siRNA transfection

4.1.2.1 Off-target effects of siRNA transfection

Transfection of cells with siRNA can induce off-target effects that are sequence-specific and non-specific either by activation of an antiviral response, by binding to non-target mRNA or by saturating the RNAi machinery and can result in induction of cell toxicity or non-target gene silencing leading to inconsistent phenotypes (Jackson et al., 2003; Hornung et al., 2005; Judge et al., 2005; Lin et al., 2005; Birmingham et al., 2006; Jackson et al., 2006b; Robbins et al., 2008). The majority of the off-target effects can be avoided by chemical modifications in the siRNA synthesis. Furthermore, selection of appropriate controls is critical for accurate validation of off-target effects (Robbins et al., 2008).

In the studies presented in this dissertation, ON-TARGET plus™ SMARTpool siRNAs (GE Healthcare, Dharmacon) consisting of 19-20 bases were used, containing a chemical dual-strand modification pattern (patent pending), which enhances the assembly of the siRNA antisense strand with the RNA-induced silencing complex complex and reduces the off-targets effects for both strands up to 90% compared to unmodified siRNA (Birmingham et al., 2006; Jackson et al., 2006a; Birmingham et al., 2007; Anderson et al., 2008; Chen et al., 2008b). Both sense and antisense strands of the siRNA contain UU 3’overhangs, crucial for double siRNA stability thus enhancing siRNA-mediated gene silencing (Bolcato-Bellemin et al., 2007; Schmitz and Chu, 2011). The 5'end of the antisense strand of

siRNA is modified with a phosphate, which contributes to stabilising the siRNA binding to RNA-induced silencing complex, improving nuclease resistance of siRNAs and allowing their entry into the RNAi pathway (Nykanen et al., 2001; Ameres et al., 2007). Each ON-TARGET plus™ SMARTpool siRNA is a mixture of four individual SMARTselection™ algorithm-designed siRNAs (Birmingham et al., 2007) targeting one gene (SMARTpool) from which three are guaranteed to silence the gene expression at the mRNA level by at least 75% under optimised transfection and detection conditions.

4.1.2.2 In vitro cationic lipid-mediated siRNA delivery: mechanism and challenges

One of the most common methods for systemic *in vitro* siRNA delivery into cells is the transfection of siRNA complexed with cationic lipids (Malone et al., 1989; Felgner et al., 1994; Spagnou et al., 2004; Leal et al., 2010). Cationic lipids, consisting mainly of a positively charged head group, one or two hydrophobic chains and a linker bond in-between (reviewed in Mahato et al., 1997), entrap the negatively charged siRNAs creating lipoplexes (Zelphati and Szoka, 1996; Leal et al., 2010). The majority of cellular uptake of siRNA using cationic lipid compounds is processed via the endocytosis pathway, by binding of the positively charged lipoplexes to the negatively charged cell surface. The siRNA content is then deposited into endosomes, followed typically by lysosome relocation and degradation or endocytic recycling (Zelphati and Szoka, 1996; Lu et al., 2009). It was proposed that cationic lipids can promote endosomal escape, whereby the siRNA is released to the cytosol and is able to associate with the RNAi mechanism contributing to the transfection efficiency (Zelphati and Szoka, 1996; Lu et al., 2009). Indeed, in a recent study, Gujrati et al., (2014), showed evidence of the siRNA endosomal escape and release to the cytosol by confocal microscopy, using multifunctional cationic lipids. Nonetheless, Lu et al., (2009), suggested that even

though the majority of the siRNA lipoplexes enters the cell through endocytosis, the functional siRNA delivery is mainly mediated by direct fusion of a small fraction of the siRNA lipoplexes with the negatively charged cell membrane (Figure 4.2). In the same vein, Gilleron et al., (2013), estimated only 1-2% siRNA escape from endosomes in transfected Hela cells using lipid nanoparticles for siRNA delivery, whilst Ming et al., (2011) and Lazebnik et al., (2016) provided evidence supporting the concept of direct fusion of the lipoplexes with the cell membrane and release of functional siRNA into the cytosol.

Cationic lipid-mediated siRNA delivery may induce toxicity in cells. The chemical composition (Bottega and Epand, 1992; Felgner et al., 1994; Aberle et al., 1998; Gao and Hui, 2001; Basha et al., 2011) and concentration (Lappalainen et al., 1994) of the cationic lipid siRNA-carrier are influential factors of siRNA transfection performance and cytotoxicity. Studies have reported cationic lipid structures and formulations exhibiting good delivery of siRNA whilst exhibiting low toxic effects (Lu et al., 2009; Li et al., 2011; Sheng et al., 2014). This emphasises the importance of careful cationic lipid design and experimental cytotoxicity evaluation. Herein, a commercially available cationic lipid-based transfection reagent called DharmaFECT#1 (GE Healthcare, Dharmacon) was used, guaranteeing high siRNA transfection in H9c2 cardiomyocytes and low cellular toxicity under optimised conditions (Lu et al., 2009).

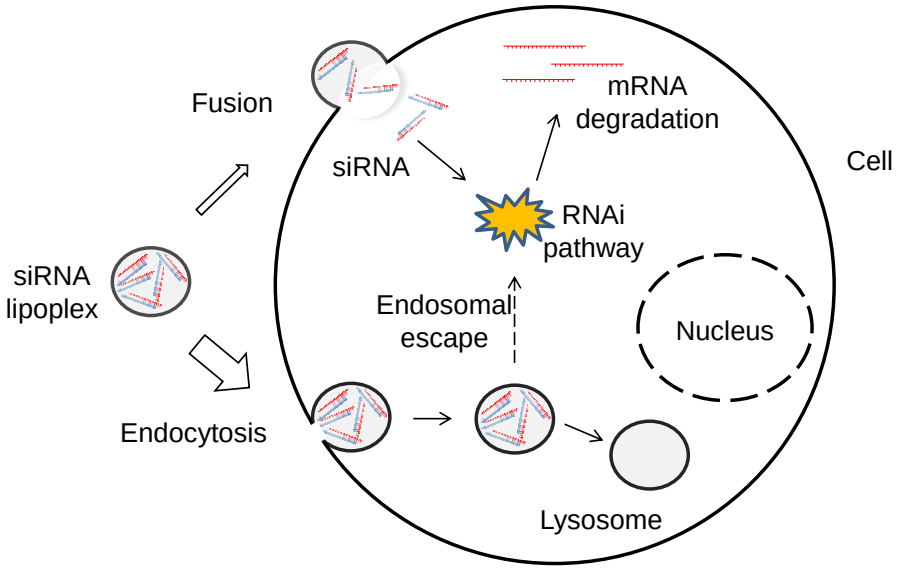

Figure 4.2 Schematic diagram of cationic lipid-mediated siRNA cellular uptake (redrawn from Lu et al., 2009). Although most of the siRNA lipoplexes cellular uptake is via endocytosis, the functional delivery of a fraction of the siRNA into the cell appears to be mediated by direct fusion between siRNA lipoplexes and the plasma membrane.

4.2 Specific objectives

In several studies, non-selective inhibitors towards the type 2A protein phosphatase catalytic subunits (PP2AC, PP4C and PP6C) have been used to investigate their role in cardiomyocytes and non-myocytes (discussed in section 4.5.1), leading to confusion about the specific targeting and potential therapeutic value of each member of this family. Therefore, siRNA-mediated knockdown technique was used to investigate the roles of individual type 2A protein phosphatase catalytic subunits (PP2ACα, PP2ACβ, PP4C, PP6C) in cardiac calcium handling and DNA repair (as shown in chapters 5 and 6) and the regulation of their expression by alpha4 (described in Chapter 4) in cardiomyocytes. Thus, the experiments presented in this study aim to:

1. increase the effectiveness of a successful, non-toxic transfection of rat PP2ACα-, PP2ACβ-, PP4C-, PP6C- and alpha4-siRNAs in H9c2 cardiomyocytes.

2. evaluate the specificity of the rat PP2ACα-, PP2ACβ -, PP4C- and PP6C-siRNAs towards the targeted genes and investigate the off-target and on-target effects of efficient PP2ACα, PP2ACβ, PP4C or PP6C mRNA and/ or protein expression knockdown towards the expression of the other catalytic subunits.

3. investigate the effects of alpha4 gene silencing on type 2A protein phosphatase catalytic subunit expression in H9c2 cardiomyocytes.

4.3 Methods

4.3.1 cDNA and protein sequence alignment

cDNA sequence of the rat PP2ACα, PP2ACβ, PP4C and PP6C genes was obtained from GenBank®[9] (Benson et al., 2000), the National Institutes of Health genetic sequence database. The open reading frame region was selected by BioEdit v7.1.3 software (Hall, 1999). The alignment between two open reading frame region sequences was performed by EMBOSS Needle[10] alignment tool (Rice et al., 2000). Protein amino acid sequence of rat PP2ACα, PP2ACβ, PP4C and PP6C was obtained by UniProtKB[11] (Magrane and UniProt Consortium, 2011). Multiple amino acid sequence alignment was performed by Clustal Omega[12] (Sievers et al., 2011).

4.3.2 Cell culture and IncuCyte® cell count proliferation assay

H9c2 cardiomyocytes were subcultured in 96 or 6-well plates as described in Chapter 2 (section 2.2). For the cell proliferation assay, cell culture confluency was monitored using an IncuCyte® ZOOM live-cell analysis system (Essen BioScience®, USA) according to the manufacturer's instructions. In brief, H9c2 cardiomyocytes were seeded in 96-well culture plates (100 µl per well) at appropriate experimental confluence density. The plates were placed in the IncuCyte inside a standard incubator (37ºC, 5% CO_2) and the instrument was typically programmed to take four pictures per well at two-hour intervals. The IncuCyte® microscope permits the automatic acquisition of multiple phase-contrast images. Images were analysed by the IncuCyte® ZOOM software v2015A to provide a

[9] Free accessed via the National Centre for Biotechnology Information (NCBI) website; http://www.ncbi.nlm.nih.gov/GenBank®/.
[10] Free accessed via the European Bioinformatics (EMBL-EBI) website; http://www.ebi.ac.uk/Tools/psa/emboss_needle/nucleotide.html.
[11] Free accessed via the Universal Protein Resource (UniProt) website; http://www.uniprot.org/help/uniprotkb.
[12] Free accessed via the European Bioinformatics (EMBL-EBI) website; http://www.ebi.ac.uk/Tools/msa/clustalo/.

representative statistical measure of confluence over longer periods of time, and the proliferation rate was calculated and presented in graphical form.

4.3.3 Optimisation of siRNA transfection in H9c2 cardiomyocytes

Efficient transfection of siRNA is crucial for effective gene silencing. To optimise the siRNA delivery conditions with minimal cell toxicity effects, cell confluency and transfection reagent concentrations were evaluated using appropriate controls and assigning a threshold of 80% cell viability.

General toxicity due to the transfection reagent DharmaFECT#1 (GE Healthcare, Dharmacon) in a specific cell density was tested. Cells were seeded in 96-well culture plates (100 µl per well) at 500, 1500 and 5000 cell density and were left to settle for 24 hours. The corresponding confluency was then estimated by an IncuCyte® ZOOM live-cell analysis system (approximately 15%, 30% and 50% respectively) and the medium was then replaced with transfection medium containing 0%, 0.1%, 0.2% or 0.4% (v/v) DharmaFECT#1 reagent only. For effective post-transcriptional silencing, cells were grown for 1-2 days (24-48 hours) for mRNA analysis and 2-4 days (48-96 hours) for protein analysis, whilst avoiding the overgrowth of cells. Cell proliferation was monitored by the IncuCyte® system for 4 days (section 4.3.2). Cell viability was measured by an MTT (3-(4, 5-dimethylthiazol-2-yl)-2, 5-diphenyltetrazolium bromide) assay as described previously (section 2.6) after 4 days of exposure to different concentrations of DharmaFECT#1.

Cytocompatible conditions of cell density and transfection reagent concentration, resulting in more than 80% cell viability without over confluency, were chosen to test the efficiency of siRNA delivery further. Cells were seeded in 96-well culture

plates (100 µl per well) at a subcultivation ratio of 1:10 and were left to settle for at least 24 hours. Once 30% confluency was reached, the medium was replaced by transfection medium containing 1% DharmaFECT#1 and 50 nM TOX Transfection Control siRNA (TOX-siRNA) or ON-TARGET plus™ Non-Targeting Control Pool (non-targeting control siRNA) (GE Healthcare, Dharmacon) which were used as a positive or a negative control, respectively. Successful cellular transfection of TOX Transfection Control siRNA promotes cell apoptosis within 24 to 48 hours (1-2 days), providing a simple method of measuring transfection efficiency. In contrast, ON-TARGET plus™ Non-Targeting Control Pool siRNA is designed for limited off-target effects against any known genes in human, mouse, or rat cells (Baum et al., 2010). For co-transfection experiments, cell viability was validated under the conditions of 0.2% (v/v) DharmaFECT#1 and 100 nM ON-TARGET plus™ Non-Targeting Control Pool siRNA. Cell viability was measured by MTT assay (section 2.6), at 1 and 4 days post-transfection.

4.3.4 Gene expression silencing of type 2A protein phosphatase catalytic subunits and alpha4 protein

The expression of PP2AC, PP4C, PP6C and alpha4 protein in H9c2 cardiomyocytes was suppressed by introducing rat catalytic subunit-specific siRNA:DharmaFECT#1 complexes into the cells as described in Chapter 2 (section 2.3.1). ON-TARGET plus™ rat PP2ACα (PP2ACα-siRNA), PP2ACβ (PP2ACβ-siRNA), PP4C (PP4C-siRNA), PP6C (siPP6-siRNA) and alpha4 (Alpha4-siRNA) siRNA SMARTpool (GE Healthcare, Dharmacon) was used to knockdown the PP2ACα, PP2ACβ, PP4C, PP6C and alpha4 expression respectively, with a ratio of 50 nM target-specific ON-TARGET plus™ SMARTpool siRNA: 0.1% (v/v) DharmaFECT#1 per well. ON-TARGET plus™ Non-Targeting Control Pool siRNA (non-targeting control siRNA) was used as a negative control with a ratio of 50 nM non-targeting siRNA:0.1%

(v/v) DharmaFECT#1 per well. Total PP2AC (both PP2ACα and PP2ACβ), PP4C, PP6C and alpha4 protein knockdown was detected by western blotting analysis and compared to the levels of the non-targeting control. Only PP2ACα and PP2ACβ mRNA knockdown were determined by qPCR analysis. A threshold of greater than 80% gene expression silencing was assigned for successful, non-toxic siRNA transfection.

4.3.5 Co-transfection of both PP2ACα and PP2ACβ siRNAs

To silence the expression of both PP2ACα and PP2ACβ simultaneously in H9c2 cardiomyocytes, both rat catalytic subunit-specific siRNAs, ON-TARGET plus™ rat PP2ACα (PP2ACα-siRNA) and PP2ACβ (PP2ACβ-siRNA) siRNA SMARTpool, were co-transfected into cells. Cells were seeded in 6-well plates at a subcultivation ratio of 1:10 and were left to settle for at least 24 hours. Once 30% confluency was reached, the medium was replaced by transfection medium (section 2.3.1). For transfection medium preparation, each siRNA:DharmaFECT#1 transfection mix was made separately, as described previously in Chapter 2 (section 2.3.1) and then added to an appropriate volume of antibiotic-free DMEM with 10% FBS, thereby achieving total siRNA concentration of 100 nM and 0.2% (v/v) DharmaFECT#1. ON-TARGET plus™ Non-Targeting Control Pool siRNA (non-targeting control siRNA): DharmaFECT#1 transfection mix was prepared in the same way and used as a negative control. Cells were incubated at 37°C in 5% CO_2 for 1-4 days and lysed for immunoblotting analysis as described in Chapter 2 (section 2.5). A threshold of greater than 80% gene silencing was assigned for successful, non-toxic siRNA transfection.

4.3.6 Verification of PP2ACα and PP2ACβ mRNA knockdown by qPCR analysis

After transfection of H9c2 cardiomyocytes with either ON-TARGET plus™ Non-

Targeting Control Pool siRNA (non-targeting control siRNA), used as a negative control, ON-TARGET plus™ rat PP2ACα (PP2ACα-siRNA) or PP2ACβ (PP2ACβ-siRNA) siRNA SMARTpool for 2 or 4 days (section 2.3.1), samples were collected and total RNA was extracted from ~$1x10^5$ or 1.5-$2x10^5$ cells respectively (section 2.4.1). Quality and quantity of total RNA were determined by NanoVue and RNA integrity was validated by a 2100 Bioanalyzer (Agilent Technologies) (section 2.4.2). The mRNA level of all genes was measured by qPCR analysis as described in Chapter 2 (section 2.4.5). Two candidate reference genes, ACTB and GAPDH, were validated by the BestKeeper© v1.0 software (section 2.4.5.1) and used in combination for more accurate normalisation. Fold change in the expression of PP2ACα or PP2ACβ in H9c2 cells transfected with either PP2ACα-siRNA or PP2ACβ-siRNA, relative to the cells transfected with non-targeting control siRNA, was calculated based on the qbase$^+$ software approach (section 2.4.5.3). Rank and selection of differentially expressed genes relevant to biological response was based on fold-change (FC) (FC≤0.5 or ≥2.0) with a *P*-value cut-off ($p<0.05$) (Guo et al., 2006; Huang et al., 2015; Qin et al., 2015; Song et al., 2015; Sun et al., 2016).

4.3.7 Verification of siRNA-mediated protein knockdown by western blotting analysis

Protein sample preparation, SDS-PAGE and western blotting analysis were performed as described in Chapter 2 (section 2.5) to detect the expression of alpha4, PP2AC (both PP2ACα and PP2ACβ), PP4C and PP6C in H9c2 cardiomyocytes. Details about the antibodies and working dilutions used in this chapter are presented in table 2.3.

4.4 Results

4.4.1 cDNA and protein alignment of PP2ACα, PP2ACβ, PP4C and PP6C

Effective siRNA-mediated degradation of the targeted mRNA results in the knockdown of protein expression corresponding to a particular gene. Therefore, it is important to analyse the target gene protein levels. Human PP2ACα and PP2ACβ share 97% amino acid identity (Arino et al., 1988), while all the type 2A protein phosphatase catalytic subunits share 60-65% amino acid homology (Kloeker et al., 2003). Similarly, homology of the amino acid sequences of rat PP2ACα and PP2ACβ, obtained from UniProtKB database, was 97.4% identical whilst, all type 2A protein phosphatase catalytic subunits share 49.4% identity in their amino acid sequence (Figure 4.3). These results indicate that the individual detection of rat PP2ACα and PP2ACβ by western blotting is extremely difficult however, detection of total PP2AC (both PP2ACα and PP2ACβ), PP4C and PP6C protein expression can be performed using catalytic subunit-specific antibodies as described by Kloeker and co-workers (Kloeker et al., 2003).

Table 4.1 shows that pair sequence alignment by EMBOSS Needle online tool between PP2ACα (NM_017039.2), PP2ACβ (NM_017040.1), PP4C (NM_134359.1) and PP6C (NM_133589.2) open reading frame of their cDNA sequences (obtained from GenBank®) revealed 59.2-64.7% nucleotide homology, with the exception of 81.6% nucleotide homology between PP2ACα and PP2ACβ pair alignment. This result highlights the importance of careful choice of the siRNA sequence used to silence the expression of PP2ACα, PP2ACβ, PP4C and PP6C to ensure specific interaction with the target mRNA.

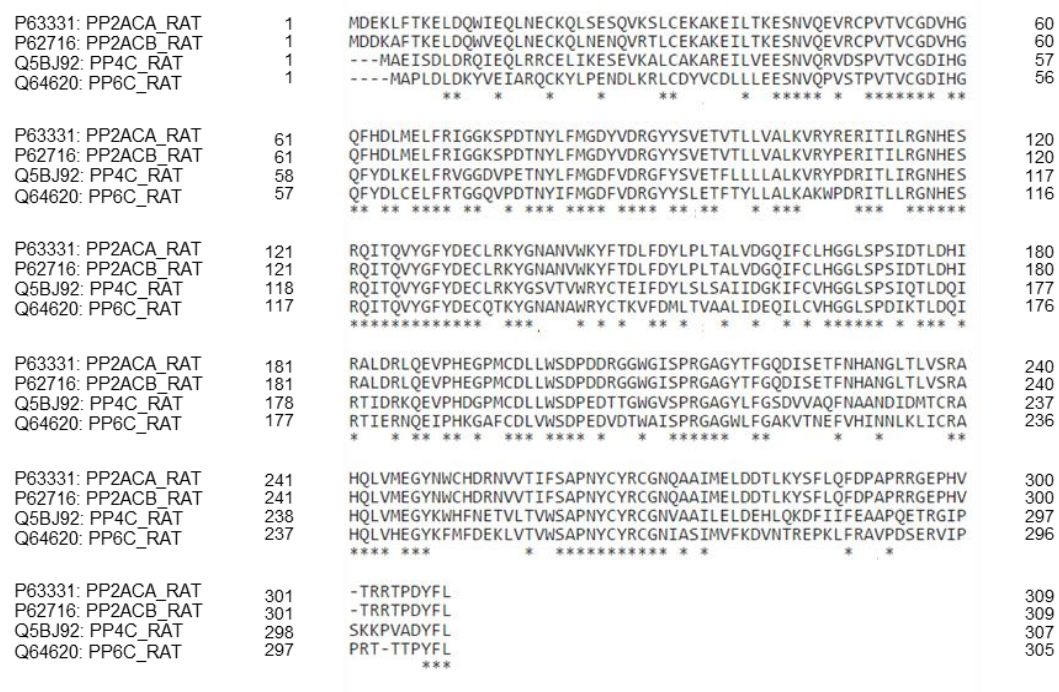

Figure 4.3 Multiple amino acid sequence alignment of PP2ACα (UniProtKB ID: P63331), PP2ACβ (UniProtKB ID: P62716), PP4C (UniProtKB ID: Q5BJ92) and PP6C (UniProtKB ID: Q64620) was performed by Clustal Omega multiple alignment tool. Amino acid residues indicated by an asterisk (*) are fully conserved.

Table 4.1 Open reading frame region sequence pair alignment by EMBOSS Needle online tool (Rice et al., 2000) of PP2ACα (GenBank® ID: NM_017039.2), PP2ACβ (GenBank® ID: NM_017040.1), PP4C (GenBank® ID: NM_134359.1) and PP6C (GenBank® ID: NM_133589.2).

Pairs	% Identity	% Gaps
PP2ACα - PP2ACβ	**81.6**	**0.2**
PP2ACα – PP4C	**64.7**	**12**
PP2ACα – PP6C	**60.6**	**17.9**
PP2ACβ – PP4C	**61.8**	**14.2**
PP2ACβ – PP6C	**59.2**	**19.9**
PP4C – PP6C	**61.9**	**15.2**

4.4.2 Confirmation of the sequence specificity of siRNAs molecules

PP2ACα (GenBank® ID: NM_017039.2), PP2ACβ (GenBank® ID: NM_017040.1),

PP4C (GenBank® ID: NM_134359.1) and PP6C (GenBank® ID: NM_133589.2) cDNA sequences were obtained from GenBank®. Each alignment showed >10 nt mismatches. Furthermore, alignment of each catalytic subunit-specific siRNA seed region (positions 1-8 nt) with the 3'-UTR of the non-target catalytic subunits, did not show 8 nt complementation. These data indicate that there is no efficient complementation between each catalytic subunit-siRNAs and the non-target catalytic subunit mRNA (open reading frame or 3'-UTR) to induce any sequence-dependent off-target effect.

4.4.3 The effects of siRNA delivery in H9c2 cardiomyocytes on viability and cell proliferation rate

4.4.3.1 DharmaFECT#1 concentration dependent screen

An initial objective of the project was to evaluate the silencing efficiency of the siRNA on protein expression of the targeted genes for up to 4 days post-transfection. Thus, the toxicity effects of the transfection reagent, DharmaFECT#1, in cell viability and proliferation rate in H9c2 cardiomyocytes was investigated, after 4 days of treatment. From figure 4.4A, it can be seen that cells seeded at 15% confluence density and treated with 0.2% or 0.4% (v/v) DharmaFECT#1 for 4 days, showed less than 80% viability (63.6 ± 1.8% or 42.6 ± 1.9 respectively). Cell viability was above 80% (87.4 ± 1.4%) only when cells were treated with 0.1% (v/v) DharmaFECT#1 for 4 days, while cell confluency reached ~60-70%. Figure 4.4B presents that cells seeded at 30% confluence and treated with 0.1% or 0.2% (v/v) DharmaFECT#1 for 4 days showed higher than 80% cells viability (87.9 ± 1.8% or 85.4 ± 3.6% respectively) and only when treated with 0.4% (v/v) DharmaFECT#1, they showed less than 80% viability (67.5 ± 7.6%). In addition, these cells reached approximately 80-90% confluency when treated with 0.1% or 0.2% DharmaFECT#1

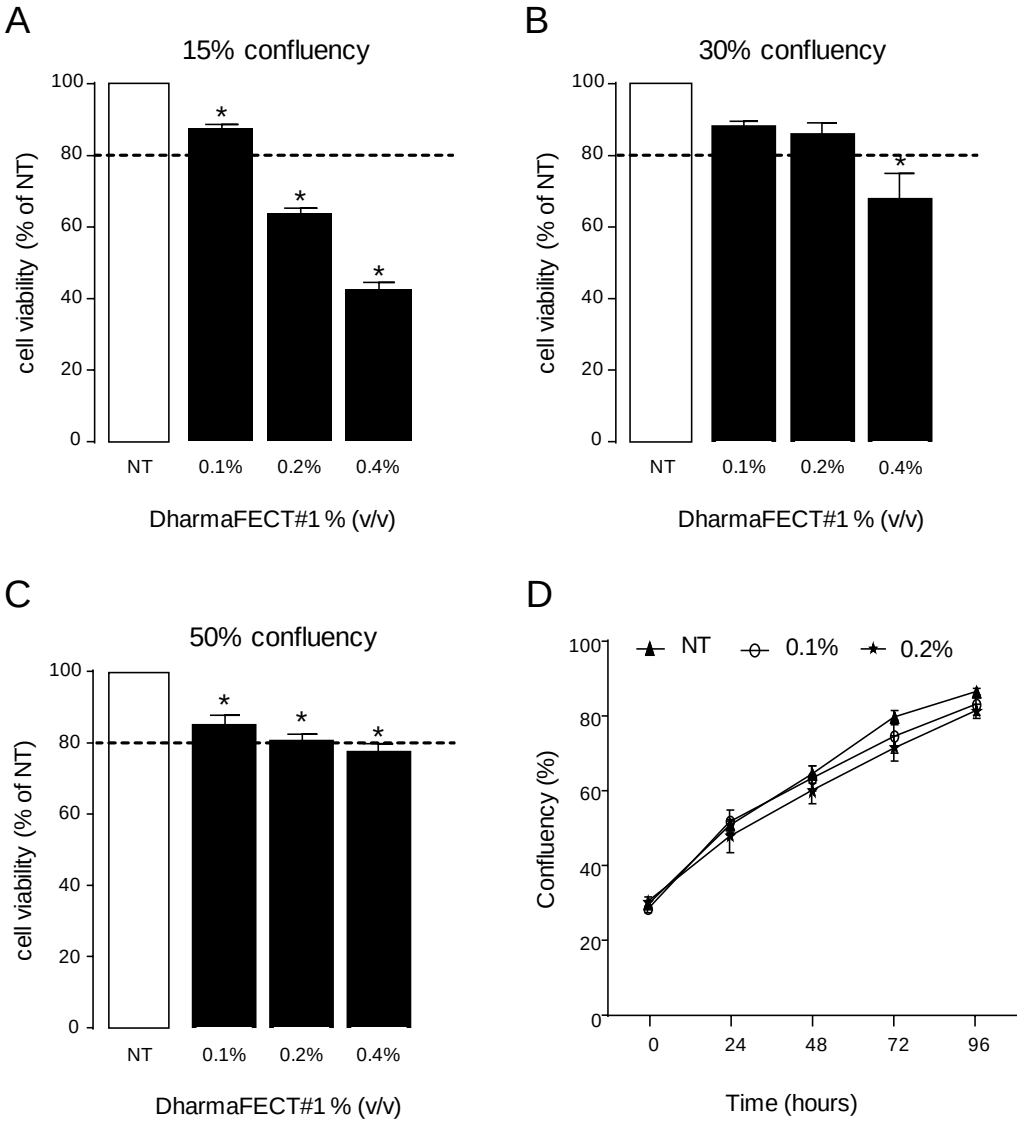

Figure 4.4 Cell viability in H9c2 cardiomyocytes seeded at (**A**) 15% (n=6), (**B**), 30% (n=6) and (**C**) 50% (n=5) confluence density and treated with 0.1%, 0.2% or 0.4% or non-treated (NT) (v/v) DharmaFECT#1 for 4 days was measured by an MTT assay. A threshold is shown at 80% cell viability. Statistical comparison was made by one-way ANOVA followed by Dunnett's post-hoc multiple comparisons tests; *p<0.05 vs non-treated (NT). (**D**) Cell proliferation rate in non-treated (NT) cells and cells treated with 0.1% or 0.2% (v/v) DharmaFECT #1 was monitored for 4 days (n=5), analysed using an IncuCyte® ZOOM live-cell analysis system and compared by two-way ANOVA. No significant change was observed at each time point, *vs* non-treated (NT). All data represent mean values ± SEM.

and proliferation rate curves, based on cell confluency, showed no significant difference between non-treated cells and cells treated with 0.1% (v/v) DharmaFECT#1 for 4 days based on two-way ANOVA analysis (Figure 4.4 D). Cells seeded at 50% confluence density, showed less than 80% viability (77.1 ±

2.5%) when treated with 0.4% (v/v) DharmaFECT#1 for 4 days (Figure 4.4C) however, they were excluded since cells overgrew and reached higher than 90% confluency after 2-3 days of treatment with either 0.1% or 0.2% (v/v) DharmaFECT#1. Taken together, these results suggest that the concentration of DharmaFECT#1 at 0.4% (v/v) was toxic for H9c2 cardiomyocytes and therefore determine that the appropriate non-toxic DharmaFECT#1 working concentration should be between 0.1% and 0.2% (v/v). Furthermore, 30% cell confluency and treatment with 0.1% (v/v) DharmaFECT#1, with the option to increase up to 0.2% (v/v) if required, was chosen as the most cytocompatible condition to further investigate the efficiency of siRNA transfection (section 4.3.3).

4.4.3.2 siRNA transfection efficiency in H9c2 cardiomyocytes

As mentioned earlier in Chapter 4 (section 4.3.3), significant siRNA-mediated mRNA knockdown can be detected after 1-2 days post-transfection and protein knockdown after 2-4 days post-transfection. Therefore, the experimental duration of siRNA transfection on H9c2 cardiomyocyte, to investigate the effects of type 2A protein phosphatase catalytic subunit knockdown in biological pathways, was initially determined at 1-4 days. To examine the toxic effects of siRNA delivery in H9c2 cardiomyocytes cell viability, cells were seeded at 30% confluence density and treated with either rat ON- TARGETplus Non-Targeting Control Pool (non-targeting control siRNA) or TOX Transfection Control siRNA (TOX-siRNA):DharmaFECT#1 mix at a ratio of 50 nM rat TOX-siRNA or non-targeting control siRNA:0.1% (v/v) DharmaFECT#1. Figures 4.5A and 4.5B clearly show that cell viability was higher than 80% when cells were incubated with non-targeting control siRNA combined with 0.1% (v/v) DharmaFECT#1 for 1 (87.8 ± 3.5%) or 4 days (89.9 ± 3.6%). Furthermore, transfection efficiency in H9c2 cardiomyocytes was confirmed by transfecting cells with 50 nM rat TOX-siRNA resulted in a significant ($p<0.05$)

~60% reduction of cell viability at 4 days post-transfection (Figure 4.5 B). These data suggest that the siRNA delivery system using 0.1% (v/v) DharmaFECT#1 and siRNA at a final concentration of 50 nM can be considered as the baseline concentration for post-transcriptional silencing of the type 2A protein phosphatase catalytic subunits and alpha4 protein.

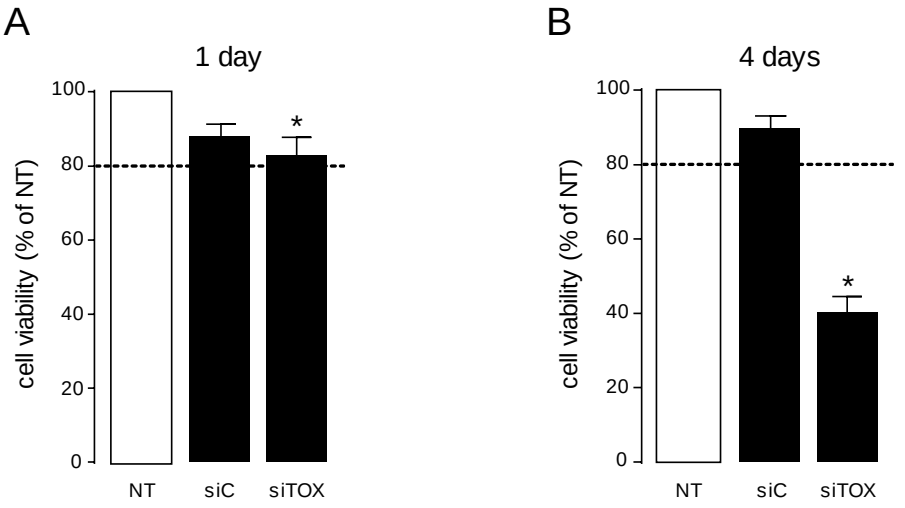

Figure 4.5 Cell viability of untreated (NT) H9c2 cardiomyocytes or transfected with either 50 nM rat non-targeting control siRNA (siC) or TOX-siRNA (siTOX) for (**A**) 1 day or (**B**) 4 days was measured by an MTT assay. A threshold is shown at 80% cell viability. Data represent mean values ± SEM of six individual experiments run in triplicates. Statistical comparison was made by one-way ANOVA followed by Dunnett's post-hoc multiple comparisons tests; *p<0.05 *vs* non-treated (NT).

An additional efficiency/toxicity test was performed using 0.2% (v/v) DharmaFECT to deliver 100 nM non-targeting control siRNA or TOX-siRNA for co-transfection experiments validation. As it can be seen in Figures 4.6A and 4.6B, cell viability was higher than 80% when cells were treated with 100 nM rat non-targeting siRNA at 1 day and 4 days post-transfection (94.9 ± 8.6% or 87.9 ± 6.2% respectively). Transfection efficiency was confirmed by transfecting cells with 100 nM rat TOX-siRNA resulting in a significant ($p<0.05$) 67.5% reduction of cell viability after 4 days post-transfection (Figure 4.6 B) thereby, establishing the appropriate reagent concentrations for siRNA co-transfection experiments.

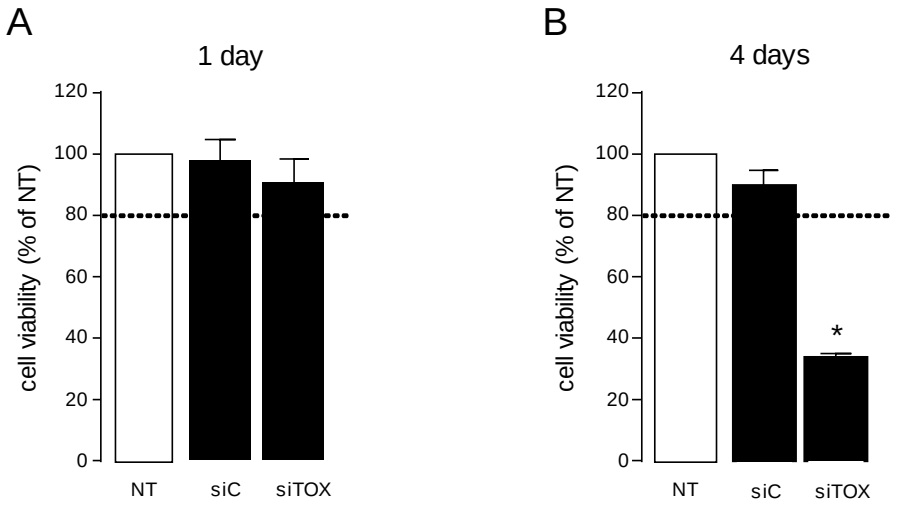

Figure 4.6 Cell viability of untreated (NT) H9c2 cardiomyocytes or transfected with either 100 nM rat non-targeting control siRNA (siC) or TOX-siRNA (siTOX) for (**A**) 1 day or (**B**) 4 days post-transfection, was measured by an MTT assay. A threshold is shown at 80% cell viability. Data represent mean values ± SEM of four individual experiments run in triplicates. Statistical comparison was made by one-way ANOVA followed by Dunnett's post-hoc multiple comparisons tests; *p<0.05 *vs* NT.

4.4.4 Evaluation of the non-targeting siRNA (siC) off-target effects towards the type 2A protein phosphatase catalytic subunits and alpha4 protein expression

To investigate off-target effects of the non-targeting control siRNA towards the protein expression levels of the type 2A protein phosphatase catalytic subunits and alpha4 protein in H9c2 cardiomyocytes, cells were transfected with non-targeting control siRNA for 4 days (maximum experimental duration of transfection). Figure 4.7 shows that protein levels of total PP2AC, PP4C, PP6C and alpha4 protein in samples transfected with 50 nM rat non-targeting control siRNA for 4 days were not significantly altered, compared to those in the non-treated cells. This data suggests that the non-targeting control siRNA has no off-target effects towards total PP2AC, PP4C, PP6C and alpha4 gene expression.

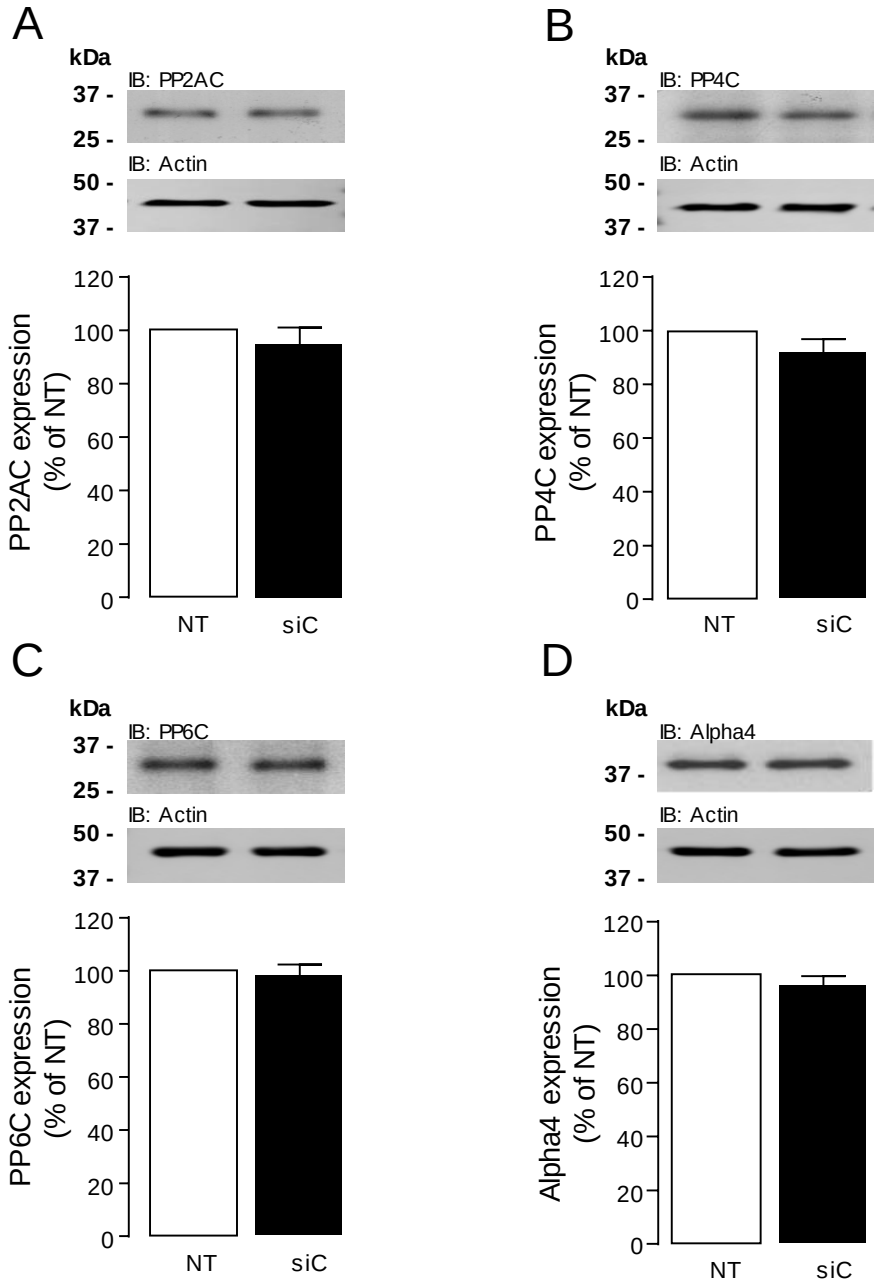

Figure 4.7 H9c2 cardiomyocytes were transfected with 50 nM non-targeting control siRNA (siC) or were non-treated (NT) for 4 days to detect any non-targeting siRNA effects of rat non-targeting control siRNA towards the total PP2AC, PP4C, PP6C and alpha4 expression. (**A**) Total PP2AC, (**B**) PP4C, (**C**) PP6C and (**D**) alpha4 protein expression level were determined by immunoblotting using subunit-specific antibodies to PP2AC, PP4C and PP6C and a rabbit polyclonal anti-alpha4 antibody. Protein levels were quantified by densitometry or LI-COR Odyssey® CLx Imaging System and were normalised to actin in each sample. All data represent mean values ± SEM of three individual experiments. Statistical comparison was made by a two-tailed unpaired Student's t-test. No significant differences were observed *vs* NT. IB: immunoblot.

4.4.5 Determination of siRNA-mediated gene silencing of PP2ACα and PP2ACβ

As shown in figure 4.3, alignment of rat PP2ACα and PP2ACβ amino acid sequence revealed 97.4% homology. Nonetheless, alignment of the open reading frame region of rat PP2ACα and PP2ACβ cDNA sequences, showed 82% nucleotide identity (Table 4.1) therefore, using qPCR analysis it is possible to detect the mRNA levels separately of PP2ACα and PP2ACβ. Efficient siRNA-mediated gene expression silencing at the mRNA level is expected to be detected at 1-2 days post-transfection. Therefore, the mRNA levels of PP2ACα and PP2ACβ were analysed by qPCR in H9c2 cardiomyocytes transfected with either 50 nM rat PP2ACα-, PP2ACβ-siRNAs or non-targeting control siRNA, for 2 and 4 days as described below, in section 4.4.5.3.

4.4.5.1 Validation of RNA quality for qPCR analysis

Only RNA samples with an absorbance ratio at OD260/280 ≥2.0 and OD260/230 >1.8 were used for qPCR analysis. Total RNA samples had RIN between 7.4 and 8.5 or between to 8.8-10 when isolated from cells transfected for 2 and 4 days, with either 50 nM PP2ACα-siRNA, PP2ACβ-siRNA or non-targeting control siRNA (Figure 4.8). In all the samples, including the ones with RIN scores between 7.4 to 8.5, clear 18S and 28S ribosomal peaks were present. These data suggest isolation of reasonable RNA quality (Schroeder et al., 2006) that can be accepted in downstream applications such as RT-PCR, with the highest quality RNA extracted after 4 days post-transfection, probably due to the larger amount of starting material (larger number of cells).

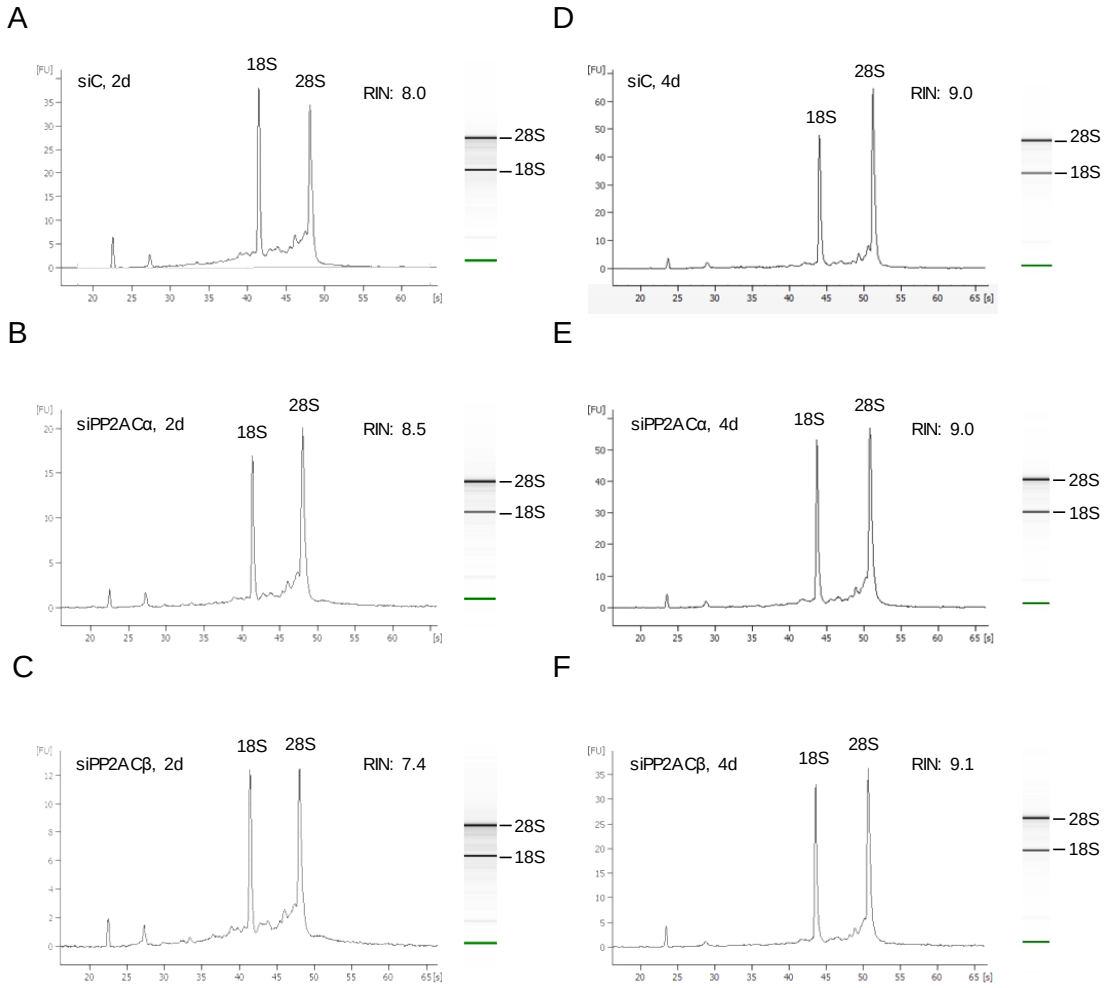

Figure 4.8 Representative electropherograms and calculated RIN values of total RNA obtained by the RNeasy protect cell mini kit (Qiagen) from H9c2 cardiomyocytes transfected with 50 nM rat (**A**) non-targeting control siRNA (siC), (**B**) PP2ACα-siRNA (siPP2ACα) or (**C**) PP2ACβ-siRNA (siPP2ACβ) for 2 days (2d) or transfected with 50 nM rat (**D**) non-targeting control siRNA (siC), (**E**) PP2ACα-siRNA (siPP2ACα) or (**F**) PP2ACβ-siRNA (siPP2ACβ) for 4 days (4d). Total RNA was analysed using an Agilent RNA 6000 Nano Assay and 2100 Bioanalyzer (Agilent Technologies). The two peaks represent the 28S and 18S ribosomal RNAs. Data are representative of 3 individual experiments.

4.4.5.2 Validation of ACTB and GAPDH reference genes

Two candidate reference genes, ACTB and GAPDH, were validated for data normalisation. Table 4.2, shows the SD of the average Cq values and Pearson coefficient of correlation (*r*) estimated by the BestKeeper© v1.0 software (Pfaffl, 2001) for each reference gene across the three biological replicates and different experimental conditions after 2 or 4 days of siRNA transfection. According to the

software criteria, both ACTB and GAPDH had SD less than 1 and showed significantly ($p<0.05$) high correlation ($r \geq 0.76$ or $r \geq 0.77$ after 2 or 4 days of siRNA transfection respectively). In addition, statistical comparison by one-way ANOVA showed no- significant change in the Cq values of each reference among cells transfected with, rat PP2ACα-siRNA, PP2ACβ-siRNA or non-targeting control siRNA for 2 or 4 days. According to these data, both reference genes were considered suitable for use in the subsequent qPCR analysis.

Table 4.2 Expression stability of the reference genes (ACTB and GAPDH) at 2 and 4 days post-transfection is determined by calculating the coefficient of variation (CV) and standard deviation (SD) and coefficient of correlation (*r*), in the Cq values (n=9) for each candidate reference gene using BestKeeper© v1.0 software (Pfaffl, 2001).

Day	Reference gene	CV(%)	SD	*r*
D2	ACTB	5.21	0.99	0.91
	GAPDH	3.05	0.54	0.76
D4	ACTB	2.63	0.44	0.77
	GAPDH	4.41	0.86	0.94

4.4.5.3 siRNA-mediated mRNA knockdown of PP2ACα and PP2ACβ

Cq values of PP2ACα, PP2ACβ, GAPDH and ACTB genes in the unknown samples, obtained from qPCR reactions, differ at least 5 Cq from the respective values in the no-RT and no-template control reactions, indicating that less 3% or less of the amplification in the unknown samples may be attributed to the genomic DNA template and was considered not significant. Cq values of the genes of interest in the unknown samples were normalised to both ACTB and GAPDH reference genes and analysed as described earlier in earlier in Chapter 4 (section 4.3.6). The mRNA levels of either PP2ACα or PP2ACβ were determined in cells transfected with

PP2ACα-siRNA or PP2ACβ-siRNA relative to the control (cells transfected with non-targeting control siRNA) as shown in table 4.3. Figure 4.9A and 4.9B clearly show that PP2ACα (43.48-fold decrease) and PP2ACβ (24.39-fold decrease) were successfully silenced in cells transfected with rat PP2ACα-siRNA or PP2ACβ-siRNA respectively for 2 days since the mRNA expression was reduced more than 10-fold compared to the siC expression levels. Interestingly, when cells were transfected with rat PP2ACα-siRNA for 2 days, mRNA levels of PP2ACβ (Figure 4.9B) were decreased (1.58-fold decrease) when compared to the siC expression levels. On the other hand, when cells were transfected with rat PP2ACβ-siRNA, mRNA levels of PP2ACα (Figure 4.9A) were decreased (1.56-fold decreases) compared to the control samples. The knockdown of PP2ACα and PP2ACβ mRNA expression at 4 days post-transfection was tested. Figure 4.10 suggests that mRNA knockdown of PP2ACα (71.43-fold decrease) and PP2ACβ (22.73-fold reduction) was sustained (more than a 10-fold reduced expression) in cells transfected with rat PP2ACα-siRNA or PP2ACβ-siRNA respectively for 4 days compared to the siC. Similar to data presented in figure 4.9, when cells were transfected with rat PP2ACα-siRNA for 4 days, mRNA levels of PP2ACβ (Figure 4.10B) were decreased (1.41-fold reduction) whilst, when cells were transfected with PP2ACβ-siRNA, mRNA levels of PP2ACα (Figure 4.10A) were decreased (1.68-fold reduction) when compared to the siC expression levels. Together these results provide evidence of efficient PP2ACα or PP2ACβ mRNA knockdown using rat PP2ACα- or PP2ACβ-siRNAs respectively (higher than a 10-fold reduced expression) in H9c2 cardiomyocytes compared to siC.

Table 4.3 mRNA expression of PP2ACα and PP2ACβ in cells transfected with PP2ACα-siRNA (siPP2ACα) or PP2ACβ-siRNA (siPP2ACβ) relative to the control respective mRNA expression values in cells transfected with non-targeting control siRNA (siC). Data with averaged fold change ($\overline{FC}$) <1, were converted to fold decrease (section 2.4.5).

	Gene	Form of data	siC	siPP2ACα	siPP2ACβ
D2	PP2ACα	$\overline{FC} \pm SEM$	1.000±0.000	0.023±0.008	0.630±0.075
		$\left\|-1/\overline{FC}\right\|$	1	43.48	1.58
	PP2ACβ	$\overline{FC} \pm SEM$	1.000±0.000	0.639±0.018	0.041±0.017
		$\left\|-1/\overline{FC}\right\|$	1	1.57	24.39
D4	PP2ACα	$\overline{FC} \pm SEM$	1.000±0.000	0.014±0.004	0.708±0.036
		$\left\|-1/\overline{FC}\right\|$	1	71.43	1.41
	PP2ACβ	$\overline{FC} \pm SEM$	1.000±0.000	0.597±0.044	0.044±0.016
		$\left\|-1/\overline{FC}\right\|$	1	1.68	22.73

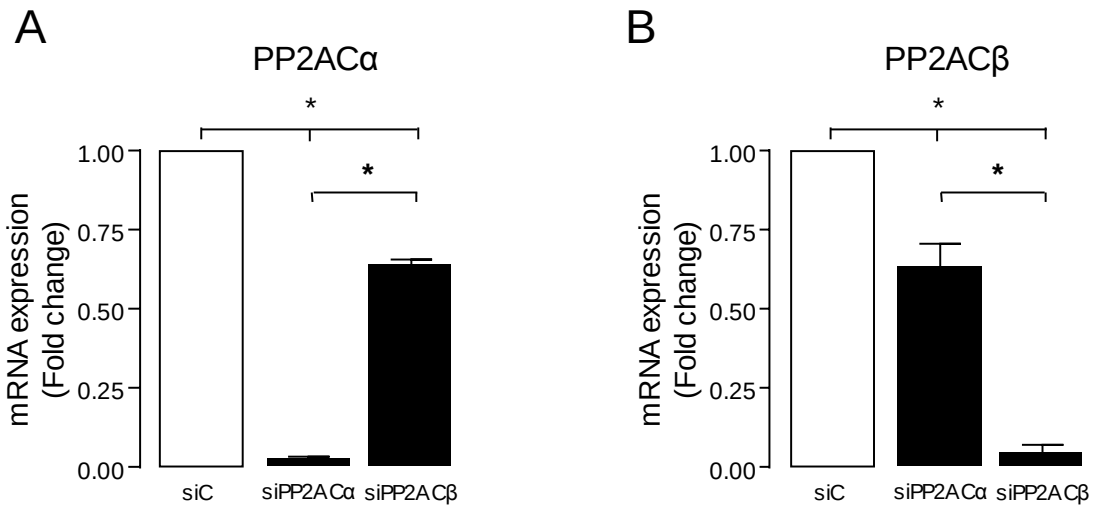

Figure 4.9 Fold change of the mRNA expression of (**A**) PP2ACα or (**B**) PP2ACβ, in H9c2 cardiomyocytes transfected with 50 nM rat non-targeting control siRNA (siC), rat PP2ACα-siRNA (siPP2ACα) or PP2ACβ-siRNA (siPP2ACβ) for 2 days, relative to the expression levels in the control samples (siC), was calculated according to qbase$^+$ software approach. Relative quantities were normalised to both ACTB and GAPDH reference genes. Data represent mean values ± SEM of 3 individual experiments. Statistical comparison was made by one-way ANOVA followed by Tukey's post-hoc multiple comparisons tests; *p<0.05.

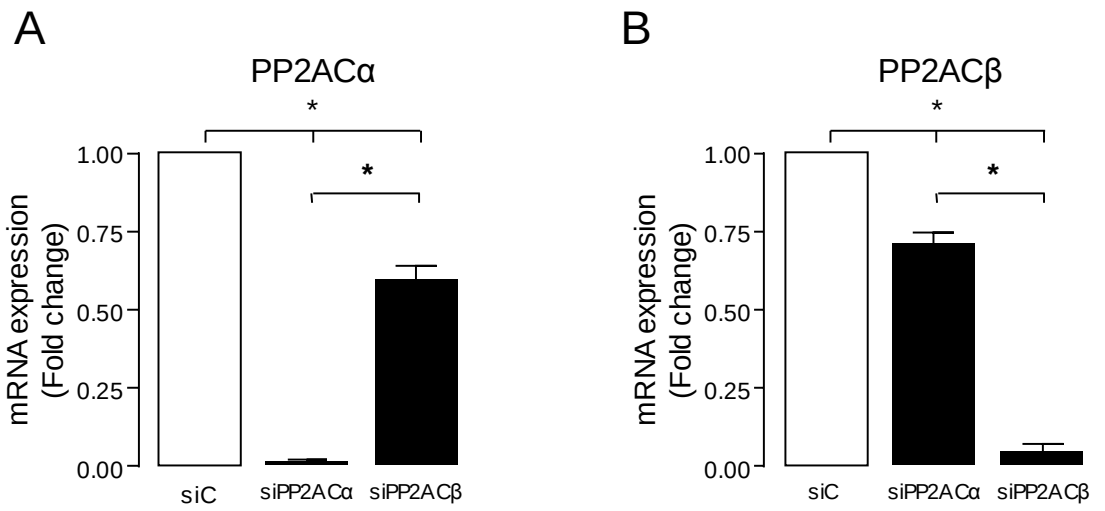

Figure 4.10 Fold change of the mRNA expression of (**A**) PP2ACα or (**B**) PP2ACβ, in H9c2 cardiomyocytes transfected with 50 nM rat non-targeting control siRNA (siC), rat PP2ACα-siRNA (siPP2ACα) or PP2ACβ-siRNA (siPP2ACβ) for 4 days, relative to the expression levels in the control samples (siC), was calculated according to qbase^{+} software approach. Relative quantities were normalised to both ACTB and GAPDH reference genes. Data represent mean values ± SEM of 3 individual experiments. Statistical comparison was made by one-way ANOVA followed by Tukey's post-hoc multiple comparisons tests; *p<0.05.

4.4.6 siRNA-mediated protein knockdown of PP2ACα/β, PP2ACα, PP2ACβ, PP4C and PP6C

Knockdown efficiency of the rat PP2ACα-, PP2ACβ -, PP4C- and PP6C-siRNAs was determined by measuring the protein levels of the targeted protein by western blotting analysis. Figure 4.11 shows that the mRNA knockdown of either PP2ACα (71.43-fold decrease) or PP2ACβ (22.73-fold decrease), analysed previously (section 4.4.5.2), in cells transfected with rat PP2ACα-siRNA (Figure 4.11A) or PP2ACβ-siRNA (Figure 4.11B) for 4 days respectively, resulted in a significant ($p<0.05$) reduction of total PP2AC protein levels (48.3 ± 2.7% or 46.7 ± 4.2% respectively) when compared to the expression levels in cells transfected with non-targeting control siRNA. Therefore, co-transfection of H9c2 cardiomyocytes with both rat PP2ACα- and PP2ACβ-siRNAs for up to 4 days should cause a larger reduction of the total PP2AC protein expression levels since both PP2ACα and PP2ACβ mRNAs are targeted simultaneously. Indeed, as shown in figure 4.12, co-transfection of the

cells with both rat PP2ACα- and PP2ACβ-siRNAs for 4 days resulted in a significant ($p<0.05$) 84% knockdown of total PP2AC protein expression (16.09 ± 8.67%), when compared to the expression levels in cells transfected with non-targeting control siRNA. Comparing the results in figures 4.11 and 4.12, it can be seen that the detected 51-53% reduction of total PP2AC protein expression, when cells are transfected with either rat PP2ACα- or PP2ACβ-siRNAs, is due to siRNA-mediated PP2ACα or PP2ACβ expression inhibition respectively. Figures 4.13 and 4.14 show significantly ($p<0.05$) reduced PP4C (4.03 ± 1.17%) PP6C (8.97 ± 2.92%) protein expression levels in H9c2 cardiomyocytes transfected with rat PP4C- or PP6C-siRNA respectively for 4 days when compared to the expression levels in cells transfected with non-targeting control siRNA. These data, along with the data presented in figures 4.9 and 4.10, demonstrate the first report of efficient siRNA-mediated post-transcriptional silencing of PP2ACα/β, PP2ACα, PP2ACβ, PP4C and PP6C in H9c2 cardiomyocytes. In addition, the data described in this section confirmed the specificity of the custom made anti-PP2CA, anti-PP4C and anti-PP6C catalytic subunit-specific antibodies used to detect protein expression of total PP2AC, PP4C and PP6C by western blotting in this study.

4.4.7 Evaluation of the off-target and on-target effects in the expression of PP2ACα/β, PP2ACα, PP2ACβ, PP4C and PP6C

As described earlier in Chapter 4 (section 4.4.1) pair sequence alignment between PP2ACα, PP2ACβ, PP4C and PP6C open reading frame of their cDNA sequences, revealed 59-65% nucleotide homology and consisted of 12-20% gaps, with the exception of PP2ACα-PP2ACβ pair alignment showing 81.6% nucleotide homology. This result raised important questions regarding the potential off-target effects of each catalytic subunit-specific siRNA towards the other non-target catalytic subunits. To analyse the potential off-target effects of each catalytic subunit-specific

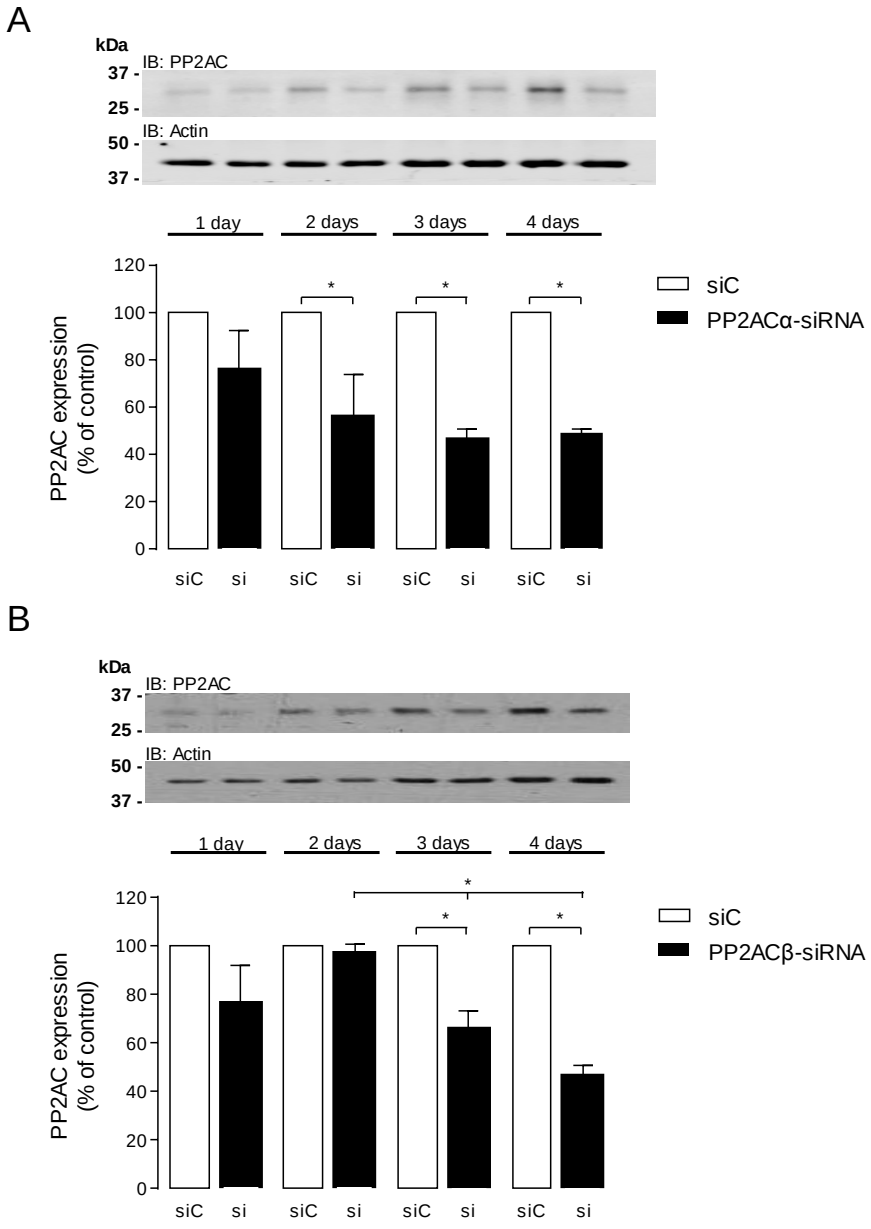

Figure 4.11 Protein expression of total PP2AC in H9c2 cardiomyocytes, transfected with 50 nM rat (**A**) PP2ACα-, (**B**) PP2ACβ-siRNAs (si) or non-targeting control siRNA (siC) for 1-4 days was determined by immunoblotting using a subunit-specific anti-PP2AC antibody. Protein levels were quantified by densitometry or LI-COR Odyssey® CLx Imaging System and were normalised to actin in each sample. All data represent mean values ± SEM of four individual experiments. Statistical comparison was made by one-way ANOVA followed by Tukey's post-hoc multiple comparisons tests; *p<0.05. IB: Immunoblot.

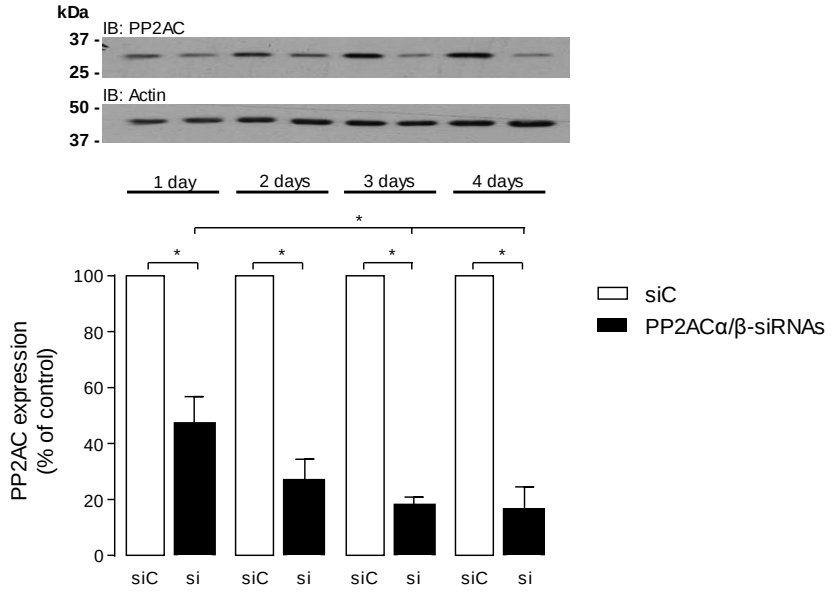

Figure 4.12 Protein expression of total PP2AC in H9c2 cardiomyocytes, co-transfected with 50 nM rat PP2ACα- and PP2ACβ-siRNAs (si) or 100 nM non-targeting control siRNA (siC) for 1-4 days was determined by immunoblotting using a subunit-specific anti-PP2AC antibody. Protein levels were quantified by densitometry or LI-COR Odyssey® CLx Imaging System and were normalised to actin in each sample. All data represent mean values ± SEM of three individual experiments. Statistical comparison was made by one-way ANOVA followed by Tukey's post-hoc multiple comparisons tests; *p<0.05. IB: Immunoblot.

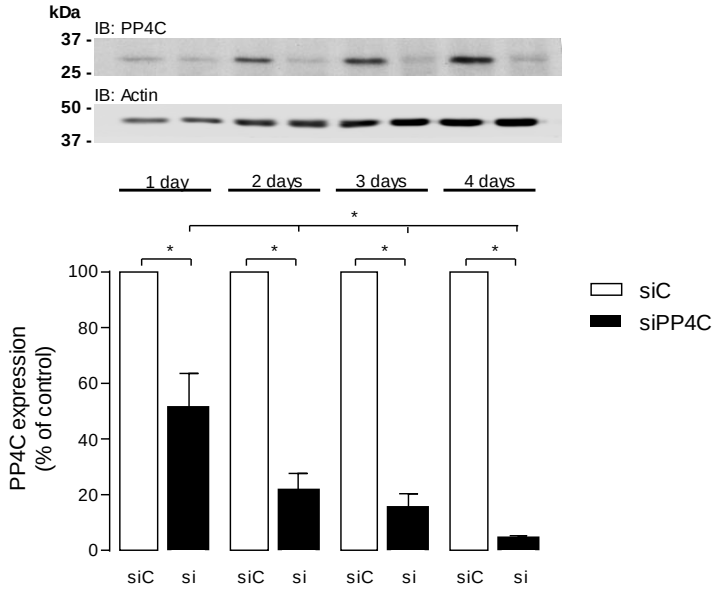

Figure 4.13 Protein expression of PP4C in H9c2 cardiomyocytes, transfected with 50 nM rat PP4C-siRNA (si) or non-targeting control siRNA (siC) for 1-4 days was determined by immunoblotting using a subunit-specific anti-PP4C antibody. Protein levels were quantified by densitometry or LI-COR Odyssey® CLx Imaging System and were normalised to actin in each sample. All data represent mean values ± SEM of five individual experiments. Statistical comparison was made by one-way ANOVA followed by Tukey's post-hoc multiple comparisons tests; *p<0.05. IB: Immunoblot.

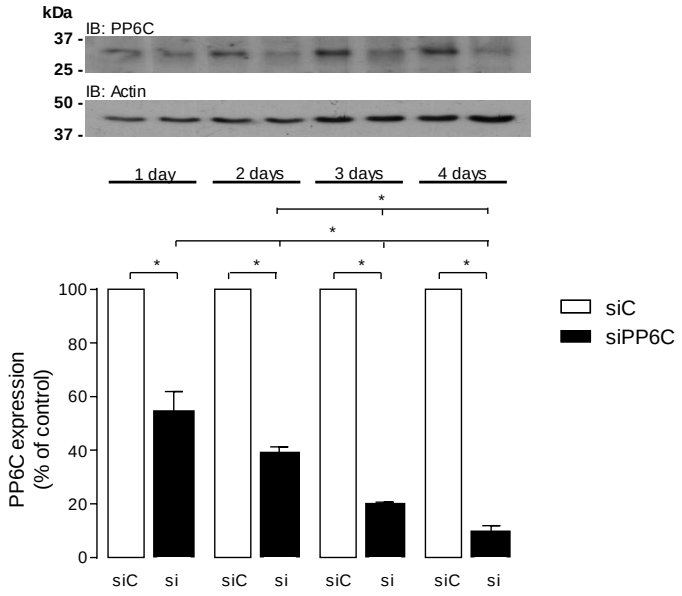

Figure 4.14 Protein expression of PP6C in H9c2 cardiomyocytes, transfected with 50 nM rat PP6C-siRNA (si) or non-targeting control siRNA (siC) for 1-4 days was determined by immunoblotting using a subunit-specific anti-PP6C antibody. Protein levels were quantified by densitometry or LI-COR Odyssey® CLx Imaging System and were normalised to actin in each sample. All data represent mean values ± SEM of five individual experiments. Statistical comparison was made by one-way ANOVA followed by Tukey's post-hoc multiple comparisons tests; *p<0.05. IB: Immunoblot.

siRNA (PP2ACα-siRNA, PP2ACβ-siRNA, PP4C-siRNA or PP6C-siRNA) and effects of the reduced levels of the target protein (on-target effects) towards the protein expression of the non-target catalytic subunits, either PP2ACα, PP2ACβ, PP4C or PP6C accordingly, a series of tests was performed by immunoblotting analysis, shown in table 4.4. Figures 4.15 and 4.16 show clearly that no significant change was detected in the protein expression levels of PP4C and PP6C when cells were transfected with either PP2ACα- or PP2ACβ-siRNA for 1-4 days, when compared to the expression levels in cells transfected with non-targeting control siRNA. Likewise, when cells were transfected with rat PP4C-siRNA for 1-4 days (Figure 4.17), there was no significant change in the total PP2AC or PP6C protein expression levels, when compared to the expression levels in cells transfected with non-targeting control siRNA. In a similar way, when cells were transfected with rat PP6C-siRNA for 1-4 days, no significant change was observed in the total PP2AC or

PP4C protein expression levels, when compared to those in cells transfected with non-targeting control siRNA (Figure 4.18).

Table 4.4 Evaluation of PP2ACα-, PP2ACβ -, PP4C- and PP6C-siRNA specificity by immunoblotting analysis.

siRNA used for transfection	mRNA target	Substrates for IB analysis	Figure
PP2ACα-siRNA	PP2ACα	PP4C	4.15A
		PP6C	4.15B
PP2ACβ-siRNA	PP2ACβ	PP4C	4.16A
		PP6C	4.16B
PP4C-siRNA	PP4C	PP2AC	4.17A
		PP6C	4.17B
PP6C-siRNA	PP6C	PP2AC	4.18A
		PP4C	4.18B

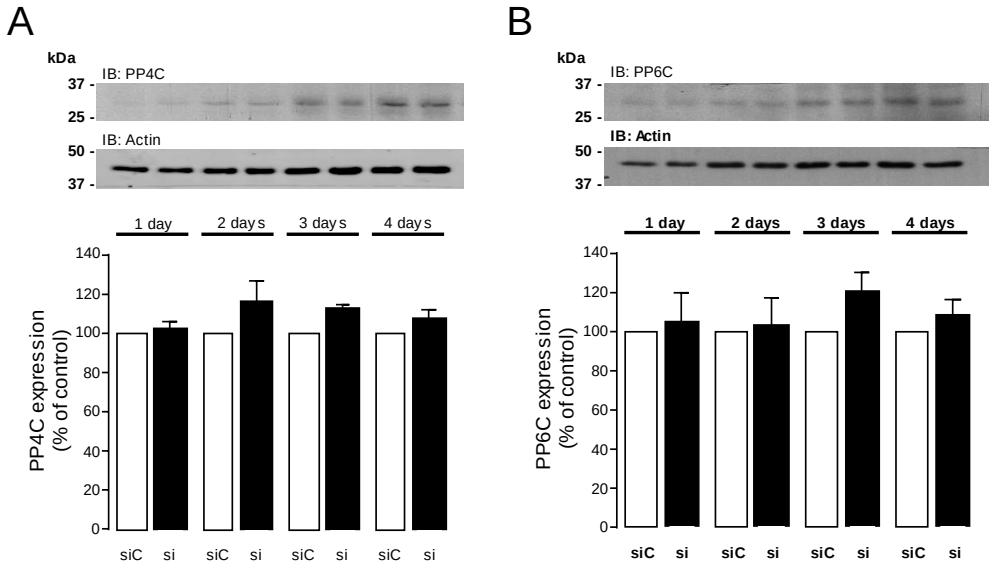

Figure 4.15 Protein expression of (**A**) PP4C and (**B**) PP6C in H9c2 cardiomyocytes, transfected with 50 nM rat PP2ACα-siRNA (si) or non-targeting control siRNA (siC) for 1-4 days. Protein expression of PP4C and PP6C was determined by immunoblotting using subunit-specific antibodies to PP4C and PP6C. Protein levels were quantified by densitometry or LI-COR Odyssey® CLx Imaging System and were normalised to actin in each sample. All data represent mean values ± SEM of four individual experiments. Statistical comparison was made by one-way ANOVA. No significant differences were observed *vs* siC. IB: Immunoblot.

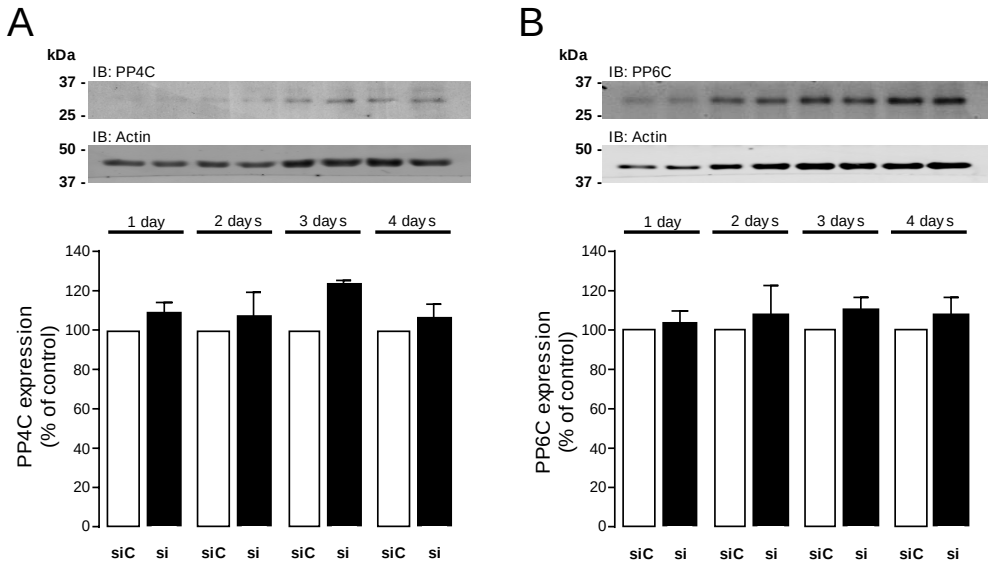

Figure 4.16 Protein expression of (**A**) PP4C (n=3) and (**B**) PP6C (n=4) in H9c2 cardiomyocytes, transfected with 50 nM rat PP2ACβ-siRNA (si) or non-targeting control siRNA (siC) for 1- 4 days was determined by immunoblotting using subunit-specific antibodies to PP4C and PP6C. Protein levels were quantified by densitometry or LI-COR Odyssey® CLx Imaging System and were normalised to actin in each sample. All data represent mean values ± SEM. Statistical comparison was made by one-way ANOVA. No significant differences were observed *vs* siC. IB: Immunoblot.

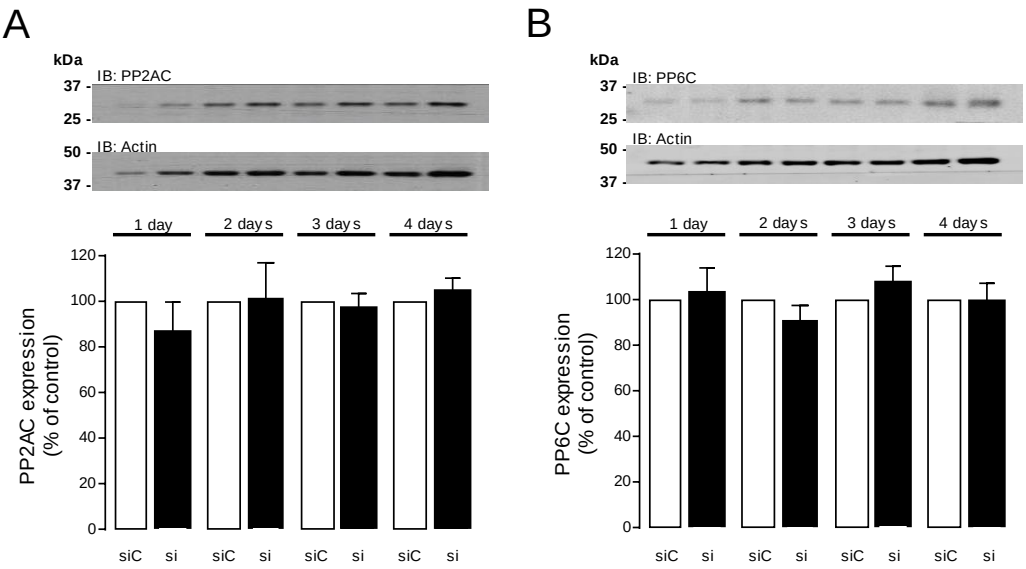

Figure 4.17 Protein expression of (**A**) total PP2AC and (**B**) PP6C in H9c2 cardiomyocytes, transfected with 50 nM rat PP4C-siRNA (si) or non-targeting control siRNA (siC) for 1-4 days was determined by immunoblotting using subunit-specific antibodies to PP2AC and PP6C. Protein levels were quantified by densitometry or LI-COR Odyssey® CLx Imaging System and were normalised to actin in each sample. All data represent mean values ± SEM of four individual experiments. Statistical comparison was made by one-way ANOVA. No significant differences were observed *vs* siC. IB: Immunoblot.

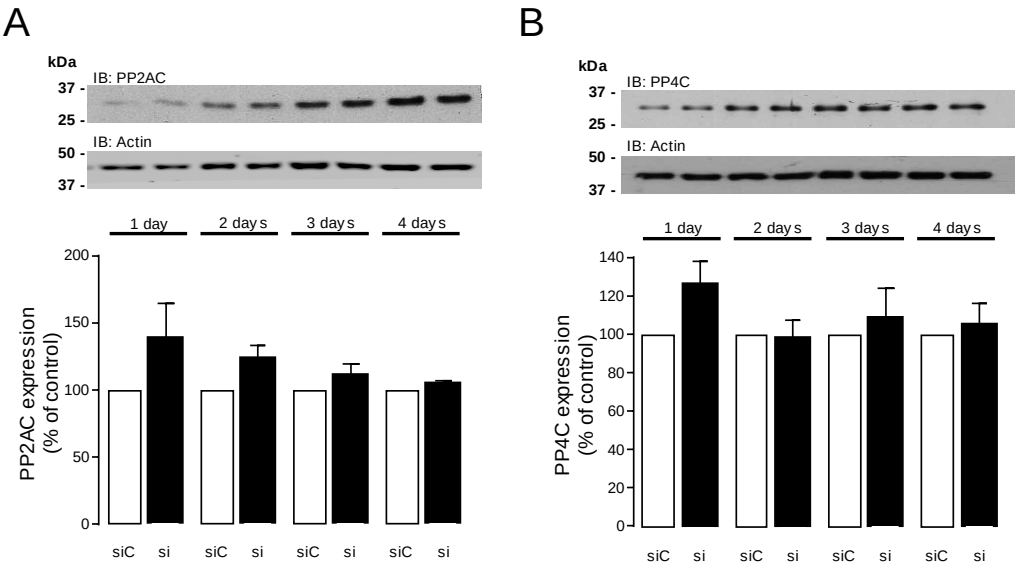

Figure 4.18 Protein expression of (**A**) total PP2AC and (**B**) PP4C in H9c2 cardiomyocytes, transfected with 50 nM rat PP6C-siRNA (si) or non-targeting control siRNA (siC) for 1-4 days was determined by immunoblotting using subunit-specific antibodies to PP2AC and PP4C. Protein levels were quantified by densitometry or LI-COR Odyssey® CLx Imaging System and were normalised to actin in each sample. All data represent mean values ± SEM relative of four individual experiments. Statistical comparison was made by one-way ANOVA. No significant differences were observed *vs* siC. IB: Immunoblot.

4.4.8 Effects of alpha4 knockdown in the expression of PP2AC, PP4C and PP6C

It has been reported previously that alpha4 protein is an essential regulator of PP2AC, PP4C and PP6C expression and activity and that deletion of alpha4 in male mouse embryonic fibroblasts results in the loss of PP2AC, PP4C and PP6C from the cells (Kong et al., 2009). To investigate whether alpha4 is similarly regulating the expression of PP2AC, PP4C and PP6C in H9c2 cardiomyocytes, the protein expression of alpha4 was inhibited by transfecting the cells with 50 nM rat alpha4-siRNA for 1-4 days. Figure 4.19 clearly shows that alpha4 protein was significantly ($p<0.05$) reduced (5.85 ± 1.90%) at 4 days post-transfection. This data demonstrates for the first time the efficient siRNA-mediated alpha4 protein knockdown in H9c2 cardiomyocytes. Consequently, lysates of H9c2 cardiomyocytes, transfected with rat alpha4-siRNA for 1-4 days, were further examined for the expression of total PP2AC, PP4C and PP6C. Figures 4.20, 4.21 and 4.22 reveal that the significant

(p<0.05) knockdown of alpha4 protein (>94%) at 4 days post-transfection, resulted in significant (p<0.05) loss of total PP2AC (16.45 ± 4.93%), PP4C (16.69 ± 3.21%) and PP6C (26.36 ± 6.89%) protein expression in cells. From these results, it is apparent that there is a tight correlation between alpha4 and type 2A protein phosphatase catalytic subunits (total PP2AC, PP4C and PP6C) protein expression. Furthermore, these data suggest that alpha4 is involved in the regulation of type 2A protein phosphatase expression in cardiomyocytes.

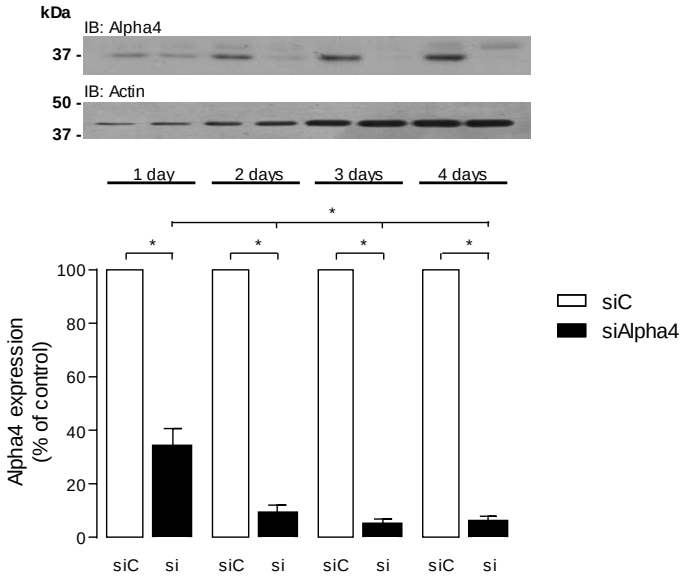

Figure 4.19 Protein expression of alpha4 in H9c2 cardiomyocytes, transfected with 50 nM rat alpha4-siRNA (si) or non-targeting control siRNA (siC) for 1-4 days was determined by immunoblotting using a rabbit polyclonal anti-alpha4 antibody. Protein levels were quantified by densitometry or LI-COR Odyssey® CLx Imaging System and were normalised to actin in each sample. All data represent mean values ± SEM of four individual experiments. Statistical comparison was made by one-way ANOVA followed by Tukey's post-hoc multiple comparisons tests; *p<0.05. IB: Immunoblot.

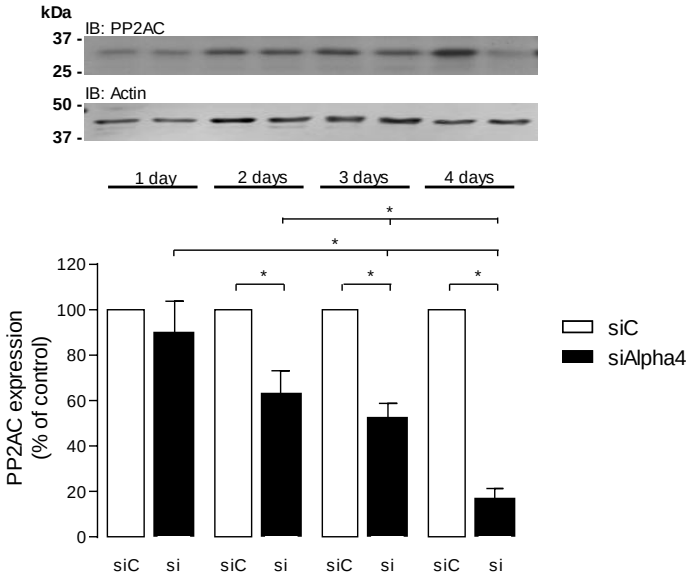

Figure 4.20 Protein expression of total PP2AC in H9c2 cardiomyocytes, transfected with 50 nM rat alpha4-siRNA (si) or non-targeting control siRNA (siC) for 1-4 days was determined by immunoblotting using a subunit-specific anti-PP2AC antibody. Protein levels were quantified by densitometry or LI-COR Odyssey® CLx Imaging System and were normalised to actin in each sample. All data represent mean values ± SEM of four individual experiments. Statistical comparison was made by one-way ANOVA followed by Tukey's post-hoc multiple comparisons tests; *p<0.05. IB: Immunoblot.

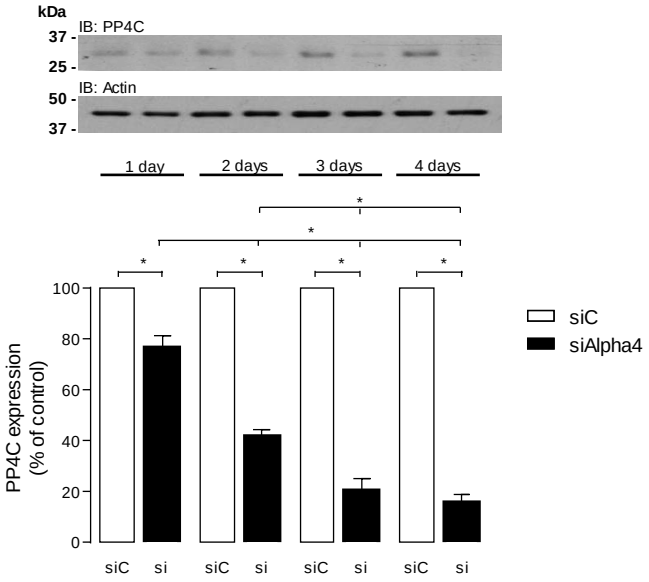

Figure 4.21 Protein expression of PP4C in H9c2 cardiomyocytes, transfected with 50 nM rat alpha4-siRNA (si) or non-targeting control siRNA (siC) for 1-4 days was determined by immunoblotting using a subunit-specific anti-PP4C antibody. Protein levels were quantified by densitometry or LI-COR Odyssey® CLx Imaging System and were normalised to actin in each sample. All data represent mean values ± SEM of three individual experiments. Statistical comparison was made by one-way ANOVA followed by Tukey's post-hoc multiple comparisons tests; *p<0.05. IB: Immunoblot.

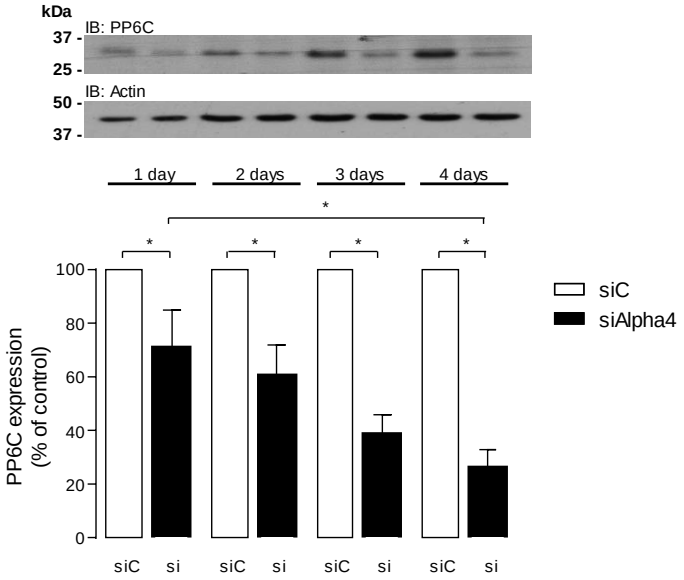

Figure 4.22 Protein expression of PP6C in H9c2 cardiomyocytes, transfected with 50 nM rat alpha4-siRNA (si) or non-targeting control siRNA (siC) for 1-4 days was determined by immunoblotting using a subunit-specific anti-PP6C antibody. Protein levels were quantified by densitometry or LI-COR Odyssey® CLx Imaging System and were normalised to actin in each sample. All data represent mean values ± SEM of four individual experiments. Statistical comparison was made by one-way ANOVA followed by Tukey's post-hoc multiple comparisons tests; *p<0.05 *vs* siC. IB: Immunoblot.

4.5 Discussion

4.5.1 Establishing siRNA-mediated knockdown of type 2A protein phosphatase catalytic subunits

In this chapter, an efficient siRNA-mediated post-transcriptional silencing of PP2ACα, PP2ACβ, PP4C, PP6C and alpha4 protein in H9c2 cardiomyocytes was demonstrated for the first time. Specifically, the siRNA delivery system was optimised in H9c2 cardiomyocytes and higher than 90% PP2ACα and PP2ACβ mRNA knockdown or PP4C, PP6C and alpha4 protein knockdown was reported, using rat -specific siRNAs to target PP2ACα, PP2ACβ, PP4C, PP6C and alpha4 protein.

To address the function of protein phosphatases in biological pathways in mammalian cells, various studies have been carried using cell-permeable chemical inhibitors (review by McConnell and Wadzinski 2009). The use of these compounds shows great advantages compared to other technologies such as RNAi (Figure 4.23), since the effect on the targets is usually assessed rapidly and the phenotype changes can be considered more direct, however, lack of specificity can be one of the main limitations. Table 4.5 presents some commonly used inhibitors of the protein phosphatase type 2A family used in the literature. Okadaic acid, a well-known inhibitor of PP2A/PP1, has been reported to inhibit not only the activity of PP2A but the activity of all three members of the type 2A protein phosphatases family (PP2A, PP4 and PP6) at similar levels of concentration, thus been recognised as a non-specific PP2A inhibitor (Brewis et al., 1993; Hastie and Cohen, 1998; Prickett and Brautigan, 2006). Despite this fact, it has been used in many inhibitor studies of PP2A activity, without distinguishing between PP2A, PP4 or PP6 (Gao et al., 1997; Baharians and Schonthal, 1998; Nowak et al., 2003; Chowdhury et al., 2005; Yang

et al., 2005; Hall et al., 2006; Zong et al., 2006; McConnell et al., 2007; De Arcangelis et al., 2008; Shi et al., 2012; Ma et al., 2016; Plácido et al., 2016). Even so, okadaic acid can be used for studies to delineate the function of more general groups of phosphatases. Another widely used PP2A inhibitor, fostriecin, has been revealed to inhibit both PP2A and PP4 catalytic subunits with similar potency (Hastie and Cohen, 1998; Buck et al., 2003). The effects of fostriecin on PP6 are currently unknown. It becomes apparent that the use of traditional pharmacological approach of protein inhibition of type 2A protein phosphatases complicates the determination of a role for each phosphatase separately. Nevertheless, the effects of these compounds on other toxin-sensitive members of the PPP family should not be ignored (i.e. PP5 activity is affected at concentrations >1-5 nM okadaic acid) (Dean et al., 2001; Swingle et al., 2007). Therefore, the siRNA-mediated PP2ACα, PP2ACβ, PP4C and PP6C protein expression knockdown in H9c2 cardiomyocytes, described in this chapter, is more appropriately selective. Efficient siRNA-mediated mRNA knockdown of PP2ACα, PP2ACβ or degradation of total PP2AC, PP4C and PP6C protein has been achieved before in other mammalian cell types (Nakada et al., 2008b; Zhong et al., 2011; Sunahori et al., 2013).

Table 4.5 Common inhibitors of type 2A protein phosphatase used in the literature.

Compound	IC_{50} (nM)			References
	PP2A	PP4	PP6	
Okadaic acid	0.1-10.0	0.1-0.2	0.1-2.0	(Brewis et al., 1993; Hastie and Cohen, 1998; Prickett and Brautigan, 2006)
Fostriecin	0.2-4.0	0.2-4.0	ND*	(Hastie and Cohen, 1998; Buck et al., 2003)
Calyculin A	1.0	0.2	1.0	(Hastie and Cohen, 1998; Prickett and Brautigan, 2006)

*ND: Not determined

Investigation of the potential off-target effects of the rat catalytic subunit-specific siRNAs (PP2ACα-, PP2ACβ -, PP4C- and PP6C-siRNAs) and on-target effects due to target protein degradation showed no significant alteration in the protein expression of the non-target catalytic subunits. Interestingly, when cells were transfected with rat PP2ACα-siRNA for 2 or 4 days (Figures 4.9B and 4.10B), the PP2ACβ gene transcript (mRNA) was decreased (1.58-fold or 1.41-fold decrease, respectively) and when cells were transfected with rat PP2ACβ-siRNA for 2 or 4 days (Figures 4.9A and 4.10A), the PP2ACα transcript was also decreased (1.57-fold or 1.68-fold change decrease, respectively), whilst the target mRNA in both transfections was decreased more than 22-fold. One of the main challenges in qPCR analysis is the determination of fold change levels indicating down- or up-regulation of a transcript influenced by treatment, such as siRNA-mediated post-transcriptional silencing of gene expression. In many recent studies of transcriptional profiling analysis, fold change ranking is established, whereby significant ($p<0.05$) 2-fold alterations suggest significant down- or up-regulation of the transcript respectively whilst, less than 2-fold increased or decreased mRNA expression indicate “normal” mRNA expression (Gao and Hui, 2001; Huang et al., 2015; Qin et al., 2015; Song et al., 2015; Sun et al., 2016). Thus, taken together, i) the 2-fold cut-off ($p<0.05$) described earlier, ii) the absence of efficient complementarity between each catalytic subunit-siRNA and the non-target catalytic subunit mRNAs, as described in section 4.4.2 and iii) the low concentration (12.5 nM) of each individual siRNA from the rat PP2ACα- and PP2ACβ-siRNA pools used in this study, the probability of an siRNA off-target effect, would be expected to be very low. Furthermore, previous studies have defined a 2-fold or more of non-target mRNA down-regulation to be considered a biologically relevant siRNA off-target effect whilst, less than 2-fold reduction in non-target mRNA expression in siRNA-transfection experiments, has been explained as experimental noise or considered biologically non-significant (Scacheri et al.,

2004; Birmingham et al., 2006; Schwarz et al., 2006; Aleman et al., 2007; Caffrey et al., 2011). Thus, the effects observed in the PP2ACα and PP2ACβ mRNAs when cells are transfected with rat PP2ACβ-siRNA or PP2ACα-siRNA, respectively, are considered biologically non-significant as a response to treatment.

Efficient siRNA-mediated post-transcriptional silencing resulted in progressive degradation of the target protein expression of all the type 2A protein catalytic subunits. From the data in figures 4.11-4.18 (sections 4.4.6 and 4.4.7), it becomes apparent that the biggest reduction of each catalytic subunit protein expression without a significant impact on the expression of the other catalytic subunit non-target proteins, was observed 4 days after siRNA-transfection with rat PP2ACα-, PP2ACβ-, PP4C- or PP6C-siRNA.

A noticeable but insignificant increase in the total PP2AC protein expression pattern was detected at 2 days post-transfection with rat PP2ACβ-siRNA compared to 1 day, 3 and 4 days post-transfection (Figure 4.11B), despite a significant ($p<0.05$) 24.39-fold decrease of the PP2ACβ mRNA expression. This result could be explained by the autoregulatory mechanism of PP2ACα and PP2ACβ at the level of translation, balancing the total PP2AC protein expression in cells, firstly described by Baharians and Schönthal (1998). In support of this study, Pandey et al., (2013), showed that total PP2AC was expressed at a constant level in human prostate cancer tissues, independently of hormone status, supporting the mechanism of PP2ACα and PP2ACβ autoregulation.

4.5.2 Effects of alpha4 protein knockdown on type 2A protein phosphatase expression

Strong evidence of the regulatory role of alpha4 protein towards the PP2AC, PP4C

and PP6C protein expression in H9c2 cardiomyocytes was found when alpha4 protein expression was significantly ($p<0.05$) reduced (>94%) at 4 days post-transfection. This led to a significant ($p<0.05$) knockdown of total PP2AC (>83%), PP4C (>84%) and PP6C (>73%) protein expression in cells. In accordance with the present results, previous reports have demonstrated that alpha4 protein deletion similarly resulted in the progressive loss of the type 2A protein phosphatase catalytic subunits in non-myocytes (Kong et al., 2009; LeNoue-Newton et al., 2016). The "protective role" of the alpha4 protein has been examined in relation to PP2AC in previous studies, proposing that three main domains of alpha4 (ubiquitin-interacting motif, E3 ligase- and PP2AC- binding domains) are required for alpha4 to inhibit PP2AC ubiquitination by the E3 ubiquitin ligase thus, "protecting" PP2AC from proteasome-mediated degradation (McConnell et al., 2010; LeNoue-Newton et al., 2011; Watkins et al., 2012). In addition, a crystal structure study by Jiang et al., in 2013, showed that the alpha4 protein interacts directly with the PP2AC and it was proposed that this binding may "protect" against PP2AC proteasome-mediated degradation by blocking access to a lysine residue in PP2AC that is targeted for polyubiquitination.

4.6 Summary

In summary, in this chapter, rat catalytic subunit specific-siRNAs were used to efficiently knockdown the expression of PP2ACα, PP2ACβ, PP4C, PP6C and alpha4 individually, in H9c2 cardiomyocytes. The concentration of the transfection reagents, cell confluency prior to transfection and experimental duration were optimised to achieve efficient knockdown of PP2ACα (>90%) and PP2ACβ (>90%) mRNA, or total PP2AC (>83%), PP4C (>95%), PP6C (>91%) and alpha4 (>94%) protein expression, without significant cytotoxicity (>80% cell viability of the control samples). The possibility of off-target effects was estimated low, based on the search for complementarity between the open reading frame or 3′ UTR sequence of the off-target mRNAs and full length or the seed region sequence of each siRNA, respectively. In the case of the type 2A protein phosphatase catalytic subunit siRNA-mediated protein knockdown, the protein expression of the non-target proteins for each siRNA assay showed non-significant siRNA off-target effects. In addition, siRNA-driven alpha4 protein knockdown (>94%) in H9c2 cardiomyocytes resulted in progressive loss of total PP2AC (>83%), PP4C (>84%) and PP6C (>73%) protein expression, suggesting that alpha4 plays a central role towards the expression stability of the type 2A protein phosphatase catalytic subunits in cardiomyocytes. The siRNA-mediated post-transcriptional silencing model of PP2ACα, PP2ACβ, PP4C, PP6C and alpha4 is further used in this study, to investigate the involvement of type 2A protein phosphatases and/ or alpha4 protein in biological pathways associated with Ca^{2+} homeostasis regulation, hypertrophy and DNA repair in H9c2 cardiomyocytes.

Chapter 5

Role of Type 2A Protein Phosphatase Catalytic Subunits in the Phosphorylation of Proteins Involved in the Regulation of Cardiomyocyte Ca^{2+} Homeostasis

5.1 Introduction

As outlined in Chapter 1 (section 1.3), electrical excitation of the cardiomyocytes activates cardiac contraction via a process called excitation-contraction coupling. Calcium (Ca^{2+}) and sodium (Na^{+}) homeostasis within the cardiomyocytes is critical for the cardiac excitation-contraction coupling process and is influenced by the phosphorylation status of many regulatory proteins (Figure 5.1). These proteins include the ryanodine receptors (RyRs), the phospholamban, the L-type calcium channel, $Ca_V1.2$, the Na^{+} channels $Na_V1.5$, the phospholemman and the myofilament proteins troponin I and myosin binding protein C (Gao et al., 1997; Marx et al., 2000a; MacLennan and Kranias, 2003; Xiao et al., 2005; Hulme et al., 2006a; Pavlović et al., 2007; Stelzer et al., 2007; Shi et al., 2012; Kooij et al., 2013). PP2A, that has been shown to be associated with many of the above cardiac cellular proteins, thereby playing a critical role in cardiac physiology (MacDougall et al., 1991; Marx et al., 2000b; Schulze et al., 2003; Ai and Pogwizd, 2005; Hall et al., 2006a; Jideama et al., 2006b; Deshmukh et al., 2007; Shi et al., 2012), however, PP4 and PP6 roles in cardiac calcium handling are yet unknown. Impaired PP2A expression and activity and dysregulation of the phosphorylation mechanism for

these regulatory proteins has been associated with cardiac dysfunction and cardiovascular diseases, atrial fibrillation and heart failure (Pieske et al., 1999; Marx et al., 2000a; Christ et al., 2004; Gergs et al., 2004; Sadayappan et al., 2005; El-Armouche et al., 2006b; Wijnker et al., 2011; Hamdani et al., 2013; Boguslavskyi et al., 2014; Li et al., 2016). Hence, the focus of this chapter is to investigate the activity of type 2A protein phosphatase catalytic subunits towards specific phosphorylation sites on L-type calcium channel ($Ca_V1.2$) and phospholemman.

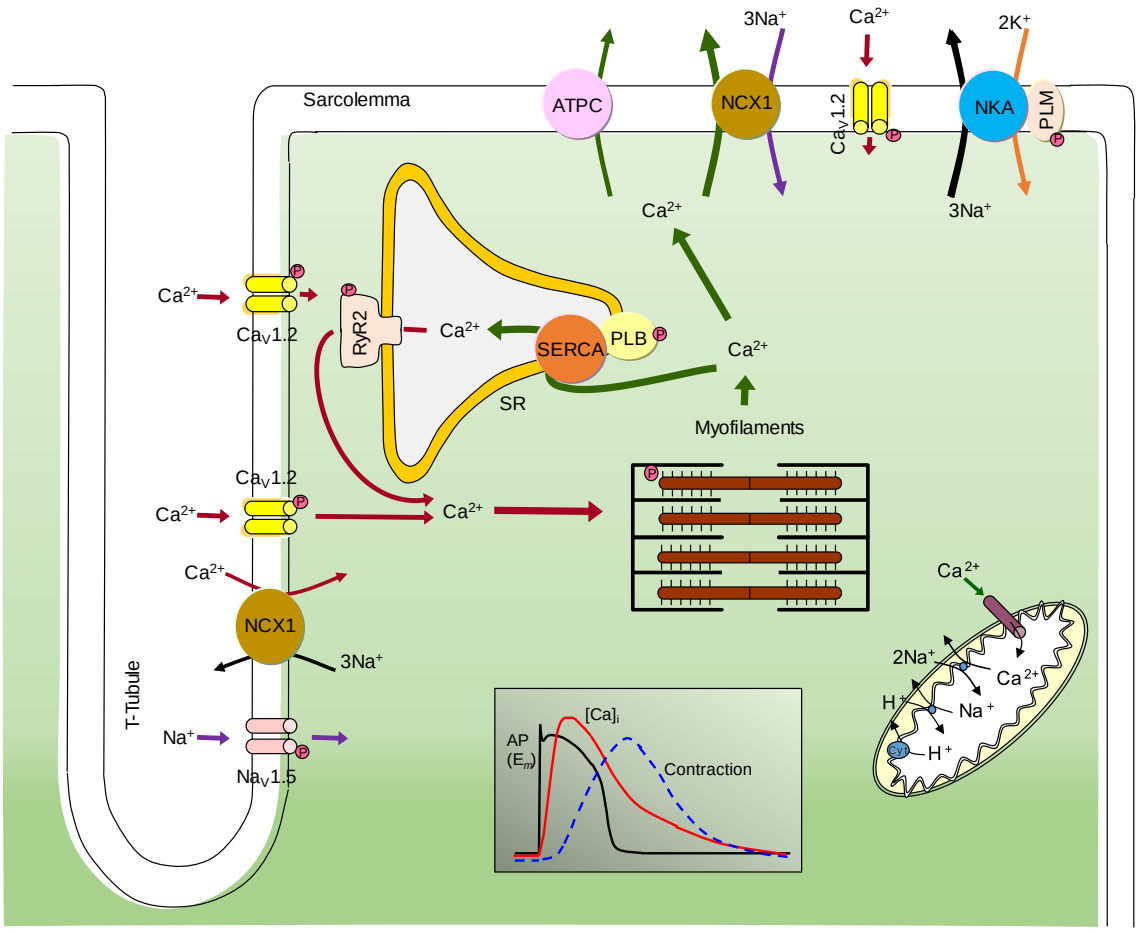

Figure 5.1 Simplified schematic representation of sodium and calcium transport during cardiac excitation-contraction coupling, including involved functional proteins which are regulated by phosphorylation (adapted from Bers, 2002). NCX1: Na^+/Ca^{2+}-exchanger; ATPC: Ca^{2+}-ATPase; NKA: Na^+/K^+-ATPase; PLB: phospholamban; PLM: phospholemman; SR: sarcoplasmic reticulum; SERCA: SR Ca^{2+}-ATPase; RyR; ryanodine receptors. NHE: Na^+/K^+-exchanger; $Na_V1.5$: Na^+ channel; P: phosphorylation site; AP: action potential; E_m: membrane potential; [Ca]i: Ca2+ intracellular concentration; Red arrows: Ca^{2+} entry into the cytosol; Green arrows: Ca^{2+} removal from the cytosol; purple arrows: Na^+ influx; black arrows: Na^+ efflux; Orange arrow: K^+ influx; Grey arrow: H^+ efflux.

5.1.1 $Ca_V1.2$-Ser1928 phosphorylation in cardiomyocytes

Ca^{2+} entry into cardiomyocytes is mainly attributable to the L-type calcium channel $Ca_V1.2$ activity during excitation-contraction coupling (Bers, 2001). L-type calcium channel consists of four subunits: the α_1, α_2, β and δ subunits (review by Harvey and Johannes, 2013). In response to the β-adrenergic receptors and cAMP/PKA signalling pathway activation, $Ca_V1.2$ is phosphorylated by the PKA at the α_1 C-terminal domain (α_{1c}) and is further activated leading to an increase in intracellular Ca^{2+} resulting in forceful heart contraction (Bers, 2001). In the α1 C-terminal domain, $Ca_V1.2$-Ser1928, a highly conserved residue across mammalian species, has been suggested as an important target residue for PKA-mediated phosphorylation (Gao et al., 1997; Hulme et al., 2006a; Shi et al., 2012). Towards dephosphorylation of $Ca_V1.2$-Ser1928, most reports, using okadaic acid, have pointed PP2A as the major phosphatase for $Ca_V1.2$-Ser1928 that downregulates its activity (Gao et al., 1997; Hall et al., 2006; Hulme et al., 2006a; Xu et al., 2010; Shi et al., 2012), potentially via the recruitment of a PP2AB' (all isoforms) or PP2AB"-PR59 regulatory subunit (Hall et al., 2006). Impaired $Ca_V1.2$ function has been associated with various cardiovascular diseases including hypertension, arrhythmia and heart failure (Schröder et al., 1998; Splawski et al., 2004; Hong et al., 2012).

5.1.2 Regulation and function of phospholemman in cardiomyocytes

Phospholemman (PLM), also known as FXYD1 (FXYD-domain containing ion transport regulator 1) (Sweadner and Rael, 2000), is a major sarcolemmal substrate for PKA and PKC in the heart that regulates the activity of the Na^+/K^+-ATPase (NKA) (Pavlovic et al., 2013). The NKA is important in Na^+ efflux from the cardiomyocyte and sodium homeostasis which in turn affects various ion exchange and transport processes, including Ca^{2+} flux via the Na^+/Ca^{2+}-exchanger (NCX1) (Pieske et al., 1999; Despa et al., 2002; Pieske et al., 2002; Baartscheer et al., 2003; Wang et al., 2011; Pavlovic et al., 2013). The mode of the NCX1 activity is

determined by the membrane potential and the intracellular Na^+ and Ca^{2+} concentrations (Kang and Hilgemann, 2004)). Thus, phospholemman appears to play an indirect but essential role in the calcium homeostasis and regulation of cardiac contractility.

Phospholemman has three established phosphorylation sites, serine 63 (Ser63), serine 68 (Ser68) and serine/ threonine-69 (Ser/Thr69) residues which alter its function. Unphosphorylated PLM inhibits NKA activity, however, following phosphorylation at Ser68 by protein kinase A (PKA) and/ or at Ser63, Ser68 or Thr/Ser69 by PKC, activity of the NKA in cardiomyocytes is elevated (Han et al., 2006; Pavlovic et al., 2007; Fuller et al., 2009; Madhani et al., 2010). Dephosphorylation of these residues is linked with the activities of protein phosphatases 1 and 2A (Bossuyt et al., 2005; Fuller et al., 2013; Wypijewski et al., 2013).

Studies in heart failure, have shown alteration of the phosphorylation status of PLM, mainly hypophosphorylation, that has been associated with increased phosphatase activity (Bossuyt et al., 2005; El-Armouche et al., 2011; Boguslavskyi et al., 2014). Thus, the regulation of phospholemman Ser63 and Ser68 phosphorylation was further investigated in this chapter, after protein knockdown of the type 2A protein phosphatase catalytic subunits (PP2ACα, PP2ACβ, PP4C and PP6C) by introducing small interfering RNA into H9c2 cardiomyocytes.

5.2 Specific objectives

The studies described in this chapter aim to provide new insights into the role of individual type 2A protein phosphatases in cardiac calcium handling by investigating:

1. the involvement of type 2A protein phosphatases in the regulation of $Ca_V1.2$ phosphorylation in H9c2 cardiomyocytes.

2. the effects of PP2ACα, PP2ACβ, PP4C or PP6C protein knockdown on the phosphorylation status of PLM-Ser63 and PLM-Ser68.

5.3 Methods

5.3.1 Western blotting analysis

Phosphorylation of PLM-Ser63 and PLM-Ser68 was detected by western blotting analysis as described in Chapter 2 (section 2.5) using custom-made antibodies. A rabbit polyclonal phospho-$Ca_V1.2$ antibody (p-$Ca_V1.2$-Ser1928) was used for the detection of $Ca_V1.2$-Ser1928 phosphorylation. Even though the p-$Ca_V1.2$-Ser1928 antibody was specific for human species, alignment of the $Ca_V1.2$ amino acid sequence between the human (Uniprot ID: Q13936) and the rat (Uniprot ID: P22002) analogues showed 100% homology 10 amino acid upstream and downstream serine 1928 within the antibody epitope. In addition, levels of actin and total levels of PLM expression (also known as FXYD1) were detected to ensure equal protein loading and/ or data normalisation. Details about the antibodies and working dilutions used in this chapter are presented in table 2.3.

5.4 Results

5.4.1 Effects of PP2ACα, PP2ACβ, PP4C or PP6C protein knockdown on the phosphorylation of $Ca_V1.2$-Ser1928

To evaluate the role of type 2A protein phosphatase catalytic subunits in regulating the phosphorylation of the $Ca_V1.2$-Ser1928, H9c2 cardiomyocytes were transfected with rat catalytic subunit-specific siRNAs as described in Chapter 2 (section 2.3.1) and lysates showing knockdown of mRNA or protein siRNA-mediated expression above 80% after 4 days post-transfection, were chosen as described in Chapter 4 (sections 4.4.5-4.4.6) and were further tested by immunoblotting analysis.

Transfection of cardiomyocytes with PP2ACα-siRNA, which resulted in significant ($p<0.05$) mRNA knockdown (71.4-fold decrease) and reduced total PP2AC protein expression (51.7%), led to a significant ($p<0.05$) increase (155.1 ± 20.9%) in the phosphorylation level of $Ca_V1.2$-Ser1928 (Figure 5.2A). Cells transfected with PP2ACβ-siRNA, which resulted in reduced PP2ACβ mRNA expression (22.7-fold decrease) and total PP2AC protein expression (53.3% less) did not cause significant alteration in the phosphorylation level of $Ca_V1.2$-Ser1928 compared to the phosphorylation levels in cells transfected with non-targeting control siRNA (Figure 5.2B). Likewise, cardiomyocytes transfected with PP4C- or PP6C-siRNA, that led to a significant knockdown of PP4C (>95%) and PP6C (>91%) protein expression did not alter the basal phosphorylation level of $Ca_V1.2$-Ser1928 (Figures 5.1C and 5.1D) significantly. These data suggest that PP2ACα may regulate the phosphorylation of $Ca_V1.2$-Ser1928 in cardiomyocytes directly.

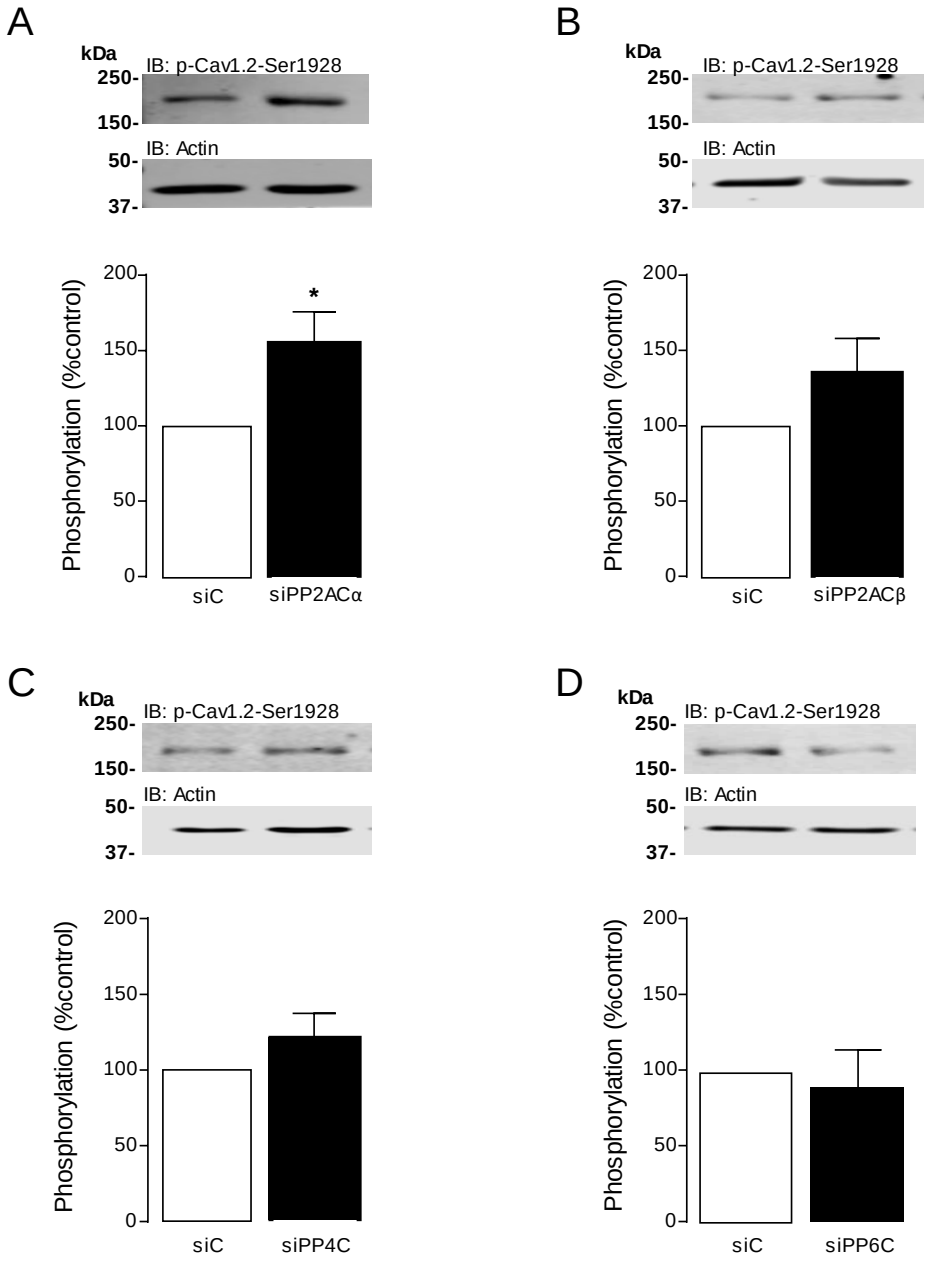

Figure 5.2 Phosphorylation level of CaV1.2-Ser1928 in H9c2 cardiomyocytes, transfected with rat PP2ACα- (siPP2ACα) (**A**), PP2ACβ- (siPP2ACβ) (**B**), PP4C- (siPP4C) (**C**), PP6C- (siPP6C) (**D**) siRNAs or non-targeting control siRNA (siC) for 4 days, was detected by immunoblotting analysis using a rabbit polyclonal anti-phospho-$Ca_V1.2$-Ser1928 antibody. Protein levels were quantified by LI-COR Odyssey® CLx Imaging System and were normalised to actin in each sample. All data represent mean values ± SEM of five individual experiments. Statistical comparison was made by a two-tailed unpaired Student's t-test; *p<0.05 *vs* siC. IB: immunoblot.

5.4.2 Effects of PP2ACα, PP2ACβ, PP4C or PP6C protein knockdown on the phosphorylation of PLM-Ser63 and PLM-Ser68

To investigate the role of type 2A protein phosphatase catalytic subunits in regulating the phosphorylation of PLM-Ser63 and/or PLM-Ser68, H9c2 cardiomyocytes were transfected with rat catalytic subunit-specific siRNAs as (section 2.3.1) and lysates showing mRNA or protein siRNA-mediated expression knockdown above 80% 4 days post-transfection, were chosen as described in Chapter 4 (sections 4.4.5-4.4.6) and were further tested by immunoblotting analysis.

Transfection of cardiomyocytes with PP2ACα-siRNA, which resulted in significant ($p<0.05$) mRNA knockdown (71.4-fold decrease) and reduction of total PP2AC protein expression (51.7%), led to in a significant ($p<0.05$) increase (331.7 ± 79.0%) of the phosphorylation level of PLM-Ser63 (Figure 5.3A). In the same cellular lysates, significantly ($p<0.05$) elevated phosphorylation level of PLM-Ser68 (471.0 ± 145.2%) was also detected compared to the control (Figure 5.3B). As it can be seen in figures 5.4A and 5.4B, cells transfected with PP2ACβ-siRNA, which resulted in reduced PP2ACβ mRNA expression (22.73-fold decrease) and total PP2AC protein expression (53.3%), led to a significant ($p<0.05$) increase in the phosphorylation level of both PLM-Ser63 and PLM-Ser68 (386.4 ± 76.3% and 408.4 ± 119.2%, respectively). Furthermore, a significant ($p<0.05$) PP4C protein knockdown (>95%) resulted in significantly ($p<0.05$) elevated phosphorylation levels of PLM-Ser63 (1082.0 ± 303.5%) and PLM-Ser68 (1101.0 ± 225.9%) (Figures 5.5A and 5.5B). On the other hand, siRNA-mediated protein knockdown of PP6C (>91%) did not cause any significant alteration in the phosphorylation status of PLM-Ser63 or PLM-Ser68 (Figures 5.6A and 5.6B). These data suggest that PP2ACα, PP2ACβ and PP4C are involved in the regulation of PLM-Ser63 and PLM-Ser68 phosphorylation.

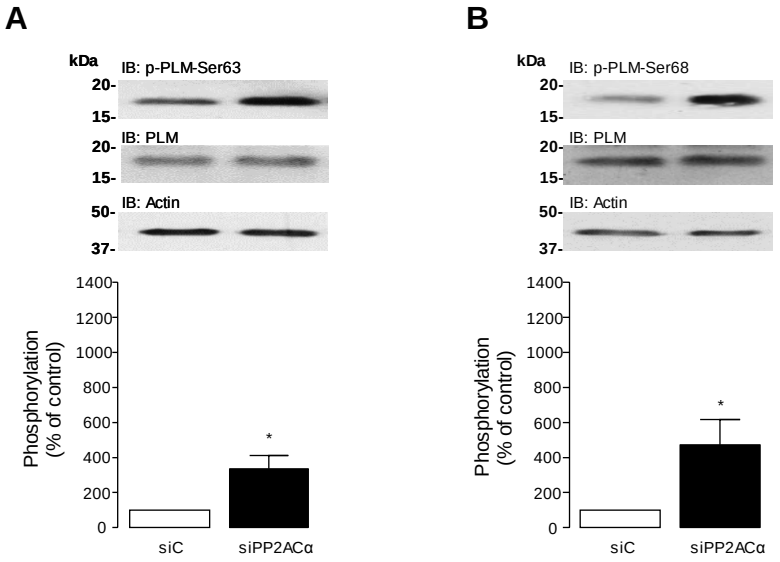

Figure 5.3 Phosphorylation level of PLM-Ser63 (**A**) or PLM-Ser68 (**B**) and total expression level of PLM in H9c2 cardiomyocytes, transfected with rat PP2ACα-siRNA (siPP2ACα) or non-targeting control siRNA (siC) for 4 days, was detected by immunoblotting analysis using specific rabbit polyclonal anti-phospho-PLM-Ser63, anti-phospho-PLM-Ser68 and rabbit monoclonal anti-PLM antibodies. Protein levels were quantified by densitometry and were normalised to total PLM in each sample. All data represent mean values ± SEM of six individual experiments. Statistical comparison was made by a two-tailed unpaired Student's t-test; *p<0.05 *vs* siC. IB: immunoblot.

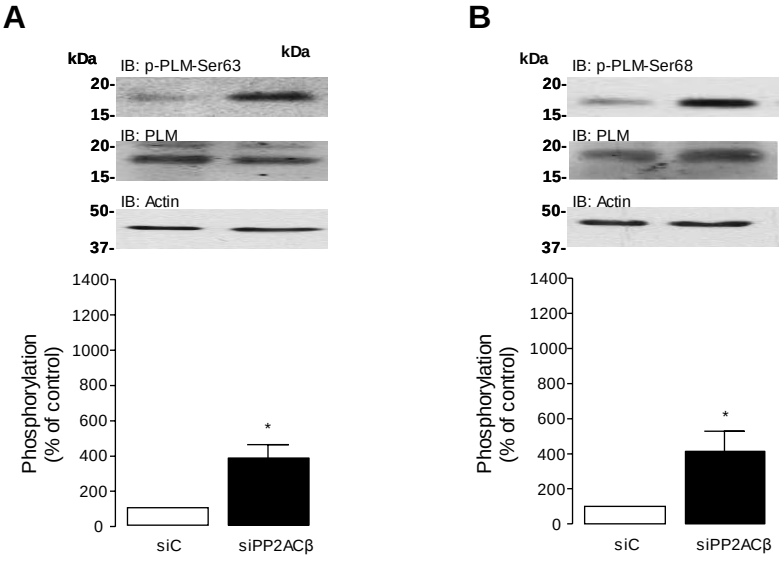

Figure 5.4 Phosphorylation level of PLM-Ser63 (**A**) or PLM-Ser68 (**B**) and total expression level of PLM in H9c2 cardiomyocytes, transfected with rat PP2ACβ-siRNA (siPP2ACβ) or non-targeting control siRNA (siC) for 4 days, was detected by immunoblotting analysis using specific rabbit polyclonal anti-phospho-PLM-Ser63, anti-phospho-PLM-Ser68 and rabbit monoclonal anti-PLM antibodies. Protein levels were quantified by densitometry and were normalised to total PLM in each sample. All data represent mean values ± SEM of six individual experiments. Statistical comparison was made by a two-tailed unpaired Student's t-test; *p<0.05 *vs* siC. IB: immunoblot.

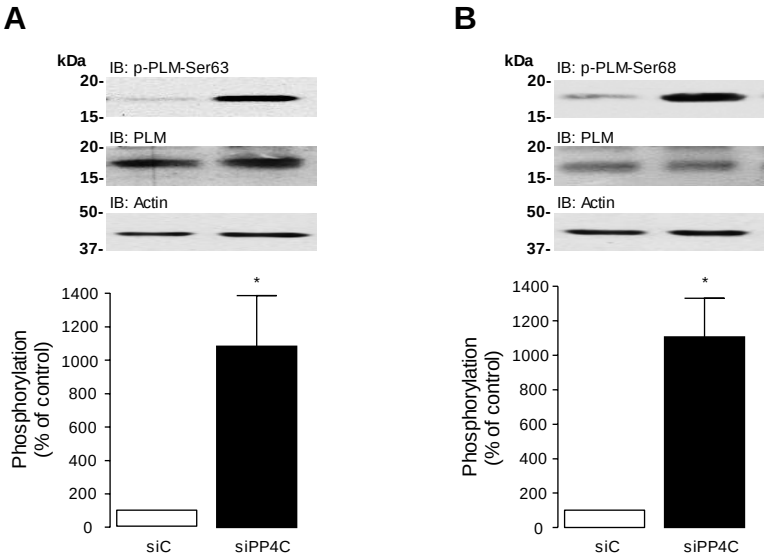

Figure 5.5 Phosphorylation level of PLM-Ser63 (**A**) or PLM-Ser68 (**B**) and total expression level of PLM in H9c2 cardiomyocytes, transfected with rat PP4C-siRNA (siPP4C) or non-targeting control siRNA (siC) for 4 days, was detected by immunoblotting analysis using specific rabbit polyclonal anti-phospho-PLM-Ser63, anti-phospho-PLM-Ser68 and rabbit monoclonal anti-PLM antibodies. Protein levels were quantified by densitometry and were normalised to total PLM in each sample. All data represent mean values ± SEM of six individual experiments. Statistical comparison was made by a two-tailed unpaired Student's t-test; *p<0.05 *vs* siC. IB: immunoblot.

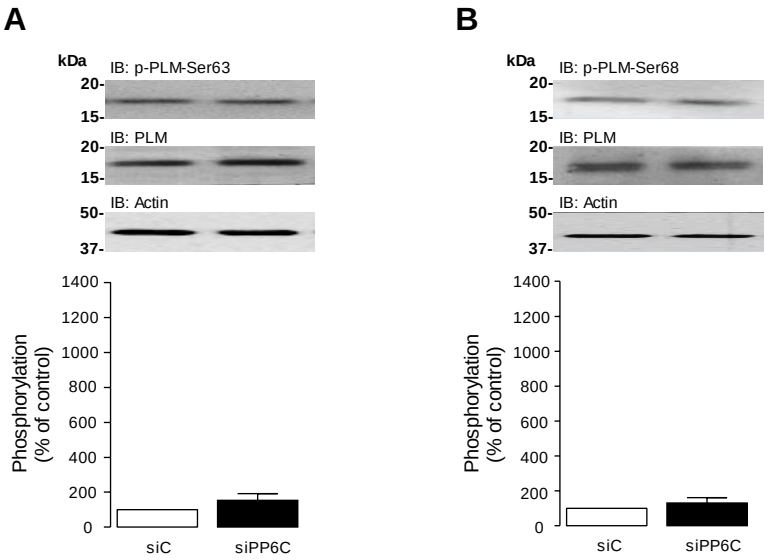

Figure 5.6 Phosphorylation level of PLM-Ser63 (**A**) or PLM-Ser68 (**B**) and total expression level of PLM in H9c2 cardiomyocytes, transfected with rat PP6C-siRNA (siPP6C) or non-targeting control siRNA (siC) for 4 days, was detected by immunoblotting analysis using specific rabbit polyclonal anti-phospho-PLM-Ser63, anti-phospho-PLM-Ser68 and rabbit monoclonal anti-PLM antibodies. Protein levels were quantified by densitometry and were normalised to total PLM in each sample. All data represent mean values ± SEM of six individual experiments. Statistical comparison was made by a two-tailed unpaired Student's t-test; *p<0.05 *vs* siC. IB: immunoblot.

5.5 Discussion

5.5.1 Regulation of $Ca_V1.2$-Ser1928 dephosphorylation by the type 2A protein phosphatase catalytic subunits

H9c2 cardiomyocytes have been shown to express L-type calcium current (I_{CaL}) with cardiac characteristics and the L-type calcium channel $\alpha 1_C$ subunit (Sipido and Marban, 1991; Mejla-Alvarez et al., 1994; Menard et al., 1999; Wang et al., 1999; Shi et al., 2012). In addition, it has been shown that the RyR2, NCX1, Na^+/K^+-ATPase are also expressed in H9c2 cardiomyocytes (Pacher et al., 2002; Maeda et al., 2005; Rahamimoff et al., 2007; Yan et al., 2016; You et al., 2016). All the above studies in combination with the demonstration of type 2A protein phosphatase catalytic subunits expression in Chapter 3 (sections 3.4.1 and 3.4.3) suggest that the rat embryonic heart-derived H9c2 cell line can be an appropriate experimental model to investigate the type 2A protein phosphatase catalytic subunit-mediated regulation of functional proteins involved in calcium regulation in cardiomyocytes.

In cardiac myocytes, activation of β_1-adrenergic receptors by catecholamines causes stimulation of the L-type Ca^{2+} channel current through a cAMP/ PKA-dependent pathway (Chapter 1, section 1.3.3). In cardiac myocytes, PKA-mediated phosphorylation occurs on the C-terminal residue Ser1928 in the α_{1c} subunit (Gao et al., 1997; Davare et al., 2001; Hulme et al., 2006a). In addition, $Ca_V1.2$-Ser1928 has been shown to be a common site for phosphorylation-mediated activation by PKC (Yang et al., 2005) and protein kinase G (PKG) (Yang et al., 2007). Even though there are many published studies, highlighting the importance of $Ca_V1.2$-Ser1928 in cAMP/ PKA pathway (Gao et al., 1997; Hal et al., 2006; Hulme et al., 2006; review by Weber et al., 2015), two studies by Ganesan et al. (2006) and Lemke et al. (2008) indicated that Ser1928 may not be involved in the regulation of $Ca_V1.2$ upon β_1-

adrenergic receptor stimulus. However, a recent study of Shi et al. (2012) proposed an important role of $Ca_V1.2$-Ser1928 phosphorylation in the regulation of basal L-type Ca^{2+} current. In that study, it was suggested that PP2A (via the PP2ACα) dephosphorylates $Ca_V1.2$-Ser1928 (Shi et al., 2012), using a PP2ACα knock-out mouse model and by treating H9c2 cardiomyocytes with okadaic acid. Interestingly, a recent study by Patriarchi et al., (2016), in neurons, suggested that PP2AC-mediated dephosphorylation of $Ca_V1.2$-Ser1928 specifically displaces the β_2-adrenergic receptors from $Ca_V1.2$, which prevented further $Ca_V1.2$ phosphorylation (Patriarchi et al., 2016). PP2AC has been shown to co-localise with β_2-adrenergic receptor and $Ca_V1.2$ in both neurons and cardiomyocytes (Davare et al., 2001; Balijepalli et al., 2006) or with $Ca_V1.2$ close to the Z-line (Shi et al., 2012).

Since in some of the studies, mentioned above, okadaic acid or other non-specific inhibitors were used to implicate the role of PP2AC in the dephosphorylation of $Ca_V1.2$-Ser1928 (Gao et al., 1997; Yang et al., 2005; Hall et al., 2006; Shi et al., 2012), however, okadaic acid is known to inhibit all three type 2A protein phosphatase catalytic subunits as discussed in Chapter 4 (section 4.5.1). In this chapter, each type 2A protein phosphatase catalytic subunit expression was knocked down, using rat catalytic subunit-specific siRNA in H9c2 cardiomyocytes. The data presented in this Chapter showed that knockdown of PP2ACα resulted in a 55% increase in basal $Ca_V1.2$-Ser1928 phosphorylation in H9c2 cardiomyocytes. These data are in line with a previous study (Hulme et al., 2006a), showing that PKA activation by stimulating β_1-adrenergic receptor with isoprenaline resulted in a 65% increase in $Ca_V1.2$-Ser1928 phosphorylation and a 3.3 ± 0.2-fold increase in the calcium current. In addition, Shi et al. (2012), showed that treatment of H9c2 cardiomyocytes with okadaic acid or deletion of PP2ACα in the mouse myocardium resulted in 80% or 100% increase of $Ca_V1.2$-Ser1928 phosphorylation, respectively

and significantly increased basal L-type calcium current in the latter (Shi et al., 2012). The biological function of $Ca_V1.2$-Ser1928 phosphorylation requires further investigation.

5.5.2 Regulation of PLM-Ser63 and PLM-Ser68 dephosphorylation by the type 2A protein phosphatase catalytic subunits

PLM is shown to co-localise with NKA (Bossuyt et al., 2005; Silverman et al., 2005) and is found that when unphosphorylated it inhibits NKA activity (Han et al., 2006; Despa et al., 2008; Fuller et al., 2009). PLM is also found to co-localise with NCX1 and has been shown to inhibit NCX1 when phosphorylated at PLM-Ser68 (Zhang et al., 2003; Wang et al., 2011). Although the latter has only been shown by one research group, additional functions of PLM cannot be ruled out. In regard to PLM-mediated regulation of NKA activity, it has been shown that phosphorylation at PLM-Ser63, PLM-Ser68 and/or PLM-Ser/Thr69 results in activation of the NKA and extrusion of Na^+ from the cytosol.

In this chapter, data showed a significant increase in PLM-Ser63 (3.3-fold) and PLM-Ser68 (4.7-fold) when PP2ACα, PP2ACβ or PP4C protein expression was silenced in H9c2 cardiomyocytes. Han et al. (2006), previously reported that activation of the cAMP/ PKA pathway by stimulating β1-adrenergic receptors in mouse ventricular myocytes resulted in a significant 2-fold increase in the PKA-mediated PLM-Ser68 phosphorylation (Han et al., 2006). In the same study, stimulation of PKC by phorbol-12,13-dibutyrate caused a significant 2-fold and 4-fold increase in PLM-Ser63 and PLM-Ser68 phosphorylation respectively and a significant increase in NKA-mediated Na^+ extrusion (Han et al., 2006). The data in this chapter suggest that silencing the expression of PP2ACα, PP2ACβ or PP4C could have a similar biological effect in the activity of NKA in cardiomyocytes.

It has been shown that PP1 regulates PLM-Ser68 phosphorylation, however, its activity is dependent on the phosphorylation status of the protein phosphatase inhibitor-1, which when phosphorylated at Thr35 by PKA, it then inhibits PP1 function (Han et al., 2006; El-Armouche et al., 2011). It has been proposed that PP2A dephosphorylates protein phosphatase inhibitor-1 at Thr35, therefore indirectly affecting the phosphorylation of PLM-Ser68 (El-Armouche et al., 2006a). Furthermore, PP2A has been suggested to dephosphorylate PLM-Ser63 (El-Armouche et al., 2006a). A recent study by Wypijewski et al., (2013), provides more evidence that PP2AC may act indirectly in the regulation of PLM-Ser68 dephosphorylation and directly dephosphorylate PLM-Ser63. In the current study, PP2ACα and PP2ACβ were shown to dephosphorylate PLM-Ser63. The activity of PP4C towards PLM dephosphorylation was investigated for the first time in this study. Interestingly data indicated that PP4C dephosphorylates both PLM-Ser63 and PLM-Ser68.

Activation of the sympathetic nervous system in response to stressor pathological conditions results in an increased cardiac performance via the activation of the sympathetic nervous system. The adrenergic receptors are stimulated, raising intracellular cAMP and activating PKA (Bers, 2001). This stimulus causes an increase in intracellular Ca^{2+} and consequently positive chronotropy. PKA, in turn, phosphorylates PLM-Ser68 (Han et al., 2006; Despa et al., 2008), thus increasing the activity of Na^{+}/K^{+}-ATPase and the extrusion of Na^{+} from cardiomyocytes. The release of Na^{+} from the cell favours the efflux of Ca^{2+} via the forward mode of NCX1, which leads to negative lusitropy and chronotropy, therefore protecting the cells from the Ca^{2+} overload effects. Regulation of this mechanism appears to be critical for the physiology of cardiomyocytes and the effective protection of the heart from triggered arrhythmias short term or pathological cardiac hypertrophy

development long term, following the chronic stimulus (Despa et al., 2008; Fuller et al., 2009).

Furthermore, increased intracellular Na^+ $[Na^+]_i$ and consequently increased cytosolic Ca^{2+} $[Ca^{2+}]_i$ concentration has been observed in many models of heart failure, indicating that dysregulation of sodium homeostasis may be involved in disease progression (Jelicks and Siri, 1995; Pieske et al., 2002; Baartscheer et al., 2003; El-Armouche et al., 2011). A possible explanation for the observed elevated $[Na^+]_i$ could be a downregulation of NKA expression or activity shown in some but not all heart failure models and/ or increased Na^+ influx by an enhanced Na^+/H^+ exchange or Na^+ channel activity (Shamraj et al., 1993; Bundgaard and Kjeldsen, 1996; Schwinger et al., 1999; Despa et al., 2002; Baartscheer et al., 2003; Maltsev et al., 2007; Nakamura et al., 2008). Nevertheless, impaired phosphorylation status of PLM has been implicated in heart failure. Bossuyt et al., (2005) showed that PLM-Ser68 was hyperphosphorylated in a rabbit heart failure model they used and concluded that the increase in the phosphorylation status is a critical mechanism for the offset of $[Na^+]_i$ increase due to downregulated NKA expression in their model (Bossuyt et al., 2005). In contrast, El-Armouche et al., (2011) reported a reduced (approximately 50%) phosphorylation of PLM-Ser68 in human heart failure compared to non-failing controls, therefore suggesting an increased inhibition of NKA activity which could explain the observed increase of $[Na^+]$i and $[Ca^{2+}]$i in heart failure and this impaired Na^+ regulation was indicated to be involved in maladaptive cardiac hypertrophy and arrhythmia (El-Armouche et al., 2011). In support of the latter study, Boguslavskyi et al., (2014) showed hypophosphorylation of PLM-Ser63 and PLM-Ser68 in pressure overload cardiac hypertrophy, developed in mice following aortic constriction (Boguslavskyi et al., 2014). In the same study, it was shown that hypertrophic response due to pressure overload was more severe in knock-in mice

for PLM-Ser63, -Ser68 and -Ser69, accompanied with a significantly higher $[Na^+]_i$, compared to the wild type phenotype (Boguslavskyi et al., 2014). The two latter studies provided evidence supporting the protective role of unphosphorylated PLM against $[Na^+]_i$ overload and consequently elevated $[Ca^{2+}]_i$ suggesting regulation of PLM activity as a potential therapeutic target for heart failure. The results in this chapter provided further insight into the regulatory mechanism of PLM-Ser63 and PLM-Ser68 phosphorylation by the type 2A protein phosphatase catalytic subunits.

5.6 Summary

In summary, in this chapter, $Ca_V1.2$-Ser1928 dephosphorylation was shown to be regulated by the activity of PP2ACα in cardiomyocytes but not PP2ACα, PP2ACβ or PP4C. Furthermore, PP2ACα, PP2ACβ and PP4C, but not PP6C, were shown to induce dephosphorylation of both PLM-Ser63 and PLM-Ser68. However, the contribution of PP1 to dephosphorylation of PLM-Ser68 due to dephosphorylation of protein phosphatase Inhibitor-1 at Thr35 by PP2AC cannot be ruled out.

Chapter 6

Role of the Type 2A Protein Phosphatases in Cardiac Hypertrophy

6.1 Introduction

6.1.1 Pressure overload-induced cardiac hypertrophy

Overall, cardiac hypertrophy can be defined as an increase in cardiac mass, in response to pressure or volume overload, to maintain a heart's pumping capacity (Grossman et al., 1975; Matsuo et al., 1998; Segers et al., 2000; reviewed by Heineke and Molkentin, 2006). Different (patho)physiological stimuli can induce different forms of (patho)physiological cardiac hypertrophy (Grossman et al., 1975; Matsuo et al., 1998; Pluim et al., 2000; Segers et al., 2000; Eghbali et al., 2005), as outlined in Chapter 1 (section 1.2). A pathological condition that can cause pressure overload, such as hypertension or aortic stenosis, produces systolic wall stress and induces concentric hypertrophy. Thereby, chronic pressure overload can cause thickening of the left ventricle wall to normalise the systolic wall stress, resulting in pathological hypertrophy (Grossman et al., 1975; Segers et al., 2000; Hein et al., 2003). Sustained stimulus and consequently prolongation of the pathological hypertrophic state is related to cardiomyocyte remodelling, fibrotic replacement, impaired cardiac function and progression to cardiovascular disease and heart failure, which is associated with high death rate (Levy et al., 1996; Hein et al., 2003; Gradman and Alfayoumi, 2006; Izumiya et al., 2006; Ying et al., 2009; Chatterjee et

al., 2014; Ponikowski et al., 2014; Bhatnagar et al., 2015; Gerber et al., 2015). Therefore, understanding the molecular mechanisms involved in the development of pathological cardiac hypertrophy is of great importance to identify new therapeutic targets for the prevention of heart failure.

Pathological cardiac hypertrophy is dependent on the activation of signalling pathways (Chapter 1, section 1.2.5), changes in gene transcription (maladaptive and/or adaptive genes) and an increased rate of protein synthesis (Gupta et al., 1996; Molkentin et a., 1998; Wang et al., 1998; Choukroun et al., 1999; Behr et al., 2001; Nicol et al., 2001; Minamino et al., 2002; Braz et al., 2003; Raman and Cobb, 2003; Harris et al., 2004; Wilkins et al., 2004; Sopontammarak et al., 2005; reviewed by Heineke and Molkentin, 2006; Liu et al., 2009; Lorenze et al., 2009; Ruppert et al., 2013). In many of these signalling pathways, serine/threonine-specific kinases are activated, such PKC, CaMKII and members of the MAPK kinases (such as ERK1/2), which in turn can phosphorylate many cardiac proteins, including PLM, RyR2, SERCA2a, phospholamban and cAMP-response element binding protein (CREB), that are involved in cardiac function and development of cardiac hypertrophy (MacDougall et al., 1991; Naraynan and Xu, 1997; Molkentin et al., 1998; Nicol et al., 2001; Zhang et al., 2002; Braz et al., 2004; Harris et al., 2004; Han et al., 2006; Li et al., 2006; El-Armouche et al., 2006a; Huke and Bers, 2008a; Backs et al., 2009; Lorenz et al., 2009; El-Armouche et al., 2011; Ruppert et al., 2013; Mutlak and Kehat, 2015). Dephosphorylation of these cardiac proteins depends on the activity of serine/threonine protein phosphatases, including the type 2A protein phosphatases (MacDougall et al., 1991; Zhang et al., 2002; Li et al., 2006; Olsen et al., 2006; El-Armouche et al., 2006a; Huke and Bers, 2008a; El-Armouche et al., 2011). Even though the involvement of PP2AC in pathological cardiac hypertrophy has been previously investigated (Gergs et al., 2004; Ling et al., 2012; Hoehn et al.,

2015; Li et al., 2016), its role and regulation is not yet well understood, whilst the role of PP4C and PP6C remains unknown. In this chapter, the expression of type 2A protein phosphatase catalytic subunits, their association with the alpha4 regulatory protein and the expression of PP6 regulatory subunits was investigated in normal and pressure overload-induced hypertrophied murine left ventricular (LV) tissue.

6.1.2 Oxidative stress and heart disease

Reactive oxygen species (ROS) is a phrase used to describe a number of free radicals (species with unpaired electron) such as superoxide ($O_2^{-\bullet}$) and hydroxyl radical ($OH^{\bullet}$) and molecules derived from molecular oxygen that are generated through a sequential reduction of oxygen, such as hydrogen peroxide (H_2O_2) (Haber and Weiss, 1934; Cohen et al., 1974; Liochev and Fridovich, 1994; Kehrer, 2000; Thomas et al., 2009). These ROS can be generated endogenously during mitochondrial oxidative phosphorylation or by ROS-generating enzymes such as nicotinamide adenine dinucleotide phosphate (NADPH) oxidase activity (McMurray et al., 1993; Liu et al., 2004; Laskowski et al., 2006; Takimoto and Kass, 2007; Dröse et al., 2009). Low levels of ROS are thought to play a role in normal cardiac signalling, growth adaptations and even cardioprotection (Zhang et al., 2002; Saotome et al., 2009; Prosser et al., 2011). However, in the presence of high levels of ROS which cannot be countered by the antioxidant capabilities of the cell (McCord and Fridovich, 1969; Matsushima et al., 2006), oxidative stress occurs (McMurray et al., 1993; review by Seddon et al., 2006; Dröse et al., 2009). Oxidative stress in cardiomyocytes can mediate DNA damage (Suematsu et al., 2003; Ye et al., 2016), reduction–oxidation (redox) signalling by affecting redox-sensitive target proteins, including activation of CAMKII, PKA, PKC and PKG (Gopalakrishna and Anderson, 1989; Kehrer, 2000; Brennan et al., 2006; Burgoyne et al., 2007; Zhu et al., 2007; Erickson et al., 2008), can induce cell arrest or

apoptosis (Kehrer, 2000; Zhu et al., 2007; Watkins et al., 2011) and has been associated with the development of pressure overload-induced pathological LV hypertrophy and progression of heart failure (McMurray et al., 1993; Siwik et al., 1999; MacCarthy et al., 2001; Li et al., 2002; Byrne et al., 2003; Maack et al., 2003; Takimoto et al., 2005; Grieve et al., 2006; Xu et al., 2008) (Figure 6.1).

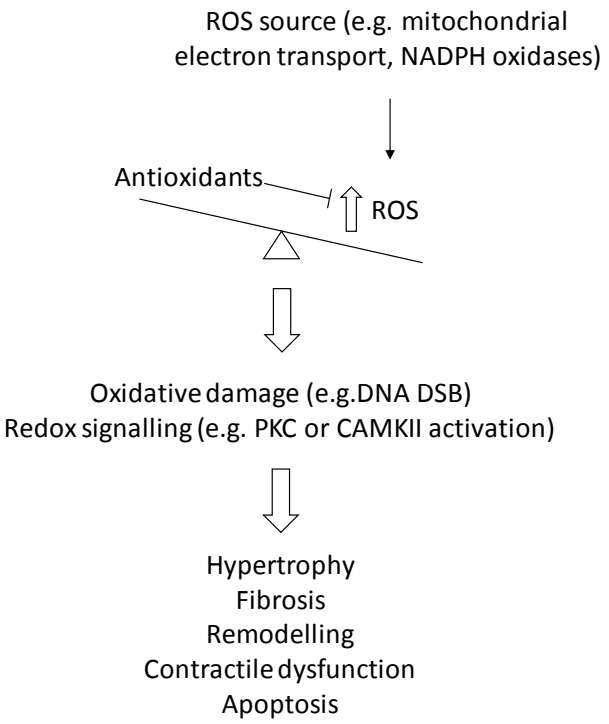

Figure 6.1 Simplified schematic diagram of the main pathophysiological effects of oxidative stress in the heart (adapted from Seddon et al. 2006; Takimoto and Kass, 2007). Higher levels of reactive oxygen species (ROS) play a role in pathophysiologic remodelling, apoptosis, and development of pathological cardiac hypertrophy and contractile dysfunction.

6.1.3 DNA double-strand break in pathological cardiac hypertrophy

As mentioned earlier, oxidative stress is a key contributor to pressure overload-induced pathological cardiac hypertrophy and heart failure (MacCarthy et al., 2001; Li et al., 2002; Byrne et al., 2003; Maack et al., 2003; Maytin et al., 2004; Takimoto et al., 2005; Grieve et al., 2006; Xu et al., 2008) and has been shown to enhance

double-strand DNA (dsDNA) break in cardiomyocytes (Ye et al., 2016). Overall, accumulation of dsDNA breaks in cells contributes to genomic instability and can lead to mutagenesis and/or cell death (Huang et al., 2005; Mirzayans et al., 2006; Jackson and Bartek, 2009; Liu et al., 2016). In mammalian cells, foci of phosphorylated H2AX at Ser139 residue are rapidly formed at dsDNA break sites (Rogakou et al., 1998; Rogakou et al., 1999; Andegeko et al., 2001; Bassing et al., 2002; Fernandez-Capetillo et al., 2002; Meador et al., 2008). H2AX is an H2A histone variant (West and Bonner, 1980), which is highly conserved across eukaryotic species (Pehrson and Fuji, 1998; review by Redon et al., 2002) and when phosphorylated is also known as γH2AX (Rogakou et al., 1998). Formation of γH2AX foci is essential for the DNA-damage response and accumulation of repair factors, such as p53 binding protein 1 (p53BP1) and breast cancer protein 1, at the break site (Paull et al., 2000; Bassing et al., 2002; Fernandez-Capetillo et al., 2002; Meador et al., 2008). Therefore, γH2AX has been considered to be a sensitive and selective biomarker for monitoring dsDNA break formation (review by Bonner et al., 2008). Phosphorylation at Ser139 is mediated by either DNA-PK (DNA-dependent protein kinase), ATM (ataxia-telangiectasia mutated) or ATR (ATM- and Rad3-Related) kinases (Andegeko et al., 2001; Falck et al., 2005) which is dephosphorylated during or after the DNA repair process (Rogakou et al., 1999; Chowdhury et al., 2005). In cardiomyocytes, γH2AX appears to be mainly ATM-dependent (Ye et al., 2016).

Furthermore, all type 2A protein phosphatases have been shown to dephosphorylate γH2AX in non-myocyte cells (Chowdhury et al., 2005; Chowdhury et al., 2008; Nakada et al., 2008a; Douglas et al., 2010; Zhong et al., 2011). In this chapter, the role of PP6 catalytic subunit and alpha4 protein in regulating γH2AX was investigated, through the siRNA-mediated knockdown of their protein expression in H9c2 cardiomyocytes.

6.2 Specific objectives

Currently, there is a lack of knowledge about the expression, regulation and role of type 2A protein phosphatase catalytic subunits and alpha4 signalling axis in pathological hypertrophy and DNA repair in cardiomyocytes. Thus, the studies described in this chapter aim to:

1. investigate the protein expression of type 2A protein phosphatase catalytic subunits, PP6C regulatory proteins (SAP1-3 (sit4 associated proteins) domain subunits and ANKRD28, 44 or 52 ankyrin repeat domain subunits) and alpha4 in SHAM- and TAC-operated mice;

2. investigate the association of alpha4 regulatory protein and type 2A protein phosphatase catalytic subunits in LV tissue of SHAM- and TAC-operated mice;

3. determine changes in the phosphorylation of γ-H2AX in between SHAM- and TAC-operated mice;

4. investigate the effects of PP6 catalytic subunit or alpha4 protein knockdown on the formation of the γH2AX foci in H9c2 cardiomyocytes in response to oxidative stress.

6.3 Methods

6.3.1 Murine myocardial hypertrophy model

Myocardial hypertrophy was induced by pressure overload via transaortic constriction (TAC) of the abdominal aorta in 6-week old male C57BL/6J mice (20–22 g) (Boguslavskyi et al., 2014). The aortic banding surgery and heart excision were carried out by Dr Andrii Boguslavskyi[13] at the BSU within the Waterloo campus of King's College London, under aseptic conditions. The operating field was disinfected with 75% isopropyl alcohol, and all surgical equipment was sterilised using a hot bead steriliser before surgery.

6.3.1.1 Transaortic constriction (TAC) of the abdominal aorta in the mouse

Male C57BL/6J mice (20–22 g), 6-week old, were anaesthetised with an isoflurane/O_2 mixture (2/98%) and were placed in a supine position on top of a 37°C heated pad to maintain their body temperature. Adequacy of anaesthesia was controlled by the inspection of the respiration rate and loss of pedal reflex. After the fur was shaved from the neckline to mid chest level, the chest was opened by a midsternal incision, and a chest retractor was applied to facilitate the view. The thymus and fat tissue were gently pulled away, and a 6-0 silk suture was placed around the abdominal aorta and tightened against a 28-guage blunt needle to assure reproducibility of the transaortic constriction (Figures 6.2-1 and 6.2-2). The needle was subsequently removed, and the stenotic aorta was created (Figure 6.2-3). Muscles and skin were closed layer by layer with 6-0 silk sutures. SHAM-operated mice underwent an identical procedure except for the transaortic banding. For post-operative analgesia, mice were injected intraperitoneally with buprenorphine

[13]Cardiovascular Division, King's College London, The Rayne Institute, St. Thomas' Hospital, London, United Kingdom.

(Vetergesic 0.3 mg/mL solution) at a dose of 20 µg/kg. After 4 weeks post-surgery, the mice were terminally anaesthetised by an intraperitoneal injection of pentobarbital (Pentoject 200 mg/mL solution) at a dose of 300 mg/kg and heparin (150 U). Once the mice were unconscious, the chest cavity was opened by cutting around the rib cage and through the diaphragm. The heart was rapidly explanted for measuring hypertrophic response and sample preparation for immunoblotting analysis.

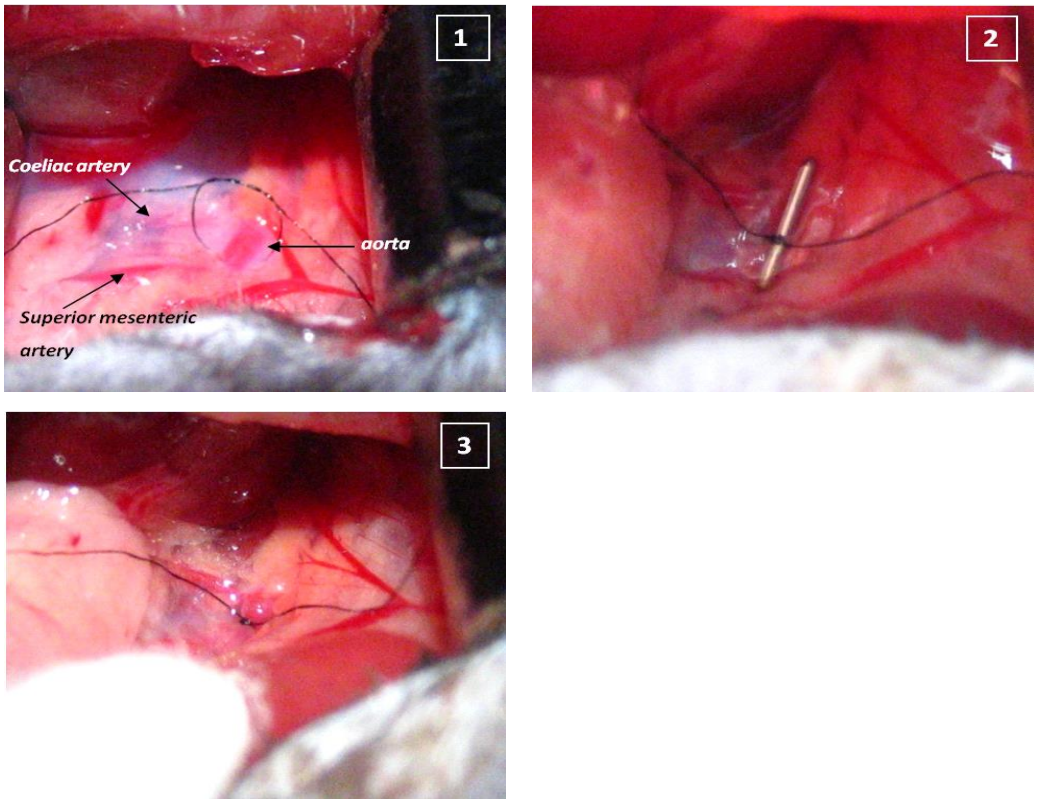

Figure 6.2 Transaortic abdominal aorta constriction model in the adult mouse (images obtained from Dr A. Boguslavskyi[14]). The abdominal aorta of the transaortic constriction (TAC)-operated mice was identified and banded by a 6-0 silk suture (**panel 1**). A 28-gauge blunt needle was placed parallel to the abdominal aorta (**panel 2**) to standardise the diameter of the loop and then removed (**panel 3**) once the suture was tied.

6.3.1.2 Assessment of hypertrophy

Following the heart excision from SHAM- and TAC-operated mice, hearts were

[14]Cardiovascular Division, King's College London, The Rayne Institute, St. Thomas' Hospital, London, United Kingdom.

rapidly flushed with ice-cold PBS to remove any residual blood. Extraneous tissue was removed, and the whole heart weight was measured. Then the left ventricle was separated from the heart and its weight was recorded. The hypertrophic response in each animal was measured and expressed as a ratio of left ventricular weight or whole heart weight versus (*vs*) body weight or tibia length (Fulton et al., 1952; Yin et al., 1982; Hangartner et al., 1985; Kitzman et al., 1988).

6.3.1.3 Homogenisation and sample preparation of murine LV tissue

After the LV free wall was dissected away and weight measured, approximately 20-30mg of the left ventricles' mass was stored in RNA*later* RNA Stabilisation Reagent (QIAGEN) and stored at -20^{o}C until required. The remainder of the left ventricle was immediately placed into liquid nitrogen for short-term storage. LV tissue was then soaked in ice-cold homogenisation buffer (100 mg tissue/ml of buffer) (20 mM MOPS, 140 mM NaCl, 5 mM KCl, 1 mM EDTA, 1% (v/v) phosphatase inhibitor cocktail #3 (Sigma), 0.1% (v/v) protease inhibitor cocktail set 3 (Calbiochem), pH 7.4) and was homogenised on ice. LV tissue soaked in buffer was initially cut into smaller pieces and was further disrupted by a hand-held homogeniser while on ice. From each homogenate, 200 µl were prepared for immunoblotting analysis as described in Chapter 2 (section 2.5) and the remainder of the homogenate was stored at -80^{o}C until required.

6.3.2 Immunoprecipitation of alpha4 from cardiomyocytes

Immunoprecipitation (IP) of alpha4 from H9c2 or ARVM lysates and mouse left ventricle homogenates, was performed using a using a protocol adapted from the publication by Snabaitis et al., (2008). On the day of the experiment, H9c2 cardiomyocytes at 80% confluency or plated freshly-isolated ARVMs (on 6-well culture plates), were washed with ice-cold PBS and lysed with 300 µl of 1X cell

lysis buffer (20 mM Tris-HCl (pH 7.5), 150 mM NaCl, 1 mM EDTA-Na_2, 1 mM EGTA, 1% (v/v) Triton X-100, 2.5 mM sodium pyrophosphate, 1 mM β-glycerophosphate, 1 mM Na_3VO_4, 1 µg/ml leupeptin; Cell Signaling Technology) supplemented with 1 tablet/10 ml mini-Complete™ protease inhibitor cocktail (freshly added) (Roche Diagnostics, Switzerland)). The plates were directly placed onto a layer of liquid nitrogen in a polystyrene ice bucket to flash-freeze the cell layer. After 5 min, the plates were removed from liquid nitrogen and left at room temperature to thaw whilst scraping the surface of each well simultaneously, to enhance cell lysis. Immediately after thawing, the lysates were transferred to safe-lock 1.5-ml centrifuge tubes (Eppendorf, Germany) on ice and then centrifuged at 14,000 *g* for 30 min at 4°C (Micro-star 17R centrifuge from VWR International, USA). Alternatively, aliquots of 30 µl from mouse left ventricle homogenates, prepared as described earlier in Chapter 6 (section 6.3.1.3), were mixed well by pipetting with 270 µl ice-cold modified 1X cell lysis buffer and centrifuged at 14,000 *g* for 30 min at 4°C. The supernatant from either H9c2 cardiomyocytes, ARVMs or mouse left ventricle lysate samples was carefully removed, and the pelleted triton-insoluble debris was discarded. Protein content in the supernatant was analysed using the BCA assay (section 6.3.3) and was then adjusted to 500 µg/ml. A sample of the supernatant was kept as a "pre-immunoprecipitation (pre-IP)" control (input) and prepared for immunoblotting analysis as described in section 2.5.1. The remaining lysate (750 µl) was equally divided into three centrifuge tubes, to which 2 µl (1 µg/µl) of rabbit IgG (Sigma-Aldrich), 2 µl PBS or 2 µl (1 µg/µl) of rabbit polyclonal anti-alpha4 antibody (Bethyl Laboratories, USA) were added individually and incubated overnight at 4ºC with gentle rocking on a tube rotator (Stuart; Bibby Scientific Ltd, UK). The samples containing Rabbit IgG (corresponding to the host species of the anti-alpha4 primary antibody; Cell Signaling Technology) or PBS were used as negative controls to detect any non-specific protein binding in the

sample to the IgG molecule or protein A magnetic beads within the IP respectively. Each tube was then incubated with 50 µl of protein A magnetic bead slurry (New England Biolabs, UK) for 2 hours at 4ºC with gentle rocking on a tube rotator. The tubes, containing the beads, were then placed into a 6-tube magnetic separation rack (New England Biolabs) and left for 30 seconds on ice until the solution was clear. The supernatant was carefully removed, from which a sample (equal proportion to the pre-IP sample) was kept as a "post-immunoprecipitation (post-IP)" control and was prepared for immunoblotting analysis as described in Chapter 2 (section 2.5.1). The magnetised pellet containing the immunocomplexes was gently washed three times with 500 µl ice-cold modified 1X cell lysis buffer and finally resuspended in 50 µl of 3X modified Laemmli sample buffer. Samples were then heated at 95°C for 5 min, followed by a brief pulse centrifugation and then analysed by immunoblotting (section 2.5) or stored at -80^{o}C until required.

6.3.3 Quantification of total protein concentration by bicinchoninic acid (BCA) assay

Protein quantification of cellular lysates was performed using the Pierce™ BCA Protein Assay Kit (Thermo Scientific) as per manufacturer's instructions. A range of protein standards (0, 0.125, 0.250, 0.5, 0.75, 1, 1.5 and 2 mg/ml Bovine serum albumin (BSA)) were made from a stock solution of BSA (2 mg/ml in 0.9% (v/v) saline and 0.05% (w/v) sodium azide). An aliquot of 10 µl from each protein standard, cell lysate sample or lysis buffer (blank control for lysate samples) was added in triplicate to a 96-well flat-bottom microplate. In each well, 200 µl of BCA solution (50:1 Reagent A:B) was added, and the plate was thoroughly mixed by shaking on an orbital plate shaker at 50 *g* for 30 seconds and incubated for 30 min at 37ºC. The plate was then cooled to room temperature for 15 min, and the absorbance was measured at 562 nm by the Infinite M200 PRO plate reader (TECAN) and

analysed using the Magellan™ data analysis software (Magellan). The concentration of the BSA standards was plotted against averaged blank (0 mg/ml BSA)-corrected absorbance responses and a standard curve was plotted using MS Excel (MS Office 2010). The concentration of the unknown samples was interpolated from the BSA standard curve using their averaged blank (lysis buffer)-corrected absorbance responses.

6.3.4 Measuring cell viability by MTT assay

Cell viability of H9c2 cardiomyocytes, under different experimental conditions, was measured using a 3-(4, 5-dimethylthiazol-2-yl)-2, 5-diphenyltetrazolium bromide (MTT) assay, as described in Chapter 2 (section 2.7). A threshold of statistically significant ($p<0.05$) more than 20% difference in cell viability (<20% or >120%) was assigned to indicate a biologically significant effect (Fan et al., 2009; Lodererova et al., 2009; Cuddington et al., 2015).

6.3.5 Hydrogen peroxide-induced oxidative stress in H9c2 cardiomyocytes

Hydrogen peroxide induces oxidative stress in cardiomyocytes (Chen et al., 2002; Oyama et al., 2009; Mojarrab et al., 2013). Cultured H9c2 cardiomyocytes were transfected with rat non-targeting siRNA and either alpha4- or PP6C-siRNA, for 4 or 8 days, respectively (section 2.3.1). When transfection lasted longer than 4 days, the transfection medium was replaced every 4 days. At day 3 (or day 7), the transfection medium was replaced with complete medium containing 300 μM H_2O_2 (condition optimised in our laboratory) or PBS as vehicle control. After 24 hours of incubation in the dark, samples were prepared for immunoblotting analysis as described in Chapter 2 (section 2.5). Hydrogen peroxide solutions were kept in the dark at 4^{o}C, before use. The treatment medium containing 300μM H_2O_2 was freshly made.

6.3.6 Western blotting analysis

Total expression of SAP1, SAP2, SAP3, ANKRD28, ANKRD44, ANKRD52, PP2AC, PP4C, PP6C, H2AX and phosphorylation status of H2AX-Ser139 (γ-H2AX) was detected by immunoblotting analysis as described in Chapter 2 (section 2.5). In addition, total levels of actin were detected to ensure equal protein loading and/ or for data normalisation. Details about the antibodies and working dilutions used in this chapter are presented in table 2.3.

6.4 Results

6.4.1 Measurement of pressure overload-induced cardiac hypertrophy

After 28 days of TAC-mediated pressure overload in mice, the heart mass was significantly ($p<0.05$) increased 60.1 ± 13.8% or 58.6 ± 9.8% when expressed as whole heart weight (HW) relative to body weight (BW) or tibia length (TL) respectively, compared to the SHAM-operated mice (Figures 6.3A and 6.3B, respectively).

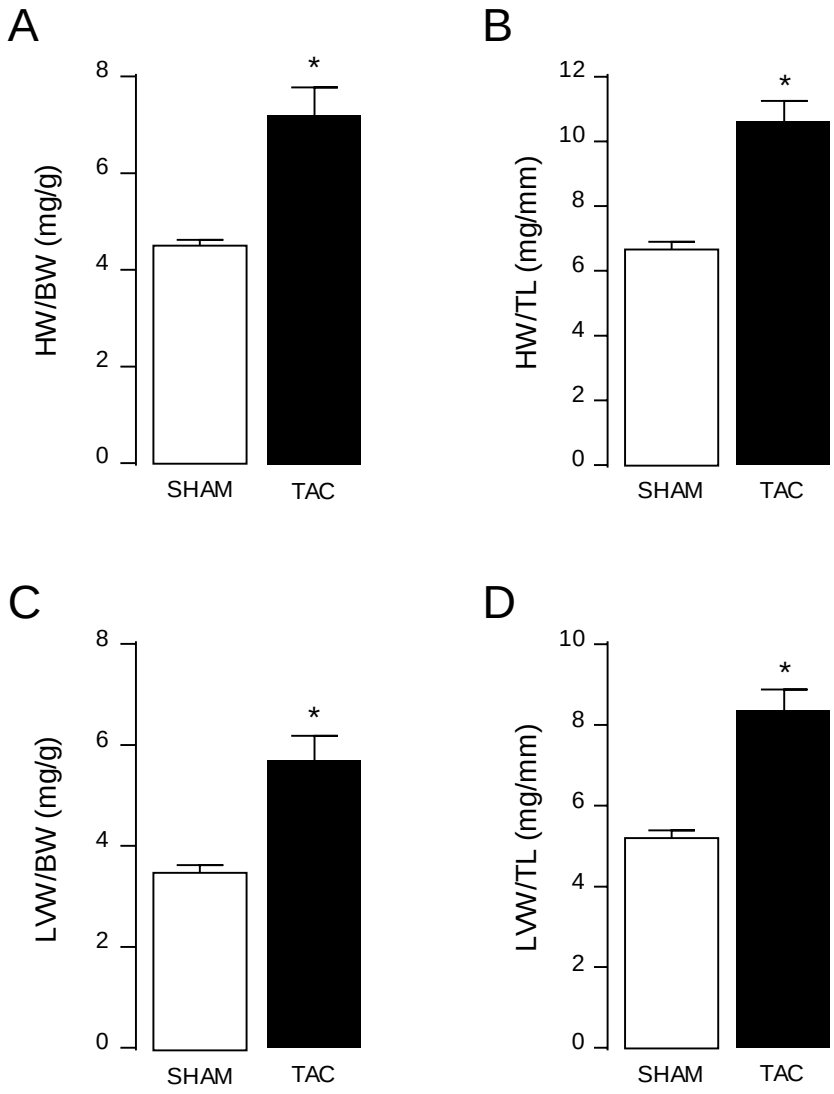

Figure 6.3 Pressure overload-induced cardiac hypertrophy in SHAM- and TAC-operated mice was measured as (**A**) whole HW to BW ratio, (**B**) HW to TL ratio, (**C**) LVW to BW ratio and (**D**) LVW to TL ratio. Bars represent mean values ± SEM, and two-tailed unpaired Student's t-test was used to compare data in SHAM- (n = 4) and TAC-operated mice (n = 6); *p<0.05.

Furthermore, the LV mass in TAC-operated mice showed a significant ($p<0.05$) 62.0 ± 13.8% or 60.4 ± 9.7 increase when expressed as left ventricular weight (LVW) relative to BW or TL, respectively (Figures 6.3C and 6.3D, respectively) compared to the SHAM-operated mice. These data suggest the development of pressure overload-induced cardiac hypertrophy in the TAC-operated mice compared to the SHAM-operated mice.

6.4.2 Protein expression of type 2A protein phosphatase catalytic subunits and alpha4 in LV hypertrophy

The expression levels of the type 2A protein phosphatase catalytic subunits were measured in the LV tissue of SHAM- and TAC-operated mice. Total PP2AC protein expression was significantly ($p<0.05$) elevated (1.7-fold) in TAC-operated mice compared to the SHAM-operated mice (Figure 6.4A). Interestingly, protein expression of PP4C was undetectable in the adult mouse myocardium (Figure 6.4B). Furthermore, PP6C protein expression was not significantly altered in left ventricles between SHAM- and TAC-operated mice (Figure 6.4C).

In addition, the protein expression of the alpha4, a regulatory protein of all type 2A protein phosphatase catalytic subunits, was investigated in hypertrophied and non-hypertrophied LV tissue. From the data in Chapter 4 (Figures 4.20-4.22), it is apparent that the maintenance of type 2A protein phosphatases in cardiomyocytes requires the expression of alpha4 protein. Figure 6.5 shows that alpha4 protein expression was significantly ($p<0.05$) increased (1.8-fold) in the LV tissue of TAC-operated mice when compared to the SHAM-operated mice.

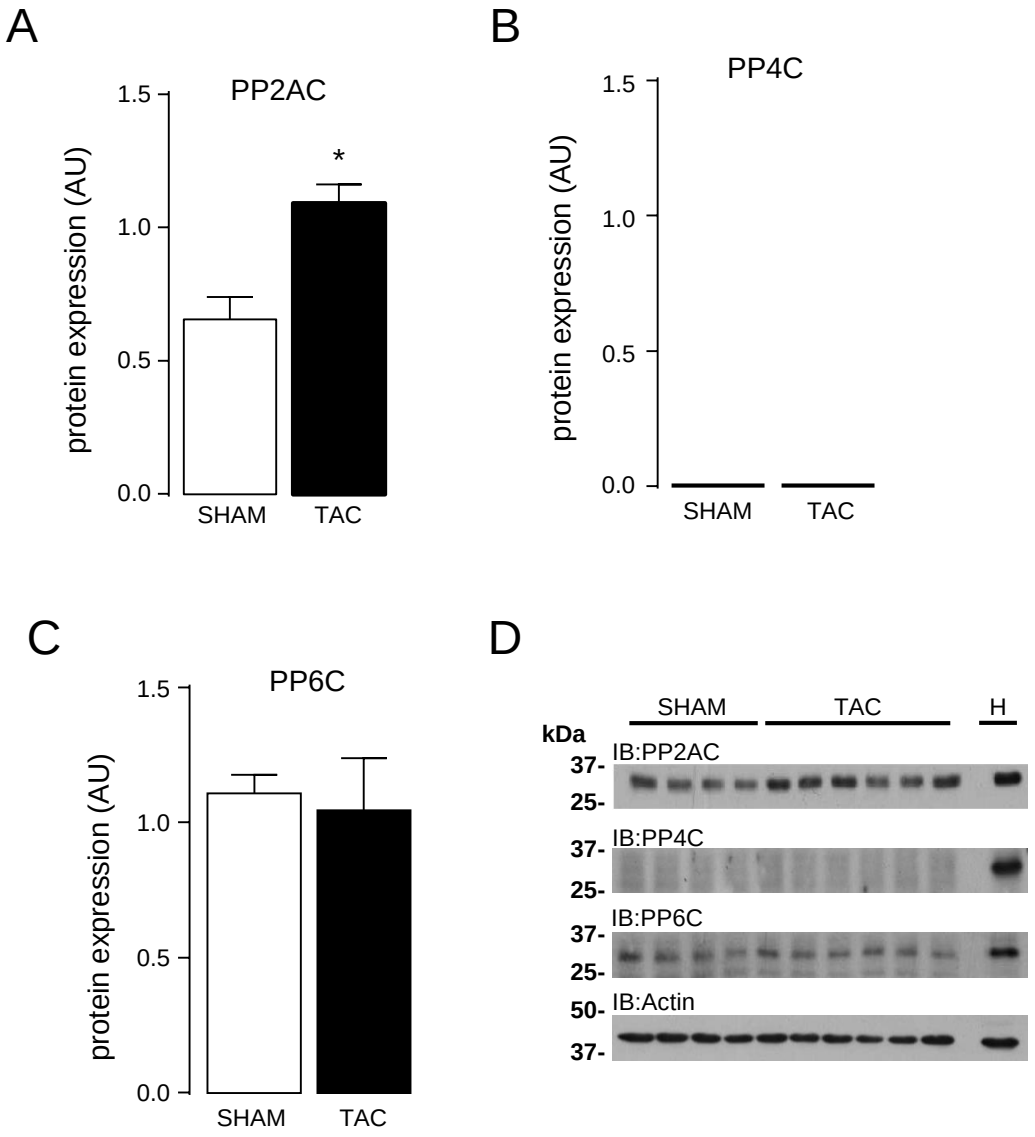

Figure 6.4 Protein expression of the type 2A protein phosphatase catalytic subunits, in the LV tissue of SHAM (n=4)- and TAC (n=6)-operated mice, 28 days post-surgery, was determined by immunoblotting analysis, using subunit-specific antibodies to PP2AC, PP4C and PP6C. An H9c2 lysate (H) run along the mouse LV tissue samples as a positive control. Prior to immunoblotting, proteins from each sample were resolved by SDS-PAGE (on 12% polyacrylamide gels). Levels of (**A**) total PP2AC, (**B**) PP4C and (**C**) PP6C protein expression were quantified by densitometry and normalised to actin. All data represent mean values ± SEM. Statistical comparison was made by a two-tailed unpaired Student's t-test; *p<0.05. (**D**) Representative immunoblots (IB) of total PP2AC, PP4C and PP6C protein expression. For clarity, the PP6C single immunoblot was spliced (white line) to have consistent order among all immunoblots.

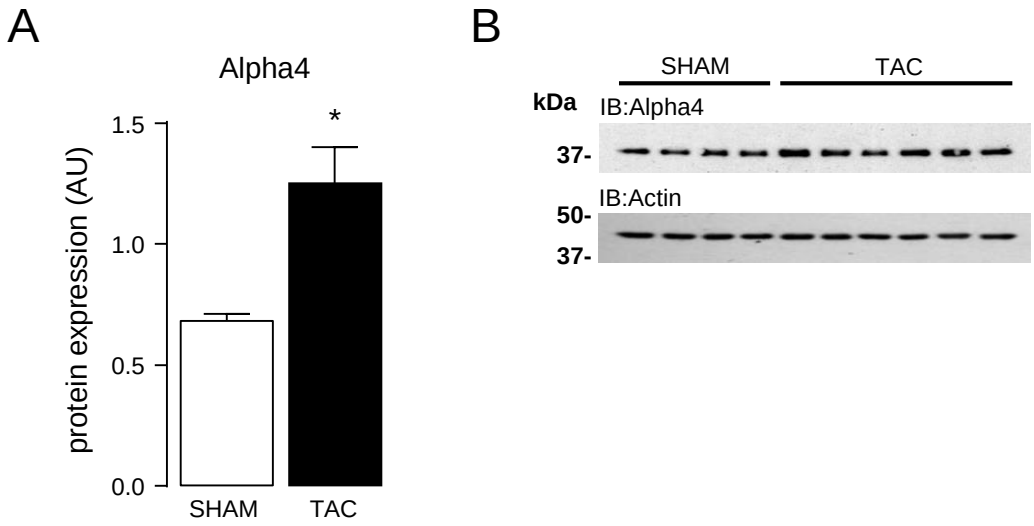

Figure 6.5 Protein expression of the alpha4, in the LV tissue of SHAM (n=4)- and TAC (n=6)-operated mice, 28 days after surgery, was determined by immunoblotting analysis, using a rabbit polyclonal anti-alpha4 antibody. Prior to immunoblotting, proteins from each sample were resolved by SDS-PAGE (on 12% polyacrylamide gels). (**A**) Levels of alpha4 protein expression were quantified by densitometry and normalised to actin. All data represent mean values ± SEM. Statistical comparison was made by a two-tailed unpaired Student's t-test; *p<0.05. (**B**) Representative immunoblots (IB) of total alpha4 protein expression.

6.4.3 Expression of PP6C regulatory subunits in LV hypertrophy

Even though PP6C expression appeared to be unchanged in the murine hypertrophied LV tissue compared to the non-hypertrophied LV tissue, as shown in figure 6.4C, PP6C activity and specificity has been proposed to be regulated by its association with a Sit4-associated domain protein (SAP1, SAP2 or SAP3) and an ankyrin repeat domain regulatory protein (ANKRD28, ANKRD44, and ANKRD52) (Stefansson et al., 2008; Guergnon et al., 2009). Therefore, the expression levels of PP6C regulatory subunits, SAP1-3, ANKRD28, ANKRD44 and ANKRD52 were determined in LV tissue obtained from SHAM- and TAC-operated mice. SAP1 was significantly ($p<0.05$) elevated (2.2-fold) (Figure 6.6A) whilst, SAP2 was significantly ($p<0.05$) reduced (2.8-fold) in TAC-operated mice (Figure 6.6B) when compared to the SHAM-operated mice. Furthermore, SAP3 protein expression level was unaltered between the cardiac LV hypertrophied and non-hypertrophied tissue (Figure 6.6C). The protein expression levels of ANKRD28 and ANKRD44 were significantly ($p<0.05$) increased (1.9-fold and 1.5-fold, respectively) in tissue from TAC-operated mice,

compared to the SHAM-operated mice (Figures 6.7A and 6.7B). Expression of the ANKRD52 protein in LV tissue lysate was unchanged between the SHAM- and TAC-operated mice (Figure 6.7C). The data in figures 6.6 and 6.7 clearly show that all the regulatory subunits of PP6C are expressed in mouse myocardium and their LV

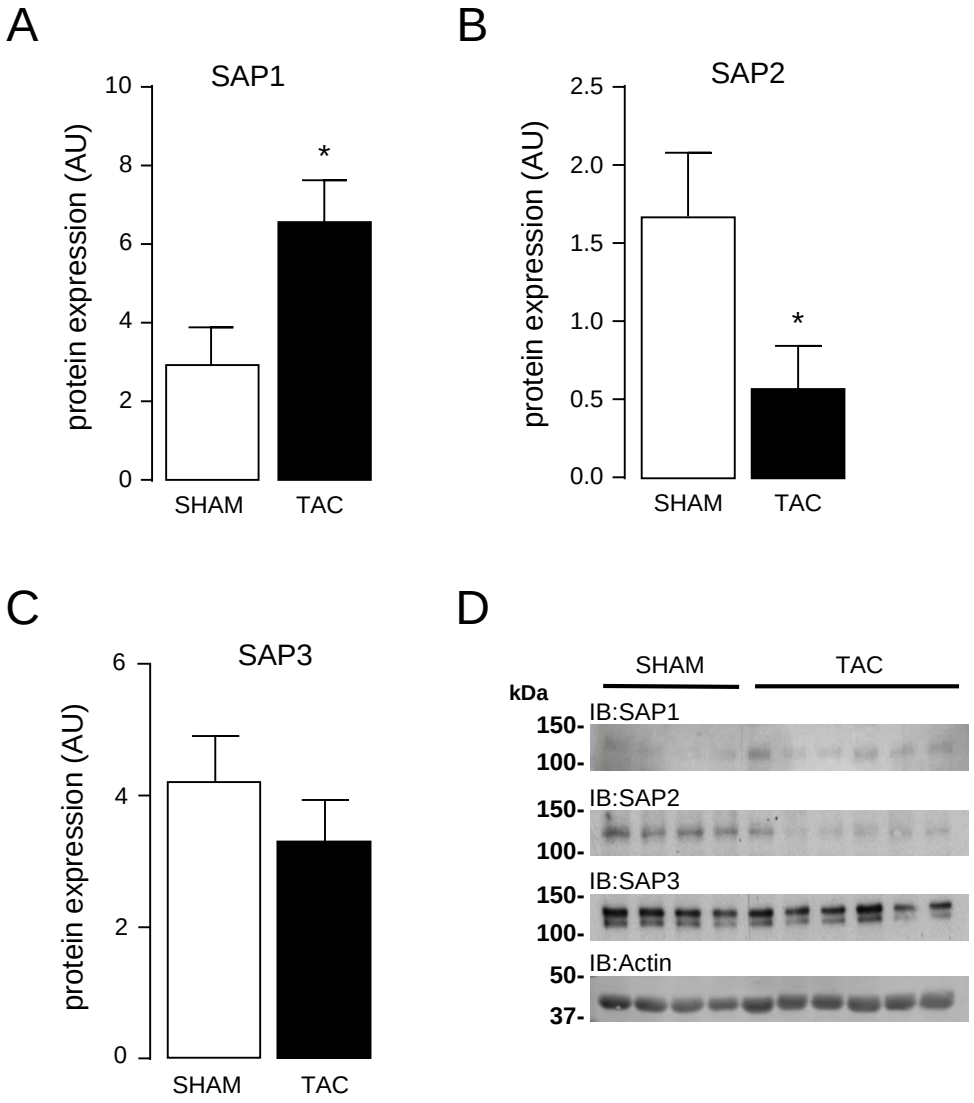

Figure 6.6 Protein expression of the PP6C sit4-associated protein domain subunits (SAP1-3), in the LV tissue of SHAM (n=4)- and TAC (n=6)-operated mice, 28 days post-surgery, was analysed by SDS-PAGE (on 9% polyacrylamide gels) and immunoblotting with antibodies specific to SAP1-3. Levels of (**A**) SAP1, (**B**) SAP2 and (**C**) SAP3 protein expression were quantified by densitometry and normalised to actin. Protein expression levels of actin were quantified by a LI-COR Odyssey® CLx Imaging System. All data represent mean values ± SEM. Statistical comparison was made by a two-tailed unpaired Student's t-test; *p<0.05. (**D**) Representative immunoblots (IB) of SAP1-3 protein expression.

expression appears to be differentially regulated in the healthy and hypertrophied mouse LV tissue.

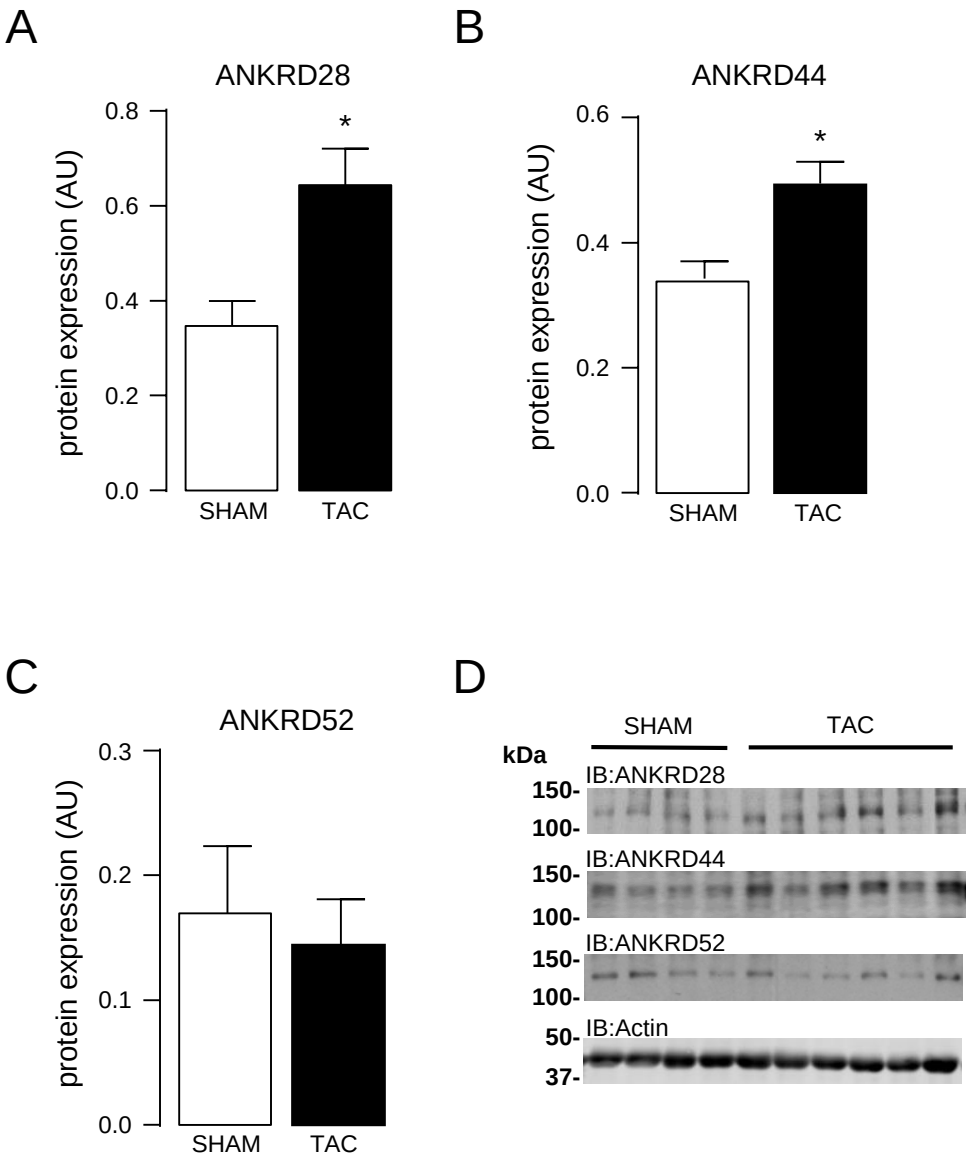

Figure 6.7 Protein expression of the PP6C regulatory ankyrin repeat domain subunits (ANKRD28/44/52), in the LV tissue obtained from SHAM (n=4)- and TAC (n=6)-operated mice, 28 days after surgery, was analysed by SDS-PAGE (on 9% polyacrylamide gels) and immunoblotting with antibodies specific to ANKRD28, ANKRD44 or ANKRD52. Levels of (**A**) ANKRD28, (**B**) ANKRD44 and (**C**) ANKRD52 protein expression were quantified by densitometry and normalised to actin. Protein expression levels of actin were quantified by a LI-COR Odyssey® CLx Imaging System. All data represent mean values ± SEM. Statistical comparison was made by a two-tailed unpaired Student's t-test; *p<0.05. (**D**) Representative immunoblots (IB) of ANKRD28/44/52 protein expression.

6.4.4 Association of alpha4 with type 2A protein phosphatase catalytic subunit complexes in normal and hypertrophic myocardium

Alpha4 is a common regulatory protein for all type 2A protein phosphatase catalytic subunits and has been shown to be essential for their stability and PP2A holoenzyme biogenesis (Chen et al., 1998; Nanahoshi et al., 1999; Kong et al., 2009; Jiang et al., 2013b; LeNoue-Newton et al., 2016). Therefore, the association of alpha4 with the type 2A protein phosphatase catalytic subunits (PP2AC, PP4C and PP6C) was investigated in murine normal and hypertrophic LV tissue. To optimise the immunoprecipitation protocol conditions, alpha4 protein complexes were initially co-immunoprecipitated from H9c2 and ARVM lysates. Figure 6.8 shows that alpha4 interacts with all type 2A protein phosphatases in H9c2 cardiomyocytes. As shown in figure 6.9, alpha4 was co-

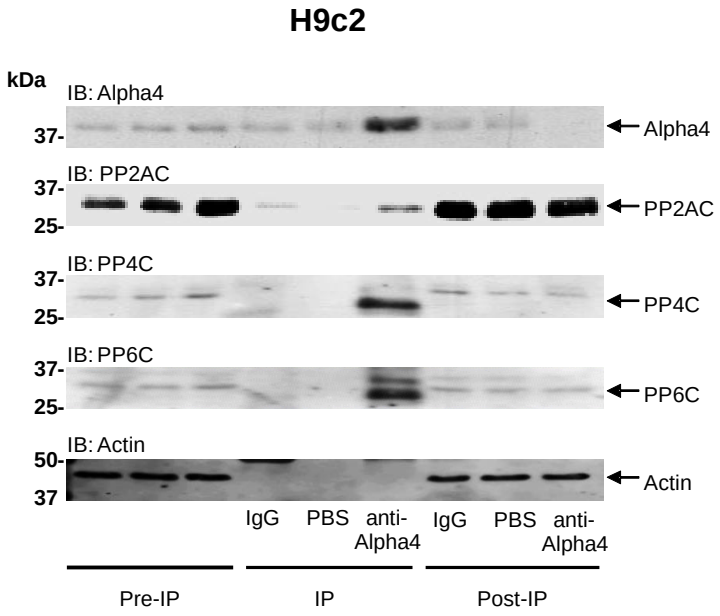

Figure 6.8 Immunoprecipitation of alpha4 in H9c2 cardiomyocyte lysates was performed using a polyclonal anti-alpha4 antibody in combination with protein A magnetic beads (Cell Signaling Technology). Equal proportions of pre-immunoprecipitation sample (pre-IP: lanes 1-3), immunoprecipitates (rabbit IgG, PBS and rabbit anti-alpha4: lanes 4-6) and post-immunoprecipitation sample (post-IP: lanes 7-9) were probed for the presence of alpha4, total PP2AC, PP4C and PP6C or actin protein by immunoblotting, using a mouse monoclonal anti-alpha4, a sheep polyclonal anti-PP2AC, anti-PP4C or anti-PP6C or a goat polyclonal anti-actin antibody, respectively. Prior to immunoblotting, proteins from each sample were resolved by SDS-PAGE (on 12% polyacrylamide gels). IB: Immunoblot.

immunoprecipitated in complex with PP2AC and PP6C in ARVMs, however, alpha4:PP4C protein complexes were not observed by immunoblotting analysis. Next, the association of alpha4 regulatory protein with PP2AC and PP6C in LV tissue from SHAM- and TAC-operated mice was investigated through co-immunoprecipitation of alpha4 protein complexes, using a polyclonal anti-alpha4 antibody. As it can be seen in figure 6.10A, alpha4 immunoprecipitation from LV tissue lysates resulted in ≥95% pull down of total cellular alpha4 protein. Moreover, alpha4 content was significantly ($p<0.05$) higher (282.0 ± 67.4%) in immunocomplexes from hypertrophied LV tissue compared to the non-hypertrophied tissue (Figure 6.10B). Actin protein content in the input (pre-IP) from SHAM- and TAC-operated mice LV tissue lysates confirmed equal protein loading between the samples for Co-IP of alpha4 immunocomplexes with type2A protein phosphatase

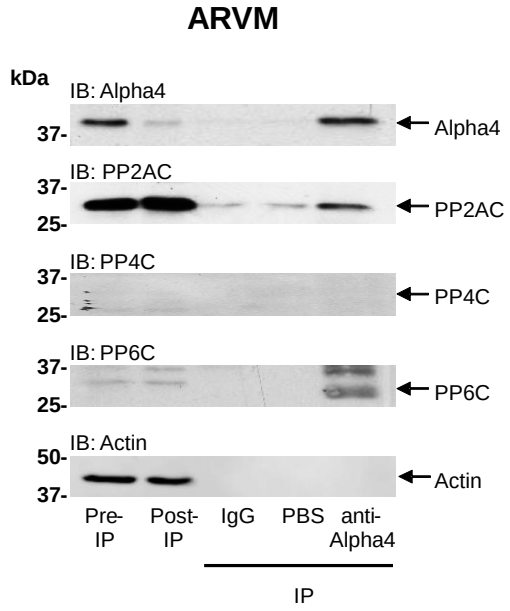

Figure 6.9 Immunoprecipitation of alpha4 in ARVM lysates was performed using a polyclonal anti-alpha4 antibody in combination with protein A magnetic beads (Cell Signaling Technology). Equal proportions of pre-immunoprecipitation sample (pre-IP: lane 1), post-immunoprecipitation sample (post-IP: lane 2) and immunoprecipitates (rabbit IgG, PBS and rabbit anti-alpha4: lanes 3-5) were probed for the presence of alpha4, total PP2AC, PP4C and PP6C or actin protein by immunoblotting, using a mouse monoclonal anti-alpha4, a sheep polyclonal anti-PP2AC, anti-PP4C or anti-PP6C or a goat polyclonal anti-actin antibody, respectively. Prior to immunoblotting, proteins from each sample were resolved by SDS-PAGE (on 12% polyacrylamide gels). IB: Immunoblot.

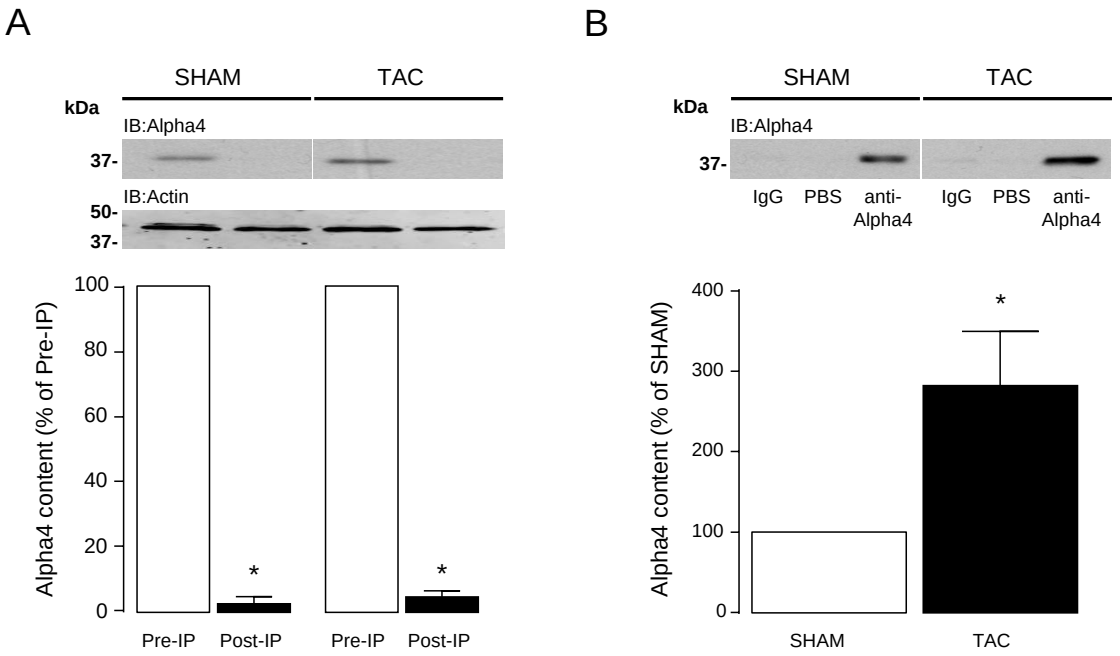

Figure 6.10 Immunoprecipitation of alpha4 in LV tissue lysates obtained from SHAM (n=4)- and TAC (n=4)-operated mice was performed using a polyclonal anti-alpha4 antibody in combination with protein A magnetic beads (Cell Signaling Technology). Equal proportions of (**A**) pre-immunoprecipitation (pre-IP: lane 1), post-immunoprecipitation sample (post-IP: lane 2) and (**B**) immunoprecipitates (rabbit IgG, PBS and rabbit anti-alpha4: lanes 3-5) were probed for the presence of alpha4 protein by immunoblotting, using a mouse monoclonal anti-alpha4 antibody. Alpha4 protein expression was quantified by densitometry. Actin in the input (pre-IP) from SHAM- and TAC-operated mice LV tissue lysates was used to indicate differences in protein loading between the samples. Prior to immunoblotting, proteins from each sample were resolved by SDS-PAGE (on 12% polyacrylamide gels). For clarity, the alpha4 single immunoblots were spliced (white line) to rearrange the order of the samples. All data represent mean values ± SEM. Statistical comparison was made by a two-tailed unpaired Student's t-test; *p<0.05. IB: Immunoblot.

catalytic subunits. PP2AC or PP6C protein present in the alpha4 immunocomplexes was quantified and normalised to the corresponding amount of alpha4 protein content in the immunoprecipitates. Figure 6.11A shows that alpha4 immunoprecipitation from normal murine LV tissue lysates significantly ($p<0.05$) removed 39% of cellular total PP2AC protein content. Comparison of the total PP2AC protein content in the immunocomplexes showed no difference between the SHAM- and TAC-operated mice (Figure 6.11B). When alpha4 was immunoprecipitated from healthy murine LV tissue, PP6C protein content was significantly ($p<0.05$) reduced to 52.0 ± 11.4% in the post-IP lysate, when compared to the pre-IP lysate (Figure 6.12A).

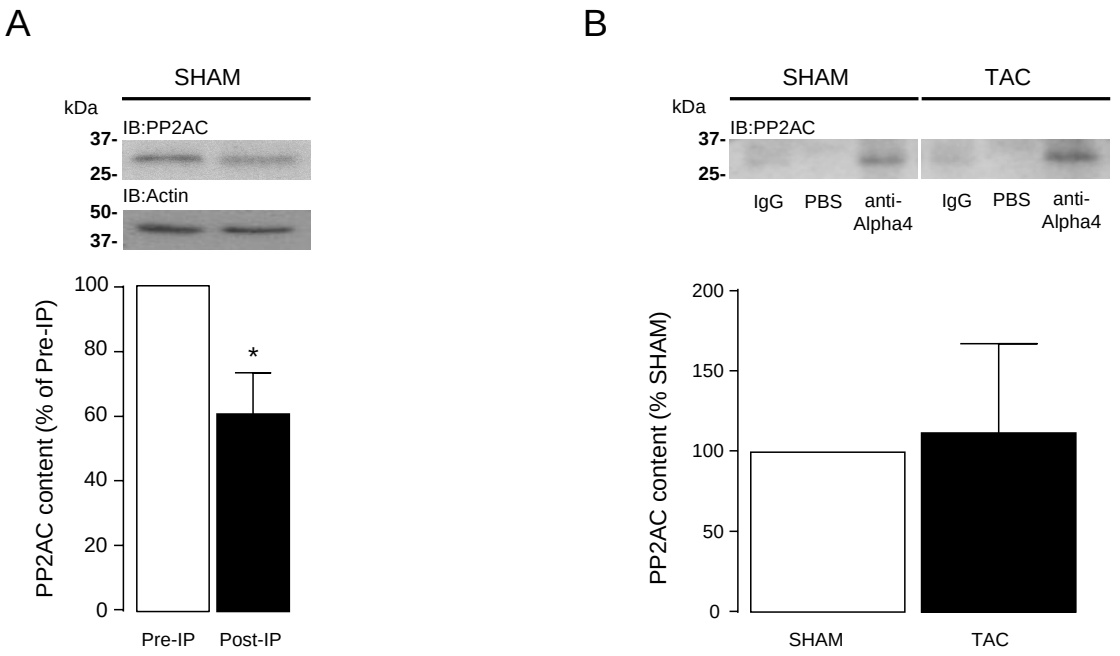

Figure 6.11 The association of PP2AC with alpha4 was investigated during LV hypertrophy. (**A**) Total PP2AC protein content was determined in equal proportions of normal murine LV tissue lysates (n=4) before (pre-IP) and after (post-IP) alpha4 immunoprecipitation, by immunoblotting analysis, using a sheep polyclonal anti-PP2AC antibody. Actin was used to indicate differences in protein loading between the samples. Graph shows the protein levels of total PP2AC in the post-IP sample relevant to the pre-IP sample. (**B**) Equal proportions of immunoprecipitates (rabbit IgG, PBS and rabbit anti-alpha4), from SHAM (n=4)- and TAC (n=4)-operated mice LV tissue lysates, were probed for the presence of total PP2AC protein by immunoblotting, using a sheep polyclonal anti-PP2AC antibody. Total PP2AC protein content in the rabbit anti-alpha4 immunoprecipitates was quantified by densitometry and normalised to the corresponding alpha4 content in the immunoprecipitates. All data represent mean values ± SEM. Statistical comparison was made by a two-tailed unpaired Student's t-test; *p<0.05. Prior to immunoblotting, proteins from each sample were resolved by SDS-PAGE (on 12% polyacrylamide gels). IB: Immunoblot.

Interestingly, a significant ($p<0.05$) reduction of PP6C protein content to 30.4 ± 7.6% was observed in alpha4 immunoprecipitates from LV tissue lysates of TAC-operated mice compared to the SHAM-operated mice (Figure 6.12B). This data indicates that even though, a significant ($p<0.05$) proportion (48%) of PP6C appeared to associate with alpha4 in the normal murine LV tissue lysates, this association was significantly ($p<0.05$) reduced in hypertrophied LV tissue. Taken together, these novel data suggest that alpha4 differentially associates with PP2AC and PP6C in the normal and hypertrophied LV tissue.

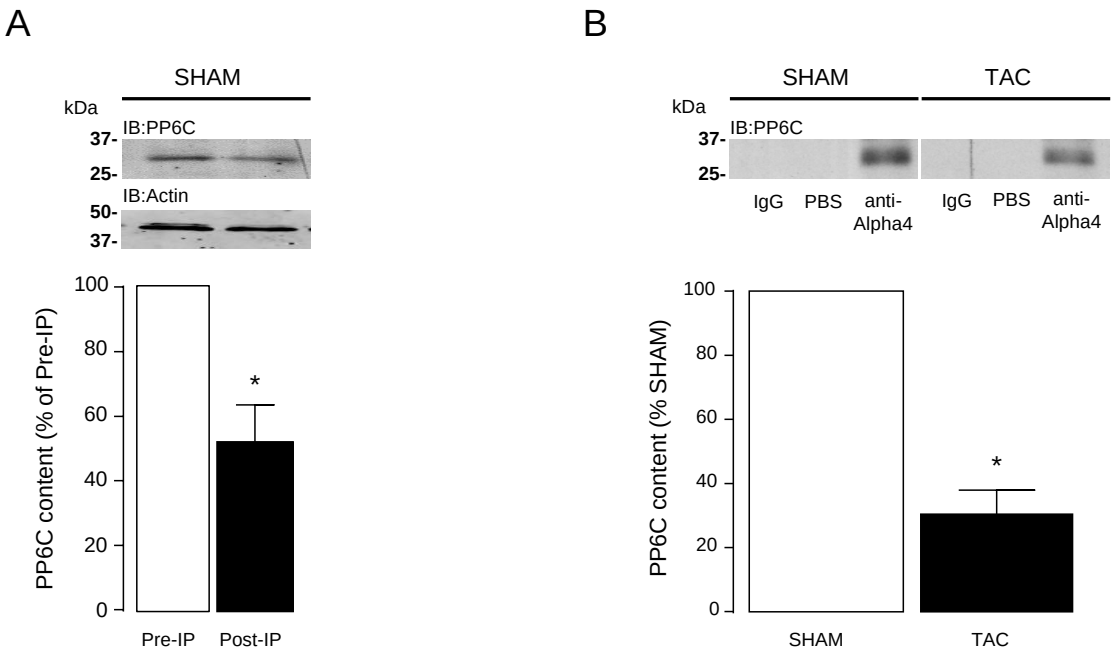

Figure 6.12 The association of PP6C with alpha4 was investigated during LV hypertrophy. (**A**) PP6C protein content was determined in equal proportions of normal murine LV tissue lysates (n=4) before (pre-IP) and after (post-IP) alpha4 immunoprecipitation, by immunoblotting analysis, using a sheep polyclonal anti-PP6C antibody. Actin was used to indicate differences in protein loading between the samples. Graph shows the protein levels of PP6C in the post-IP sample relevant to the pre-IP sample. (**B**) Equal proportions of immunoprecipitates (rabbit IgG, PBS and rabbit anti-alpha4), from SHAM (n=4)- and TAC (n=4)-operated mice LV tissue lysates, were probed for the presence of PP6C protein by immunoblotting, using a sheep polyclonal anti-PP6C antibody. PP6C protein content in the rabbit anti-alpha4 immunoprecipitates was quantified by densitometry and normalised to the corresponding alpha4 content in the immunoprecipitates. All data represent mean values ± SEM. Statistical comparison was made by a two-tailed unpaired Student's t-test; *p<0.05. Prior to immunoblotting, proteins from each sample were resolved by SDS-PAGE (on 12% polyacrylamide gels). The spliced image (white line) was from a single immunoblot to rearrange the order of the samples. IB: Immunoblot.

6.4.5 Effects of PP6C protein knockdown on H9c2 cardiomyocyte viability

PP6C is considered to be a survival protein in HeLa cells (MacKeigan et al., 2005). To investigate whether PP6C can regulate cardiomyocyte survival, H9c2 cardiomyocytes were transfected with rat PP6C-siRNA or non-targeting control siRNA and cell viability was measured after 4, 6 and 8 days of transfection. As it can be seen in figure 6.13A, PP6C protein expression was significantly ($p<0.05$) reduced more than 80% in H9c2 cardiomyocytes incubated with rat PP6C-siRNA for

4, 6 or 8, compared to the control. However, only PP6C-siRNA at 8 days post-transfection led to a significant ($p<0.05$) reduction of cell viability (92.3 ± 0.2%) in H9c2 cardiomyocytes (Figure 6.13B). Although this result was statistically significant, since cell viability was above 80%, it was considered not biologically significant (section 6.3.4).

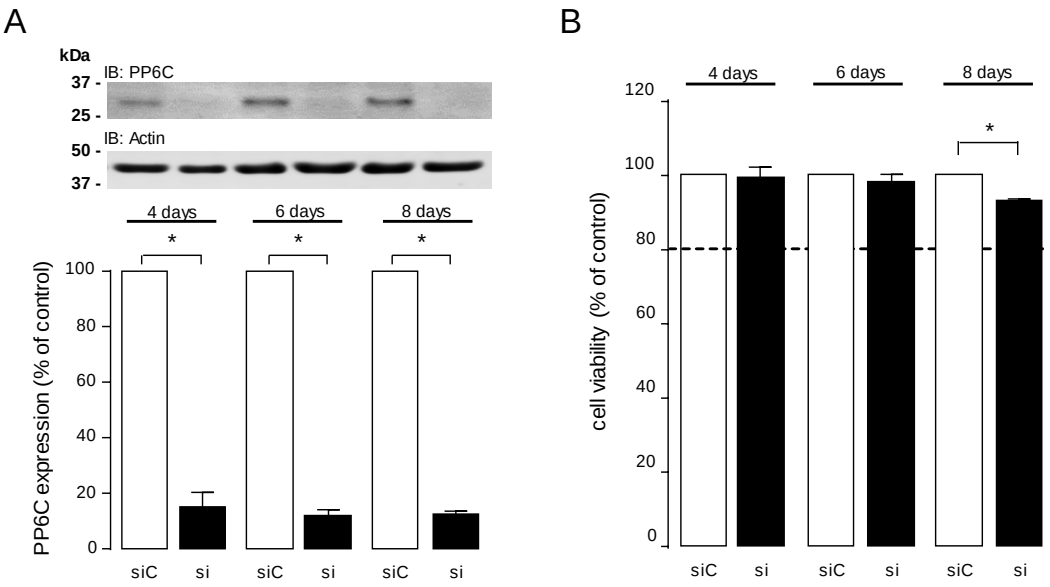

Figure 6.13 Effects of siRNA-mediated PP6C protein expression knockdown on cell viability. (**A**) Protein expression of PP6C (n=3) in H9c2 cardiomyocytes, transfected with 50 nM rat PP6C-siRNA (si) or non-targeting control siRNA (siC) for 4,6 or 8 days was analysed by immunoblotting using a subunit-specific anti-PP6C antibody. Protein levels were quantified by densitometry and were normalised to actin in each sample. Protein expression levels of actin were quantified by a LI-COR Odyssey® CLx Imaging System. Before the immunoblotting analysis, proteins from each sample were resolved by SDS-PAGE (on 12% polyacrylamide gels). (**B**) Cell viability (n=5) in H9c2 cardiomyocytes incubated with 50 nM rat PP6C-siRNA (si) or non-targeting control siRNA (siC) for 4,6 or 8 days post-transfection, was measured by an MTT assay. A threshold is shown at 80% cell viability. All data represent mean values ± SEM of four individual experiments run in triplicates. Statistical comparison was made by one-way ANOVA followed by Tukey's post-hoc multiple comparisons tests; *$p<0.05$ *vs* siC. IB: Immunoblot.

6.4.6 Effects of PP6C protein knockdown on γH2AX in response to oxidative stress

PP6C has been previously reported to directly affect H2AX phosphorylation in non-myocytes (Douglas et al., 2010). Therefore, the role of PP6 catalytic subunit (PP6C) in H2AX phosphorylation in cardiomyocytes, under normal and oxidative stress conditions,

was investigated. According to the data in figure 6.13B, only H9c2 cardiomyocytes, transfected with rat PP6C-siRNA for 8 days, showed a statistically significant reduction in cell viability, even though, it was not considered biologically significant. Therefore, H9c2 cardiomyocytes were transfected with rat PP6C-siRNA or non-targeting control for 8 days and were either treated with H_2O_2 or PBS (vehicle control), 24 hours before harvesting of the samples. As shown in figure 6.14, PP6C protein expression was successfully knocked down (>93%) at 8 days post- transfection in H9c2 cardiomyocytes. Interestingly, treatment with H_2O_2 caused a significant ($p<0.05$) reduction of PP6C expression to 68.2 ± 10.5% in H9c2 cardiomyocytes. The off-target effects of PP6C-siRNA towards the expression of PP2AC and PP4C were examined at 8 days post-transfection. Figures 6.15A and 6.15B

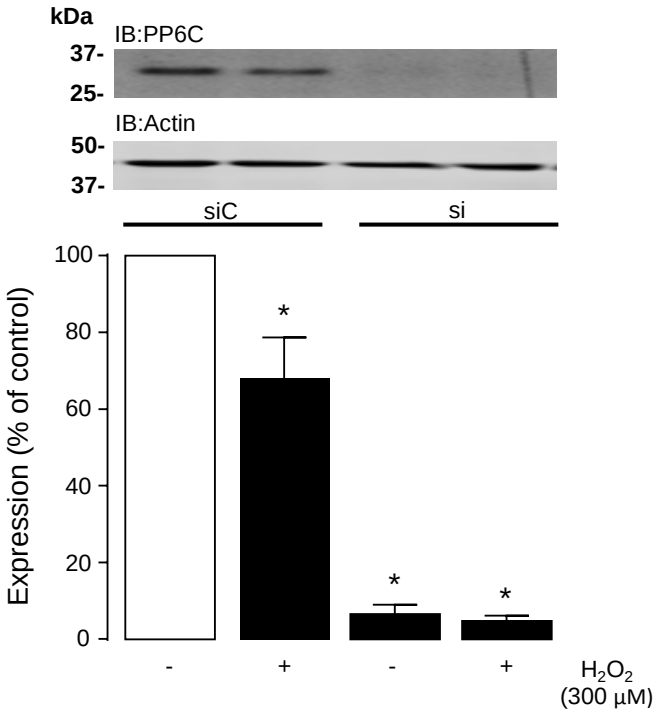

Figure 6.14 Protein expression of PP6C in H9c2 cardiomyocytes, transfected with 50 nM rat PP6C-siRNA (si) or non-targeting control siRNA (siC) for 8 days and treated with 300 µM H2O2 or PBS (vehicle control), was analysed by SDS-PAGE (12% polyacrylamide gels) and immunoblotting using a sheep polyclonal anti-PP6C antibody. Protein levels were quantified by densitometry and were normalised to actin in each sample. Protein expression levels of actin were quantified by a LI-COR Odyssey® CLx Imaging System. All data represent mean values ± SEM of five individual experiments. Statistical comparison was made by one-way ANOVA followed by Dunnett's post-hoc multiple comparisons tests; *$p<0.05$ *vs* siC without H_2O_2 (control). IB: Immunoblot.

show that the protein expression of total PP2AC and PP4C was not significantly altered in cells were transfected with rat PP6C-siRNA for 8 days, compared to the cells transfected with the non-targeting control siRNA. In addition, H_2O_2 treatment appeared to have a non-significant effect on the expression of total PP2AC and PP4C compared to the control samples. These data demonstrate an efficient siRNA-mediated post-transcriptional silencing of PP6C in H9c2 cardiomyocytes, 8 days post-transfection and the specificity of the rat PP6C-siRNA towards PP6C. Furthermore, PP6C protein expression appeared to be hydrogen peroxide-sensitive, compared to total PP2AC or PP4C.

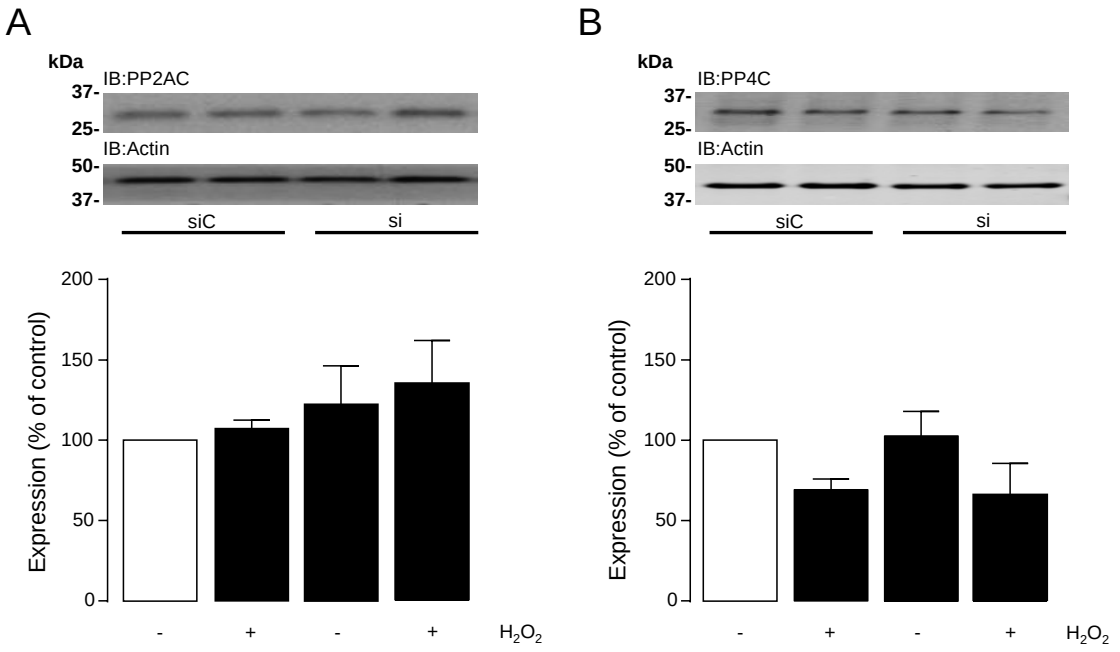

Figure 6.15 Protein expression of (**A**) total PP2AC (n=5) and (**B**) PP4C (n=4) in H9c2 cardiomyocytes, transfected with 50 nM rat PP6C-siRNA (si) or non-targeting control siRNA (siC) for 8 days and treated with 300 µM H2O2 or PBS (vehicle control), was analysed by SDS-PAGE (12% polyacrylamide gels) and immunoblotting using a sheep polyclonal anti-PP2AC and anti-PP4C antibodies. Protein levels were quantified by densitometry and were normalised to actin in each sample. Protein expression levels of actin were quantified by a LI-COR Odyssey® CLx Imaging System. All data represent mean values ± SEM. Statistical comparison was made by one-way ANOVA. No significant changes were observed (*vs* siC without H_2O_2). IB: Immunoblot.

Lysates were further tested by immunoblotting analysis for the expression of γH2AX, total H2AX and the ratio of γH2AX/ H2AX. Figure 6.16A shows that treatment of H9c2

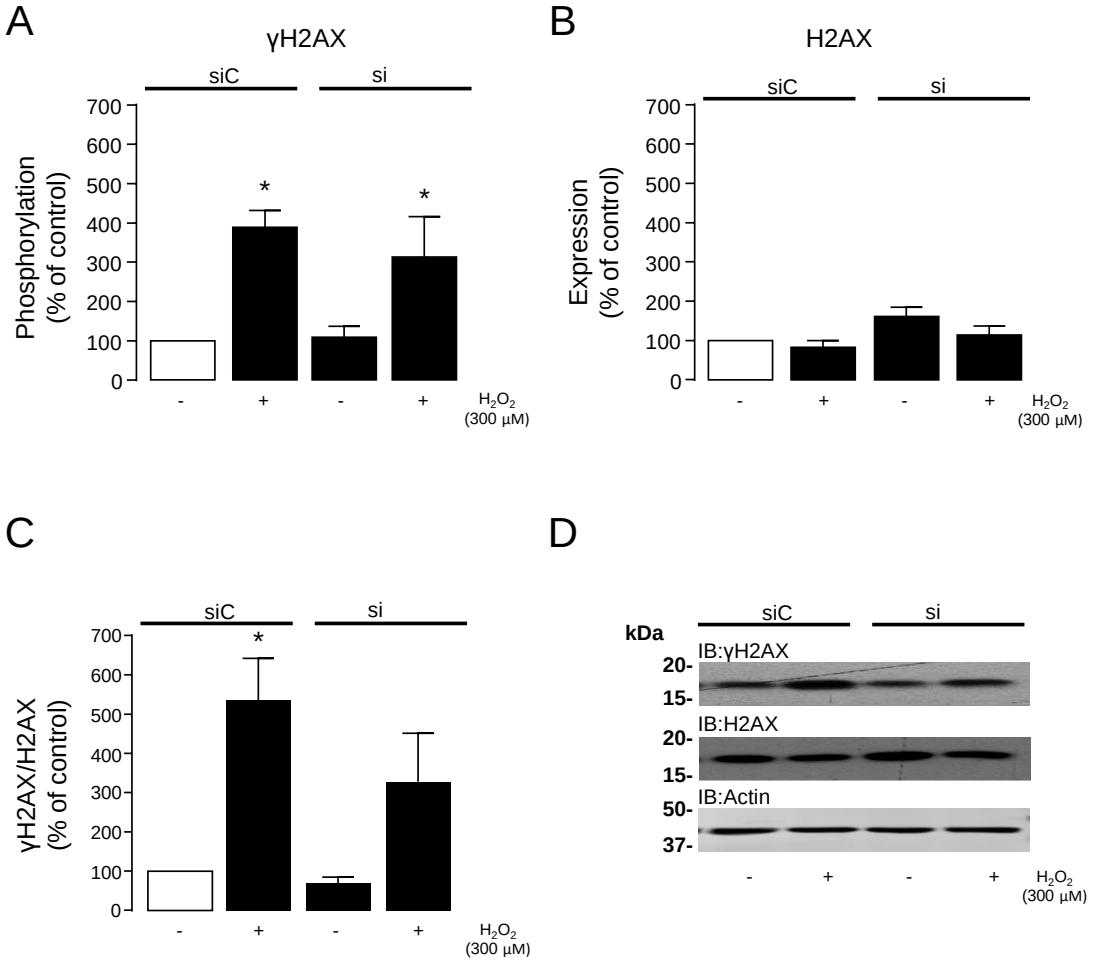

Figure 6.16 Protein expression of (**A**) γH2AX, (**B**) H2AX and (**C**) γH2AX/H2AX ratio in H9c2 cardiomyocytes, transfected with 50 nM rat PP6C-siRNA (si) or non-targeting control siRNA (siC) for 8 days and treated with 300 µM H2O2 or PBS (vehicle control), was analysed by SDS-PAGE (15% polyacrylamide gels) and immunoblotting using specific anti-γH2AX and anti-H2AX antibodies. Protein levels were quantified by densitometry and were normalised to actin in (**A**) and (**B**). Protein expression levels of actin were quantified by a LI-COR Odyssey® CLx Imaging System. All data represent mean values ± SEM of five individual experiments. Statistical comparison was made by one-way ANOVA followed by Dunnett's post-hoc multiple comparisons tests; *p<0.05 *vs* siC without H_2O_2 (control). (**D**) Representative immunoblots (IB) of γH2AX and H2AX protein expression.

cardiomyocytes with 300 µM H_2O_2 for 24 hours, significantly ($p<0.05$) elevated the phosphorylation level of γH2AX when cells were transfected with either non-targeting control siRNA (388 ±42.7 %) or rat PP6C-siRNA (312.6 ± 103.4%), compared to the non-targeting vehicle control sample. When the same samples were tested for the protein expression levels of total H2AX, non-significant change was detected (Figure 6.16B). Nevertheless, in figure 6.16C it is shown that the ratio

γH2AX/ H2AX was significantly ($p<0.05$) increased (535.7 ± 106.3%) in H9c2 cells transfected with non-targeting control siRNA and treated with 300 µM H_2O_2, compared to the cells treated with PBS. Even though γH2AX/ H2AX ratio was increased in cells transfected with rat PP6C-siRNA under oxidative stress (328.1 ± 123.4%), the change was not statistically significant ($p=0.156$), compared to the vehicle control samples. Taken together, these data suggest that oxidative stress induces the formation of γH2AX foci in H9c2 cardiomyocytes. Nevertheless, PP6C appears not to be involved in regulating H2AX phosphorylation, in response to H_2O_2 treatment, in cardiomyocytes.

6.4.7 Effects of alpha4 protein knockdown on γH2AX in response to oxidative stress

Phosphorylation of H2AX can be affected by all type 2A protein phosphatase catalytic subunits (Chowdhury et al., 2005; Chowdhury et al., 2008; Nakada et al., 2008a; Douglas et al., 2010; Zhong et al., 2011). Furthermore, the protein expression levels of total PP2AC, PP4C and PP6C is severely reduced (>70%) when alpha4 protein is depleted (>94%) in cardiomyocytes, as shown in Chapter 4 (Figures 4.19-4.22). Therefore, the role of alpha4 in H2AX phosphorylation was investigated in H9c2 cardiomyocytes, under normal and oxidative stress condition. Cells were transfected with either non-targeting control siRNA or rat alpha4-siRNA for 4 days and were either treated with H_2O_2 or PBS (vehicle control), 24 hours before harvesting of the samples. H_2O_2 treatment induced basal formation of γH2AX foci (196.4 ± 15.7%) in H9c2 cardiomyocytes, transfected with non-targeting control siRNA (Figure 6.18A). Surprisingly, when expression of alpha4 protein was significantly ($p<0.05$) knocked down (>98%) (Figure 6.17), the basal formation of γH2AX foci in cells was significantly ($p<0.05$) abolished (18.4 ± 5.6%) (Figure 6.18A) compared to the non-targeting control samples. This effect was consistent even in response to H_2O_2 treatment (28.7 ± 20.9%) (Figure 6.18A). Interestingly, the

expression of total H2AX protein was significantly ($p<0.05$) reduced (>73%) when the alpha4 protein expression was knocked down (>98%) either combined or not with H_2O_2 treatment (Figure 6.18B). The ratio of γH2AX/H2AX was then calculated. As shown in figure 6.18C, γH2AX/H2AX ratio was significantly increased in response to H_2O_2 treatment (278.9 ± 47.9%) compared to the vehicle control. However, γH2AX/ H2AX ratio was not significantly changed when alpha4 protein expression was knocked down in H9c2 cardiomyocytes with or without H_2O_2 treatment when compared to vehicle control (Figure 6.18C). These data suggest that loss of alpha4 in H9c2 cardiomyocytes efficiently reduces γH2AX foci formation and cellular total H2AX protein content.

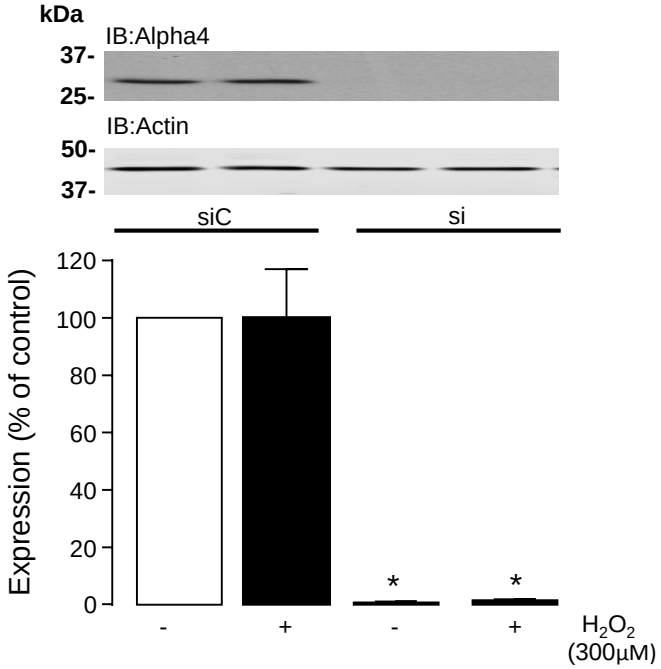

Figure 6.17 Protein expression of alpha4 in H9c2 cardiomyocytes, transfected with 50 nM rat alpha4-siRNA (si) or non-targeting control siRNA (siC) for 4 days and treated with 300 μM H2O2 or PBS (vehicle control), was analysed by SDS-PAGE (12% polyacrylamide gels) and immunoblotting using a rabbit monoclonal anti-alpha4 antibody. Protein levels were quantified by densitometry and were normalised to actin in each sample. Protein expression levels of actin were quantified by a LI-COR Odyssey® CLx Imaging System. All data represent mean values ± SEM of three individual experiments. Statistical comparison was made by one-way ANOVA followed by Dunnett's post-hoc multiple comparisons tests; *$p<0.05$ *vs* siC without H_2O_2 (control). IB: Immunoblot.

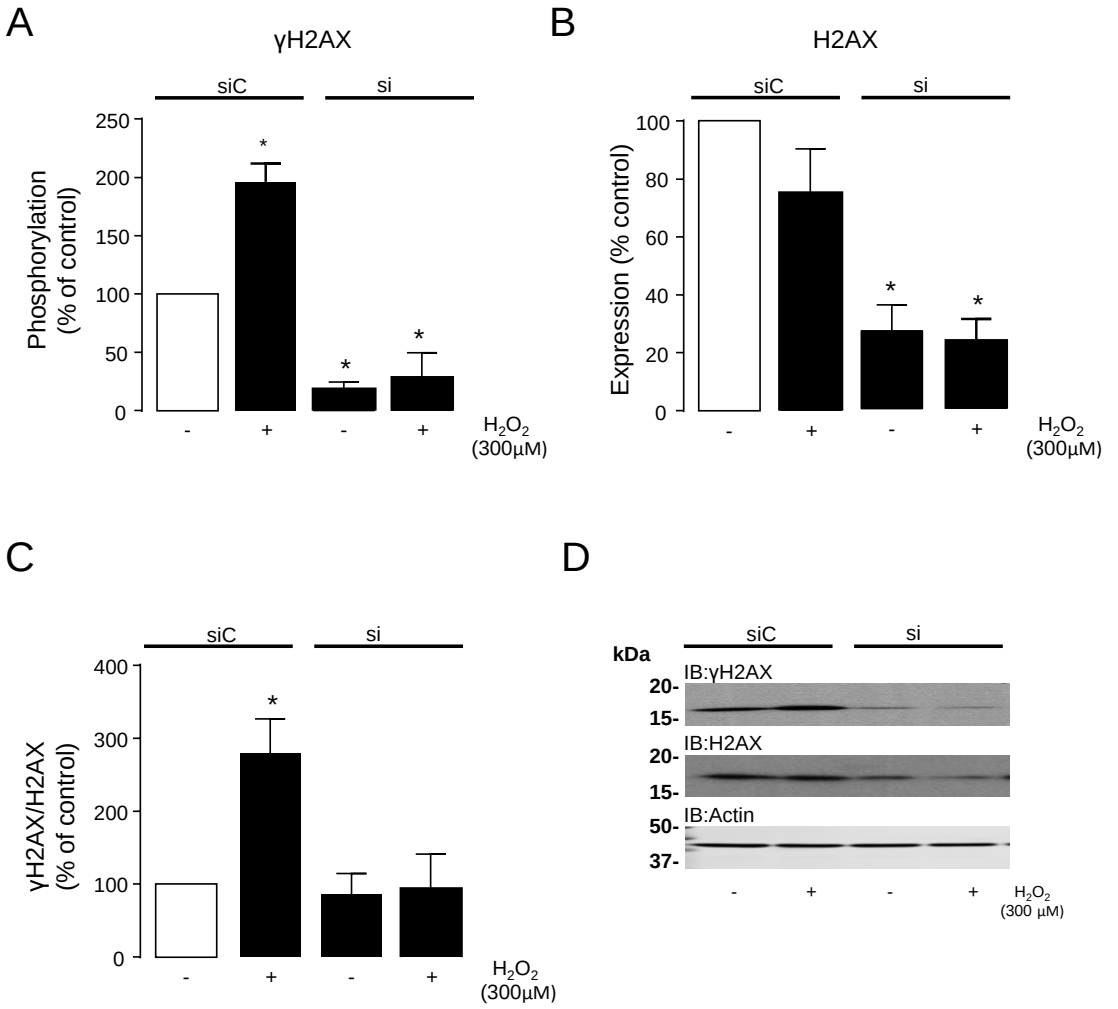

Figure 6.18 Protein expression of (**A**) γH2AX, (**B**) H2AX and (**C**) γH2AX/H2AX ratio in H9c2 cardiomyocytes, transfected with 50 nM rat alpha4-siRNA (si) or non-targeting control siRNA (siC) for 4 days and treated with 300 μM H2O2 or PBS (vehicle control), was analysed by SDS-PAGE (15% polyacrylamide gels) and immunoblotting using specific anti-γH2AX and anti-H2AX antibodies. Protein levels were quantified by densitometry and were normalised to actin in (**A**) and (**B**). Protein expression levels of actin were quantified by a LI-COR Odyssey® CLx Imaging System. All data represent mean values ± SEM of three individual experiments. Statistical comparison was made by one-way ANOVA followed by Dunnett's post-hoc multiple comparisons tests; *p<0.05 *vs* siC without H_2O_2 (control). (**D**) Representative immunoblots (IB) of γH2AX and H2AX protein expression.

6.4.8 Investigation of sequence complementation-dependent alpha4-siRNA-mediated off-target effects against H2AX expression

Since alpha4 protein knockdown in H9c2 cardiomyocytes resulted in a significant ($p<0.05$) reduction (>73%) of total H2AX protein levels, the probability of alpha4-siRNA-mediated off-target effects towards H2AX mRNA was examined as described

in Chapter 2 (section 2.3.2). Alignment between the rat H2AX mRNA (GenBank® ID: NM_001109291.1) open reading frame and each rat alpha4-siRNA sequence showed >10 nt mismatches. Furthermore, alignment of each siRNA seed region (positions 1-8 nt) with the 3'-UTR of H2AX did not show 8 nt complementation. These data indicate that there is no efficient complementation between the rat alpha4-siRNAs and the H2AX mRNA (open reading frame or 3'-UTR) to induce any sequence-dependent off-target effect.

6.4.9 Phosphorylation status of H2AX in pressure overload-induced LV hypertrophy

The formation of γH2AX foci was investigated in pressure overload-induced murine hypertrophied LV tissue lysates and compared to the SHAM control tissue. Figures 6.19A and 6.19B, show that γH2AX and H2AX protein levels, respectively, remained unchanged between the hypertrophied and non-hypertrophied LV tissue lysates. Furthermore, the γH2AX/ H2AX ratio was not significantly altered in LV tissue obtained from TAC-operated mice, when compared to the SHAM-operated mice (Figure 6.19C). These data indicate that the amount of γH2AX foci formation was similar in murine normal and hypertrophied LV tissue.

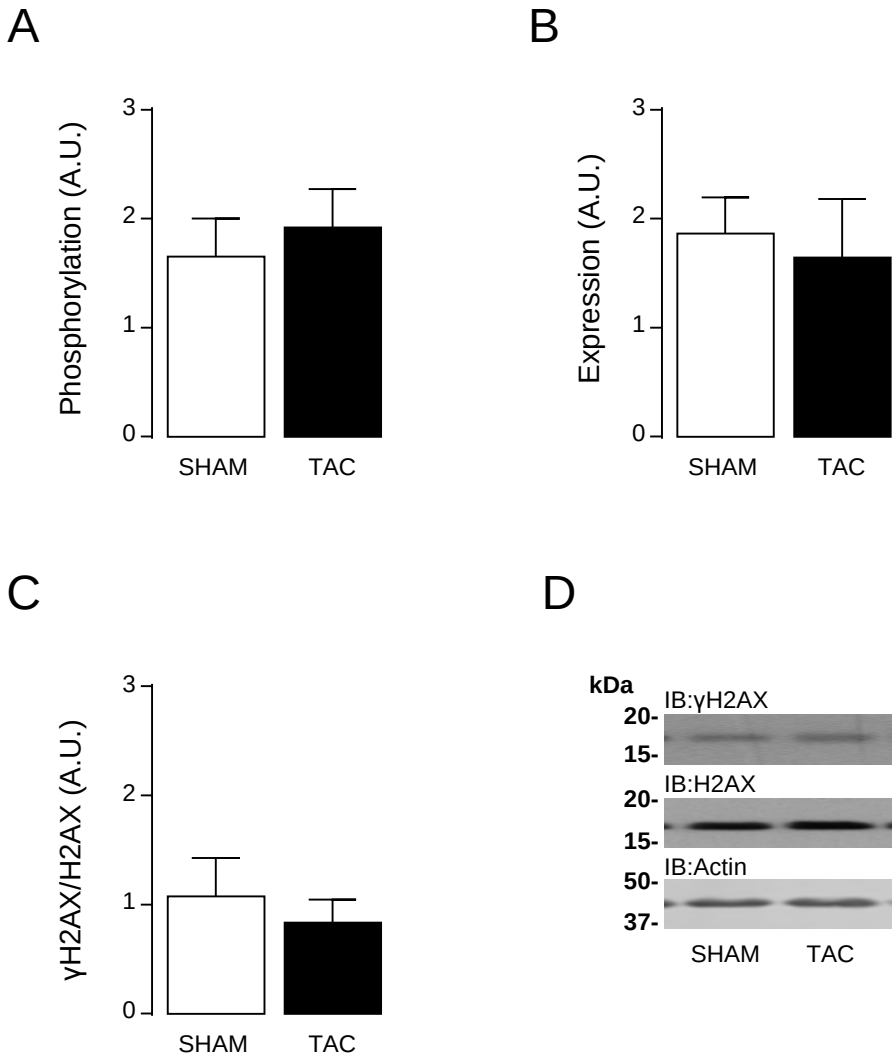

Figure 6.19 Protein expression of (**A**) γH2AX, (**B**) H2AX and (**C**) γH2AX/ H2AX enrichment in the LV tissue of SHAM (n=4)- and TAC (n=6)-operated mice, 28 days after surgery, was determined by immunoblotting analysis, using specific anti-γH2AX and anti-H2AX antibodies. Prior to immunoblotting, proteins from each sample were resolved by SDS-PAGE (on 15% polyacrylamide gels). Protein levels were quantified by densitometry and were normalised to actin in (**A**) and (**B**). Protein expression levels of actin were quantified by a LI-COR Odyssey® CLx Imaging System. All data represent mean values ± SEM. Statistical comparison was made by a two-tailed unpaired Student's t-test. No significant changes were observed between the SHAM and TAC. (**D**) Representative immunoblots (IB) of γH2AX and H2AX protein expression.

6.5 Discussion

6.5.1 Pressure overload-induced LV hypertrophy in mice

Aortic binding initiates a rapid increase in cardiac afterload and consequently a hypertrophic response in the left ventricle. *In vivo* animal models of partial abdominal aortic constriction-induced cardiac hypertrophy have been used extensively in previous studies to investigate pressure overload-induced pathological cardiac hypertrophy (Cutilletta et al., 1975; Balakumar and Singh, 2006; Seymour et al., 2015; Singh et al., 2015). The data in the current study showed that transaortic constriction (TAC) of the abdominal aorta of mice for 28 days resulted in a significant ($p<0.05$) 60-62% increase of LV mass compared to the SHAM-operated mice. These data are in agreement with previous reports where the abdominal aorta was bound or show a more severe phenotype. Balakumar and Singh (2006) and Singh et al. (2015) demonstrated an approximate 56% increase in LV mass, in TAC-operated rats 4 weeks post-surgery, whilst Seymour et al. (2015) showed only 17% significant increase in LV mass in TAC-operated mice 4 weeks post-surgery.

6.5.2 Expression of PP2AC, PP4C, PP6C and their association with alpha4 regulatory protein in LV hypertrophy

In the present study, the development of LV hypertrophy in response to pressure overload, in the TAC-operated mice, was sufficient to significantly ($p<0.05$) elevate PP2AC (1.7-fold) and alpha4 (1.8-fold) protein expression in murine LV hypertrophied tissue. Furthermore, PP2AC showed significant interaction with alpha4 protein (Figure 6.10A) in LV tissue. In addition, the novel data in figures 6.10B and 6.11B suggest an increase in PP2AC:alpha4 complex formation in LV hypertrophied tissue.

Previous studies have demonstrated the elevation of PP2AC expression or activity in the diseased myocardium (Gergs et al., 2004; DeGrande et al., 2013). Gergs et al., (2004), showed that overexpression of PP2AC (2.1-fold) in the myocardium was associated with LV hypertrophy (22% mass increase). However, no change in the expression of the type 2A protein phosphatase regulatory protein alpha4 was observed. Furthermore, DeGrande et al. (2013) reported a significant 2-fold PP2AC protein increase in human heart failure cardiac tissue.

A critical role of the alpha4 protein is the protection of the type 2A protein phosphatase catalytic subunits from proteasome-mediated degradation (Kong et al., 2009; McConnell et al., 2010; LeNoue-Newton et al., 2011; Watkins et al., 2012; Jiang et al., 2013b; LeNoue-Newton et al., 2016). Thus, it becomes apparent that the association of alpha4 with PP2AC, PP4C and PP6C is of great importance for normal cellular function. The data in Gergs and co-workers' study, (2004), indicate that PP2AC overexpression *per se* was not sufficient to alter alpha4 protein expression levels. However, in a recent study, LeNoue-Newton et al. (2016) showed that protein knockdown of alpha4 led to a reduction of PP2AC protein expression, which was recovered when alpha4 protein expression was rescued in HEK293T cells. In addition, the data in Chapter 4 (figures 4.19-4.22) demonstrated that alpha4 protein knockdown significantly reduced the protein expression levels of the type 2A protein phosphatase catalytic subunits in H9c2 cardiomyocytes.

Taken together the above studies and the findings in this thesis, offer an explanatory theory for the augmentation of PP2AC protein levels in the diseased LV tissue, which may be facilitated through a pressure overload-induced increase in alpha4 protein expression, which in turn may protect PP2AC from proteasome-mediated degradation through an increased PP2AC:alpha4 complex formation.

In the present study, the protein expression of PP4C was not detectable in the adult mouse LV tissue, suggesting that PP4C was either absent or of a very low abundance. This result agrees with the data shown in Chapter 3 (Figure 3.6) where PP4C was undetectable at the protein level in the ARVMs unless the 26S proteasome was inhibited with MG132 (Figure 3.8). The latter finding indicates that PP4C may be post-translationally regulated by the ubiquitin-proteasome system in the adult myocardium. In addition, alpha4 protein knockdown (>94%) in Chapter 4 (Figure 4.19) resulted in significant reduction of PP4C expression (>84%) (Figure 4.21), suggesting that alpha4 may play a protective role towards PP4C against proteasome activity, similarly to PP2AC. Hence, 1.8-fold upregulation of alpha4 expression in the hypertrophied myocardium was speculated to cause an increase in the intact PP4C, which was not the case. In support to this data, LeNoue-Newton et al. (2016), demonstrated that even though alpha4 protein expression knockdown led to a reduction of PP4C protein expression in HEK293T cells, this effect was not reversed when alpha4 protein was re-expressed. Thus, PP4C regulation by alpha4 protein appears to be more complex. Since PP4C protein expression was not detectable in alpha4 immunoprecipitates from ARVMs (Figure 6.9) or in the LV tissue of mice, the association of alpha4 with PP4C in the adult murine myocardium was not investigated.

PP6C expression was not significantly changed in LV hypertrophy and showed significant interaction with the alpha4 protein in the mouse adult myocardium. Interestingly, PP6C:alpha4 complex formation appeared to be significantly reduced in the hypertrophied LV tissue (Figure 6.12B). Besides the protective role of alpha4 towards PP6C, the interaction of PP6C with alpha4 has been suggested to inhibit PP6C activity in non-myocytes (Nanahoshi et al., 1999; Jacinto et al., 2001; Prickett and Brautigan, 2006). Since the total expression of PP6C was not knocked down

(Figure 6.4C), by the observed reduction of PP6C:alpha complex (Figure 6.12) and "free" PP6C is thought to be unstable, it is proposed here that PP6C holoenzyme complex formation and consequently PP6C activity might be enhanced in cardiac hypertrophy.

The present study is the first study to compare the expression of alpha4 protein in normal and hypertrophied LV tissue. As mentioned earlier, alpha4 protein was significantly ($p<0.05$) upregulated (1.8-fold increase) in the LV tissue obtained from the TAC-operated mice compared to the SHAM-operated mice. Pathological cardiac hypertrophy is characterised by an abnormal increase in protein synthesis and cell size, which is considered a "tumor-like" growth (Gupta et al., 1996; Molkentin et a., 1998; Harris et al., 2004; Lorenze et al., 2009). Notably, alpha4 overexpression has been detected in many types of cancer, and it has been suggested to be involved in increased cell migration and proliferation (Chen et al., 2011; Liu et al., 2014).

6.5.3 Expression of PP6 regulatory subunits in LV hypertrophy

PP6C has been shown to interact with multiple regulatory subunits: the SAPs domain regulatory proteins (SAP1-3) (Luke et al., 1996; Stefansson and Brautigan, 2006; Zeng et al., 2010) and ankyrin repeat domain proteins (ANKRD28, ANKRD44, and ANKRD52) (Stefansson et al., 2008; Zeng et al., 2010). It is thought to assemble like the classical PP2A holoenzyme (discussed below), where the SAPs domain subunits act as adaptors to bridge PP6C and the ankyrin repeat domain subunits (Stefansson et al., 2008). SAP1 and SAP2 were significantly increased and decreased, respectively, whilst SAP3 remained unchanged in the LV tissue from TAC-operated mice compared to the SHAM-operated mice. Moreover, ANKRD28 and ANKRD44 were found to be significantly increased in LV hypertrophied tissue compared to the normal tissue, whilst ANKRD52 remained

unchanged. To date, there is no information in the literature regarding the expression and role of SAPs1-3, ANKRD28, ANKRD44, and ANKRD52 in cardiomyocytes. The novel data in the current study presented differential expression of the PP6 regulatory subunits between the normal and hypertrophied murine LV tissue, even though, PP6C expression was unchanged, which may indicate a redundant function of each subunit or involvement in PP6 localisation.

6.5.4 Oxidative stress and γH2AX foci formation in cardiomyocytes

Previous studies have demonstrated that neurohormones, such as angiotensin II (Ang-II), endothelin-1 (ET-1) or norepinephrine (NE), which are released in response to pathological pressure overload and induce a cardiac hypertrophic phenotype (Schunkert et al., 1990; Arai et al., 1995; Rapacciuolo et al., 2001; Yayama et al., 2004), can mediate an increase in ROS formation and oxidative stress (Liu et al., 2004; Laskowski et al., 2006). Furthermore, there is evidence that oxidative stress contributes to the progression of pathological hypertrophy and heart failure (McMurray et al., 1993; Siwik et al., 1999; Takimoto et al., 2005; Grieve et al., 2006; Xu et al., 2008; Oyama et al., 2009). In addition, oxidative stress is known to cause DNA damage (Suematsu et al., 2003; Ye et al., 2016), therefore, increase the risk of genomic instability and cell death (Huang et al., 2005; Mirzayans et al., 2006; Jackson and Bartek, 2009; Liu et al., 2016). Hence, to investigate the role of type 2A protein phosphatases in dsDNA break repair process in cardiomyocytes, a cell culture model for oxidative stress was initially evaluated, by treating H9c2 cardiomyocytes with H_2O_2, which is known to induce dsDNA breaks (Driessens et al., 2009; Ye et al., 2016). Indeed, as shown in figures 6.16 and 6.18, H_2O_2 treatment in H9c2 cardiomyocytes resulted in a significant increase (≥196.4 %) of γH2AX foci formation. This data is in line with a previous study by Ye et al., (2016), showing that oxidative stress is implicated in DNA double-strand break in cardiomyocytes,

by monitoring a significantly increased formation of γH2AX in neonatal rat ventricular myocytes treated with H_2O_2 (Ye et al., 2016).

6.5.5 Does PP6C affect γH2AX and cell viability in cardiomyocytes?

The phosphorylation of the nuclear histone variant H2AX at ser139 (γH2AX) initiates the DNA double-strand break repair response in cells (Rogakou et al., 1998; Rogakou et al., 1999; Andegeko et al., 2001; Bassing et al., 2002; Fernandez-Capetillo et al., 2002; Meador et al., 2008). Oxidant stress is a potent inducer of DNA damage and consequent formation of γH2AX foci in myocytes (Figures 6.16A and 6.18A). In addition, persistent oxidative stress and dsDNA break may increase the risk of cell death (Huang et al., 2005; Mirzayans et al., 2006; Jackson and Bartek, 2009; Liu et al., 2009). PP6C had been implicated in regulating the formation of γH2AX foci in non-myocytes (Douglas et al., 2010) and was found to be a survival protein in HeLa cells in a large-scale RNA interference (RNAi) screen, (MacKeigan et al., 2005). MacKeigan and co-workers (2005), demonstrated that a greater than 80% PP6C mRNA knockdown in HeLa cells by a PP6C-siRNA pool, for 3 days, initiated a 4.6-fold increase in apoptosis. However, in the present study, H9c2 cardiomyocyte transfection with rat PP6C-siRNA for 4 and 6 days, which resulted in >80% PP6C protein expression knockdown, did not affect cell viability significantly. When H9c2 cells were transfected with rat PP6C-siRNA for 8 days, a statistically significant reduction (7%) was observed in cell viability, and cell lysates were further tested for γH2AX foci formation. However, 8 days post-transfection with PP6C-siRNA, the basal γH2AX foci formation was unchanged compared to H9c2 cells transfected with non-targeting control siRNA (Figure 6.16). These data indicate that PP6C protein knockdown (>93%) per se, in cardiomyocytes, does not initiate cell death or γH2AX foci formation. Douglas and co-workers (2010), showed that when PP6C protein expression was knocked down (90%) by

siRNA transfection in HeLa cells exposed to ionising radiation, γH2AX was significantly increased, compared to cells transfected with a control siRNA. Thus, the role of PP6C in the regulation of H2AX phosphorylation status was investigated in cardiomyocytes under oxidative stress conditions (by exogenous H_2O_2). Nonetheless, siRNA-driven knockdown (>93%) of PP6C protein expression in H9c2 cardiomyocytes treated with H_2O_2, induced the formation of γH2AX foci at similar levels to cells transfected with non-targeting control siRNA (Figure 6.16). This data suggests that either PP6C does not target γH2AX in cardiomyocytes or that γH2AX dephosphorylation by PP2AC and/ or PP4C (Chowdhury et al., 2005; Chowdhury et al., 2008; Nakada et al., 2008a) can compensate for the lack of PP6C and thereby maintain low levels of cellular γH2AX.

Notably, in the same experiments, a significant ($p<0.05$) reduction of basal PP6C protein expression was observed (Figure 6.14), when oxidative stress was induced (exogenous H_2O_2). This rather interesting result could be related to a possible oxidative modification of PP6C by ROS. Oxidised proteins (Stadtman, 2006; Wani et al., 2014) are usually degraded either by the 20S proteasome free form (Davies, 2001; reviewed by Raynes et al., 2016) or by autophagy (Kiffin et al., 2004). However, this explanation can only be speculated due to lack of studies in the literature that investigated oxidation of PP6C.

6.5.6 Role of alpha4 in regulating γH2AX in cardiomyocytes

Alpha4 is a regulatory protein of all type 2A protein phosphatase catalytic subunits (Murata et al., 1997; Chen et al., 1998; Nanahoshi et al., 1999; Kloeker et al., 2003; Kong et al., 2009; Watkins et al., 2012; Jiang et al., 2013b). As shown in Chapter 4 (Figures 4.19-4.22), knockdown of alpha4 protein expression (>94% decrease) in cardiomyocytes had severe consequences on the expression of total PP2AC, PP4C

and PP6C and led to their progressive loss (>83%, >84% and >73%, respectively) at 4 days post-transfection with alpha4-siRNA. γH2AX has been shown to be dephosphorylated by all three type 2A protein phosphatases (Chowdhury et al., 2005; Chowdhury et al., 2008; Nakada et al., 2008a; Douglas et al., 2010; Zhong et al., 2011). Hence, it was hypothesised that siRNA-mediated knockdown of alpha4 protein expression and consequent significant reduction of PP2AC, PP4C and PP6C expression at 4 days post-transfection, would cause an increase in γH2AX under oxidative stress conditions (by exogenous H_2O_2). Surprisingly, as shown in figure 6.18A, protein expression knockdown of alpha4 (>98%) resulted in a significant ($p<0.05$) reduction of γH2AX foci formation in the absence and presence of H_2O_2 treatment in H9c2 cardiomyocytes. This result contrasted with a previous report, showing an increase in γH2AX in non-myocytes when alpha4 protein expression was silenced (Kong et al., 2009). In addition, protein levels of total H2AX expression were significantly reduced (>73%) when alpha4 protein expression was knocked down (Figure 6.18B). Thus, the reduction in the expression of total H2AX explains the observed decrease of γH2AX levels in alpha4 deficient H9c2 cardiomyocytes, as the γH2AX/H2AX ratio remained unchanged in cells transfected with either non-targeting control siRNA or rat alpha4-siRNA, without H_2O_2 treatment. This novel data was considered an alpha4-siRNA-mediated on-target effect, since no efficient sequence complementation was detected between the alpha4-siRNAs and H2AX mRNA (section 6.4.8).

It is notable that Kong et al. (2009) did not investigate the effects of alpha4 knockdown on the expression of total H2AX. Chowdhury et al. (2008), showed that protein silencing of PP2AC or PP4C expression in HeLa cells, increased γH2AX foci formation when cells were treated with camptothecin, a compound that mediates dsDNA breaks, whilst PP4C also affected the basal level of γH2AX foci. In the same

study, total H2AX was unchanged (Chowdhury et al., 2008). The data in this study showed that knockdown of PP6C in cardiomyocytes, in the absence or presence of H_2O_2, did not affect the γH2AX or total H2AX protein expression. In support of these data, Zhong et al. (2011), showed no change in the protein expression of total H2AX when PP6C was knocked down by siRNA in MCF-7 cells, however in the same paper γH2AX also remained unchanged (Zhong et al., 2011). In contrast, Douglas et al. (2010), showed that siRNA-driven PP6C protein knockdown could increase γH2AX in HeLa cells after exposure to ionising radiation, but also did not investigate the expression of total H2AX under the same experimental conditions. Taken together, these findings seem to suggest that individual protein expression knockdown of each phosphatase per se, may not affect the expression of total H2AX. Hence, it is proposed, that in the current study, the degree of alpha4 knockdown, and consequent loss of all type 2A protein phosphatase catalytic subunits in H9c2 cardiomyocytes, 4 days post-transfection with rat alpha4-siRNA, creates a severe insult to the cells followed by the loss of H2AX and their inability to form γH2AX foci and undergo DNA repair. Furthermore, γH2AX was not increased, even when alpha4-deficient cardiomyocytes were treated with H_2O_2, which supports the previous statement. Thereby, delayed repair of damaged DNA in cardiomyocytes would be expected to lead to genomic instability and eventually apoptotic cell death, as it has been demonstrated previously in non-myocytes (Bensaad and Vousden, 2005; Christophorou et al., 2006; Jackson and Bartek, 2009).

A model that could explain the loss of H2AX in cardiomyocytes, in the absence of alpha4 and low γH2AX foci formation under oxidative stress (exogenous H_2O_2) would be the loss of total H2AX protein expression due to an increased proteasome-mediated degradation, in settings of disease. This model, in turn, could be interpreted in two ways.

Gruosso et al. (2016) recently demonstrated that H2AX (consequently γH2AX foci formation) was significantly reduced in the presence of accumulated ROS under oxidative stress conditions, in non-myocytes with a defective antioxidant response. This degradation was driven by the H2AX polyubiquitination of Lys119 residue by the E3 ubiquitin ligase RNF168 and proteasome activity (Gruosso et al., 2016). Prevention of γH2AX formation, in turn, has been shown to enhance cell apoptosis (Taneja et al., 2004). Fernandez-Capetillo et al. (2002), showed that deletion of H2AX in transgenic mice resulted in enhancing the entry of damaged cells into mitosis, instead of cell arrest at the G_2/M checkpoint (reviewed by Smith et al., 2010) until DNA repair and replication completion. This result was confirmed later by Meador et al. (2008) in H2AX null mouse embryonic stem cells and fibroblasts, showing a lack of G_2/M checkpoint, increased G_1 cell arrest and apoptosis rate. Many other previous studies provided evidence of genomic instability when H2AX was deleted either in transgenic mice or mammalian non-myocyte cells (Bassing et al., 2002; Celeste et al., 2002). Thus, more damaged DNA was clustered, resulting in genomic instability and high risk of apoptotic cell death (Li et al., 2004). In support to the proteasome-mediated degradation of H2AX, (Zong et al., 2006). Zong et al. (2006), demonstrated that inhibition of PP2AC (and potentially PP4C and PP6C) by okadaic acid in murine heart caused an increased activity of cardiac proteasome 20S, which is the core unit of all proteasomes (Eytan et al., 1989; Davies, 2001; review by Dahlmann et al., 2016). In the present study, all type 2A protein phosphatase catalytic subunits were inhibited by the siRNA-driven knockdown of alpha4 in H9c2 cardiomyocytes (Figures 4.19-4.22). In addition, initial observations by Kong et al. (2009), showed apoptotic cell death of non-myocytes, when alpha4 protein expression was knocked down. Thus, delayed DNA repair in embryonic, neonatal and adult (without re-entering the cell cycle) cardiomyocytes due to increased proteasome-mediated degradation of H2AX to oxidative stress, could potentially

lead to accumulation of damaged DNA and enhanced cell death.

Alternatively, it has been shown that during the DNA repair response (DRR) process, proteasome activator PA200/Blm10 re-localises to nuclear foci formation at the DNA damaged region (Blickwedehl et al., 2008). In a recent review by Qian et al. (2013), authors concluded that activation of the proteasome by PA200/Blm10 at the DNA damaged area, results in the removal of acetylated core histones, including H2AX (Jiang et al., 2010) to facilitate DNA unravelling and accessibility of DNA repair proteins to damaged DNA. In this case, initiation of H2AX proteasome-mediated degradation in cardiomyocytes may promote cell viability.

Collectively these findings indicate that H2AX expression, γH2AX foci formation and their regulation by alpha4 protein in cardiomyocytes, may be important for cell viability under stress conditions (e.g. pressure overload/ oxidative stress). A question, raised by the current study, is whether loss of alpha4 protein in cardiomyocytes could be a severe enough insult to induce cell death and/ or increase ROS sensitivity.

6.5.7 Pressure overload-induced LV hypertrophy and DNA damage repair

Many studies have shown that pressure overload-mediated cardiac hypertrophy is associated with increased levels of ROS and oxidative stress (McMurray et al., 1993; Siwik et al., 1999; MacCarthy et al., 2001; Li et al., 2002; Byrne et al., 2003; Maack et al., 2003; Maytin et al., 2004; Takimoto et al., 2005; Grieve et al., 2006; Xu et al., 2008). Oxidative stress, in turn, can initiate DNA double strand breaks and consequent DNA damage repair response in cardiomyocytes, detected by the formation of γH2AX foci as it was shown in the present study (Figures 6.16A and 6.18A) and a previous report (Ye et al., 2016). Increased levels of PP2AC in the

hypertrophied left ventricles are expected to promote γH2AX dephosphorylation (Chowdhury et al., 2008; Nakada et al., 2008a). Moreover, PP6C/SAP1 association is known to activate DNA-PK (Mi et al., 2009; Douglas et al., 2010; Hosing et al., 2012), which targets Ser139 residue of H2AX, hence, the elevated SAP1 protein levels (Figure 6.6A) in the hypertrophied LV tissue may indirectly increase γH2AX foci, but may also directly dephosphorylate it (Douglas et al., 2010). On the contrary, PP6C/SAP2 association is responsible for γH2AX dephosphorylation (Zhong et al., 2011). Therefore, the decreased levels of SAP2 (Figure 6.6B) in the hypertrophied myocardium would suggest an increase in γH2AX foci. Most of the above evidence in previous reports and observations in this study would argue for an increase in the γH2AX foci formation in LV hypertrophy. However, no significant alteration was observed in γH2AX or H2AX in the LV tissue from TAC-operated mice compared to the SHAM-operated mice (Figure 6.19).

PP2AC and PP6C have been shown to be present in the nucleus of non-myocytes (Turowski et al., 1995; Mi et al., 2009). Therefore, the increased PP2AC protein expression and "free" intact PP6C presence observed in the cellular lysates of murine hypertrophied LV tissue, in the current study, could contribute to an increased PP2AC and PP6C activity in the nucleus of the cardiomyocytes, which may be responsible for keeping γH2AX foci levels low, thereby delaying DNA repair. Moreover, further research is required to confirm the potential implication of alpha4 overexpression in the DNA repair process in the adult hypertrophied myocardium.

Nevertheless, a positive correlation between the elevated ROS and γH2AX foci formation has been shown previously in heart failure compared to non-heart failure patients (Mondal et al., 2013). Furthermore, progression of cardiac hypertrophy to

heart failure is related to enhanced ROS levels (Hill and Singal, 1996; Ide et al., 2000; Li et al., 2002; Heymes et al., 2003; Mondal et al., 2013), DNA damage (Olivetti et al., 1997; Bartunek et al., 2002; Wencker et al., 2003; Mondal et al., 2013) and cell death (Olivetti et al., 1997; Chen et al., 2002; Hein et al., 2003; Wencker et al., 2003). Therefore, another possible explanation for the unchanged γH2AX between the hypertrophied and non-hypertrophied LV tissue could be the level of DNA damage severity compared to heart failure, at least in the mice used in the current study.

Moreover, the formation of γH2AX foci is essential for the initiation of the DNA damage repair response and recruitment of DNA damage repair proteins (Paull et al., 2000; Bassing et al., 2002; Fernandez-Capetillo et al., 2002; Meador et al., 2008). As discussed in the previous section, one possible consequence of delaying the repair of damaged DNA due to lack of γH2AX foci, with persistent DNA damage, would be the accumulation of irreparable DNA and initiation of apoptotic cell death (Bensaad and Vousden, 2005; Christophorou et al., 2006; Jackson and Bartek, 2009). Hence, the abnormal regulation of the DNA repair process observed in the hypertrophied myocardium might be a primary event, contributing to the progressive loss of cardiomyocytes and transition of hypertrophy to heart failure, but this requires further study.

6.6 Summary

In summary, in this chapter, it was shown that pressure overload-induced LV hypertrophy (60-62% increase of LV mass) was associated with a significant ($p<0.05$) increase in PP2AC (1.7-fold) and alpha4 (1.8-fold) protein expression whilst, PP4C was not detectable in the murine myocardium. Even though PP6C expression was unaltered in the hypertrophied murine LV tissue, expression of PP6C regulatory subunits (i) SAP1 (2.2-fold) and (ii) ANKRD28 (1.9-fold) and ANKRD44 (1.5-fold) proteins was significantly ($p<0.05$) increased, whereas SAP2 expression was significantly ($p<0.05$) reduced (2.8-fold) and expression of SAP3 and ANKRD52 remained unchanged, compared to the normal LV tissue. Co-immunoprecipitation of alpha4 regulatory protein and type 2A protein phosphatase catalytic subunits, from LV tissue of SHAM- and TAC-operated mice, revealed that the cellular association between alpha4 protein and PP2AC or PP6C subunits was either unchanged or significantly reduced ($p<0.05$) in the hypertrophied LV tissue, respectively. DNA damage determined by γH2AX was unaltered between the normal and hypertrophic tissue. However, exposure of H9c2 cardiomyocytes to 300 μM H_2O_2 for 24 hours significantly elevated ($p<0.05$) levels of γH2AX, which was unaffected when PP6C protein expression was knocked down long-term (8 days) and significantly reduced along with the expression levels of total H2AX by the short-term knockdown (4 days) of alpha4 protein.

Chapter 7

Conclusions

One of the aims of this study was to identify the expression of type 2A protein phosphatase catalytic subunits in cardiomyocytes. Using qPCR and immunoblotting analysis, I demonstrated that all the type 2A protein phosphatase catalytic subunits were expressed in H9c2 cardiomyocytes, NRVMs and ARVMs, except for PP4C protein expression which was not detected in ARVMs. Similar results were obtained from the adult murine myocardium, where PP4C protein expression was not detectable by immunoblotting analysis. This novel data also revealed that the gene transcription profile and protein expression pattern of the type 2A protein phosphatase catalytic subunits were similar in H9c2 cardiomyocytes and NRVMs. Based on the data presented in the current study and data in the existing literature, the rat embryonic heart-derived H9c2 cell line can be an appropriate experimental model to investigate the type 2A protein phosphatase catalytic subunit-mediated regulation of functional protein involved in calcium regulation in cardiomyocytes.

Subsequent proteasome inhibition experiments in ARVMs revealed that PP4C expression might be at least partly regulated by the proteasome-mediated degradation mechanism, during heart development. This result seems to be of great importance as PP4C activity has been implicated in cell cycle re-entry in mammalian cells (Shaltiel et al., 2014). It is of great interest to me, to investigate whether overexpression of PP4C, in the adult heart of transgenic mice, promotes cell cycle

re-entry and cardiomyocyte regeneration, in the settings of myocardial infarction. In this case, enhancement of cardiac functional recovery following myocardial infarction, would provide strong evidence that PP4C could be a promising gene therapy candidate for myocardial infarction-associated LV pathological hypertrophy and heart failure.

In the present study, an efficient and well-characterised loss-of-function model based on RNAi was established in H9c2 cardiomyocytes. Novel data, presented in this thesis, demonstrated the regulation of L-type voltage-dependent Ca^{2+} channel $Ca_V1.2$-Ser1928 by the PP2ACα specifically, among the type 2A protein phosphatase catalytic subunits, at comparable levels with the existing literature. However, further experiments are required involving I_{CaL} measurement, to confirm the biological significance of this post-translational modification. Collectively, findings in this thesis consisted of the identification of PP2ACα, PP2ACβ and PP4C as regulators of PLM-Ser63 and PLM-Ser68 phosphorylation status. However, the data cannot rule out PP2AC (PP2ACα and PP2ACβ) and potential PP4C indirect dephosphorylation on PLM-Ser68 via protein phosphatase inhibitor-1-Thr35 dephosphorylation and subsequent PP1 inhibition. Future studies, focused on defining which phosphatase(s) may regulate the dephosphorylation status of protein phosphatase inhibitor-1-Thr35 and the direct measurement on $[Na^+]_i$ would provide more insights into this mechanism. Furthermore, since, PP4C was not present in the adult myocardium, it may play an important role in regulating the phosphorylation of PLM at an earlier stage of the heart development. The impaired activity of phosphatases and NKA function has been observed in patients with heart failure and has raised the importance of regulating NKA activity via potentially the therapeutic manipulation of PLM phosphorylation.

In this study, pathological LV hypertrophy was developed in a mouse model in

response to pressure overload stimulus. Most importantly, the data presented here, demonstrated changes in the expression of the type 2A protein phosphatase catalytic subunits, alpha4 protein, PP6 regulatory subunits and altered association of PP2AC and PP6C with alpha4 protein in murine hypertrophied LV tissue compared to the normal tissue. Here, the altered expression of the PP6 regulatory subunits and the differential association of the PP6C with alpha4 protein, as shown by co-immunoprecipitation experiments, strongly suggest that PP6 activity and targeting may be altered in cardiac health and disease. Evaluation of the subcellular localisation of the PP6 catalytic and regulatory subunits in H9c2 and primary adult cardiomyocytes, using confocal microscopy, would be important to define potential novel targets for PP6.

Initial results suggest that PP6C may not target γH2AX in cardiomyocytes. Findings in this thesis provided strong evidence of the regulatory and protective role of alpha4 towards the protein expression of type 2A protein phosphatase catalytic subunits in cardiomyocytes. Interestingly, alpha4 short-term knockdown (4 days), resulted in a significant loss of H2AX (and γH2AX) that may suggest delayed DNA repair. A more in-depth study of the consequences of this effect, in cardiomyocyte viability and pathophysiology, will require prolonged knockdown and/ or overexpression of alpha4 protein in cardiomyocytes.

References

Aberle, A.M., Tablin, F., Zhu, J., Walker, N.J., Gruenert, D.C. and Nantz, M.H., 1998. A novel tetraester construct that reduces cationic lipid-associated cytotoxicity. Implications for the onset of cytotoxicity. Biochemistry 37, 6533-40.

Ai, X., Jiang, A., Ke, Y., Solaro, R.J. and Pogwizd, S.M., 2011. Enhanced activation of p21-activated kinase 1 in heart failure contributes to dephosphorylation of connexin 43. Cardiovascular Research 92, 106-114.

Aleman, L.M., Doench, J. and Sharp, P.A., 2007. Comparison of siRNA-induced off-target RNA and protein effects. RNA 13, 385-95.

Alkass, K., Panula, J., Westman, M., Wu, T.-D., Guerquin-Kern, J.-L. and Bergmann, O., 2015. No evidence for cardiomyocyte number expansion in preadolescent mice. Cell 163, 1026-1036.

Amarzguioui, M., Holen, T., Babaie, E. and Prydz, H., 2003. Tolerance for mutations and chemical modifications in a siRNA. Nucleic Acids Research 31, 589-595.

Ameres, S.L., Martinez, J. and Schroeder, R., 2007. Molecular basis for target RNA recognition and cleavage by human RISC. Cell 130, 101-12.

Andegeko, Y., Moyal, L., Mittelman, L., Tsarfaty, I., Shiloh, Y. and Rotman, G., 2001. Nuclear retention of ATM at sites of DNA double strand breaks. Journal of Biological Chemistry 276, 38224-30.

Anderson, E.M., Birmingham, A., Baskerville, S., Reynolds, A., Maksimova, E., Leake, D., Fedorov, Y., Karpilow, J. and Khvorova, A., 2008. Experimental validation of the importance of seed complement frequency to siRNA specificity. RNA 14, 853-61.

Anderson, M.E., Higgins, L.S. and Schulman, H., 2006. Disease mechanisms and emerging therapies: protein kinases and their inhibitors in myocardial disease. Nature Clinical Practice Cardiovascular Medicine 3, 437-445.

Antos, C.L., Frey, N., Marx, S.O., Reiken, S., Gaburjakova, M., Richardson, J.A., Marks, A.R. and Olson, E.N., 2001. Dilated cardiomyopathy and sudden death resulting from constitutive activation of protein kinase A. Circulation Research 89, 997-1004.

Anversa, P., Leri, A., Kajstura, J. and Nadal-Ginard, B., 2002. Myocyte growth and cardiac repair. Journal of Molecular and Cellular Cardiology 34, 91-105.

Arai, M., Yoguchi, A., Iso, T., Takahashi, T., Imai, S., Murata, K. and Suzuki, T., 1995. Endothelin-1 and its binding sites are upregulated in pressure overload cardiac hypertrophy. American Journal of Physiology - Heart and Circulatory Physiology 268, H2084.

Arino, J., Woon, C.W., Brautigan, D.L., Miller, T.B., Jr. and Johnson, G.L., 1988. Human liver phosphatase 2A: cDNA and amino acid sequence of two catalytic subunit isotypes. Proceedings of the National Academy of Sciences of the United States of America 85, 4252-6.

Arndt, K.T., Styles, C.A. and Fink, G.R., 1989. A suppressor of a HIS4 transcriptional defect encodes a protein with homology to the catalytic subunit of phosphatases. Cell 56, 527-537.

Baartscheer, A., Schumacher, C.A., van Borren, M.M.G.J., Belterman, C.N.W., Coronel, R. and Fiolet, J.W.T., 2003. Increased Na^+/H^+-exchange activity is the cause of increased $[Na^+]i$ and underlies disturbed calcium handling in the rabbit pressure and volume overload heart failure model. Cardiovascular Research 57, 1015-1024.

Baba, S., Dun, W. and Boyden, P.A., 2004. Can PKA activators rescue Na^+ channel function in epicardial border zone cells that survive in the infarcted canine heart? Cardiovascular Research 64, 260-267.

Backs, J., Backs, T., Neef, S., Kreusser, M.M., Lehmann, L.H., Patrick, D.M., Grueter,

C.E., Qi, X., Richardson, J.A., Hill, J.A., Katus, H.A., Bassel-Duby, R., Maier, L.S. and Olson, E.N., 2009. The δ isoform of CaM kinase II is required for pathological cardiac hypertrophy and remodeling after pressure overload. Proceedings of the National Academy of Sciences of the United States of America 106, 2342-2347.

Baharians, Z. and Schonthal, A.H., 1998. Autoregulation of protein phosphatase type 2A expression. Journal of Biological Chemistry 273, 19019-24.

Balakumar, P. and Singh, M., 2006. The possible role of caspase-3 in pathological and physiological cardiac hypertrophy in rats. Basic & Clinical Pharmacology & Toxicology 99, 418-424.

Balijepalli, R.C., Foell, J.D., Hall, D.D., Hell, J.W. and Kamp, T.J., 2006. Localization of cardiac L-type Ca^{2+} channels to a caveolar macromolecular signaling complex is required for β(2)-adrenergic regulation. Proceedings of the National Academy of Sciences of the United States of America 103, 7500-7505.

Banerjee, I., Fuseler, J.W., Price, R.L., Borg, T.K. and Baudino, T.A., 2007. Determination of cell types and numbers during cardiac development in the neonatal and adult rat and mouse. American Journal of Physiology - Heart and Circulatory Physiology 293, H1883.

Bart, R., Chern, M., Park, C.J., Bartley, L. and Ronald, P.C., 2006. A novel system for gene silencing using siRNAs in rice leaf and stem-derived protoplasts. Plant Methods 2, 13.

Bartunek, J., Vanderheyden, M., Knaapen, M.W.M., Tack, W., Kockx, M.M. and Goethals, M., 2002. Deoxyribonucleic acid damage/repairproteins are elevated in the failing human myocardium due to idiopathic dilated cardiomyopathy. Journal of the American College of Cardiology 40, 1097-1103.

Basha, G., Novobrantseva, T.I., Rosin, N., Tam, Y.Y., Hafez, I.M., Wong, M.K., Sugo, T., Ruda, V.M., Qin, J., Klebanov, B., Ciufolini, M., Akinc, A., Tam, Y.K., Hope, M.J. and Cullis, P.R., 2011. Influence of cationic lipid composition on gene silencing properties of lipid nanoparticle formulations of siRNA in antigen-presenting cells. Molecular Therapy 19, 2186-200.

Bassing, C.H., Chua, K.F., Sekiguchi, J., Suh, H., Whitlow, S.R., Fleming, J.C., Monroe, B.C., Ciccone, D.N., Yan, C., Vlasakova, K., Livingston, D.M., Ferguson, D.O., Scully, R. and Alt, F.W., 2002. Increased ionizing radiation sensitivity and genomic instability in the absence of histone H2AX. Proceedings of the National Academy of Sciences of the United States of America 99, 8173-8178.

Bastians, H., Krebber, H., Hoheisel, J., Ohl, S., Lichter, P., Ponstingl, H. and Joos, S., 1997a. Assignment of the human serine/threonine protein phosphatase 4 gene (PPP4C) to chromosome 16p11-p12 by fluorescence in situ hybridization. Genomics 42, 181-2.

Bastians, H., Krebber, H., Vertrie, D., Hoheisel, J., Lichter, P., Ponstingl, H. and Joos, S., 1997b. Localization of the novel serine/threonine protein phosphatase 6 gene (*PPP6C*) to human chromosome Xq22.3. Genomics 41, 296-297.

Bastians, H. and Ponstingl, H., 1996. The novel human protein serine/threonine phosphatase 6 is a functional homologue of budding yeast Sit4p and fission yeast ppe1, which are involved in cell cycle regulation. Journal of Cell Science 109, 2865-74.

Baum, P., Fundel-Clemens, K., Kreuz, S., Kontermann, R.E., Weith, A., Mennerich, D. and Rippmann, J.F., 2010. Off-target analysis of control siRNA molecules reveals important differences in the cytokine profile and inflammation response of human fibroblasts. Oligonucleotides 20, 17-26.

Behr, T.M., Nerurkar, S.S., Nelson, A.H., Coatney, R.W., Woods, T.N., Sulpizio, A., Chandra, S., Brooks, D.P., Kumar, S., Lee, J.C., Ohlstein, E.H., Angermann, C.E., Adams, J.L., Sisko, J., Sackner-Bernstein, J.D. and Willette, R.N., 2001. Hypertensive end-organ damage and premature mortality are p38 mitogen-activated protein kinase–dependent in a rat model of cardiac hypertrophy and dysfunction. Circulation 104, 1292.

Belevych, A.E., Sansom, S.E., Terentyeva, R., Ho, H.-T., Nishijima, Y., Martin, M.M., Jindal, H.K., Rochira, J.A., Kunitomo, Y., Abdellatif, M., Carnes, C.A., Elton, T.S., Györke, S. and Terentyev, D., 2011. MicroRNA-1 and -133 increase arrhythmogenesis in heart failure by dissociating phosphatase activity from RyR2 complex. PLoS ONE 6, e28324.

Benoit, D.S. and Boutin, M.E., 2012. Controlling mesenchymal stem cell gene expression using polymer-mediated delivery of siRNA. Biomacromolecules 13, 3841-9.

Bensaad, K. and Vousden, K.H., 2005. Savior and slayer: the two faces of p53. Nature Medicine 11, 1278-1279.

Benson, D.A., Karsch-Mizrachi, I., Lipman, D.J., Ostell, J., Rapp, B.A. and Wheeler, D.L., 2000. GenBank. Nucleic Acids Research 28, 15-8.

Berg, J.M., Tymoczko, J.L., J. Gatto, J., Gregory and Stryer, L., 2015. Biochemistry, 8th ed. W. H. Freeman and Company, New York.

Bergmann, O., Bhardwaj, R.D., Bernard, S., Zdunek, S., Barnabé-Heider, F., Walsh, S., Zupicich, J., Alkass, K., Buchholz, B.A., Druid, H., Jovinge, S. and Frisén, J., 2009. Evidence for cardiomyocyte renewal in humans. Science 324, 98-102.

Bergmann, O., Zdunek, S., Felker, A., Salehpour, M., Alkass, K., Bernard, S., Sjostrom, S.L., Szewczykowska, M., Jackowska, T., Dos Remedios, C., Malm, T., Andra, M., Jashari, R., Nyengaard, J.R., Possnert, G., Jovinge, S., Druid, H. and Frisen, J., 2015. Dynamics of cell generation and turnover in the human heart. Cell 161, 1566-75.

Bernardo, B.C., Weeks, K.L., Pretorius, L. and McMullen, J.R., 2010. Molecular distinction between physiological and pathological cardiac hypertrophy: Experimental findings and therapeutic strategies. Pharmacology & Therapeutics 128, 191-227.

Bernstein, E., Caudy, A.A., Hammond, S.M. and Hannon, G.J., 2001. Role for a bidentate ribonuclease in the initiation step of RNA interference. Nature 409, 363-6.

Bers, D.M., 1997. Ca transport during contraction and relaxation in mammalian ventricular muscle. Basic Research in Cardiology 92, 1-10.

Bers, D.M., 2001. Excitation-contraction coupling and cardiac contractile force. Kluwer Academic Publishers, Dordrecht, Neth.

Bers, D.M., 2002. Cardiac excitation-contraction coupling. Nature 415, 198-205.

Bhatnagar, P., Wickramasinghe, K., Williams, J., Rayner, M. and Townsend, N., 2015. The epidemiology of cardiovascular disease in the UK 2014. Heart 101, 1182-9.

Birmingham, A., Anderson, E., Sullivan, K., Reynolds, A., Boese, Q., Leake, D., Karpilow, J. and Khvorova, A., 2007. A protocol for designing siRNAs with high functionality and specificity. Nature Protocols 2, 2068-78.

Birmingham, A., Anderson, E.M., Reynolds, A., Ilsley-Tyree, D., Leake, D., Fedorov, Y., Baskerville, S., Maksimova, E., Robinson, K., Karpilow, J., Marshall, W.S. and Khvorova, A., 2006. 3' UTR seed matches, but not overall identity, are associated with RNAi off-targets. Nature Methods 3, 199-204.

Blaich, A., Welling, A., Fischer, S., Wegener, J.W., Köstner, K., Hofmann, F. and Moosmang, S., 2010. Facilitation of murine cardiac L-type $Ca_V1.2$ channel is modulated by Calmodulin kinase II–dependent phosphorylation of S1512 and S1570. Proceedings of the National Academy of Sciences of the United States of America 107, 10285-10289.

Blechschmidt, S., Haufe, V., Benndorf, K. and Zimmer, T., 2008. Voltage-gated Na^+ channel transcript patterns in the mammalian heart are species-dependent. Progress in Biophysics and Molecular Biology 98, 309-318.

Blickwedehl, J., Agarwal, M., Seong, C., Pandita, R.K., Melendy, T., Sung, P., Pandita, T.K. and Bangia, N., 2008. Role for proteasome activator PA200 and postglutamyl proteasome activity in genomic stability. Proceedings of the National Academy of Sciences of the United States of America 105, 16165-16170.

Blitzer, R.D., Connor, J.H., Brown, G.P., Wong, T., Shenolikar, S., Iyengar, R. and Landau, E.M., 1998. Gating of CaMKII by cAMP-regulated protein phosphatase activity

during LTP. Science 280, 1940.
Bogoyevitch, M.A., Andreson, M.B., Gillespie-Brown, J., Clerk, A., Glennon, P.E., Fuller, S.J. and Sugden, P.H., 1996. Adrenergic receptor stimulation of the mitogen-activated protein kinase cascade and cardiac hypertrophy. Biochem J 314, 115-121.
Boguslavskyi, A., Pavlovic, D., Aughton, K., Clark, J.E., Howie, J., Fuller, W. and Shattock, M.J., 2014. Cardiac hypertrophy in mice expressing unphosphorylatable phospholemman. Cardiovascular Research 104, 72.
Bolcato-Bellemin, A.L., Bonnet, M.E., Creusat, G., Erbacher, P. and Behr, J.P., 2007. Sticky overhangs enhance siRNA-mediated gene silencing. Proceedings of the National Academy of Sciences of the United States of America 104, 16050-5.
Bonner, W.M., Redon, C.E., Dickey, J.S., Nakamura, A.J., Sedelnikova, O.A., Solier, S. and Pommier, Y., 2008. γH2AX and cancer. Nature Reviews. Cancer 8, 957-967.
Bossuyt, J., Ai, X., Moorman, J.R., Pogwizd, S.M. and Bers, D.M., 2005. Expression and Phosphorylation of the Na-Pump Regulatory Subunit Phospholemman in Heart Failure. Circulation Research 97, 558-565.
Bottega, R. and Epand, R.M., 1992. Inhibition of protein kinase C by cationic amphiphiles. Biochemistry 31, 9025-30.
Boyett, M.R., Inada, S., Yoo, S., Li, J., Liu, J., Tellez, J., Greener, I.D., Honjo, H., Billeter, R., Lei, M., Zhang, H., Efimov, I.R. and Dobrzynski, H., 2006. Connexins in the sinoatrial and atrioventricular nodes. Advances in Cardiology 42, 175-97.
Braten, O., Livneh, I., Ziv, T., Admon, A., Kehat, I., Caspi, L.H., Gonen, H., Bercovich, B., Godzik, A., Jahandideh, S., Jaroszewski, L., Sommer, T., Kwon, Y.T., Guharoy, M., Tompa, P. and Ciechanover, A., 2016. Numerous proteins with unique characteristics are degraded by the 26S proteasome following monoubiquitination. Proceedings of the National Academy of Sciences of the United States of America 113, E4639-47.
Brautigan, D.L., 2013. Protein Ser/Thr phosphatases – the ugly ducklings of cell signalling. FEBS Journal 280, 324-325.
Braz, J.C., Bueno, O.F., Liang, Q., Wilkins, B.J., Dai, Y.-S., Parsons, S., Braunwart, J., Glascock, B.J., Klevitsky, R., Kimball, T.F., Hewett, T.E. and Molkentin, J.D., 2003. Targeted inhibition of p38 MAPK promotes hypertrophic cardiomyopathy through upregulation of calcineurin-NFAT signaling. Journal of Clinical Investigation 111, 1475-1486.
Braz, J.C., Gregory, K., Pathak, A., Zhao, W., Sahin, B., Klevitsky, R., Kimball, T.F., Lorenz, J.N., Nairn, A.C., Liggett, S.B., Bodi, I., Wang, S., Schwartz, A., Lakatta, E.G., DePaoli-Roach, A.A., Robbins, J., Hewett, T.E., Bibb, J.A., Westfall, M.V., Kranias, E.G. and Molkentin, J.D., 2004. PKC-alpha regulates cardiac contractility and propensity toward heart failure. Nature Medicine 10, 248-254.
Brennan, J.P., Bardswell, S.C., Burgoyne, J.R., Fuller, W., Schröder, E., Wait, R., Begum, S., Kentish, J.C. and Eaton, P., 2006. Oxidant-induced activation of type I protein kinase A is mediated by RI subunit interprotein disulfide bond formation. Journal of Biological Chemistry 281, 21827-21836.
Brette, F., Sallé, L. and Orchard, C.H., 2004. Differential modulation of L-type Ca^{2+} current by SR Ca^{2+} release at the T-tubules and surface membrane of rat ventricular myocytes. Circulation Research 95, e1.
Brewis, N.D. and Cohen, P.T., 1992. Protein phosphatase X has been highly conserved during mammalian evolution. Biochimica et Biophysica Acta 1171, 231-3.
Brewis, N.D., Street, A.J., Prescott, A.R. and Cohen, P.T.W., 1993. PPX, a novel protein serine/threonine phosphatase localized to centrosomes. EMBO J 12, 987-996.
Brodde, O.E., 1991. β_1- and β_2-adrenoceptors in the human heart: Properties, function, and alterations in chronic heart failure. Pharmacological Reviews 43, 203-242.
Brown, D.W., Giles, W.H. and Croft, J.B., 2000. Left ventricular hypertrophy as a predictor of coronary heart disease mortality and the effect of hypertension. American Heart Journal 140, 848-856.

Buck, S.B., Hardouin, C., Ichikawa, S., Soenen, D.R., Gauss, C.M., Hwang, I., Swingle, M.R., Bonness, K.M., Honkanen, R.E. and Boger, D.L., 2003. Fundamental role of the fostriecin unsaturated lactone and implications for selective protein phosphatase inhibition. Journal of The American Chemical Society 125, 15694-5.

Bueno, O.F. and Molkentin, J.D., 2002. Involvement of Extracellular Signal-Regulated Kinases 1/2 in Cardiac Hypertrophy and Cell Death. Circulation Research 91, 776.

Bulteau, A.L., Lundberg, K.C., Humphries, K.M., Sadek, H.A., Szweda, P.A., Friguet, B. and Szweda, L.I., 2001. Oxidative modification and inactivation of the proteasome during coronary occlusion/reperfusion. Journal of Biochemistry 276, 30057-63.

Bundgaard, H. and Kjeldsen, K., 1996. Human myocardial Na,K-ATPase concentration in heart failure. Molecular and Cellular Biochemistry 163, 277-283.

Burgoyne, J.R., Madhani, M., Cuello, F., Charles, R.L., Brennan, J.P., Schröder, E., Browning, D.D. and Eaton, P., 2007. Cysteine redox sensor in PKGIa enables oxidant-induced activation. Science 317, 1393.

Bustin, S.A., Benes, V., Garson, J.A., Hellemans, J., Huggett, J., Kubista, M., Mueller, R., Nolan, T., Pfaffl, M.W., Shipley, G.L., Vandesompele, J. and Wittwer, C.T., 2009. The MIQE guidelines: minimum information for publication of quatitative real-time PCR experiments. Clinical Chemistry 55, 611-622.

Byrne, J.A., Grieve, D.J., Bendall, J.K., Li, J.-M., Gove, C., Lambeth, J.D., Cave, A.C. and Shah, A.M., 2003. Contrasting roles of NADPH oxidase isoforms in pressure-overload versus angiotensin II–induced cardiac hypertrophy. Circulation Research 93, 802.

Caffrey, D.R., Zhao, J., Song, Z., Schaffer, M.E., Haney, S.A., Subramanian, R.R., Seymour, A.B. and Hughes, J.D., 2011. siRNA off-target effects can be reduced at concentrations that match their individual potency. PLoS One 6, e21503.

Celeste, A., Petersen, S., Romanienko, P.J., Fernandez-Capetillo, O., Chen, H.T., Sedelnikova, O.A., Reina-San-Martin, B., Coppola, V., Meffre, E., Difilippantonio, M.J., Redon, C., Pilch, D.R., Olaru, A., Eckhaus, M., Camerini-Otero, R.D., Tessarollo, L., Livak, F., Manova, K., Bonner, W.M., Nussenzweig, M.C. and Nussenzweig, A., 2002. Genomic instability in mice lacking histone H2AX. Science 296, 922-927.

Chatterjee, S., Bavishi, C., Sardar, P., Agarwal, V., Krishnamoorthy, P., Grodzicki, T. and Messerli, F.H., 2014. Meta-analysis of left ventricular hypertrophy and sustained arrhythmias. American Journal of Cardiology 114, 1049-1052.

Chau, V., Tobias, J.W., Bachmair, A., Marriott, D., Ecker, D.J., Gonda, D.K. and Varshavsky, A., 1989. A multiubiquitin chain is confined to specific lysine in a targeted short-lived protein. Science 243, 1576-83.

Chen-Izu, Y., Xiao, R.P., Izu, L.T., Cheng, H., Kuschel, M., Spurgeon, H. and Lakatta, E.G., 2000. G(i)-dependent localization of beta(2)-adrenergic receptor signaling to L-type Ca^{2+} channels. Biophysical Journal 79, 2547-2556.

Chen, G.I., Tisayakorn, S., Jorgensen, C., D'Ambrosio, L.M., Goudreault, M. and Gingras, A.-C., 2008a. PPR4/KIAA1622 forms a novel stable cytosolic complex with phosphoprotein phosphatase 4. Journal of Biological Chemistry 283, 29273-29284.

Chen, H.W., Chien, C.T., Yu, S.L., Lee, Y.T. and Chen, W.J., 2002. Cyclosporine A regulate oxidative stress-induced apoptosis in cardiomyocytes: mechanisms via ROS generation, iNOS and Hsp70. British Journal of Pharmacology 137, 771-781.

Chen, J., Martin, B.L. and Brautigan, D.L., 1992. Regulation of protein serine-threonine phosphatase type-2A by tyrosine phosphorylation. Science 257, 1261-1264.

Chen, J., Peterson, R.T. and Schreiber, S.L., 1998. α4 associates with protein phosphatase 2A, 4, and 6. Biochemical and Biophysical Research Communications 247, 827-832.

Chen, L.P., Lai, Y.D., Li, D.C., Zhu, X.N., Yang, P., Li, W.X., Zhu, W., Zhao, J., Li, X.D., Xiao, Y.M., Zhang, Y., Xing, X.M., Wang, Q., Zhang, B., Lin, Y.C., Zeng, J.L., Zhang, S.X., Liu, C.X., Li, Z.F., Zeng, X.W., Lin, Z.N., Zhuang, Z.X. and Chen,

W., 2011. Alpha4 is highly expressed in carcinogen-transformed human cells and primary human cancers. Oncogene 30, 2943-2953.

Chen, P.Y., Weinmann, L., Gaidatzis, D., Pei, Y., Zavolan, M., Tuschl, T. and Meister, G., 2008b. Strand-specific 5'-O-methylation of siRNA duplexes controls guide strand selection and targeting specificity. RNA 14, 263-74.

Cho, U.S. and Xu, W., 2007. Crystal structure of a protein phosphatase 2A heterotrimeric holoenzyme. Nature 445, 53-57.

Choukroun, G., Hajjar, R., Fry, S., Del Monte, F., Haq, S., Guerrero, J.L., Picard, M., Rosenzwig, A. and Force, T., 1999. Regulation of cardiac hypertrophy in vivo by the stress-activated protein kinases/c-Jun NH_2-terminal kinases. Journal of Clinical Investigation 104, 391-398.

Chowdhury, D., Keogh, M.-C., Ishii, H., Peterson, C.L., Buratowski, S. and Lieberman, J., 2005. H2AX dephosphorylation by protein phosphatase 2A facilitates DNA double-strand break repair. Molecular Cell 20, 801-809.

Chowdhury, D., Xu, X., Zhong, X., Ahmed, F., Zhong, J., Liao, J., Dykxhoorn, D.M., Weinstock, D.M., Pfeifer, G.P. and Lieberman, J., 2008. A PP4-phosphatase complex dephosphorylates γ-H2AX generated during DNA replication. Molecular Cell 31, 33-46.

Christ, T., Boknik, P., Wöhrl, S., Wettwer, E., Graf, E.M., Bosch, R.F., Knaut, M., Schmitz, W., Ravens, U. and Dobrev, D., 2004. L-type Ca^{2+} current downregulation in chronic human atrial fibrillation is associated with increased activity of protein phosphatases. Circulation 110, 2651.

Christophorou, M.A., Ringshausen, I., Finch, A.J., Swigart, L.B. and Evan, G.I., 2006. The pathological response to DNA damage does not contribute to p53-mediated tumour suppression. Nature 443, 214-217.

Cleaver, O. and Krieg, P.A., 2010. Vascular development, Heart Development and Regeneration. Academic Press, Boston, pp. 487-488.

Cohen, G., Heikkila, R.E. and MacNamee, W.t.t.a.o.D., 1974. The generation of hydrogen peroxide, superoxide radical, and hydroxyl radical by 6-hydroxydopamine, dialuric acid, and related cytotoxic agents. Journal of Biological Chemistry 249, 2447-2452.

Cohen, P.T., Brewis, N.D., Hughes, V. and Mann, D.J., 1990. Protein serine/threonine phosphatases; an expanding family. FEBS Letters 268, 355-9.

Cohen, P.T.W., 2002. Protein phosphatase 1 – targeted in many directions. Journal of Cell Science 115, 241.

Cohen, P.T.W., 2004. Overview of protein serine/threonine phosphatases, in: Ariño, J.n. and Alexander, D.R. (Eds.), Protein Phosphatases. Springer Berlin Heidelberg, Berlin, Heidelberg, pp. 1-20.

Communal, C., Singh, K., Pimentel, D.R. and Colucci, W.S., 1998. Norepinephrine stimulates apoptosis in adult rat ventricular myocytes by activation of the β-adrenergic pathway. Circulation 98, 1329-1334.

Cros, C. and Brette, F., 2013. Functional subcellular distribution of β1- and β2-adrenergic receptors in rat ventricular cardiac myocytes. Physiological Reports 1, e00038.

Cuddington, B.P., Verschoor, M., Ashkar, A. and Mossman, K.L., 2015. Enhanced efficacy with azacytidine and oncolytic BHV-1 in a tolerized cotton rat model of breast adenocarcinoma. Molecular Therapy Oncolytics 2, 15004.

Cutilletta, A.F., Dowell, R.T., Rudnik, M., Arcilla, R.A. and Zak, R., 1975. Regression of myocardial hypertrophy I. Experimental model, changes in heart weight, nucleic acids and collagen. Journal of Molecular and Cellular Cardiology 7, 767-781.

D'Haene, B., Vandesompele, J. and Hellemans, J., 2010. Accurate and objective copy number profiling using real-time quantitative PCR. Methods 50, 262-70.

da Fonseca, P.C., He, J. and Morris, E.P., 2012. Molecular model of the human 26S proteasome. Molecular Cell 46, 54-66.

Dahlmann, B., 2016. Mammalian proteasome subtypes: Their diversity in structure and function. Archives of Biochemistry and Biophysics 591, 132-140.

Davare, M.A., Avdonin, V., Hall, D.D., Peden, E.M., Burette, A., Weinberg, R.J., Horne, M.C., Hoshi, T. and Hell, J.W., 2001. A β2 adrenergic receptor signaling complex assembled with the Ca^{2+} channel $Ca_V1.2$. Science 293, 98-101.

Davies, K.J.A., 2001. Degradation of oxidized proteins by the 20S proteasome. Biochimie 83, 301-310.

De Arcangelis, V., Soto, D. and Xiang, Y., 2008. Phosphodiesterase 4 and phosphatase 2A differentially regulate cAMP/protein kinase A signaling for cardiac myocyte contraction under stimulation of β(1) adrenergic receptor. Molecular Pharmacology 74, 1453-1462.

de Simone, G., Gottdiener, J.S., Chinali, M. and Maurer, M.S., 2008. Left ventricular mass predicts heart failure not related to previous myocardial infarction: the Cardiovascular Health Study. European Heart Journal 29, 741.

Dean, D.A., Urban, G., Aragon, I.V., Swingle, M., Miller, B., Rusconi, S., Bueno, M., Dean, N.M. and Honkanen, R.E., 2001. Serine / threonine protein phosphatase 5 (PP5) participates in the regulation of glucocorticoid receptor nucleocytoplasmic shuttling. BMC Cell Biology 2, 6.

Defer, N., Best-Belpomme, M. and Hanoune, J., 2000. Tissue specificity and physiological relevance of various isoforms of adenylyl cyclase. American Journal of Physiology - Renal Physiology 279, F400-16.

DeGrande, S.T., Little, S.C., Nixon, D.J., Wright, P., Snyder, J., Dun, W., Murphy, N., Kilic, A., Higgins, R., Binkley, P.F., Boyden, P.A., Carnes, C.A., Anderson, M.E., Hund, T.J. and Mohler, P.J., 2013. Molecular mechanisms underlying cardiac protein phosphatase 2A regulation in heart. Journal of Biological Chemistry 288, 1032-46.

Deng, L., Wang, C., Spencer, E., Yang, L., Braun, A., You, J., Slaughter, C., Pickart, C. and Chen, Z.J., 2000. Activation of the IkappaB kinase complex by TRAF6 requires a dimeric ubiquitin-conjugating enzyme complex and a unique polyubiquitin chain. Cell 103, 351-61.

Depre, C., Wang, Q., Yan, L., Hedhli, N., Peter, P., Chen, L., Hong, C., Hittinger, L., Ghaleh, B., Sadoshima, J., Vatner, D.E., Vatner, S.F. and Madura, K., 2006. Activation of the cardiac proteasome during pressure overload promotes ventricular hypertrophy. Circulation 114, 1821-8.

Despa, S., Islam, M.A., Weber, C.R., Pogwizd, S.M. and Bers, D.M., 2002. Intracellular Na^+ concentration is elevated in heart failure but Na/K pump function is unchanged. Circulation 105, 2543-2548.

Despa, S., Tucker, A.L. and Bers, D.M., 2008. Phospholemman-mediated activation of Na/K-ATPase Limits [Na](i) and inotropic state during β-adrenergic stimulation in mouse ventricular myocytes. Circulation 117, 1849-1855.

Di Como, C.J. and Arndt, K.T., 1996. Nutrients, via the Tor proteins, stimulate the association of Tap42 with type 2A phosphatases. Genes Dev 10, 1904-16.

Diviani, D., Dodge-Kafka, K.L., Li, J. and Kapiloff, M.S., 2011. A-kinase anchoring proteins: scaffolding proteins in the heart. American Journal of Physiology - Heart and Circulatory Physiology 301, H1742-H1753.

Dong, D., Li, L., Gu, P., Jin, T., Wen, M., Yuan, C., Gao, X., Liu, C. and Zhang, Z., 2015. Profiling metabolic remodeling in PP2Acalpha deficiency and chronic pressure overload mouse hearts. FEBS Letters 589, 3631-9.

Douglas, P., Zhong, J., Ye, R., Moorhead, G.B.G., Xu, X. and Lees-Miller, S.P., 2010. Protein phosphatase 6 interacts with the DNA-dependent protein kinase catalytic subunit and dephosphorylates γ-H2AX. Molecular and Cellular Biology 30, 1368-1381.

Drazner, M.H., Rame, J.E., Marino, E.K., Gottdiener, J.S., Kitzman, D.W., Gardin, J.M., Manolio, T.A., Dries, D.L. and Siscovick, D.S., 2004. Increased left ventricular mass is a risk factor for the development of a depressed left ventricular ejection fraction within five years: The Cardiovascular Health Study. Journal of the

American College of Cardiology 43, 2207-2215.

Driessens, N., Versteyhe, S., Ghaddhab, C., Burniat, A., De Deken, X., Van Sande, J., Dumont, J.-E., Miot, F. and Corvilain, B., 2009. Hydrogen peroxide induces DNA single- and double-strand breaks in thyroid cells and is therefore a potential mutagen for this organ. Endocrine-Related Cancer 16, 845-856.

Dröse, S., Hanley, P.J. and Brandt, U., 2009. Ambivalent effects of diazoxide on mitochondrial ROS production at respiratory chain complexes I and III. Biochimica et biophysica acta 1790, 558-565.

Dunlay, S.M., Weston, S.A., Jacobsen, S.J. and Roger, V.L., 2009. Risk Factors for Heart Failure: A Population-Based Case-Control Study. The American journal of medicine 122, 1023-1028.

East, M.A., Jollis, J.G., Nelson, C.L., Marks, D. and Peterson, E.D., 2003. The influence of left ventricular hypertrophyon survival in patients with coronaryartery disease: do race and gender matter? Journal of the American College of Cardiology 41, 949-954.

Eghbali, M., Deva, R., Alioua, A., Minosyan, T.Y., Ruan, H., Wang, Y., Toro, L. and Stefani, E., 2005. Molecular and functional signature of heart hypertrophy during pregnancy. Circulation Research 96, 1208.

El-Armouche, A., Bednorz, A., Pamminger, T., Ditz, D., Didié, M., Dobrev, D. and Eschenhagen, T., 2006a. Role of calcineurin and protein phosphatase-2A in the regulation of phosphatase inhibitor-1 in cardiac myocytes. Biochemical and Biophysical Research Communications 346, 700-706.

El-Armouche, A., Boknik, P., Eschenhagen, T., Carrier, L., Knaut, M., Ravens, U. and Dobrev, D., 2006b. Molecular determinants of altered Ca^{2+} handling in human chronic atrial fibrillation. Circulation 114, 670.

El-Armouche, A. and Eschenhagen, T., 2008. β-Adrenergic stimulation and myocardial function in the failing heart. Heart Failure Reviews 14, 225.

El-Armouche, A., Rau, T., Zolk, O., Ditz, D., Pamminger, T., Zimmermann, W.-H., Jackal, E., Harding, S.E., Boknik, P., Neumann, J. and Eschenhagen, T., 2003. Evidence for protein phosphatase inhibitor-1 playing an amplifier role in β-adrenergic signaling in cardiac myocytes. The FASEB Journal 17, 437-439.

El-Armouche, A., Wittköpper, K., Fuller, W., Howie, J., Shattock, M.J. and Pavlovic, D., 2011. Phospholemman-dependent regulation of the cardiac Na/K-ATPase activity is modulated by inhibitor-1 sensitive type-1 phosphatase. FASEB Journal 25, 4467-4475.

El-Khodor, B.F., Kholodilov, N.G., Yarygina, O. and Burke, R.E., 2001. The expression of mRNAs for the proteasome complex is developmentally regulated in the rat mesencephalon. Developmental Brain Research 129, 47-56.

Elbashir, S.M., Harborth, J., Lendeckel, W., Yalcin, A., Weber, K. and Tuschl, T., 2001b. Duplexes of 21-nucleotide RNAs mediate RNA interference in cultured mammalian cells. Nature 411, 494-8.

Elbashir, S.M., Lendeckel, W. and Tuschl, T., 2001a. RNA interference is mediated by 21- and 22-nucleotide RNAs. Genes & Development 15, 188-200.

Elbashir, S.M., Martinez, J., Patkaniowska, A., Lendeckel, W. and Tuschl, T., 2001c. Functional anatomy of siRNAs for mediating efficient RNAi in *Drosophila melanogaster* embryo lysate. EMBO Journal 20, 6877-6888.

Ellison, G.M., Vicinanza, C., Smith, A.J., Aquila, I., Leone, A., Waring, C.D., Henning, B.J., Stirparo, G.G., Papait, R., Scarfo, M., Agosti, V., Viglietto, G., Condorelli, G., Indolfi, C., Ottolenghi, S., Torella, D. and Nadal-Ginard, B., 2013. Adult c-kit(pos) cardiac stem cells are necessary and sufficient for functional cardiac regeneration and repair. Cell 154, 827-42.

Erickson, J.R., Joiner, M.-l.A., Guan, X., Kutschke, W., Yang, J., Oddis, C.V., Bartlett, R.K., Lowe, J.S., O'Donnell, S., Aykin-Burns, N., Zimmerman, M.C., Zimmerman, K., Ham, A.-J.L., Weiss, R.M., Spitz, D.R., Shea, M.A., Colbran, R.J., Mohler, P.J.

and Anderson, M.E., 2008. A dynamic pathway for calcium-independent activation of CaMKII by methionine oxidation. Cell 133, 462-474.

Eytan, E., Ganoth, D., Armon, T. and Hershko, A., 1989a. ATP-dependent incorporation of 20S protease into the 26S complex that degrades proteins conjugated to ubiquitin. Proceedings of the National Academy of Sciences of the United States of America 86, 7751-7755.

Eytan, E., Ganoth, D., Armon, T. and Hershko, A., 1989b. ATP-dependent incorporation of 20S protease into the 26S complex that degrades proteins conjugated to ubiquitin. Proceedings of the National Academy of Sciences of the United States of America 86, 7751-5.

Falck, J., Coates, J. and Jackson, S.P., 2005. Conserved modes of recruitment of ATM, ATR and DNA-PKcs to sites of DNA damage. Nature 434, 605-11.

Fan, J.H., Hung, W.I., Li, W.T. and Yeh, J.M., 2009. Biocompatibility study of gold nanoparticles to human cells, in: Lim, C.T. and Goh, J.C.H. (Eds.), 13th International Conference on Biomedical Engineering: ICBME 2008 3–6 December 2008 Singapore. Springer Berlin Heidelberg, Berlin, Heidelberg, pp. 870-873.

Favre, B., Zolnierowicz, S., Turowski, P. and Hemmings, B.A., 1994. The catalytic subunit of protein phosphatase 2A is carboxyl-methylated *in vivo*. Journal of Biological Chemistry 269, 16311-16317.

Felgner, J.H., Kumar, R., Sridhar, C.N., Wheeler, C.J., Tsai, Y.J., Border, R., Ramsey, P., Martin, M. and Felgner, P.L., 1994. Enhanced gene delivery and mechanism studies with a novel series of cationic lipid formulations. Journal of Biological Chemistry 269, 2550-61.

Fernandez-Capetillo, O., Chen, H.-T., Celeste, A., Ward, I., Romanienko, P.J., Morales, J.C., Naka, K., Xia, Z., Camerini-Otero, R.D., Motoyama, N., Carpenter, P.B., Bonner, W.M., Chen, J. and Nussenzweig, A., 2002. DNA damage-induced G2-M checkpoint activation by histone H2AX and 53BP1. Nature Cell Biology 4, 993-997.

Fire, A., Xu, S., Montgomery, M.K., Kostas, S.A., Driver, S.E. and Mello, C.C., 1998. Potent and specific genetic interference by double-stranded RNA in *Caenorhabditis elegans*. Nature 391, 806-11.

Fleige, S. and Pfaffl, M.W., 2006. RNA integrity and the effect on the real-time qRT-PCR performance. Molecular Aspects of Medicine 27, 126-139.

Frenneaux, M.P., 2004. Assessing the risk of sudden cardiac death in a patient with hypertrophic cardiomyopathy. Heart 90, 570-575.

Fuchs, S.Y., Fried, V.A. and Ronai, Z., 1998. Stress-activated kinases regulate protein stability. Oncogene 17, 1483-90.

Fuller, W., Howie, J., McLatchie, L.M., Weber, R.J., Hastie, C.J., Burness, K., Pavlovic, D. and Shattock, M.J., 2009. FXYD1 phosphorylation in vitro and in adult rat cardiac myocytes: threonine 69 is a novel substrate for protein kinase C. American Journal of Physiology - Cell Physiology 296, C1346.

Fuller, W., Tulloch, L.B., Shattock, M.J., Calaghan, S.C., Howie, J. and Wypijewski, K.J., 2013. Regulation of the cardiac sodium pump. Cellular and Molecular Life Sciences 70, 1357-1380.

Fulton, R.M., Hutchinson, E.C. and Jones, A.M., 1952. Ventricular weight in cardiac hypertrophy. British Heart Journal 14, 413-420.

Ganesan, A.N., Maack, C., Johns, D.C., Sidor, A. and O'Rourke, B., 2006. β-adrenergic stimulation of L-type Ca^{2+} channels in cardiac myocytes requires the distal carboxyl terminus of α1C but not serine 1928. Circulation Research 98, e11-e18.

Gao, H. and Hui, K.M., 2001. Synthesis of a novel series of cationic lipids that can act as efficient gene delivery vehicles through systematic heterocyclic substitution of cholesterol derivatives. Gene Therapy 8, 855-63.

Gao, T., Yatanio, A., Dell'Acqua, M.L., Sako, H., Green, S.A., Dascal, N., Scott, J.D. and Hosey, M.M., 1997. cAMP-dependent regulation of cardiac L-type Ca^{2+} channels

requires membrane targeting of PKA and phosphorylation of channel subunits. Neuron 18, 185-196.

Gerber, Y., Weston, S.A., Redfield, M.M., Chamberlain, A.M., Manemann, S.M., Jiang, R., Killian, J.M. and Roger, V.L., 2015. A contemporary appraisal of the heart failure epidemic in Olmsted County, Minnesota, 2000 to 2010. JAMA Internal Medicine 175, 996-1004.

Gergs, U., Boknik, P., Buchwalow, I., Fabritz, L., Matus, M., Justus, I., Hanske, G., Schmitz, W. and Neumann, J., 2004. Overexpression of the catalytic subunit of protein phosphatase 2A impairs cardiac function. Journal of Biological Chemistry 279, 40827-34.

Gilleron, J., Querbes, W., Zeigerer, A., Borodovsky, A., Marsico, G., Schubert, U., Manygoats, K., Seifert, S., Andree, C., Stoter, M., Epstein-Barash, H., Zhang, L., Koteliansky, V., Fitzgerald, K., Fava, E., Bickle, M., Kalaidzidis, Y., Akinc, A., Maier, M. and Zerial, M., 2013. Image-based analysis of lipid nanoparticle-mediated siRNA delivery, intracellular trafficking and endosomal escape. Nature Biotechnology 31, 638-46.

Gingras, A.-C., Caballero, M., Zarske, M., Sanchez, A., Hazbun, T.R., Fields, S., Sonenberg, N., Hafen, E., Raught, B. and Aebersold, R., 2005. A novel evolutionary conserved protein phosphatase complex involved in cisplatin sensitivity. Mol Cell Prot 4, 1725-1740.

Giudicessi, J.R. and Ackerman, M.J., 2012. Potassium-channel mutations and cardiac arrhythmias[mdash]diagnosis and therapy. Nature Reviews Cardiology 9, 319-332.

Gopalakrishna, R. and Anderson, W.B., 1989. Ca^{2+}- and phospholipid-independent activation of protein kinase C by selective oxidative modification of the regulatory domain. Proceedings of the National Academy of Sciences of the United States of America 86, 6758-6762.

Gradman, A.H. and Alfayoumi, F., 2006. From left ventricular hypertrophy to congestive heart failure: management of hypertensive heart disease. Progress in Cardiovascular Diseases 48, 326-341.

Green, D.D., Yang, S.I. and Mumby, M.C., 1987. Molecular cloning and sequence analysis of the catalytic subunit of bovine type 2A protein phosphatase. Proceedings of the National Academy of Sciences (USA) 84, 4880-4884.

Grieve, D.J., Byrne, J.A., Siva, A., Layland, J., Johar, S., Cave, A.C. and Shah, A.M., 2006. Involvement of the nicotinamide adenosine dinucleotide phosphate oxidase isoform Nox2 in cardiac contractile dysfunction occurring in response to pressure overload. Journal of the American College of Cardiology 47, 817-826.

Griffiths, E.J., Balaska, D. and Cheng, W.H.Y., 2010. The ups and downs of mitochondrial calcium signalling in the heart. Biochimica et Biophysica Acta (BBA) - Bioenergetics 1797, 856-864.

Grossman, W., Jones, D. and McLaurin, L.P., 1975. Wall stress and patterns of hypertrophy in the human left ventricle. Journal of Clinical Investigation 56, 56-64.

Gruosso, T., Mieulet, V., Cardon, M., Bourachot, B., Kieffer, Y., Devun, F., Dubois, T., Dutreix, M., Vincent-Salomon, A., Miller, K.M. and Mechta-Grigoriou, F., 2016. Chronic oxidative stress promotes H2AX protein degradation and enhances chemosensitivity in breast cancer patients. EMBO Molecular Medicine 8, 527.

Guergnon, J., Derewenda, U., Edelson, J.R. and Brautigan, D.L., 2009. Mapping of protein phosphatase-6 association with its SAPS domain regulatory subunit using a model of helical repeats. BMC Biochemistry 10, 24.

Guha, K. and McDonagh, T., 2013. Heart Failure Epidemiology: European Perspective. Current Cardiology Reviews 9, 123-127.

Gujrati, M., Malamas, A., Shin, T., Jin, E., Sun, Y. and Lu, Z.R., 2014. Multifunctional cationic lipid-based nanoparticles facilitate endosomal escape and reduction-triggered cytosolic siRNA release. Molecular Pharmaceutics 11, 2734-44.

Guo, L., Lobenhofer, E.K., Wang, C., Shippy, R., Harris, S.C., Zhang, L., Mei, N., Chen,

T., Herman, D., Goodsaid, F.M., Hurban, P., Phillips, K.L., Xu, J., Deng, X., Sun, Y.A., Tong, W., Dragan, Y.P. and Shi, L., 2006. Rat toxicogenomic study reveals analytical consistency across microarray platforms. Nature Biotechnology 24, 1162-9.

Gupta, S., Barrett, T., Whitmarsh, A.J., Cavanagh, J., Sluss, H.K., Dérijard, B. and Davis, R.J., 1996. Selective interaction of JNK protein kinase isoforms with transcription factors. EMBO Journal 15, 2760-2770.

Haber, F. and Weiss, J., 1934. The catalytic decomposition of hydrogen peroxide by iron salts. Proceedings of the Royal Society of London. Series A - Mathematical and Physical Sciences 147, 332.

Hall, D.D., Feekes, J.A., Arachchige Don, A.S., Shi, M., Hamid, J., Chen, L., Strack, S., Zamponi, G.W., Horne, M.C. and Hell, J.W., 2006. Binding of protein phosphatase 2A to the L-type Calcium channel $Ca_V1.2$ next to Ser1928, its main PKA site, is critical for Ser1928 dephosphorylation. Biochemistry 45, 3448-3459.

Hall, T.A., 1999. BioEdit: a user-friendly biological sequence alignment editor and analysis program for Windows 95/98/NT. Nucleic Acids Symposium Series 41, 95-98.

Hamdani, N., Bishu, K.G., von Frieling-Salewsky, M., Redfield, M.M. and Linke, W.A., 2013. Deranged myofilament phosphorylation and function in experimental heart failure with preserved ejection fraction. Cardiovascular Research 97, 464-71.

Hamilton, A.J. and Baulcombe, D.C., 1999. A species of small antisense RNA in posttranscriptional gene silencing in plants. Science 286, 950-2.

Hammond, S.M., Bernstein, E., Beach, D. and Hannon, G.J., 2000. An RNA-directed nuclease mediates post-transcriptional gene silencing in Drosophila cells. Nature 404, 293-6.

Han, F., Bossuyt, J., Despa, S., Tucker, A.L. and Bers, D.M., 2006. Phospholemman phosphorylation mediates the protein kinase C-dependent effects on Na/K pump function in cardiac myocytes. Circulation Research 99, 1376.

Hangartner, J.R.W., Marley, N.J., Whitehead, A., Thomas, A.C. and Davies, M.J., 1985. The assessment of cardiac hypertrophy at autopsy. Histopathology 9, 1295-1306.

Harris, I.S., Zhang, S., Treskov, I., Kovacs, A., Weinheimer, C. and Muslin, A.J., 2004. Raf-1 kinase is required for cardiac hypertrophy and cardiomyocyte survival in response to pressure overload. Circulation 110, 718.

Harvey, R.D. and Hell, J.W., 2013. $Ca_V1.2$ signaling complexes in the heart. Journal of Molecular and Cellular Cardiology 58, 143-152.

Hastie, C.J., Carnegie, G.K., Morrice, N. and Cohen, P.T.W., 2000. A novel 50 kDa protein forms complexes with protein phosphatase 4 and is located at centrosomal microtube organizing centres. Biochemical Journal 347, 845-855.

Hastie, C.J. and Cohen, P.T., 1998. Purification of protein phosphatase 4 catalytic subunit: inhibition by the antitumour drug fostriecin and other tumour suppressors and promoters. FEBS Letters 431, 357-61.

Hastie, C.J., Vazquez-Martin, C., Philp, A., Stark, M.J.R. and Cohen, P.T.W., 2006. The *Saccharomyces cerevisiae* orthologue of the human protein phosphatase 4 core regulatory subunit R2 confers resistance to the anticancer drug cisplatin. FEBS Journal 273, 3322-3334.

Havranek, E.P., Froshaug, D.B., Emserman, C.D.B., Hanratty, R., Krantz, M.J., Masoudi, F.A., Dickinson, L. and Steiner, J.F., 2008. Left ventricular hypertrophy and cardiovascular mortality by race and ethnicity. The American journal of medicine 121, 870-875.

Hazard, A.L., Kohout, S.C., Stricker, N.L., Putkey, J.A. and Falke, J.J., 1998. The kinetic cycle of cardiac troponin C: calcium binding and dissociation at site II trigger slow conformational rearrangements. Protein Science 7, 2451-2459.

Heijman, J., Dewenter, M., El-Armouche, A. and Dobrev, D., 2013. Function and regulation of serine/threonine phosphatases in the healthy and diseased heart. Journal of Molecular and Cellular Cardiology 64, 90-98.

Hein, S., Arnon, E., Kostin, S., Schönburg, M., Elsässer, A., Polyakova, V., Bauer, E.P., Klövekorn, W.-P. and Schaper, J., 2003. Progression From Compensated Hypertrophy to Failure in the Pressure-Overloaded Human Heart. Circulation 107, 984.

Heineke, J. and Molkentin, J.D., 2006. Regulation of cardiac hypertrophy by intracellular signalling pathways. Nature Reviews Molecular Cell Biology 7, 589-600.

Hellemans, J., Mortier, G., De Paepe, A., Speleman, F. and Vandesompele, J., 2007. qBase relative quantification framework and software for management and automated analysis of real-time quantitative PCR data. Genome Biology 8, R19.

Helps, N.R., Brewis, N.D., Lineruth, K., Davis, T., Kaiser, K. and Cohen, P.T., 1998. Protein phosphatase 4 is an essential enzyme required for organisation of microtubules at centrosomes in Drosophila embryos. Journal of Cell Science 111, 1331-40.

Hemmings, B.A., Adams-Pearson, C., Maurer, F., Muller, P., Goris, J., Merlevde, W., Hofsteenge, J. and Stone, S.R., 1990. α- and β-forms of the 65-kDa subunit of protein phosphatase 2A have a similar 39 amino acid repeating structure. Biochemistry 29, 3166-3173.

Herrmann, J., Gulati, R., Napoli, C., Woodrum, J.E., Lerman, L.O., Rodriguez-Porcel, M., Sica, V., Simari, R.D., Ciechanover, A. and Lerman, A., 2003. Oxidative stress-related increase in ubiquitination in early coronary atherogenesis. FASEB Journal.

Hershko, A., Heller, H., Elias, S. and Ciechanover, A., 1983. Components of ubiquitin-protein ligase system. Resolution, affinity purification, and role in protein breakdown. Journal of Biochemistry 258, 8206-14.

Heymes, C., Bendall, J.K., Ratajczak, P., Cave, A.C., Samuel, J.-L., Hasenfuss, G. and Shah, A.M., 2003. Increased myocardial NADPH oxidase activity in human heart failure. Journal of the American College of Cardiology 41, 2164-2171.

Hill, M.F. and Singal, P.K., 1996. Antioxidant and oxidative stress changes during heart failure subsequent to myocardial infarction in rats. The American Journal of Pathology 148, 291-300.

Hoege, C., Pfander, B., Moldovan, G.L., Pyrowolakis, G. and Jentsch, S., 2002. RAD6-dependent DNA repair is linked to modification of PCNA by ubiquitin and SUMO. Nature 419, 135-41.

Hoehn, M., Zhang, Y., Xu, J., Gergs, U., Boknik, P., Werdan, K., Neumann, J. and Ebelt, H., 2015. Overexpression of protein phosphatase 2A in a murine model of chronic myocardial infarction leads to increased adverse remodeling but restores the regulation of β-catenin by glycogen synthase kinase 3β. International Journal of Cardiology 183, 39-46.

Holen, T., Amarzguioui, M., Wiiger, M.T., Babaie, E. and Prydz, H., 2002. Positional effects of short interfering RNAs targeting the human coagulation trigger Tissue Factor. Nucleic Acids Research 30, 1757-1766.

Hong, T.-T., Smyth, J.W., Chu, K.Y., Vogan, J.M., Fong, T.S., Jensen, B.C., Fang, K., Halushka, M.K., Russell, S.D., Colecraft, H., Hoopes, C.W., Ocorr, K., Chi, N.C. and Shaw, R.M., 2012. BIN1 is reduced and $Ca_V1.2$ trafficking is impaired in human failing cardiomyocytes. Heart Rhythm 9, 812-820.

Hornung, V., Guenthner-Biller, M., Bourquin, C., Ablasser, A., Schlee, M., Uematsu, S., Noronha, A., Manoharan, M., Akira, S., de Fougerolles, A., Endres, S. and Hartmann, G., 2005. Sequence-specific potent induction of IFN-alpha by short interfering RNA in plasmacytoid dendritic cells through TLR7. Nature Medicine 11, 263-70.

Hosing, A.S., Valerie, N.C.K., Dziegielewski, J., Brautigan, D.L. and Larner, J.M., 2012. PP6 regulatory subunit R1 is bidentate anchor for targeting protein phosphatase-6 to DNA-dependent protein kinase. Journal of Biological Chemistry 287, 9230-9239.

Hough, R., Pratt, G. and Rechsteiner, M., 1986. Ubiquitin-lysozyme conjugates. Identification and characterization of an ATP-dependent protease from rabbit

reticulocyte lysates. Journal of Biochemistry 261, 2400-8.
Hu, M.C.-T., Shui, J.-W., Mihindukulasuriya, K.A. and Tan, T.-H., 2001. Genomic structure of mouse the PP4 gene: a developmentally regulated protein phosphatase. Gene 278, 89-99.
Hu, M.C.-T., Tang-Oxley, Q., Qiu, W.R., Wang, Y.-P., Mihindukulasuriya, K.A., Afshar, R. and Tan, T.-H., 1998. Protein phosphatase X interacts with c-Rel and stimulates c-Rel/nuclear factor kB activity. Journal of Biological Chemistry 273, 33561-33565.
Huang, H.Y., Liu, R.R., Zhao, G.P., Li, Q.H., Zheng, M.Q., Zhang, J.J., Li, S.F., Liang, Z. and Wen, J., 2015. Integrated analysis of microRNA and mRNA expression profiles in abdominal adipose tissues in chickens. Scientific Reports 5, 16132.
Huang, X., Cheng, A. and Honkanen, R.E., 1997. Genomic organization of the human PP4 gene encoding a serine/threonine protein phosphatase (PP4) suggests a common ancestry with PP2A. Genomics 44, 336-343.
Huang, X., Halicka, H.D., Traganos, F., Tanaka, T., Kurose, A. and Darzynkiewicz, Z., 2005. Cytometric assessment of DNA damage in relation to cell cycle phase and apoptosis. Cell Proliferation 38, 223-243.
Huke, S. and Bers, D.M., 2008a. Ryanodine receptor phosphorylation at serine 2030, 2808 and 2814 in rat cardiomyocytes. Biochemical and Biophysical Research Communications 376, 80-85.
Huke, S. and Bers, D.M., 2008b. Ryanodine receptor phosphorylation at Serine 2030, 2808 and 2814 in rat cardiomyocytes. Biochemical and Biophysical Research Communications 376, 80-85.
Hulme, J.T., Westenbroek, R.E., Scheuer, T. and Catterall, W.A., 2006a. Phosphorylation of serine 1928 in the distal C-terminal domain of cardiac $Ca_V1.2$ channels during β1-adrenergic regulation. Proceedings of the National Academy of Sciences of the United States of America 103, 16574-16579.
Hwang, J., Lee, J.A. and Pallas, D.C., 2016. Leucine carboxyl methyltransferase 1 (LCMT-1) methylates protein phosphatase 4 (PP4) and protein phosphatase 6 (PP6) and differentially regulates the stable formation of different PP4 holoenzymes. Journal of Biological Chemistry.
Ide, T., Tsutsui, H., Kinugawa, S., Suematsu, N., Hayashidani, S., Ichikawa, K., Utsumi, H., Machida, Y., Egashira, K. and Takeshita, A., 2000. Direct evidence for increased hydroxyl radicals originating from superoxide in the failing myocardium. Circulation Research 86, 152.
Iemitsu, M., Miyauchi, T., Maeda, S., Sakai, S., Fujii, N., Miyazaki, H., Kakinuma, Y., Matsuda, M. and Yamaguchi, I., 2003. Cardiac hypertrophy by hypertension and exercise training exhibits different gene expression of enzymes in energy metabolism. Hypertension Research 26, 829-837.
Imbert, A., Chaffanet, M., Essioux, L., Noguchi, T., Adelaide, J., Kerangueven, F., Le Paslier, D., Bonaiti-Pellie, C., Sobol, H., Birnbaum, D. and Pebusque, M.J., 1996. Integrated map of the chromosome 8p12-p21 region, a region involved in human cancers and Werner syndrome. Genomics 32, 29-38.
Inagaki, N., Gonoi, T., Iv, J.P.C., Wang, C.-Z., Aguilar-Bryan, L., Bryan, J. and Seino, S., 1996. A Family of sulfonylurea receptors determines the pharmacological properties of ATP-sensitive K^+ channels. Neuron 16, 1011-1017.
Inui, S., Kuwahara, K., Mizutani, J., Maeda, K., Kawai, T., Nakayasu, H. and Sakaguchi, N., 1995. Molecular cloning of a cDNA clone encoding a phosphoprotein component related to the Ig receptor-mediatred signal transduction. Journal of Immunology 154, 2714-2723.
Izumiya, Y., Shiojima, I., Sato, K., Sawyer, D.B., Colucci, W.S. and Walsh, K., 2006. Vascular endothelial growth factor blockade promotes the transition from compensatory cardiac hypertrophy to failure in response to pressure overload. Hypertension 47, 887-893.
Jacinto, E., Guo, B., Arndt, K.T., Schmelzle, T. and Hall, M.N., 2001. TIP41 interacts with

Tap42 and negatively regulates the Tor signaling pathway. Molecular Cell 8, 1017-1026.

Jackson, A.L., Bartz, S.R., Schelter, J., Kobayashi, S.V., Burchard, J., Mao, M., Li, B., Cavet, G. and Linsley, P.S., 2003. Expression profiling reveals off-target gene regulation by RNAi. Nature Biotechnology 21, 635-7.

Jackson, A.L., Burchard, J., Leake, D., Reynolds, A., Schelter, J., Guo, J., Johnson, J.M., Lim, L., Karpilow, J., Nichols, K., Marshall, W., Khvorova, A. and Linsley, P.S., 2006a. Position-specific chemical modification of siRNAs reduces "off-target" transcript silencing. RNA 12, 1197-205.

Jackson, A.L., Burchard, J., Schelter, J., Chau, B.N., Cleary, M., Lim, L. and Linsley, P.S., 2006b. Widespread siRNA "off-target" transcript silencing mediated by seed region sequence complementarity. RNA 12, 1179-87.

Jackson, A.L. and Linsley, P.S., 2010. Recognizing and avoiding siRNA off-target effects for target identification and therapeutic application. Nature Reviews Drug Discovery 9, 57-67.

Jackson, S.P. and Bartek, J., 2009. The DNA-damage response in human biology and disease. Nature 461, 1071-1078.

Janssens, V. and Goris, J., 2001. Protein phosphatase 2A: a highly regulated family of serine/threonine phosphatases implicated in cell growth and signalling. Biochemical Journal 353, 417-439.

Jelicks, L.A. and Siri, F.M., 1995. Effects of hypertrophy and heart failure on $[Na^+]i$ in pressure-overloaded guinea pig heart. American Journal of Hypertension 8, 934-943.

Jiang, L., Stanevich, V., Satyshur, K.A., Kong, M., Watkins, G.R., Wadzinski, B.E., Sengupta, R. and Xing, Y., 2013a. Structural basis of protein phosphatase 2A stable latency. Nature Communications 4, 1699.

Jiang, L., Stanevich, V., Satyshur, K.A., Kong, M., Watkins, G.R., Wadzinski, B.E., Sengupta, R. and Xing, Y., 2013b. Structural basis of protein phosphatase 2A stable latency. Nature Communications 4, 1-11.

Jiang, X., Xu, Y. and Price, B.D., 2010. Acetylation of H2AX on lysine 36 plays a key role in the DNA double-strand break repair pathway. FEBS Letters 584, 2926-2930.

Jiang, Y. and Broach, J.R., 1999. Tor proteins and protein phosphatase 2A reciprocally regulate Tap42 in controlling cell growth in yeast. The EMBO Journal 18, 2782-2792.

Jideama, N.M., Crawford, B.H., Hussain, A.A. and Raynor, R.L., 2006. Dephosphorylation specificities of protein phosphatase for cardiac troponin I, troponin T, and sites within troponin T. International Journal of Biological Sciences 2, 1-9.

Jin, L., Williamson, A., Banerjee, S., Philipp, I. and Rape, M., 2008. Mechanism of ubiquitin-chain formation by the human anaphase-promoting complex. Cell 133, 653-65.

Jones, T.A., Barker, H.M., da Cruz e Silva, E.F., Mayer-Jaekel, R.E., Hemmings, B.A., Spurr, N.K., Sheer, D. and Cohen, P.T., 1993. Localization of the genes encoding the catalytic subunits of protein phosphatase 2A to human chromosome bands 5q23-->q31 and 8p12-->p11.2, respectively. Cytogenetics and Cell Genetics 63, 35-41.

Judge, A.D., Sood, V., Shaw, J.R., Fang, D., McClintock, K. and MacLachlan, I., 2005. Sequence-dependent stimulation of the mammalian innate immune response by synthetic siRNA. Nature Biotechnology 23, 457-62.

Kaiser, R.A., Bueno, O.F., Lips, D.J., Doevendans, P.A., Jones, F., Kimball, T.F. and Molkentin, J.D., 2004. Targeted inhibition of p38 mitogen-activated protein kinase antagonizes cardiac injury and cell death following ischemia-reperfusion *in vivo*. Journal of Biological Chemistry 279, 15524-15530.

Kang, T.M. and Hilgemann, D.W., 2004. Multiple transport modes of the cardiac Na^+/Ca^{2+} exchanger. Nature 427, 544-548.

Kannel, W.B., Levy, D. and Cupples, L.A., 1987. Left ventricular hypertrophy and risk of

cardiac failure: insights from the Framingham study. Journal of Cardiovascular Pharmacology 10, S135-S140.

Kanzaki, Y., Terasaki, F., Okabe, M., Fujita, S., Katashima, T., Otsuka, K. and Ishizaka, N., 2010. Three-dimensional architecture of cardiomyocytes and connective tissue in human heart revealed by scanning electron microscopy. Circulation 122, 1973.

Katz, A.M., 2002. Ernest Henry Starling, His Predecessors, and the "Law of the Heart". Circulation 106, 2986-2992.

Kehrer, J.P., 2000. The Haber–Weiss reaction and mechanisms of toxicity. Toxicology 149, 43-50.

Khatri, M. and Rajam, M.V., 2007. Targeting polyamines of Aspergillus nidulans by siRNA specific to fungal ornithine decarboxylase gene. Medical Mycology 45, 211-20.

Khew-Goodall, Y. and Hemmings, B.A., 1988. Tissue-specific expression of mRNAs encoding alpha- and beta-catalytic subunits of protein phosphatase 2A. FEBS Letters 238, 265-8.

Khew-Goodall, Y., Mayer, R.E., Maurer, F., Stone, S.R. and Hemmings, B.A., 1991. Structure and transcriptional regulation of protein phosphatase 2A catalytic subunit genes. Biochemistry 30, 89-97.

Kiffin, R., Christian, C., Knecht, E. and Cuervo, A.M., 2004. Activation of chaperone-mediated autophagy during oxidative Stress. Molecular Biology of the Cell 15, 4829-4840.

Kilts, J.D., Gerhardt, M.A., Richardson, M.D., Sreeram, G., Mackensen, G.B., Grocott, H.P., White, W.D., Davis, R.D., Newman, M.F., Reves, J.G., Schwinn, D.A. and Kwatra, M.M., 2000. β2-adrenergic and several other G protein–coupled receptors in human atrial membranes activate both Gs and Gi. Circulation Research 87, 705-709.

Kitzman, D.W., Scholz, D.G., Hagen, P.T., Ilstrup, D.M. and Edwards, W.D., 1988. Age-related changes in normal human hearts during the first 10 decades of life. Part II (Maturity): A quantitative anatomic study of 765 specimens from subjects 20 to 99 years old. Mayo Clinic Proceedings 63, 137-146.

Kloeker, S., Bryant, J.C., Strack, S., Colbran, R.J. and Wadzinski, B.R., 1997. Carboxymethylation of nuclear protein serine/threonine phosphatase X. Biochemical Journal 327, 481-486.

Kloeker, S., Reed, R., McConnell, J.L., Chang, D., Tran, K., S., W.R., Law, B.K., Colbran, R.J., Kamoun, M., Campbell, K.S. and Wadzinski, B.E., 2003. Parallel purification of three catalytic subunits of the protein serine.threonine phosphatase 2A family (PP2Ac, PP4c, and PP6c) and anaylsis of the interaction of PP2Ac with alpha4 protein. Protein Expression & Purification 31, 19-33.

Kloeker, S. and Wadzinski, B.E., 1999. Purification and identification of a novel subunit of protein serine/threonine phosphatase 4. Journal of Biological Chemistry 274, 5339-5347.

Komander, D., Clague, M.J. and Urbe, S., 2009. Breaking the chains: structure and function of the deubiquitinases. Nature Reviews Molecular Cell Biology 10, 550-63.

Kong, M., Ditsworth, D., Lindsten, T. and Thompson, C.B., 2009. α4 is an essential regulator of PP2A phosphatase activity. Molecular Cell 36, 51-60.

Konhilas, J.P., Maass, A.H., Luckey, S.W., Stauffer, B.L., Olson, E.N. and Leinwand, L.A., 2004. Sex modifies exercise and cardiac adaptation in mice. American Journal of Physiology. Heart and Circulatory Physiology 287, H2768-H2776.

Kooij, V., Holewinski, R.J., Murphy, A.M. and Van Eyk, J.E., 2013. Characterization of the cardiac myosin binding protein-C phosphoproteome in healthy and failing human hearts. Journal of Molecular and Cellular Cardiology 60, 116-120.

Koren, M.J., Devereux, R.B., Casale, P.N., Savage, D.D. and Laragh, J.H., 1991. Relation of left ventricular mass and geometry to morbidity and mortality in uncomplicated essential hypertension. Annals of Internal Medicine 114, 345-352.

Kremmer, E., Ohst, K., Kiefer, J., Brewis, N. and Walter, G., 1997. Separation of PP2A

core enzyme and holoenzyme with monoclonal antibodies against the regulatory A subunit: abundant expression of both forms in cells. Molecular and Cellular Biology 17, 1692-1701.

Kuschel, M., Zhou, Y.-Y., Spurgeon, H.A., Bartel, S., Karczewski, P., Zhang, S.-J., Krause, E.-G., Lakatta, E.G. and Xiao, R.-P., 1999. β2-adrenergic cAMP signaling is uncoupled from phosphorylation of cytoplasmic proteins in canine heart. Circulation 99, 2458-2465.

Laemmli, U.K., 1970. Cleavage of structural proteins during the assembly of the head of bacteriophage T4. Nature 227, 680-5.

Lambright, D.G., Noel, J.P., Hamm, H.E. and Sigler, P.B., 1994. Structural determinants for activation of the [alpha]-subunit of a heterotrimeric G protein. Nature 369, 621-628.

Lappalainen, K., Jaaskelainen, I., Syrjanen, K., Urtti, A. and Syrjanen, S., 1994. Comparison of cell proliferation and toxicity assays using two cationic liposomes. Pharmaceutical Research 11, 1127-31.

Laskowski, A., Woodman, O.L., Cao, A.H., Drummond, G.R., Marshall, T., Kaye, D.M. and Ritchie, R.H., 2006. Antioxidant actions contribute to the antihypertrophic effects of atrial natriuretic peptide in neonatal rat cardiomyocytes. Cardiovascular Research 72, 112.

Lazebnik, M., Keswani, R.K. and Pack, D.W., 2016. Endocytic transport of polyplex and lipoplex siRNA vectors in HeLa cells. Pharmaceutical Research.

Leal, C., Bouxsein, N.F., Ewert, K.K. and Safinya, C.R., 2010. Highly efficient gene silencing activity of siRNA embedded in a nanostructured gyroid cubic lipid matrix. Journal of The American Chemical Society 132, 16841-7.

Lee, D.H. and Goldberg, A.L., 1996. Selective inhibitors of the proteasome-dependent and vacuolar pathways of protein degradation in *Saccharomyces cerevisiae*. Journal of Biochemistry 271, 27280-4.

Lee, J., Chen, Y., Tolstykh, T. and Stock, J., 1996. A specific protein carboxyl methylesterase that demethylates phosphoprotein phosphatase 2A in bovine brain. Proceedings of the National Academy of Sciences of the United States of America 93, 6043-6047.

Lee, J. and Lee, D.-H., 2014. Leucine methylation of protein phosphatase PP4C at C-terminal is critical for its cellular functions. Biochemical and Biophysical Research Communications 452, 42-47.

Lemke, T., Welling, A., Christel, C.J., Blaich, A., Bernhard, D., Lenhardt, P., Hofmann, F. and Moosmang, S., 2008. Unchanged β-adrenergic stimulation of cardiac L-type calcium channels in $Ca_V1.2$ phosphorylation site S1928A mutant mice. Journal of Biological Chemistry 283, 34738-34744.

LeNoue-Newton, M., Wadzinski, B.E. and Spiller, B.W., 2016. The three type 2A protein phosphatases, PP2Ac, PP4c and PP6c, are differentially regulated by Alpha4. Biochemical and Biophysical Research Communications 475, 64-69.

LeNoue-Newton, M., Watkins, G.R., Zou, P., Germane, K.L., McCorvey, L.R., Wadzinski, B.E. and Spiller, B.W., 2011. The E3 ubiquitin ligase- and protein phophatase 2A (PP2A)-binding domains of the alpha4 protein are both required for alpha4 to inhibit PP2A degradation. Journal of Biological Chemistry 286, 17665-17671.

Levy, D., Garrison, R.J., Savage, D.D., Kannel, W.B. and Castelli, W.P., 1990. Prognostic implications of echocardiographically determined left ventricular mass in the Framingham heart study. New England Journal of Medicine 322, 1561-1566.

Levy, D., Larson, M.G., Vasan, R.S., Kannel, W.B. and Ho, K.L., 1996. The progression from hypertension to congestive heart failure. JAMA 275, 1557-1562.

Li, B., Kaetzel, M.A. and Dedman, J.R., 2006. Signaling pathways regulating murine cardiac CREB phosphorylation. Biochemical and Biophysical Research Communications 350, 179-184.

Li, F., Wang, X., Capasso, J.M. and Gerdes, A.M., 1996. Rapid transition of cardiac myocytes from hyperplasia to hypertrophy during postnatal development. Journal of

Molecular and Cellular Cardiology 28, 1737-1746.
Li, H.-H., Li, A.G., Sheppard, H.M. and Liu, X., 2004. Phosphorylation on Thr-55 by TAF1 mediates degradation of p53. Molecular Cell 13, 867-878.
Li, J.-M., Gall, N.P., Grieve, D.J., Chen, M. and Shah, A.M., 2002. Activation of NADPH oxidase during progression of cardiac hypertrophy to failure. Hypertension 40, 477.
Li, L., Fang, C., Xu, D., Xu, Y., Fu, H. and Li, J., 2016. Cardiomyocyte specific deletion of PP2A causes cardiac hypertrophy. American Journal of Translational Research 8, 1769-79.
Li, L., Song, H., Luo, K., He, B., Nie, Y., Yang, Y., Wu, Y. and Gu, Z., 2011. Gene transfer efficacies of serum-resistant amino acids-based cationic lipids: dependence on headgroup, lipoplex stability and cellular uptake. International Journal of Pharmaceutics 408, 183-90.
Liang, Q. and Molkentin, J.D., 2003. Redefining the roles of p38 and JNK signaling in cardiac hypertrophy" dichotomy between cultured myocytes and animal models. Journal of Molecular and Cellular Cardiology 35, 1385-1394.
Liao, J., Li, H., Zeng, W., Sauer, D.B., Belmares, R. and Jiang, Y., 2012. Structural insight into the ion-exchange mechanism of the sodium/calcium exchanger. Science 335, 686.
Lillo, C., Kataya, A.R., Heidari, B., Creighton, M.T., Nemie-Feyissa, D., Ginbot, Z. and Jonassen, E.M., 2014. Protein phosphatases PP2A, PP4 and PP6: mediators and regulators in development and responses to environmental cues. Plant, Cell & Environment 37, 2631-48.
Lin, X., Ruan, X., Anderson, M.G., McDowell, J.A., Kroeger, P.E., Fesik, S.W. and Shen, Y., 2005. siRNA-mediated off-target gene silencing triggered by a 7 nt complementation. Nucleic Acids Research 33, 4527-35.
Lines, G.T., Sande, J.B., Louch, W.E., Mørk, H.K., Grøttum, P. and Sejersted, O.M., 2006. Contribution of the Na^+/Ca^{2+} exchanger to rapid Ca^{2+} release in cardiomyocytes. Biophysical Journal 91, 779-792.
Ling, S., Sun, Q., Li, Y., Zhang, L., Zhang, P., Wang, X., Tian, C., Li, Q., Song, J., Liu, H., Kan, G., Cao, H., Huang, Z., Nie, J., Bai, Y., Chen, S., Li, Y., He, F., Zhang, L. and Li, Y., 2012. CKIP-1 inhibits cardiac hypertrophy by regulating class II histone deacetylase phosphorylation through recruiting PP2A. Circulation 126, 3028.
Liochev, S.I. and Fridovich, I., 1994. The role of $O2^{\cdot-}$ in the production of HO.: in vitro and in vivo. Free Radical Biology and Medicine 16, 29-33.
Liu, J., Cai, M., Chen, J., Liao, Y., Mai, S., Li, Y., Huang, X., Liu, Y., Zhang, J., Kung, H., Zeng, Y., Zhou, F. and Xie, D., 2014. α4 contributes to bladder urothelial carcinoma cell invasion and/or metastasis via regulation of E-cadherin and is a predictor of outcome in bladder urothelial carcinoma patients. European Journal of Cancer 50, 840-851.
Liu, J., Xu, L., Zhong, J., Liao, J., Li, J. and Xu, X., 2012. Protein phosphatase PP4 is involved in NHEJ-mediated repair of DNA double-strand breaks. Cell Cycle 11, 2643-9.
Liu, J.C., Chan, P., Chen, J.J., Lee, H.M., Lee, W.S., Shih, N.L., Chen, Y.L., Hong, H.J. and Cheng, T.H., 2004. The inhibitory effect of trilinolein on norepinephrine-induced beta-myosin heavy chain promoter activity, reactive oxygen species generation, and extracellular signal-regulated kinase phosphorylation in neonatal rat cardiomyocytes. Journal of Biomedical Science 11, 11-8.
Liu, W., Zi, M., Jin, J., Prehar, S., Oceandy, D., Kimura, T.E., Lei, M., Neyses, L., Weston, A.H., Cartwright, E.J. and Wang, X., 2009. Cardiac-specific deletion of *Mkk4* reveals its role in pathological hypertrophic remodeling but not in physiological cardiac growth. Circulation Research 104, 905.
Liu, Z., Liu, H., Gao, F., Dahlstrom, K.R., Sturgis, E.M. and Wei, Q., 2016. Reduced DNA double-strand break repair capacity and risk of squamous cell carcinoma of the head and neck – A case-control study. DNA Repair 40, 18-26.

Livak, K.J. and Schmittgen, T.D., 2001. Analysis of relative gene expression data using real-time quantitative PCR and the 2(-Delta Delta C(T)) Method. Methods 25, 402-8.

Lodererova, M., Rybnicek, J., Steidl, J., Richter, J., Boivie, K., Karlsen, R. and Åsebø, O., 2009. Biocompatibility of metal sintered materials in dependence on multi-material graded structure, in: Lim, C.T. and Goh, J.C.H. (Eds.), 13th International Conference on Biomedical Engineering: ICBME 2008 3–6 December 2008 Singapore. Springer Berlin Heidelberg, Berlin, Heidelberg, pp. 1204-1207.

Longin, S., Zwaenepoel, K., Louis, J.V., Dilworth, S., Goris, J. and Janssens, V., 2007. Selection of protein phosphatase 2A regulatory subunits is mediated by the C terminus of the catalytic subunit. Journal of Biological Chemistry 282, 26971-26980.

Longman, M.R., Ranieri, A., Avkiran, M. and Snabaitis, A.K., 2014. Regulation of PP2AC carboxylmethylation and cellular localisation by inhibitory class G-protein coupled receptors in cardiomyocytes. PLoS One 9, e86234.

Lorenz, K., Schmitt, J.P., Schmitteckert, E.M. and Lohse, M.J., 2009. A new type of ERK1/2 autophosphorylation causes cardiac hypertrophy. Nature Medicine 15, 75-83.

Lu, J.J., Langer, R. and Chen, J., 2009. A novel mechanism is involved in cationic lipid-mediated functional siRNA delivery. Molecular Pharmaceutics 6, 763-71.

Luke, M.M., Della Seta, F., Di como, C.J., Sugimoto, H., Kobayashi, R. and Arndt, K.T., 1996. The SAPs, a new family of proteins, associate and function positively with the SIT4 phosphatase. Molecular and Cellular Biology 16, 2744-2755.

Luo, J., McMullen, J.R., Sobkiw, C.L., Zhang, L., Dorfman, A.L., Sherwood, M.C., Logsdon, M.N., Horner, J.W., DePinho, R.A., Izumo, S. and Cantley, L.C., 2005. Class I(A) phosphoinositide 3-kinase regulates heart size and physiological cardiac hypertrophy. Molecular and Cellular Biology 25, 9491-9502.

Lüss, H., Klein-Wiele, O., Bokník, P., Herzig, S., Knapp, J., Linck, B., Müller, F.U., Scheld, H.H., Schmid, C., Schmitz, W. and Neumann, J., 2000. Regional expression of protein phosphatase type 1 and 2A catalytic subunit isoforms in the human heart. Journal of Molecular and Cellular Cardiology 32, 2349-2359.

Ma, R., Xu, S., Zhao, Y., Xia, B. and Wang, R., 2016. Selection and validation of appropriate reference genes for quantitative real-time PCR analysis of gene expression in lycoris aurea. Frontiers in Plant Science 7, 536.

Maack, C., Kartes, T., Kilter, H., Schäfers, H.-J., Nickenig, G., Böhm, M. and Laufs, U., 2003. Oxygen free radical release in human failing myocardium is associated with increased activity of Rac1-GTPase and represents a target for statin treatment. Circulation 108, 1567.

MacCarthy, P.A., Grieve, D.J., Li, J.-M., Dunster, C., Kelly, F.J. and Shah, A.M., 2001. Impaired endothelial regulation of ventricular relaxation in cardiac hypertrophy. Circulation 104, 2967.

MacDougall, L.K., Jones, L.R. and Cohen, P., 1991. Identification of the major protein phosphatases in mammalian cardiac muscle which dephosphorylate phospholamban. European Journal of Biochemistry 196, 725-734.

MacKeigan, J.P., Murphy, L.O. and Blenis, J., 2005. Sensitized RNAi screen of human kinases and phosphatases identifies new regulators of apoptosis and chemoresistance. Nature Cell Biology 7, 591-600.

Mackenzie, L., Roderick, H.L., Proven, A., Conway, S.J. and Bootman, M.D., 2004. Inositol 1,4,5-trisphosphate receptors in the heart. Biological Research 37, 553-7.

MacLennan, D.H. and Kranias, E.G., 2003. Phospholamban: a crucial regulator of cardiac contractility. Nature Reviews Molecular Cell Biology 4, 566-577.

Madhani, M., Hall, A.R., Cuello, F., Charles, R.L., Burgoyne, J.R., Fuller, W., Hobbs, A.J., Shattock, M.J. and Eaton, P., 2010. Phospholemman Ser69 phosphorylation contributes to sildenafil-induced cardioprotection against reperfusion injury.

American Journal of Physiology - Heart and Circulatory Physiology 299, H827-H836.

Maeda, S., Matsuoka, I., Iwamoto, T., Kurose, H. and Kimura, J., 2005. Down-regulation of Na^+/Ca^{2+} exchanger by fluvastatin in rat cardiomyoblast H9c2 cells; involvement of RhoB in Na^+/Ca^{2+} Exchanger mRNA stability. Molecular Pharmacology 68, 414.

Mahato, R.I., Rolland, A. and Tomlinson, E., 1997. Cationic lipid-based gene delivery systems: pharmaceutical perspectives. Pharmaceutical Research 14, 853-9.

Maier, S.K.G., Westenbroek, R.E., Schenkman, K.A., Feigl, E.O., Scheuer, T. and Catterall, W.A., 2002. An unexpected role for brain-type sodium channels in coupling of cell surface depolarization to contraction in the heart. Proceedings of the National Academy of Sciences of the United States of America 99, 4073-4078.

Maillet, M., van Berlo, J.H. and Molkentin, J.D., 2013. Molecular basis of physiological heart growth: fundamental concepts and new players. Nature Reviews Molecular Cell Biology 14, 38-48.

Malone, R.W., Felgner, P.L. and Verma, I.M., 1989. Cationic liposome-mediated RNA transfection. Proceedings of the National Academy of Sciences of the United States of America 86, 6077-81.

Maltsev, V.A., Silverman, N., Sabbah, H.N. and Undrovinas, A.I., 2007. Chronic heart failure slows late sodium current in human and canine ventricular myocytes: implications for repolarization variability. European Journal of Heart Failure 9, 219-227.

Mangoni, M.E., Couette, B., Bourinet, E., Platzer, J., Reimer, D., Striessnig, J. and Nargeot, J., 2003. Functional role of L-type $Ca_V1.3$ Ca^{2+} channels in cardiac pacemaker activity. Proceedings of the National Academy of Sciences of the United States of America 100, 5543-5548.

Marks, A.R., 2001. Ryanodine Receptors/Calcium Release channels in Heart Failure and Sudden Cardiac Death. Journal of Molecular and Cellular Cardiology 33, 615-624.

Marx, S.O., Reiken, S., Hisamatsu, Y., Jayaraman, T., Burkhoff, D., Rosemblit, N. and Marks, A.R., 2000a. PKA phosphorylation dissociates FKBP12.6 from the calcium release channel (ryanodine receptor). Cell 101, 365-376.

Marx, S.O., Reiken, S., Hisamatsu, Y., Jayaraman, T., Burkhoff, D., Rosemblit, N. and Marks, A.R., 2000b. PKA phosphorylation dissociates FKBP12.6 from the calcium release channel (ryanodine receptor): defective regulation in failing hearts. Cell 101, 365-375.

Matsuo, T., Carabello, B.A., Nagatomo, Y., Koide, M., Hamawaki, M., Zile, M.R. and McDermott, P.J., 1998. Mechanisms of cardiac hypertrophy in canine volume overload. American Journal of Physiology - Heart and Circulatory Physiology 275, H65.

Matsushima, S., Ide, T., Yamato, M., Matsusaka, H., Hattori, F., Ikeuchi, M., Kubota, T., Sunagawa, K., Hasegawa, Y., Kurihara, T., Oikawa, S., Kinugawa, S. and Tsutsui, H., 2006. Overexpression of mitochondrial peroxiredoxin-3 prevents left ventricular remodeling and failure after myocardial infarction in mice. Circulation 113, 1779.

Maytin, M., Siwik, D.A., Ito, M., Xiao, L., Sawyer, D.B., Liao, R. and Colucci, W.S., 2004. Pressure Overload–Induced Myocardial Hypertrophy in Mice Does Not Require gp91. Circulation 109, 1168.

McConnell, J.L., GOmez, R.J., McCorvey, L.R.A., Law, B.K. and Wadzinski, B.E., 2007. Identification of a PP2A-interacting protein that functions as a negative regulator of phosphatase activity in the ATM/ATR signaling pathway. Oncogene, 1-10.

McConnell, J.L. and Wadzinski, B.E., 2009. Targeting protein serine/threonine phosphatases for drug development. Molecular Pharmacology 75, 1249-61.

McConnell, J.L., Watkins, G.R., Soss, S.E., Franz, H.S., McCorvey, L.R., Spiller, B.W., Chazin, W.J. and Wadzinski, B.E., 2010. Alpha4 is a ubiquitin-binding protein that regulates protein serine/threonine phosphatase 2A ubiquitination. Biochemistry 49, 1713-1718.

McCord, J.M. and Fridovich, I., 1969. Superoxide dismutas:. An enzymic function for erythrocuprein (hemocuprein). Journal of Biological Chemistry 244, 6049-6055.

McDonald, W.J., Thomas, L.N., Koirata, S. and Too, C.K.L., 2014. Progestin-inducible EDD E3 ubiquitin ligase binds to α4 phosphoprotein to regulate ubiquitination and degradation of protein phosphatase PP2AC. Molecular and Cellular Endocrinology 382, 254-261.

McMullen, J.R., Shioi, T., Zhang, L., Tarnavski, O., Sherwood, M.C., Kang, P.M. and Izumo, S., 2003. Phosphoinositide 3-kinase(p110α) plays a critical role for the induction of physiological, but not pathological, cardiac hypertrophy. Proceedings of the National Academy of Sciences of the United States of America 100, 12355-12360.

McMurray, J., Chopra, M., Abdullah, I., Smith, W.E. and Dargie, H.J., 1993. Evidence of oxidative stress in chronic heart failure in humans. European Heart Journal 14, 1493.

McMurray, J.J.V., Adamopoulos, S., Anker, S.D., Auricchio, A., Böhm, M., Dickstein, K., Falk, V., Filippatos, G., Fonseca, C., Gomez-Sanchez, M.A., Jaarsma, T., Køber, L., Lip, G.Y.H., Maggioni, A.P., Parkhomenko, A., et al., 2012. ESC guidelines for the diagnosis and treatment of acute and chronic heart failure 2012: The task force for the diagnosis and treatment of acute and chronic heart failure 2012 of the European Society of Cardiology. Developed in collaboration with the Heart Failure Association (HFA) of the ESC. European Heart Journal 33, 1787-1847.

Meador, J.A., Zhao, M., Su, Y., Narayan, G., Geard, C.R. and Balajee, A.S., 2008. Histone H2AX is a critical factor for cellular protection against DNA alkylating agents. Oncogene 27, 5662-5671.

Meijs, M.F.L., Bots, M.L., Vonken, E.J., Cramer, M.J., Melman, P.G., Velthuis, B.K., van der Graaf, Y., Mali, W., Doevendans, P.A. and on behalf of the, S.S.G., 2007. Rationale and design of the SMART heart study: A prediction model for left ventricular hypertrophy in hypertension. Netherlands Heart Journal 15, 295-298.

Mejla-Alvarez, R., Tomaselli, G.F. and Marban, E., 1994. Simultaneous expression of cardiac and skeletal muscle isoforms of the L-type Ca^{2+} channel in a rat heart muscle cell line. J Physiol 478, 315-329.

Menard, C., Pupier, S., Mornet, D., Kitzmann, M., Nargeot, J. and Lory, P., 1999. Modulation of L-type calcium channel expression during retinoic acid-induced differentiation of H9c2 cardiac cells. Journal of Biological Chemistry 274, 29063-29070.

Mesquita, R.F., Paul, M.A., Valmaseda, A., Francois, A., Jabr, R., Anjum, S., Marber, M.S., Budhram-Mahadeo, V. and Heads, R.J., 2014. Protein kinase Cepsilon-calcineurin cosignaling downstream of toll-like receptor 4 downregulates fibrosis and induces wound healing gene expression in cardiac myofibroblasts. Molecular and Cellular Biology 34, 574-94.

Mi, J., Dziegielewski, J., Bolesta, E., Brautigan, D.L. and Larner, J.M., 2009. Activation of DNA-PK by ionizing radiation is mediated by protein phosphatase 6. PLoS ONE 4, e4395.

Mihl, C., Dassen, W.R.M. and Kuipers, H., 2008. Cardiac remodelling: concentric versus eccentric hypertrophy in strength and endurance athletes. Netherlands Heart Journal 16, 129-133.

Minamino, T., Yujiri, T., Terada, N., Taffet, G.E., Michael, L.H., Johnson, G.L. and Schneider, M.D., 2002. MEKK1 is essential for cardiac hypertrophy and dysfunction induced by Gq. Proceedings of the National Academy of Sciences of the United States of America 99, 3866-3871.

Minsky, N., Shema, E., Field, Y., Schuster, M., Segal, E. and Oren, M., 2008. Monoubiquitinated H2B is associated with the transcribed region of highly expressed genes in human cells. Nature Cell Biology 10, 483-8.

Mirzayans, R., Severin, D. and Murray, D., 2006. Relationship between DNA double-strand

break rejoining and cell survival after exposure to ionizing radiation in human fibroblast strains with differing ATM/p53 status: Implications for evaluation of clinical radiosensitivity. International Journal of Radiation Oncology, Biology, Physics 66, 1498-1505.

Mojarrab, M., Jamshidi, M., Ahmadi, F., Alizadeh, E. and Hosseinzadeh, L., 2013. Extracts of Artemisia ciniformis Protect Cytotoxicity Induced by Hydrogen Peroxide in H9c2 Cardiac Muscle Cells through the Inhibition of Reactive Oxygen Species. Advances in Pharmacological Sciences 2013, 141683.

Molkentin, J.D., Lu, J.-R., Antos, C.L., Markham, B., Richardson, J., Robbins, J., Grant, S.R. and Olson, E.N., 1998. A calcineurin-dependent transcriptional pathway for cardiac hypertrophy. Cell 93, 215-228.

Mollova, M., Bersell, K., Walsh, S., Savla, J., Das, L.T., Park, S.-Y., Silvberstein, L.E., dos Remedios, C.G., Graham, D., Colan, S. and Kuhn, B., 2013. Cardiomyocyte proliferation contributes to heart growth in young humans. Proceedings of the National Academy of Sciences of the United States of America
110, 1446-1451.

Mondal, N.K., Sorensen, E., Hiivala, N., Feller, E., Griffith, B. and Wu, Z.J., 2013. Oxidative stress, DNA damage and repair in heart failure patients after implantation of continuous flow left ventricular assist devices. International Journal of Medical Sciences 10, 883-893.

Moniotte, S., Vaerman, J.L., Kockx, M.M., Larrouy, D., Langin, D., Noirhomme, P. and Balligand, J.L., 2001. Real-time RT-PCR for the detection of beta-adrenoceptor messenger RNAs in small human endomyocardial biopsies. Journal of Molecular and Cellular Cardiology 33, 2121-2133.

Morales-Johansson, H., Puria, R., Brautigan, D.L. and Cardenas, M.E., 2009. Human protein phosphatase PP6 regulatory subunits provide sit4-dependent and rapamycin-sensitive sap function in *Saccharomyces cerevisiae*. Plos One 4, e6331.

Mosmann, T., 1983. Rapid colorimetric assay for cellular growth and survival: application to proliferation and cytotoxicity assays. Journal of Immunological Methods 65, 55-63.

Murata, K., Wu, J. and Brautigan, D.L., 1997. B cell receptor-associated protein α4 displays rapamycin-sensitive binding directly to the catalytic subunit of protein phosphatase 2A. Proceedings of the National Academy of Sciences of the United States of America 94, 10624-10629.

Mutlak, M. and Kehat, I., 2015. Extracellular signal-regulated kinases 1/2 as regulators of cardiac hypertrophy. Frontiers in Pharmacology 6, 149.

Nag, A.C., 1980. Study of non-muscle cells of the adult mammalian heart: a fine structural analysis and distribution. Cytobios 28, 41-61.

Naghavi M, Wang H, Lozano R, Davis A, Liang X, Zhou M, Vollset SE, Ozgoren AA, Abdalla S, Abd-Allah F, Abdel Aziz MI, A.S., Aboyans V, Abraham B, A.J., Abuabara KE, Abubakar I, et al., 2015. Global, regional, and national age-sex specific all-cause and cause-specific mortality for 240 causes of death, 1990-2013: a systematic analysis for the Global Burden of Disease Study 2013. The Lancet 385, 117-171.

Nakada, S., Chen, G.I., Gingras, A.-C. and Durocher, D., 2008a. PP4 is a γH2AX phosphatase required for recovery from the DNA damage checkpoint. EMBO Reports 9, 1019-1026.

Nakada, S., Chen, G.I., Gingras, A.C. and Durocher, D., 2008b. PP4 is a gamma H2AX phosphatase required for recovery from the DNA damage checkpoint. EMBO Reports 9, 1019-26.

Nakai, J., Imagawa, T., Hakamata, Y., Shigekawa, M., Takeshima, H. and Numa, S., 1990. Primary structure and functional expression from cDNA of the cardiac ryanodine receptor/calcium release channel. FEBS Letters 271, 169-177.

Nakamura, T.Y., Iwata, Y., Arai, Y., Komamura, K. and Wakabayashi, S., 2008. Activation

of Na^+/H^+ exchanger 1 is sufficient to generate Ca^{2+} signals that induce cardiac hypertrophy and heart failure. Circulation Research 103, 891-899.

Nakayama, H., Bodi, I., Maillet, M., DeSantiago, J., Domeier, T.L., Mikoshiba, K., Lorenz, J.N., Blatter, L.A., Bers, D.M. and Molkentin, J.D., 2010. The IP(3) Receptor regulates cardiac hypertrophy in response to select stimuli. Circulation Research 107, 659-666.

Nanahoshi, M., Tsujishita, Y., Tokunaga, C., Inui, S., Sakaguchi, N., Hara, K. and Yonezawa, K., 1999. Alpha4 protein as a common regulator of type 2A-related serine/threonine protein phosphatases. FEBS Letters 446, 108-112.

Nanduri, S., Carpick, B.W., Yang, Y., Williams, B.R. and Qin, J., 1998. Structure of the double-stranded RNA-binding domain of the protein kinase PKR reveals the molecular basis of its dsRNA-mediated activation. EMBO Journal 17, 5458-65.

Naraynan, N. and Xu, A., 1997. Phosphorylation and regulation of the Ca^{2+}-pumping ATPase in cardiac sarcoplasmic reticulum by calcium/calmodulin-dependent protein kinase. Basic Research in Cardiology 92, 25-35.

Nathan, J.A., Kim, H.T., Ting, L., Gygi, S.P. and Goldberg, A.L., 2013. Why do cellular proteins linked to K63-polyubiquitin chains not associate with proteasomes? EMBO Journal 32, 552-65.

Nattel, S. and Carlsson, L., 2006. Innovative approaches to anti-arrhythmic drug therapy. Nature Reviews Drug Discovery 5, 1034-1049.

Nguyen, L.K., Dobrzynski, M., Fey, D. and Kholodenko, B.N., 2014. Polyubiquitin chain assembly and organization determine the dynamics of protein activation and degradation. Frontiers in Physiology 5, 4.

Nicol, E.D., Fittall, B., Roughton, M., Cleland, J.G.F., Dargie, H. and Cowie, M.R., 2008. NHS heart failure survey: a survey of acute heart failure admissions in England, Wales and Northern Ireland. Heart 94, 172-177.

Nicol, R.L., Frey, N., Pearson, G., Cobb, M., Richardson, J. and Olson, E.N., 2001. Activated MEK5 induces serial assembly of sarcomeres and eccentric cardiac hypertrophy. EMBO Journal 20, 2757-2767.

Nishida, K., Yamaguchi, O., Hirotani, S., Hikoso, S., Higuchi, Y., Watanabe, T., Takeda, T., Osuka, S., Morita, T., Kondoh, G., Uno, Y., Kashiwase, K., Taniike, M., Nakai, A., Matsumura, Y., Miyazaki, J.-i., Sudo, T., Hongo, K., Kusakari, Y., Kurihara, S., Chien, K.R., Takeda, J., Hori, M. and Otsu, K., 2004. p38α mitogen-activated protein kinase plays a critical role in cardiomyocyte survival but not in cardiac hypertrophic growth in response to pressure overload. Molecular and Cellular Biology 24, 10611-10620.

Novoyatleva, T., Diehl, F., van Amerongen, M.J., Patra, C., Ferrazzi, F., Bellazzi, R. and Engel, F.B., 2010. TWEAK is a positive regulator of cardiomyocyte proliferation. Cardiovascular Research 85, 681-90.

Nowak, S.J., Pai, C.Y. and Corces, V.G., 2003. Protein phosphatase 2A activity affects histone H3 phosphorylation and transcription in *Drosophila melanogaster*. Molecular & Cellular Biology 23, 6129-38.

Nykanen, A., Haley, B. and Zamore, P.D., 2001. ATP requirements and small interfering RNA structure in the RNA interference pathway. Cell 107, 309-21.

Ogris, E., Du, X., Nelson, K.C., Mak, E.K., Yu, X.X., Lane, W.S. and Pallas, D.C., 1999. A protein phosphatase methylesterase (PME-1) is one of several novel proteins stably associating with two inactive mutants of protein phosphatase 2A. The Journal of biological chemistry 274, 14382-14391.

Ohama, T., Wang, L., Griner, E.M. and Brautigan, D.L., 2013. Protein Ser/Thr phosphatase-6 is required for maintenance of E-cadherin at adherens junctions. BMC Cell Biology 14, 42.

Okwuosa, T.M., Soliman, E.Z., Lopez, F., Williams, K.A., Alonso, A. and Ferdinand, K.C., 2015. Left ventricular hypertrophy and cardiovascular disease risk prediction and reclassification in Blacks and Whites: the ARIC study. American heart journal 169,

155-161.e5.

Olivetti, G., Abbi, R., Quaini, F., Kajstura, J., Cheng, W., Nitahara, J.A., Quaini, E., Di Loreto, C., Beltrami, C.A., Krajewski, S., Reed, J.C. and Anversa, P., 1997. Apoptosis in the failing human heart. New England Journal of Medicine 336, 1131-1141.

Olsen, J.V., Blagoev, B., Gnad, F., Macek, B., Kumar, C., Mortensen, P. and Mann, M., 2006. Global, in vivo, and site-specific phosphorylation dynamics in signaling networks. Cell 127, 635-48.

Onda, M., Inui, S., Maeda, K., Suzuki, M., Takahashi, E.-i. and Sakaguchi, N., 1997. Expression and chromosomal localization of the human *α4/IGBP1* gene, the structure of which is closely related to the yeast TAP42 protein of the rapamycin-sensitive signal transduction pathway. Genomics 46, 373-378.

Osterrieder, W., Brum, G., Hescheler, J., Trautwein, W., Flockerzi, V. and Hofmann, F., 1982. Injection of subunits of cyclic AMP-dependent protein kinase into cardiac myocytes modulates Ca^{2+} current. Nature 298, 576-578.

Oyama, K., Takahashi, K. and Sakurai, K., 2009. Cardiomyocyte H9c2 Cells exhibit differential sensitivity to intracellular reactive oxygen species generation with regard to their hypertrophic vs death responses to exogenously added hydrogen peroxide. Journal of Clinical Biochemistry and Nutrition 45, 361-369.

Oyama, K., Takahashi, K. and Sakurai, K., 2011. Hydrogen peroxide induces cell cycle arrest in cardiomyoblast H9c2 cells, which is related to hypertrophy. Biological & Pharmaceutical Bulletin 34, 501-6.

Pacher, P., Thomas, A.P. and Hajnoczky, G., 2002. Ca^{2+} sparks: miniature calcium signals in single mitochondria driven by ryanodine receptors. Proceedings of the National Academy of Sciences (USA) 99, 2380-2385.

Pandey, P., Seshacharyulu, P., Das, S., Rachagani, S., Ponnusamy, M.P., Yan, Y., Johansson, S.L., Datta, K., Fong Lin, M. and Batra, S.K., 2013. Impaired expression of protein phosphatase 2A subunits enhances metastatic potential of human prostate cancer cells through activation of AKT pathway. British Journal of Cancer 108, 2590-600.

Patriarchi, T., Qian, H., Di Biase, V., Malik, Z.A., Chowdhury, D., Price, J.L., Hammes, E.A., Buonarati, O.R., Westenbroek, R.E., Catterall, W.A., Hofmann, F., Xiang, Y.K., Murphy, G.G., Chen, C.-Y., Navedo, M.F. and Hell, J.W., 2016. Phosphorylation of $Ca_V1.2$ on S1928 uncouples the L-type Ca^{2+} channel from the β2 adrenergic receptor. The EMBO Journal 35, 1330-1345.

Patten, R.D. and Hall-Porter, M.R., 2009. Small animal models of heart failure: development of novel therapies, past and present. Circulation. Heart Failure 2, 138-44.

Paull, T.T., Rogakou, E.P., Yamazaki, V., Kirchgessner, C.U., Gellert, M. and Bonner, W.M., 2000. A critical role for histone H2AX in recruitment of repair factors to nuclear foci after DNA damage. Current Biology 10, 886-895.

Pavlovic, D., Fuller, W. and Shattock, M.J., 2007. The intracellular region of FXYD1 is sufficient to regulate cardiac Na/K ATPase. FASEB Journal 21, 1539-1546.

Pavlovic, D., Fuller, W. and Shattock, M.J., 2013. Novel regulation of cardiac Na pump via phospholemman. Journal of Molecular and Cellular Cardiology 61, 83-93.

Pavlović, D., Fuller, W. and Shattock, M.J., 2007. The intracellular region of FXYD1 is sufficient to regulate cardiac Na/K ATPase. The FASEB Journal 21, 1539-1546.

Pehrson, J.R. and Fuji, R.N., 1998. Evolutionary conservation of histone macroH2A subtypes and domains. Nucleic Acids Research 26, 2837-2842.

Pfaffl, M.W., 2001. A new mathematical model for relative quantification in real-time RT-PCR. Nucleic Acids Research 29.

Pfaffl, M.W., Tichopad, A., Prgomet, C. and Neuvians, T.P., 2004. Determination of stable housekeeping genes, differentially regulated target genes and sample integrity: BestKeeper--Excel-based tool using pair-wise correlations. Biotechnology Letters

26, 509-15.

Pierce, K.L., Premont, R.T. and Lefkowitz, R.J., 2002. Seven-transmembrane receptors. Nature Reviews Molecular Cell Biology 3, 639-650.

Pieske, B., Maier, L.S., Bers, D.M. and Hasenfuss, G., 1999. Ca^{2+} handling and sarcoplasmic reticulum Ca^{2+} content in isolated failing and nonfailing human myocardium. Circulation Research 85, 38.

Pieske, B., Maier, L.S., Piacentino, V., Weisser, J., Hasenfuss, G. and Houser, S., 2002. Rate dependence of $[Na^{+}]i$ and contractility in nonfailing and failing human myocardium. Circulation 106, 447.

Plácido, A.I., Pereira, C.M.F., Correira, S.C., Carvalho, C., Oliveira, C.R. and Moreira, P.I., 2016. Phosphatase 2A inhibition affects endoplasmic reticulum and mitochondria homeostasis via cytoskeletal alterations in brain endothelial cells. Molecular Neurobiology, 1-15.

Pluim, B.M., Zwinderman, A.H., van der Laarse, A. and van der Wall, E.E., 2000. The Athlete's Heart. Circulation 101, 336.

Ponikowski, P., Anker, S.D., AlHabib, K.F., Cowie, M.R., Force, T.L., Hu, S., Jaarsma, T., Krum, H., Rastogi, V., Rohde, L.E., Samal, U.C., Shimokawa, H., Budi Siswanto, B., Sliwa, K. and Filippatos, G., 2014. Heart failure: preventing disease and death worldwide. ESC Heart Failure 1, 4-25.

Pooja, S., Pushpanathan, M., Gunasekaran, P. and Rajendhran, J., 2015. Endocytosis mediated invasion and pathogenicity of Streptococcus agalactiae in rat cardiomyocyte (H9C2). PLoS One 10, e0139733.

Popescu, L.M., Gherghiceanu, M., Hinescu, M.E., Cretoiu, D., Ceafalan, L., Regalia, T., Popescu, A.C., Ardeleanu, C. and Mandache, E., 2006. Insights into the interstitium of ventricular myocardium: interstitial Cajal-like cells (ICLC). Journal of Cellular and Molecular Medicine 10, 429-458.

Porrello, E.R., Widdop, R.E. and Delbridge, L.M., 2008. Early origins of cardiac hypertrophy: does cardiomyocyte attrition programme for pathological 'catch-up' growth of the heart? Clinical and Experimental Pharmacology and Physiology 35, 1358-64.

Powell, S.R., Wang, P., Katzeff, H., Shringarpure, R., Teoh, C., Khaliulin, I., Das, D.K., Davies, K.J. and Schwalb, H., 2005. Oxidized and ubiquitinated proteins may predict recovery of postischemic cardiac function: essential role of the proteasome. Antioxidants and Redox Signaling 7, 538-46.

Predmore, J.M., Wang, P., Davis, F., Bartolone, S., Westfall, M.V., Dyke, D.B., Pagani, F., Powell, S.R. and Day, S.M., 2010. Ubiquitin proteasome dysfunction in human hypertrophic and dilated cardiomyopathies. Circulation 121, 997-1004.

Prickett, T.D. and Brautigan, D.L., 2006. The α4 regulatory subunit exerts opposing allosteric effects on protein phosphatases PP6 and PP2A. Journal of Biological Chemistry 281, 30503-30511.

Prosser, B.L., Ward, C.W. and Lederer, W.J., 2011. X-ROS signaling: rapid mechano-chemo transduction in heart. Science 333, 1440.

Puglisi, J.L., Yuan, W., Bassani, J.W.M. and Bers, D.M., 1999. Ca^{2+} influx through Ca^{2+} channels in rabbit ventricular myocytes during action potential clamp. Circulation Research 85, e7.

Punn, A., Mockridge, J.W., Farooqui, S., Marber, M.S. and Heads, R.J., 2000. Sustained activation of p42/p44 mitogen-activated protein kinase during recovery from simulated ischaemia mediates adaptive cytoprotection in cardiomyocytes. Biochemical Journal 350 Pt 3, 891-9.

Qin, B. and Cheng, K., 2010. Silencing of the IKKepsilon gene by siRNA inhibits invasiveness and growth of breast cancer cells. Breast Cancer Research 12, R74.

Qin, Q., Wang, X., Yan, N., Song, R.H., Cai, T.T., Zhang, W., Guan, L.J., Muhali, F.S. and Zhang, J.A., 2015. Aberrant expression of miRNA and mRNAs in lesioned tissues of Graves' disease. Cellular Physiology and Biochemistry 35, 1934-42.

Rahamimoff, H., Elbaz, B., Alperovich, A., Kimchi-Sarfaty, C., Gottesman, M.M., Lichtenstein, Y., Eskin-Shwartz, M. and Kasir, J., 2007. Cyclosporin A-dependent downregulation of the Na^{+}/Ca^{2+} exchanger expression. Annals of the New York Academy of Sciences 1099, 204-214.

Raman, M. and Cobb, M.H., 2003. MAP Kinase modules: Many roads home. Current Biology 13, R886-R888.

Rana, T.M., 2007. Illuminating the silence: understanding the structure and function of small RNAs. Nature Reviews Molecular Cell Biology 8, 23-36.

Rapacciuolo, A., Esposito, G., Caron, K., Mao, L., Thomas, S.A. and Rockman, H.A., 2001. Important role of endogenous norepinephrine and epinephrine in the development of in vivo pressure-overload cardiac hypertrophy. Journal of the American College of Cardiology 38, 876-882.

Raynes, R., Pomatto, L.C.D. and Davies, K.J.A., 2016. Degradation of oxidized proteins by the proteasome: Distinguishing between the 20S, 26S, and immunoproteasome proteolytic pathways. Molecular Aspects of Medicine 50, 41-55.

Redon, C., Pilch, D., Rogakou, E., Sedelnikova, O., Newrock, K. and Bonner, W., 2002. Histone H2A variants H2AX and H2AZ. Current Opinion in Genetics & Development 12, 162-169.

Rice, P., Longden, I. and Bleasby, A., 2000. EMBOSS: the European Molecular Biology Open Software Suite. Trends in Genetics 16, 276-7.

Rio, D.C., Ares, M., Jr., Hannon, G.J. and Nilsen, T.W., 2010. Nondenaturing agarose gel electrophoresis of RNA. Cold Spring Harbor Protocols 2010, pdb prot5445.

Robbins, M., Judge, A., Ambegia, E., Choi, C., Yaworski, E., Palmer, L., McClintock, K. and MacLachlan, I., 2008. Misinterpreting the therapeutic effects of small interfering RNA caused by immune stimulation. Human Gene Therapy 19, 991-9.

Rockman, H.A., Koch, W.J. and Lefkowitz, R.J., 2002. Seven-transmembrane-spanning receptors and heart function. Nature 415, 206-212.

Rodriguez, P., Bhogal, M.S. and Colyer, J., 2003. Stoichiometric phosphorylation of cardiac ryanodine receptor on serine 2809 by calmodulin-dependent kinase II and protein kinase A. Journal of Biological Chemistry 278, 38593-38600.

Rogakou, E.P., Boon, C., Redon, C. and Bonner, W.M., 1999. Megabase chromatin domains involved in DNA double-strand breaks in vivo. Journal of Cell Biology 146, 905-916.

Rogakou, E.P., Pilch, D.R., Orr, A.H., Ivanova, V.S. and Bonner, W.M., 1998. DNA double-stranded breaks induce histone H2AX phosphorylation on serine 139. Journal of Biological Chemistry 273, 5858-68.

Roth, G.A., Forouzanfar, M.H., Moran, A.E., Barber, R., Nguyen, G., Feigin, V.L., Naghavi, M., Mensah, G.A. and Murray, C.J.L., 2015. Demographic and epidemiologic drivers of global cardiovascular mortality. New England Journal of Medicine 372, 1333-1341.

Rozengurt, E., 1986. Early signals in the mitogenic response. Science 234, 161.

Ruppert, C., Deiss, K., Herrmann, S., Vidal, M., Oezkur, M., Gorski, A., Weidemann, F., Lohse, M.J. and Lorenz, K., 2013. Interference with ERKThr188 phosphorylation impairs pathological but not physiological cardiac hypertrophy. Proceedings of the National Academy of Sciences of the United States of America 110, 7440-7445.

Sadayappan, S., Gulick, J., Osinska, H., Martin, L.A., Hahn, H.S., Dorn, G.W., Klevitsky, R., Seidman, C.E., Seidman, J.G. and Robbins, J., 2005. Cardiac myosin-binding protein-C phosphorylation and cardiac function. Circulation Research 97, 1156.

Sadoshima, J., Montagne, O., Wang, Q., Yang, G., Warden, J., Liu, J., Takagi, G., Karoor, V., Hong, C., Johnson, G.L., Vatner, D.E. and Vatner, S.F., 2002. The MEKK1-JNK pathway plays a protective role in pressure overload but does not mediate cardiac hypertrophy. Journal of Clinical Investigation 110, 271-9.

Saotome, M., Katoh, H., Yaguchi, Y., Tanaka, T., Urushida, T., Satoh, H. and Hayashi, H., 2009. Transient opening of mitochondrial permeability transition pore by reactive

oxygen species protects myocardium from ischemia-reperfusion injury. American Journal of Physiology - Heart and Circulatory Physiology 296, H1125.

Saucerman, J.J. and Bers, D.M., 2008. Calmodulin mediates differential sensitivity of CaMKII and calcineurin to local Ca^{2+} in cardiac myocytes. Biophysical Journal 95, 4597-4612.

Scacheri, P.C., Rozenblatt-Rosen, O., Caplen, N.J., Wolfsberg, T.G., Umayam, L., Lee, J.C., Hughes, C.M., Shanmugam, K.S., Bhattacharjee, A., Meyerson, M. and Collins, F.S., 2004. Short interfering RNAs can induce unexpected and divergent changes in the levels of untargeted proteins in mammalian cells. Proceedings of the National Academy of Sciences of the United States of America 101, 1892-7.

Schannwell, C.M., Zimmermann, T., Schneppenheim, M., Plehn, G., Marx, R. and Strauer, B.E., 2002. Left ventricular hypertrophy and diastolic dysfunction in healthy pregnant women. Cardiology 97, 73-78.

Schmittgen, T.D. and Livak, K.J., 2008. Analyzing real-time PCR data by the comparative C(T) method. Nature Protocols 3, 1101-8.

Schmitz, J.C. and Chu, E., 2011. Effect of small interfering RNA 3'-end overhangs on chemosensitivity to thymidylate synthase inhibitors. Silence 2, 1.

Schmitz, M.H.A., Held, M., Janssens, V., Hutchins, J.R.A., Hudecz, O., Ivanova, E., Goris, J., Trinkle-Mulcahy, L., Lamond, A.I., Poser, I., Hyman, A.A., Mechtler, K., Peters, J.-M. and Gerlich, D.W., 2010. Live-cell imaging RNAi screen identifies PP2A–B55α and importin-β1 as key mitotic exit regulators in human cells. Nature cell biology 12, 10.1038/ncb2092.

Schröder, F., Handrock, R., Beuckelmann, D.J., Hirt, S., Hullin, R., Priebe, L., Schwinger, R.H.G., Weil, J. and Herzig, S., 1998. Increased availability and open probability of single L-type calcium channels from failing compared with nonfailing human ventricle. Circulation 98, 969-976.

Schroeder, A., Mueller, O., Stocker, S., Salowsky, R., Leiber, M., Gassmann, M., Lightfoot, S., Menzel, W., Granzow, M. and Ragg, T., 2006. The RIN: an RNA integrity number for assigning integrity values to RNA measurements. BMC Molecular Biology 7, 3.

Schunkert, H., Dzau, V.J., Tang, S.S., Hirsch, A.T., Apstein, C.S. and Lorell, B.H., 1990. Increased rat cardiac angiotensin converting enzyme activity and mRNA expression in pressure overload left ventricular hypertrophy. Effects on coronary resistance, contractility, and relaxation. Journal of Clinical Investigation 86, 1913-1920.

Schwarz, D.S., Ding, H., Kennington, L., Moore, J.T., Schelter, J., Burchard, J., Linsley, P.S., Aronin, N., Xu, Z. and Zamore, P.D., 2006. Designing siRNA that distinguish between genes that differ by a single nucleotide. PLoS Genetics 2, e140.

Schwinger, R.H.G., Wang, J., Frank, K., Müller-Ehmsen, J., Brixius, K., McDonough, A.A. and Erdmann, E., 1999. Reduced sodium pump α1, α3, and β1-isoform protein levels and Na^{+},K^{+}-ATPase activity but unchanged Na^{+}-Ca^{2+} exchanger protein levels in human heart failure. Circulation 99, 2105-2112.

Scriven, D.R., Dan, P. and Moore, E.D., 2000. Distribution of proteins implicated in excitation-contraction coupling in rat ventricular myocytes. Biophysical Journal 79, 2682-2691.

Seddon, M., Looi, Y.H. and Shah, A.M., 2007. Oxidative stress and redox signalling in cardiac hypertrophy and heart failure. Heart 93, 903-907.

Segers, P., Stergiopulos, N., Schreuder, J.J., Westerhof, B.E. and Westerhof, N., 2000. Left ventricular wall stress normalization in chronic pressure-overloaded heart: a mathematical model study. American Journal of Physiology - Heart and Circulatory Physiology 279, H1120.

Sents, W., Ivanova, E., Lambrecht, C., Haesen, D. and Janssens, V., 2013. The biogenesis of active protein phosphatase 2A holoenzymes: a tightly regulated process creating phosphatase specificity. Febs Journal 280, 644-661.

Senyo, S.E., Steinhauser, M.L., Pizzimenti, C.L., Yang, V.K., Cai, L., Wang, M., Wu, T.-

D., Guerquin-Kern, J.-L., Lechene, C.P. and Lee, R.T., 2013. Mammalian heart renewal by preexisting cardiomyocytes. Nature 493, 433-436.

Seymour, A.-M.L., Giles, L., Ball, V., Miller, J.J., Clarke, K., Carr, C.A. and Tyler, D.J., 2015. In vivo assessment of cardiac metabolism and function in the abdominal aortic banding model of compensated cardiac hypertrophy. Cardiovascular Research 106, 249-260.

Shaltiel, I.A., Aprelia, M., Saurin, A.T., Chowdury, D., Kops, G.J.P.L., Voest, E.E. and Medema, R.H., 2014. Distinct phosphatases antagonize the p53 response in different phases of the cell cycle. Proceedings of the National Academy of Sciences (USA) 111, 7313-7318.

Shamraj, O.I., Grupp, I.L., Grupp, G., Melvin, D., Gradoux, N., Kremers, W., Lingrel, J.B. and Pover, A.D., 1993. Characterisation of Na/K-ATPase, its isoforms, and the inotropic response to ouabain in isolated failing human hearts. Cardiovascular Research 27, 2229.

Shannon, T.R., Ginsburg, K.S. and Bers, D.M., 2000. Potentiation of fractional sarcoplasmic reticulum calcium release by total and free intra-sarcoplasmic reticulum calcium concentration. Biophysical Journal 78, 334-343.

Shen, M.J., Choi, E.-K., Tan, A.Y., Lin, S.-F., Fishbein, M.C., Chen, L.S. and Chen, P.-S., 2012. Neural mechanisms of atrial arrhythmias. Nature Reviews Cardiology 9, 30-39.

Sheng, R., Luo, T., Li, H., Sun, J., Wang, Z. and Cao, A., 2014. Cholesterol-based cationic lipids for gene delivery: contribution of molecular structure factors to physico-chemical and biological properties. Colloids and Surfaces B: Biointerfaces 116, 32-40.

Sherwood, L., 2011. Fundamentals of Human Physiology, Fundamentals of Human Physiology. Brooks/Cole, Cengage Learning, Florence, KY, pp. 229-259.

Shi, J., Gu, P., Zhu, Z., Liu, J., Chen, Z., Sun, X., Chen, W., Gao, X. and Zhang, Z., 2012. Protein phosphatase 2A effectively modulates basal L-type Ca^{2+} current by dephosphorylating $Ca_V1.2$ at serine 1866 in mouse cardiac myocytes. Biochemical and Biophysical Research Communications 418, 792-798.

Shi, Y., 2009. Serine/Threonine Phosphatases: Mechanism through Structure. Cell 139, 468-484.

Shrivastav, M., De Haro, L.P. and Nickoloff, J.A., 2008a. Regulation of DNA double-strand break repair pathway choice. Cell Research 18, 134-147.

Shrivastav, M., De Haro, L.P. and Nickoloff, J.A., 2008b. Regulation of DNA double-strand break repair pathway choice. Cell Res 18, 134-147.

Sievers, F., Wilm, A., Dineen, D., Gibson, T.J., Karplus, K., Li, W., Lopez, R., McWilliam, H., Remmert, M., Soding, J., Thompson, J.D. and Higgins, D.G., 2011. Fast, scalable generation of high-quality protein multiple sequence alignments using Clustal Omega. Molecular Systems Biology 7, 539.

Sigg, D.C. and Hezi-Yamit, A., 2009. Cardiac and vascular receptors and signal transduction, in: Iaizzo, P.A. (Ed.), Handbook of Cardiac Anatomy, Physiology, and Devices. Humana Press, Totowa, NJ, pp. 191-218.

Silverman, B.d.Z., Fuller, W., Eaton, P., Deng, J., Moorman, J.R., Cheung, J.Y., James, A.F. and Shattock, M.J., 2005. Serine 68 phosphorylation of phospholemman: acute isoform-specific activation of cardiac Na/K ATPase. Cardiovascular Research 65, 93-103.

Simon, M.I., Strathmann, M.P. and Gautam, N., 1991. Diversity of G proteins in signal transduction. Science 252, 802.

Simpson, P., McGrath, A. and Savion, S., 1982. Myocyte hypertrophy in neonatal rat heart cultures and its regulation by serum and by catecholamines. Circulation Research 51, 787-801.

Singh, A.P., Singh, R. and Krishan, P., 2015. Ameliorative role of gemfibrozil against partial abdominal aortic constriction-induced cardiac hypertrophy in rats.

Cardiology in the Young 25, 725-730.
Sipido, K.R. and Marban, E., 1991. L-type calcium channels, potassium channels, and novel nonspecific cation channels in a clonal muscle cells line derived from embryonic rat ventricle. Circ Res 69, 1487-1499.
Siu, P.M., Teng, B.T., Pei, X.M. and Tam, E.W., 2011. Proteasome inhibition alleviates prolonged moderate compression-induced muscle pathology. BMC Musculoskeletal Disorders 12, 58.
Siwik, D.A., Tzortzis, J.D., Pimental, D.R., Chang, D.L.F., Pagano, P.J., Singh, K., Sawyer, D.B. and Colucci, W.S., 1999. Inhibition of copper-zinc superoxide dismutase induces cell growth, hypertrophic phenotype, and apoptosis in neonatal rat cardiac myocytes in vitro. Circulation Research 85, 147.
Smith, J., Mun Tho, L., Xu, N. and A. Gillespie, D., 2010. Chapter 3 - The ATM–Chk2 and ATR–Chk1 pathways in DNA damage signaling and cancer, in: George, F.V.W. and George, K. (Eds.), Advances in Cancer Research. Academic Press, pp. 73-112.
Smits, A.M. and Smits, J.F.M., 2004. Ischemic heart disease: models of myocardial hypertrophy and infarction. Drug Discovery Today: Disease Models 1, 273-278.
Snabaitis, A.K., Cuello, F. and Avkiran, M., 2008. Protein kinase B/Akt phosphorylates and inhibits the cardiac Na^+/H^+ exchanger NHE1. Circulation Research 103, 881-890.
Snabaitis, A.K., Muntendorff, A., Wieland, T. and Avkiran, M., 2005. Regulation of the extracellular signal-regulated kinase pathway in adult myocardium: differential roles of $G_{q/11}$, G_i and $G_{12/13}$ proteins in signalling by α_1-adrenergic, endothelin-1 and thrombin-sensitive protease-activated receptors. Cellular Signalling 17, 655-664.
Sondek, J., Bohm, A., Lambright, D.G., Hamm, H.E. and Sigler, P.B., 1996. Crystal structure of a GA protein [beta][gamma]dimer at 2.1 A resolution. Nature 379, 369-374.
Song, Z.T., Sun, L., Lu, S.J., Tian, Y., Ding, Y. and Liu, J.X., 2015. Transcription factor interaction with COMPASS-like complex regulates histone H3K4 trimethylation for specific gene expression in plants. Proceedings of the National Academy of Sciences of the United States of America 112, 2900-5.
Sopontammarak, S., Aliharoob, A., Ocampo, C., Arcilla, R.A., Gupta, M.P. and Gupta, M., 2005. Mitogen-activated protein kinases (p38 and c-Jun NH2-terminal kinase) are differentially regulated during cardiac volume and pressure overload hypertrophy. Cell Biochemistry and Biophysics 43, 61-76.
Spagnou, S., Miller, A.D. and Keller, M., 2004. Lipidic carriers of siRNA: differences in the formulation, cellular uptake, and delivery with plasmid DNA. Biochemistry 43, 13348-56.
Splawski, I., Timothy, K.W., Sharpe, L.M., Decher, N., Kumar, P., Bloise, R., Napolitano, C., Schwartz, P.J., Joseph, R.M., Condouris, K., Tager-Flusberg, H., Priori, S.G., Sanguinetti, M.C. and Keating, M.T., 2004. $Ca_V1.2$ calcium channel dysfunction causes a multisystem disorder including arrhythmia and autism. Cell 119, 19-31.
Spragg, D.D. and Kass, D.A., 2005. Controlling the gap: Myocytes, matrix, and mechanics. Circulation Research 96, 485-487.
Stadtman, E.R., 2006. Protein oxidation and aging. Free Radical Research 40, 1250-1258.
Stanevich, V., Jiang, L., Satyshur, K.A., Li, Y., Jeffrey, P.D., Li, Z., Menden, P., Semmelhack, M.F. and Xing, Y., 2011. The structural basis for tight control of PP2A methylation and function by LCMT-1. Molecular cell 41, 331-342.
Stefansson, B. and Brautigan, D.L., 2006. Protein phosphatase 6 subunit with conserved sit4-associated protein domain targets I*k*B∑. Journal of Biological Chemistry 281, 22624-22634.
Stefansson, B., Ohama, T., Daugherty, A.E. and Brautigan, D.L., 2008. Protein phosphatase 6 regulatory subunits composed of ankyrin repeat domains. Biochemistry 47, 1442-1451.
Stelzer, J.E., Patel, J.R., Walker, J.W. and Moss, R.L., 2007. Differential roles of cardiac myosin-binding protein C and cardiac troponin I in the myofibrillar force responses

to protein kinase A phosphorylation. Circulation Research 101, 503.

Suematsu, N., Tsutsui, H., Wen, J., Kang, D., Ikeuchi, M., Ide, T., Hayashidani, S., Shiomi, T., Kubota, T., Hamasaki, N. and Takeshita, A., 2003. Oxidative stress mediates tumor necrosis factor-alpha-induced mitochondrial DNA damage and dysfunction in cardiac myocytes. Circulation 107, 1418-23.

Sumiyoshi, E., Sugimoto, A. and Yamamoto, M., 2002. Protein phosphatase 4 is required for centrosome maturation in mitosis and sperm meiosis in *C. elegans*. Journal of Cell Science 115, 1403-10.

Sun, J., Ruan, Y., Wang, M., Chen, R., Yu, N., Sun, L., Liu, T. and Chen, H., 2016. Differentially expressed circulating LncRNAs and mRNA identified by microarray analysis in obese patients. Scientific Reports 6, 35421.

Sun, X., Momen, A., Wu, J., Noyan, H., Li, R., von Harsdorf, R. and Husain, M., 2014. p27 Protein Protects Metabolically Stressed Cardiomyocytes from Apoptosis by Promoting Autophagy. Journal of Biological Chemistry 289, 16924-16935.

Sunahori, K., Juang, Y.-T. and Tsokos, G.C., 2009. Methylation Status of CpG Islands Flanking a cAMP Response Element Motif on the Protein Phosphatase 2Acα Promoter Determines CREB Binding and Activity. Journal of Immunology 182, 1500-1508.

Sunahori, K., Juang, Y.T., Kyttaris, V.C. and Tsokos, G.C., 2011. Promoter hypomethylation results in increased expression of protein phosphatase 2A in T cells from patients with systemic lupus erythematosus. Journal of Immunology 186, 4508-17.

Sunahori, K., Nagpal, K., Hedrich, C.M., Mizui, M., Fitzgerald, L.M. and Tsokos, G.C., 2013. The catalytic subunit of protein phosphatase 2A (PP2Ac) promotes DNA hypomethylation by suppressing the phosphorylated mitogen-activated protein kinase/extracellular signal-regulated kinase (ERK) kinase (MEK)/phosphorylated ERK/DNMT1 protein pathway in T-cells from controls and systemic lupus erythematosus patients. Journal of Biological Chemistry 288, 21936-44.

Sweadner, K.J. and Rael, E., 2000. The FXYD gene family of small ion transport regulators or channels: cDNA sequence, protein signature sequence, and expression. Genomics 68, 41-56.

Swingle, M., Ni, L. and Honkanen, R.E., 2007. Small-molecule inhibitors of ser/thr protein phosphatases: specificity, use and common forms of abuse. Methods in Molecular Biology 365, 23-38.

Takemura, H., Yasui, K., Opthof, T., Niwa, N., Horiba, M., Shimizu, A., Lee, J.-K., Honjo, H., Kamiya, K., Ueda, Y. and Kodama, I., 2005. Subtype Switching of L-Type Ca^{2+} Channel From $Ca_V1.3$ to $Ca_V1.2$ in Embryonic Murine Ventricle. Circulation Journal 69, 1405-1411.

Takimoto, E., Champion, H.C., Li, M., Ren, S., Rodriguez, E.R., Tavazzi, B., Lazzarino, G., Paolocci, N., Gabrielson, K.L., Wang, Y. and Kass, D.A., 2005. Oxidant stress from nitric oxide synthase–3 uncoupling stimulates cardiac pathologic remodeling from chronic pressure load. Journal of Clinical Investigation 115, 1221-1231.

Takimoto, E. and Kass, D.A., 2007. Role of Oxidative Stress in Cardiac Hypertrophy and Remodeling. Hypertension 49, 241.

Tan, S.C., Carr, C.A., Yeoh, K.K., Schofield, C.J., Davies, K.E. and Clarke, K., 2012. Identification of valid housekeeping genes for quantitative RT-PCR analysis of cardiosphere-derived cells preconditioned under hypoxia or with prolyl-4-hydroxylase inhibitors. Molecular Biology Reports 39, 4857-67.

Tanaka, M., Ito, H., Adachi, S., Akimoto, H., Nishikawa, T., Kasajima, T., Marumo, F. and Hiroe, M., 1994. Hypoxia induces apoptosis with enhanced expression of Fas antigen messenger RNA in cultured neonatal rat cardiomyocytes. Circulation Research 75, 426-33.

Taneja, N., Davis, M., Choy, J.S., Beckett, M.A., Singh, R., Kron, S.J. and Weichselbaum, R.R., 2004. Histone H2AX phosphorylation as a predictor of radiosensitivity and

target for radiotherapy. Journal of Biological Chemistry 279, 2273-2280.

Terentyev, D., Belevych, A.E., Terentyeva, R., Martin, M.M., Malana, G.E., Kuhn, D.E., Abdellatif, M., Feldman, D.S., Elton, T.S. and Györke, S., 2009. miR-1 Overexpression enhances Ca^{2+} release and promotes cardiac arrhythmogenesis by targeting PP2A regulatory subunit B56α and causing CaMKII-dependent hyperphosphorylation of RyR2. Circulation Research 104, 514.

Terret, M.E., Wassmann, K., Waizenegger, I., Maro, B., Peters, J.M. and Verlhac, M.H., 2003. The meiosis I-to-meiosis II transition in mouse oocytes requires separase activity. Current Biology 13, 1797-802.

Territo, P.R., Mootha, V.K., French, S.A. and Balaban, R.S., 2000. Ca^{2+} activation of heart mitochondrial oxidative phosphorylation: role of the F0/F1-ATPase. American Journal of Physiology - Cell Physiology 278, C423.

Thomas, C., Mackey, M.M., Diaz, A.A. and Cox, D.P., 2009. Hydroxyl radical is produced via the Fenton reaction in submitochondrial particles under oxidative stress: implications for diseases associated with iron accumulation. Redox Report 14, 102-108.

Thrower, J.S., Hoffman, L., Rechsteiner, M. and Pickart, C.M., 2000. Recognition of the polyubiquitin proteolytic signal. EMBO Journal 19, 94-102.

Townsend, N., Wilson, L., Bhatnagar, P., Wickramasinghe, K., Rayner, M. and Nichols, M., 2016. Cardiovascular disease in Europe: epidemiological update 2016. European Heart Journal 37, 3232-3245.

Trepel, J.B., Moyer, J.D., Heikkila, R. and Sausville, E.A., 1988. Modulation of bombesin-induced phosphatidylinositol hydrolysis in a small-cell lung-cancer cell line. Biochemical Journal 255, 403.

Trockenbacher, A., Suckow, V., Foerster, K., Winter, J., Kraub, J., Ropers, H.-H., Schneider, R. and Schweiger, S., 2001. *MID1*, mutated in Opitz syndrome, encodes an ubiquitin ligase that targets phohphatase 2A for degradation. Nature Genetics 29, 287-294.

Troegeler, A., Lastrucci, C., Duval, C., Tanne, A., Cougoule, C., Maridonneau-Parini, I., Neyrolles, O. and Lugo-Villarino, G., 2014. An efficient siRNA-mediated gene silencing in primary human monocytes, dendritic cells and macrophages. Immunology & Cell Biology 92, 699-708.

Tsubuki, S., Saito, Y., Tomioka, M., Ito, H. and Kawashima, S., 1996. Differential inhibition of calpain and proteasome activities by peptidyl aldehydes of di-leucine and tri-leucine. Journal of Biochemistry 119, 572-6.

Turowski, P., Fernandez, A., Favre, B., Lamb, N.J.C. and Hemmings, B., 1995. Differential methylation and altered conformation of cytoplasmic and nuclear forms of protein phosphatase 2A during cell cycle progression. Journal of Cell Biology 129, 397-410.

Udeshi, N.D., Svinkina, T., Mertins, P., Kuhn, E., Mani, D.R., Qiao, J.W. and Carr, S.A., 2013. Refined preparation and use of anti-diglycine remnant (K-epsilon-GG) antibody enables routine quantification of 10,000s of ubiquitination sites in single proteomics experiments. Molecular & Cellular Proteomics 12, 825-31.

Ui-Tei, K., 2013. Optimal choice of functional and off-target effect-reduced siRNAs for RNAi therapeutics. Frontiers in Genetics 4, 107.

Vandesompele, J., De Preter, K., Pattyn, F., Poppe, B., Van Roy, N., De Paepe, A. and Speleman, F., 2002. Accurate normalization of real-time quantitative RT-PCR data by geometric averaging of multiple internal control genes. Genome Biology 3, RESEARCH0034.

Vangheluwe, P., Schuermans, M., ZÁDor, E., Waelkens, E., Raeymaekers, L. and Wuytack, F., 2005. Sarcolipin and phospholamban mRNA and protein expression in cardiac and skeletal muscle of different species. Biochemical Journal 389, 151.

Velagaleti, R. and Vasan, R.S., 2007. Heart failure in the 21st century: Is it a coronary artery disease problem or hypertension problem? Cardiology clinics 25, 487-v.

Villeneuve, C., Caudrillier, A., Ordener, C., Pizzinat, N., Parini, A. and Mialet-Perez, J., 2009. Dose-dependent activation of distinct hypertrophic pathways by serotonin in cardiac cells. American Journal of Physiology - Heart and Circulatory Physiology 297, H821-8.

Vincent, A., Berthel, E., Dacheux, E., Magnard, C. and Dalla Venezia, N.L., 2016. BRCA1 affects protein phosphatase 6 signalling through its interaction with ANKRD28. Biochemical Journal 473, 949-960.

Virshup, D.M. and Shenolikar, S., 2009. From promiscuity to precision: protein phosphatases get a makeover. Molecular Cell 33, 537-545.

Wang, J., Gao, E., Rabinowitz, J., Song, J., Zhang, X.-Q., Koch, W.J., Tucker, A.L., Chan, T.O., Feldman, A.M. and Cheung, J.Y., 2011. Regulation of in vivo cardiac contractility by phospholemman: role of Na^{+}/Ca^{2+} exchange. American Journal of Physiology - Heart and Circulatory Physiology 300, H859-H868.

Wang, L. and Proud, C.G., 2002. Regulation of the phosphorylation of elongation factor 2 by MEK-dependent signalling in adult rat cardiomyocytes. FEBS Letters 531, 285-9.

Wang, W., Watanabe, M., Nakamura, T., Kudo, Y. and Ochi, R., 1999. Properties and expression of Ca^{2+}-activated K^{+} channels in H9c2 cells derived from rat ventricle. American Journal of Physiology-Heart and Circulatory Physiology 276, H1559-H1566.

Wang, Y., Huang, S., Sah, V.P., Ross, J., Brown, J.H., Han, J. and Chien, K.R., 1998. Cardiac muscle cell hypertrophy and apoptosis induced by distinct members of the p38 mitogen-activated protein kinase family. Journal of Biological Chemistry 273, 2161-2168.

Wani, R., Nagata, A. and Murray, B.W., 2014. Protein redox chemistry: post-translational cysteine modifications that regulate signal transduction and drug pharmacology. Frontiers in Pharmacology 5, 224.

Waterhouse, P.M., Graham, M.W. and Wang, M.B., 1998. Virus resistance and gene silencing in plants can be induced by simultaneous expression of sense and antisense RNA. Proceedings of the National Academy of Sciences of the United States of America 95, 13959-64.

Watkins, G.R., Wang, N., Mazalouskas, M.D., Gomez, R.J., Guthrie, C.R., Kraemer, B.C., Schweiger, S., Spiller, B.W. and Wadzinski, B.E., 2012. Monoubiquitination promotes calpain cleavage of the protein phosphatase 2A (PP2A) regulatory subunit α4, altering PP2A stability and mictotubule-associated protein phosphorylation. Journal of Biological Chemistry 287, 24207-24215.

Watkins, S.J., Borthwick, G.M. and Arthur, H.M., 2011. The H9C2 cell line and primary neonatal cardiomyocyte cells show similar hypertrophic responses in vitro. In Vitro Cellular & Developmental Biology 47, 125-31.

Weber, S., Meyer-Roxlau, S., Wagner, M., Dobrev, D. and El-Armouche, A., 2015. Counteracting protein kinase activity in the heart: the multiple roles of protein phosphatases. Frontiers in Pharmacology 6, 270.

Weinberg, E.O., Thienelt, C.D., Katz, S.E., Bartunek, J., Tajima, M., Rohrbach, S., Douglas, P.S. and Lorell, B.H., 1999. Gender differences in molecular remodeling in pressure overload hypertrophy. Journal of the American College of Cardiology 34, 264-273.

Wencker, D., Chandra, M., Nguyen, K., Miao, W., Garantziotis, S., Factor, S.M., Shirani, J., Armstrong, R.C. and Kitsis, R.N., 2003. A mechanistic role for cardiac myocyte apoptosis in heart failure. Journal of Clinical Investigation 111, 1497-1504.

Wengrod, J., Wang, D., Weiss, S., Zhong, H., Osman, I. and Gardner, L.B., 2015. Phosphorylation of eIF2α by mTORC1 inhibition and PP6C activation is required for autophagy and is aberrant in PP6C-mutated melanoma. Science signaling 8, ra27-ra27.

West, M.H. and Bonner, W.M., 1980. Histone 2A, a heteromorphous family of eight protein

species. Biochemistry 19, 3238-45.
Wianny, F. and Zernicka-Goetz, M., 2000. Specific interference with gene function by double-stranded RNA in early mouse development. Nature Cell Biology 2, 70-5.
Wijnker, P.J., Boknik, P., Gergs, U., Muller, F.U., Neumann, J., dos Remedios, C., Schmitz, W., Sindermann, J.R., Stienen, G.J., van der Velden, J. and Kirchhefer, U., 2011. Protein phosphatase 2A affects myofilament contractility in non-failing but not in failing human myocardium. Journal of Muscle Research and Cell Motility 32, 221-33.
Wilkins, B.J., Dai, Y.-S., Bueno, O.F., Parsons, S.A., Xu, J., Plank, D.M., Jones, F., Kimball, T.R. and Molkentin, J.D., 2004. Calcineurin/NFAT coupling participates in pathological, but not physiological, cardiac hypertrophy. Circulation Research 94, 110.
Wlodarchak, N. and Xing, Y., 2016. PP2A as a master regulator of the cell cycle. Critical reviews in biochemistry and molecular biology 51, 162-184.
Wong, M.L. and Medrano, J.F., 2005. Real-time PCR for mRNA quantitation. BioTechniques 39, 75-85.
Wu, X., Eder, P., Chang, B. and Molkentin, J.D., 2010. TRPC channels are necessary mediators of pathologic cardiac hypertrophy. Proceedings of the National Academy of Sciences of the United States of America 107, 7000-7005.
Wypijewski, K.J., Howie, J., Reilly, L., Tulloch, L.B., Aughton, K.L., McLatchie, L.M., Shattock, M.J., Calaghan, S.C. and Fuller, W., 2013. A separate pool of cardiac phospholemman that does not regulate or associate with the sodium pump: Multimers of phospholemman in ventricular muscle. The Journal of Biological Chemistry 288, 13808-13820.
Xiao, B., Jiang, M.T., Zhao, M., Yang, D., C., S., Lai, F.A., Walsh, M.P., Warltier, D.C., Cheng, H. and Chen, S.R.W., 2005. Characterization of a novel PKA phosphorylation site, serine-2030, reveals no PKA hyperphosphorylation of the cardiac ryanodine receptor in canine heart failure. Circulation Research 96, 847-855.
Xiao, B., Zhong, G., Obayashi, M., Yang, D., Chen, K., Walsh, M.P., Shimoni, Y., Cheng, H., ter Keurs, H. and Chen, S.R.W., 2006. Ser-2030, but not ser-2808, is the major phosphorylation site in cardiac ryanodine receptors responding to protein kinase A activation upon b-adrenergic stimulation in normal and failing hearts. Biochemical Journal 396, 7-16.
Xiao, J., Li, J., Xu, T., Lv, D., Shen, B., Song, Y. and Xu, J., 2014. Pregnancy-induced physiological hypertrophy protects against cardiac ischemia-reperfusion injury. International Journal of Clinical and Experimental Pathology 7, 229-235.
Xiao, R.P., Hohl, C., Altschuld, R., Jones, L., Livingston, B., Ziman, B., Tantini, B. and Lakatta, E.G., 1994. Beta 2-adrenergic receptor-stimulated increase in cAMP in rat heart cells is not coupled to changes in Ca^{2+} dynamics, contractility, or phospholamban phosphorylation. Journal of Biological Chemistry 269, 19151-19156.
Xiao, R.P., Ji, X. and Lakatta, E.G., 1995. Functional coupling of the beta 2-adrenoceptor to a pertussis toxin-sensitive G protein in cardiac myocytes. Molecular Pharmacology 47, 322.
Xu, H., Ginsburg, K.S., Hall, D.D., Zimmermann, M., Stein, I.S., Zhang, M., Tandan, S., Hill, J.A., Horne, M.C., Bers, D.M. and Hell, J.W., 2010. Targeting of protein phosphatases PP2A and PP2B to the C-terminus of the L-type calcium channel $Ca_V1.2$. Biochemistry 49, 10298-10307.
Xu, J., Zhou, J.-Y., Xu, Z., Kho, D.-H., Zhuang, Z., Raz, A. and Wu, G.S., 2014. The role of Cullin3-mediated ubiquitination of the catalytic subunit of PP2A in TRAIL signaling. Cell Cycle 13, 3750-3758.
Xu, X., Hu, X., Lu, Z., Zhang, P., Zhao, L., Wessale, J.L., Bache, R.J. and Chen, Y., 2008. Xanthine oxidase inhibition with febuxostat attenuates systolic overload-induced

left ventricular hypertrophy and dysfunction in mice. Journal of Cardiac Failure 14, 746-753.

Xu, Y., Xing, Y., Chen, Y., Chao, Y., Lin, Z., Fan, E., Yu, J.W., Strack, S., Jeffrey, P.D. and Shi, Y., 2006. Structure of the protein phosphatase 2A holoenzyme. Cell 127, 1239-1251.

Yan, X., Xun, M., Li, J., Wu, L., Dou, X. and Zheng, J., 2016. Activation of Na^+/K^+-ATPase attenuates high glucose-induced H9c2 cell apoptosis via suppressing ROS accumulation and MAPKs activities by DRm217. Acta Biochimica et Biophysica Sinica.

Yang, L., Liu, G., Zakharov, S.I., Bellinger, A.M., Mongillo, M. and Marx, S.O., 2007. Protein kinase G phosphorylates $Ca_V1.2$ alpha1c and beta2 subunits. Circulation Research 101, 465-474.

Yang, L., Liu, G., Zakharov, S.I., Morrow, J.P., Rybin, V.O., Steinberg, S.F. and Marx, S.O., 2005. Ser1928 is a common site for $Ca_V1.2$ phosphorylation by protein kinase C isoforms. Journal of Biological Chemistry 280, 207-214.

Yayama, K., Horii, M., Hiyoshi, H., Takano, M., Okamoto, H., Kagota, S. and Kunitomo, M., 2004. Up-regulation of angiotensin II type 2 receptor in rat thoracic aorta by pressure-overload. Journal of Pharmacology and Experimental Therapeutics 308, 736.

Ye, B., Hou, N., Xiao, L., Xu, Y., Xu, H. and Li, F., 2016. Dynamic monitoring of oxidative DNA double-strand break and repair in cardiomyocytes. Cardiovascular Pathology 25, 93-100.

Yin, F.C., Spurgeon, H.A., Rakusan, K., Weisfeldt, M.L. and Lakatta, E.G., 1982. Use of tibial length to quantify cardiac hypertrophy: application in the aging rat. American Journal of Physiology - Heart and Circulatory Physiology 243, H941.

Ying, X., Lee, K., Li, N., Corbett, D., Mendoza, L. and Frangogiannis, N.G., 2009. Characterization of the inflammatory and fibrotic response in a mouse model of cardiac pressure overload. Histochemistry and Cell Biology 131, 471-481.

You, W.-t., Zhou, T., Ma, Z.-c., Liang, Q.-d., Xiao, C.-r., Tang, X.-l., Tan, H.-l., Zhang, B.-l., Wang, Y.-g. and Gao, Y., 2016. Ophiopogonin D maintains Ca^{2+} homeostasis in rat cardiomyocytes in vitro by upregulating CYP2J3/EETs and suppressing ER stress. Acta Pharmacologica Sinica 37, 368-381.

Zamore, P.D., Tuschl, T., Sharp, P.A. and Bartel, D.P., 2000. RNAi: double-stranded RNA directs the ATP-dependent cleavage of mRNA at 21 to 23 nucleotide intervals. Cell 101, 25-33.

Zelphati, O. and Szoka, F.C., Jr., 1996. Mechanism of oligonucleotide release from cationic liposomes. Proceedings of the National Academy of Sciences of the United States of America 93, 11493-8.

Zender, L., Hutker, S., Liedtke, C., Tillmann, H.L., Zender, S., Mundt, B., Waltemathe, M., Gosling, T., Flemming, P., Malek, N.P., Trautwein, C., Manns, M.P., Kuhnel, F. and Kubicka, S., 2003. Caspase 8 small interfering RNA prevents acute liver failure in mice. Proceedings of the National Academy of Sciences of the United States of America 100, 7797-802.

Zeng, K., Bastos, R.N., Barr, F.A. and Gruneberg, U., 2010. Protein phosphatase 6 regulates mitotic spindle formation by controlling the T-loop phosphorylation state of Aurora A bound to its activator TPX2. Journal of Cell Biology 191, 1315-1332.

Zhang, D., Gaussin, V., Taffet, G.E., Belaguli, N.S., Yamada, M., Schwartz, R.J., Michael, L.H., Overbeek, P.A. and Schneider, M.D., 2000. TAK1 is activated in the myocardium after pressure overload and is sufficient to provoke heart failure in transgenic mice. Nature Medicine 6, 556-563.

Zhang, H.-B., Li, R.-C., Xu, M., Xu, S.-M., Lai, Y.-S., Wu, H.-D., Xie, X.-J., Gao, W., Ye, H., Zhang, Y.-Y., Meng, X. and Wang, S.-Q., 2013. Ultrastructural uncoupling between T-tubules and sarcoplasmic reticulum in human heart failure. Cardiovascular Research 98, 269.

Zhang, T., Johnson, E.N., Gu, Y., Morissette, M.R., Sah, V.P., Gigena, M.S., Belke, D.D., Dillmann, W.H., Rogers, T.B., Schulman, H., Ross, J. and Brown, J.H., 2002. The Cardiac-specific Nuclear δB Isoform of Ca^{2+}/Calmodulin-dependent Protein Kinase II Induces Hypertrophy and Dilated Cardiomyopathy Associated with Increased Protein Phosphatase 2A Activity. Journal of Biological Chemistry 277, 1261-1267.

Zhang, X.-Q., Qureshi, A., Song, J., Carl, L.L., Tian, Q., Stahl, R.C., Carey, D.J., Rothblum, L.I. and Cheung, J.Y., 2003. Phospholemman modulates Na^{+}/Ca^{2+} exchange in adult rat cardiac myocytes. American Journal of Physiology - Heart and Circulatory Physiology 284, H225-H233.

Zhang, Z., He, Y., Tuteja, D., Xu, D., Timofeyev, V., Zhang, Q., Glatter, K.A., Xu, Y., Shin, H.-S., Low, R. and Chiamvimonvat, N., 2005. Functional roles of $Ca_V1.3$(alpha1D) calcium channels in atria: insights gained from gene-targeted null mutant mice. Circulation 112, 1936-1944.

Zheng, M., Zhu, J., Lv, T., Liu, L., Sun, H. and Tian, J., 2013. Bone morphogenetic protein2 enhances the expression of cardiac transcription factors by increasing histone H3 acetylation in H9c2 cells. Molecular Biology Reports 7, 953-8.

Zhong, J., Liao, J.K., Liu, X., Wang, P.H., Liu, J., Hou, W., Zhu, B., Yao, L., Wang, J., Li, J., Stark, M.J.R., Xie, Y. and Xu, X., 2011. Protein phosphatase PP6 is required for homology-directed repair of DNA double-strand breaks. Cell Cycle 10, 1411-1419.

Zhou, X., Oi, F.M. and Scharf, M.E., 2006. Social exploitation of hexamerin: RNAi reveals a major caste-regulatory factor in termites. Proceedings of the National Academy of Sciences of the United States of America 103, 4499-504.

Zhu, W., Woo, A.Y.-H., Yang, D., Cheng, H., Crow, M.T. and Xiao, R.-P., 2007. Activation of CaMKIIδC is a common intermediate of diverse death stimuli-induced heart muscle cell apoptosis. Journal of Biological Chemistry 282, 10833-10839.

Zong, C., Gomes, A.V., Drews, O., Li, X., Young, G.W., Berhane, B., Qiao, X., French, S.W., Bardag-Gorce, F. and Ping, P., 2006. Regulation of murine cardiac 20S proteasomes: Role of associating partners. Circulation Research 99, 372.

Zornhagen, K.W., Kristensen, A.T., Hansen, A.E., Oxboel, J. and Kjær, A., 2015. Selection of suitable reference genes for normalization of genes of interest in canine soft tissue sarcomas using quantitative real-time polymerase chain reaction. Veterinary and Comparative Oncology 13, 485-493.

Zwaenepoel, K., Louis, J.V., Goris, J. and Janssens, V., 2008. Diversity in genomic organisation, developmental regulation and distribution of the murine PR72/B" subunits of protein phosphatase 2A. BMC Genomics 9, 393-393.